Volume 16, Issue 4, December 2026
pISSN 2158-0510 eISSN - 2158-0529

IJBM

International Journal of BIOMEDICINE

www.ijbm.org

IJBM

INTERNATIONAL JOURNAL OF BIOMEDICINE

International Journal of Biomedicine (print ISSN - 2158-0510 and online ISSN - 2158-0529) is published four times a year by International Medical Research and Development Corp. (IMRDC). International Journal of Biomedicine (IJBM) is an international, peer-reviewed, open access journal. IJBM publishes scientific articles related to basic, applied, and translational research in biology and medicine. The main purpose of IJBM is to promote new scientific ideas and biomedical technologies. The distribution of freely accessible, high-quality content is a central mission of IJBM, aimed at increasing research visibility and accelerating scientific discovery. IJBM articles are published under a Creative Commons Attribution–NonCommercial–NoDerivatives 4.0 International (CC BY-NC ND 4.0) license.

International Journal of Biomedicine endorses and behaves in accordance with the codes of conduct and international standards established by the Committee on Publication Ethics (COPE).

Photocopying and Permissions: Published papers appear electronically and are freely available from our website. Authors may also use their published .pdf's for any non-commercial use on their personal or non-commercial institution's website. Users are free to read, download, copy, print, search, or link to the full texts of these articles for any non-commercial purpose. Articles from IJBM website may be reproduced, in any media or format, or linked to for any commercial purpose, subject to a selected user license.

Manuscript Submission: Original works will be accepted with the understanding that they are contributed solely to the Journal, are not under review by another publication, and have not previously been published except in abstract form.

Copyright

• Copyright for the article remains with the author(s) or the author's employer.

• By signing an Open Access Publishing Agreement, the authors authorize the publisher to publish the article and the right to identify itself as the original publisher. The Open Access Publishing Agreement encompasses all rights to publish, distribute, and make the article available in all media (print, digital, and online), as well as the right to protect these rights against third parties.

• The authors grant any third party the right to freely use the article under the terms of the Creative Commons Attribution (CC BY-NC-ND 4.0) license. The CC BY-NC-ND 4.0 license permits the use and distribution of all published articles in any medium, provided that the original work is properly cited and contains a DOI link to the version of record on www.ijbm.org. It is prohibited to distribute materials for commercial purposes or to modify or adapt the original works.

Notice: No responsibility is assumed by the Publisher, Corporation, or Editors for any injury and/or damage to persons or property as a matter of products liability, negligence, or otherwise, or from any use or operation of any methods, products, instructions, or ideas contained in the material herein. Because of rapid advances in the medical and biological sciences, in particular, independent verification of diagnoses, drug dosages, and devices recommended should be made. Although all advertising material is expected to conform to ethical (medical) standards, inclusion in this publication does not constitute a guarantee or endorsement of the quality or value of such product or of the claims made of it by its manufacturer.

IJBM

INTERNATIONAL JOURNAL OF BIOMEDICINE

Editor-in-Chief
Marietta Eliseyeva
IMRDC, New York, USA

Founding Editor
Simon Edelstein
Berry Moorman P.C., Birmingham, USA

EDITORIAL BOARD

Mary Ann Lila
North Carolina State University
Kannapolis, NC, USA

Ilya Raskin
Rutgers University
New Brunswick, NJ, USA

Gulnoz Khamidullaeva
National Center of Cardiology
Tashkent, Uzbekistan

Randy Lieberman
Detroit Medical Center
Detroit, MI, USA

Seung H. Kim
Hanyang University Medical Center
Seoul, South Korea

Karunakaran Rohini
AIMST University
Bedong, Malaysia

Shaoling Wu
Qingdao University, Qingdao
Shandong, China

Biao Xu
Nanjing University,
Nanjing, China

Bruna Scaggiante
University of Trieste
Trieste, Italy

Bhaskar Behera
Agharkar Research Institute
Pune, India

Gundu H.R. Rao
Lillehei Heart Institute, University
of Minnesota, Minneapolis, USA

Roy Beran
Griffith University, Queensland
UNSW, Sydney, Australia

Tetsuya Sugiyama
Nakano Eye Clinic
Nakagyo-ku, Kyoto, Japan

Timur Melkumyan
Tashkent State Medical University
Tashkent, Uzbekistan
RUDN University,
Moscow, Russia

Yue Wang
National Institute for Viral Disease
Control and Prevention, CCDC
Beijing, China

Zahir Hussain
Umm Al-Qura University
Makkah, Saudi Arabia

Pulat Sultanov
Republican Research Centre of
Emergency Medicine
Tashkent, Uzbekistan

Hesham Abdel-Hady
University of Mansoura
Mansoura, Egypt

EDITORIAL STAFF

Paul Edelstein *(Managing Editor)*
Paul Clee *(Copy Editor)*

Dmitriy Eliseyev *(Associate Editor)*
Paul Ogan *(Bilingual Interpreter)*

Nigora Srojidinova *(Editorial Assistant)*
Natalya Kozlova *(Editorial Assistant)*

IJBM
INTERNATIONAL JOURNAL OF BIOMEDICINE
www.ijbm.org
Volume 16 Issue 4 December 2026

CONTENTS

REVIEW ARTICLES

Contemporary Lipid-Lowering Strategies in Patients with Subclinical Coronary Atherosclerosis and Moderate Coronary Artery Calcification (CACS 100-299 AU)
Georgi Bradov, Tatyana Chalakova, Georgi Bachvarov, Maria Tsvetkova, Djeni Cherneva, Mariya Negreva 419

Ex Vivo and In Vivo Gene Therapy Strategies via Viral Vectors: Paving the Way toward a Cure for Hemophilia
Jie Gong, QiuYi Li1, Hong Du, Rui Yang 430

The Clinical Application of AI in Advanced Medical Imaging and Image Processing in Diagnostic Radiology
Rowa Aljondi 442

Microtubular Organization and Dynamics: Synthetic Chemistry, Chemical Biology, Biotechnology, Medicine and Biomedicine Perspectives
Zahir Hussain 455

ORIGINAL ARTICLES

Clinical and Pathological Characteristics Associated with BRAF V600E Mutation in Vietnamese Patients with Papillary Thyroid Carcinoma
Nguyen Thanh Hai, Tran Quang Phuc, Nguyen Huu Le, Nguyen Van Chuyen, Nguyen Thi Thu Trang, Cao Ba Loi 462

Short-Term Cancer Trends in Tabuk City, Saudi Arabia: A Retrospective Study (2023–2025)
Khalid Alhazmi 469

Enhanced Oxidative Phosphorylation Induces Autophagy in Prolactinomas
Yutao Shen 477

Evaluation of Mortality Using the PRISM Score System in a Pediatric Intensive Care Unit
Inva Gjeta, Iliriana Bakalli, Durim Sala, Ermela Çelaj, Vladimir Hoxha, Marsela Biqiku, Elmira Kola.....486

Hematological Consequences of Dengue–Malaria Co-infection Compared to Mono-infections: A Retrospective Cross-sectional Study in Omdurman, Sudan
Noha Osama, Roaa Mohammad, Sahwaa Jalal, Razan Altayeb, Nada Osman, Tyseer Ahmed, et al. 492

CONTENTS

ORIGINAL ARTICLES

Proinflammatory Mediators in Normal Weight Hypertensive Women of Reproductive Age
Zahir Hussain 499

Clinical Evaluation of a Novel Nanostructural Calcium Silicate–Hydroxyapatite Cement for Pulp Capping
Marija Lalović, Slavoljub Živković, Marijana Popović Bajić, Vukoman Jokanović, Vladimir Biočanin 505

CASE REPORTS

Diagnosis of ANCA-Negative Eosinophilic Granulomatosis with Polyangiitis with Cardiac Involvement and Progressive Neuropathy via Cardiac Magnetic Resonance Imaging and Bone Marrow Biopsy
Musab A. bin Shuayl 513

CORRIGENDUM

[Corrigendum] Deep Learning-Based Convolutional Neural Networks for Brain Tumor Detection on CT Scans: A Systematic Review
Sara Ali, Meaad Elbashir, Noor Hamzi, Imad Akour, Anwar Sheikhain, Raed Al-Shahri, Turkey Refaee, Ali Abdelrazig, Awatif M. Omer 517

READER SERVICES

Instructions for Authors 518

International Journal of Biomedicine 16(4) (2026) 419-429
http://dx.doi.org/10.21103/Article16(4)_RA1

REVIEW ARTICLE

INTERNATIONAL JOURNAL OF BIOMEDICINE

Contemporary Lipid-Lowering Strategies in Patients with Subclinical Coronary Atherosclerosis and Moderate Coronary Artery Calcification (CACS 100-299 AU)

Georgi Bradov[1*], Tatyana Chalakova[2], Georgi Bachvarov[3], Maria Tsvetkova[4], Djeni Cherneva[4], Mariya Negreva[1]

[1]*First Cardiology Clinic, University Hospital "St. Marina", Varna, BGR*
[2]*Department of Cardiology and Rheumatology, Medical University "Prof. Dr. Paraskev Stoyanov", Varna, BGR*
[3]*Department of Cardiac Surgery, Medical University "Prof. Dr. Paraskev Stoyanov", Varna, BGR*
[4]*Department of Biology, Faculty of Pharmacy, Medical University "Prof. Dr. Paraskev Stoyanov", Varna, BGR*

Abstract

Subclinical coronary atherosclerosis represents one of the earliest detectable manifestations of coronary artery disease and is associated with an increased risk of future cardiovascular events. Coronary artery calcium scoring (CACS) is a well-established non-invasive imaging biomarker that complements conventional cardiovascular risk prediction models and improves risk stratification, particularly in asymptomatic individuals with borderline or intermediate estimated cardiovascular risk. Accumulating evidence indicates that a moderate coronary artery calcium score (CACS 100–299 AU) is associated with a substantially increased risk of future cardiovascular events compared with that estimated by traditional risk prediction models alone. Consequently, CACS may facilitate the timely initiation and appropriate intensification of lipid-lowering therapy. This review summarizes the current evidence regarding the management of dyslipidemia in patients with subclinical coronary atherosclerosis and a moderate coronary artery calcium score (CACS 100–299 AU), with particular emphasis on contemporary therapeutic strategies and recent advances in lipid-lowering treatment. (**International Journal of Biomedicine. 2026;16(4):419-429**.)

Keywords: coronary artery calcium • coronary artery calcium score • dyslipidemia • subclinical coronary atherosclerosis • lipid-lowering therapy • cardiovascular risk stratification • primary prevention

For citation: Bradov G, Chalakova T, Bachvarov G, Tsvetkova M, Cherneva D, Negreva M. Contemporary Lipid-Lowering Strategies in Patients with Subclinical Coronary Atherosclerosis and Moderate Coronary Artery Calcification (CACS 100-299 AU). International Journal of Biomedicine. 2026;16(4):419-429. doi:10.21103/ Article16(4)_RA1

Introduction

Subclinical atherosclerosis is defined as the presence of structural atherosclerotic changes within one or more vascular territories before the onset of clinically manifest cardiovascular disease. It represents one of the earliest detectable manifestations of atherosclerotic disease, and its identification has become increasingly important in contemporary preventive cardiology, as it enables cardiovascular risk assessment before clinical events.[1]

Cardiovascular disease (CVD) remains the leading cause of mortality both in Europe and worldwide despite substantial advances in prevention and treatment. Current epidemiological projections indicate that the global burden of CVD will continue to increase over the coming decades, with ischemic heart disease remaining the most prevalent cardiovascular disorder.[2]

Coronary artery disease (CAD) remains one of the leading causes of death and disability worldwide, accounting for approximately seven million deaths annually. Although the incidence of CAD has declined in many high-income countries owing to improvements in preventive strategies and evidence-based therapies, its overall burden continues to increase due to population aging and the rising prevalence of cardiometabolic risk factors.[3] The classical cardiovascular risk factors identified in the Framingham Heart Study established the foundation of contemporary preventive cardiology and introduced the concept of cardiovascular risk prediction.[4] Subsequently, the

© 2026 The Author(s). *International Journal of Biomedicine* is published by IMRDC.
This is an open access article under the CC BY-NC-ND 4.0 license.

INTERHEART study demonstrated that the vast majority of myocardial infarctions worldwide are attributable to a limited number of potentially modifiable cardiovascular risk factors.[5] Furthermore, validation of the SCORE2 algorithms in the EPIC-Norfolk cohort demonstrated satisfactory predictive performance in middle-aged individuals while highlighting important limitations in risk discrimination among older adults.[6]

Data from the CARDIA study, which included 3,980 participants aged 22–36 years, demonstrated that the Framingham Risk Score (FRS) frequently underestimates cardiovascular risk in young adults because chronological age is a dominant component of the algorithm. Consequently, individuals with prolonged exposure to multiple cardiovascular risk factors may remain classified as low risk despite already having developed subclinical atherosclerosis.[7]

Similar findings were reported in a cohort of 2,447 asymptomatic women, in whom a substantial proportion of individuals with coronary artery calcification were still classified as being at low cardiovascular risk according to conventional risk assessment tools.[8] Collectively, these observations indicate that conventional cardiovascular risk prediction models may underestimate the true burden of subclinical coronary atherosclerosis in a considerable proportion of asymptomatic individuals.

Endothelial dysfunction is a key pathophysiological mechanism across the entire spectrum of atherogenesis and independently predicts future cardiovascular events, regardless of conventional cardiovascular risk scores.[9] Accordingly, assessment of endothelial function has emerged as an additional tool for cardiovascular risk stratification. A meta-analysis including 32 studies and more than 15,000 participants demonstrated that impaired endothelial function, assessed by peripheral arterial tonometry or brachial artery flow-mediated dilation during reactive hyperemia, is independently associated with an increased risk of future cardiovascular events.[10]

Taken together, these findings support the use of non-invasive imaging modalities, particularly coronary artery calcium scoring (CACS) and coronary computed tomography angiography (CCTA), for the detection of subclinical coronary atherosclerosis and refinement of cardiovascular risk stratification. Particular attention should be paid to asymptomatic individuals with a moderate coronary artery calcium score (CACS 100–299 AU), in whom cardiovascular risk is frequently underestimated by conventional risk prediction models such as SCORE2 and SCORE2-OP. Early initiation and appropriate intensification of lipid-lowering therapy in these patients may reduce cumulative exposure to LDL cholesterol and slow the progression of atherosclerotic plaque development.[11]

The rapid development of novel lipid-lowering therapies has substantially expanded the therapeutic armamentarium for the management of dyslipidemia. In addition to statins and ezetimibe, PCSK9-targeted therapies, bempedoic acid, inclisiran, and emerging RNA-based therapeutic approaches are progressively reshaping contemporary lipid management, while several additional therapeutic strategies remain under active clinical investigation.

Materials and Methods

This narrative review was based on a literature search performed in the PubMed/MEDLINE database covering publications from January 2000 to January 2025. The search strategy included the following keywords and MeSH terms: “coronary artery calcium score,” “subclinical atherosclerosis,” “coronary artery calcification,” “dyslipidemia,” and “lipid-lowering therapy”. Original research articles, systematic reviews, meta-analyses, narrative reviews, and relevant clinical practice guidelines published in English were considered for inclusion. Publications were selected based on their relevance to coronary artery calcium assessment, cardiovascular risk stratification, and the role of lipid-lowering therapies in patients with subclinical coronary atherosclerosis.

Publications were excluded if they were duplicate records, editorials, letters to the editor, or not directly relevant to the objectives of this review. Preference was given to peer-reviewed full-text publications; however, conference proceedings were included when they provided relevant information that complemented the available published evidence.

Additional relevant studies were identified by manually screening the reference lists of selected publications and major guideline documents from the European Society of Cardiology (ESC), European Atherosclerosis Society (EAS), and American College of Cardiology/American Heart Association (ACC/AHA). The available evidence was synthesized narratively according to the main themes of this review.

Pathogenesis and Clinical Significance of Atherosclerosis

Atherosclerosis is a chronic inflammatory disease that underlies the development of both cardiovascular and cerebrovascular disorders and is characterized by lipid accumulation and plaque formation within the arterial intima.[12,13] Endothelial dysfunction represents the initiating event in atherogenesis by facilitating the retention of low-density lipoprotein (LDL) particles within the arterial wall and triggering a local inflammatory response. Subsequently, circulating monocytes infiltrate the vessel wall, differentiate into macrophages, and internalize oxidized LDL (oxLDL), leading to the formation of lipid-laden foam cells. Migration and proliferation of vascular smooth muscle cells promote the development of a fibrous cap, whereas plaque rupture or erosion activates platelets and the coagulation cascade, ultimately resulting in thrombus formation.[14,15]

Assessment of plaque stability has become a cornerstone of contemporary cardiovascular risk evaluation.[13] The randomized SCOT-HEART trial demonstrated that patient prognosis is determined not only by the severity of coronary stenosis but also by plaque characteristics. In particular, the presence of high-risk plaque features was independently associated with an increased incidence of future cardiovascular events.[16]

Lipid-lowering therapy has consistently been shown to reduce cardiovascular morbidity and mortality.[17] Furthermore, evidence from multiple cohort studies and meta-analyses

indicates that early initiation of lipid-lowering therapy is justified in individuals with elevated LDL cholesterol concentrations (>130 mg/dL), particularly when additional cardiovascular risk factors are present.[18,19]

Imaging Modalities for the Assessment of Subclinical Atherosclerosis

The 2021 European Society of Cardiology (ESC) Guidelines introduced the SCORE2 and SCORE2-Older Persons (SCORE2-OP) algorithms for estimating the 10-year risk of fatal and non-fatal cardiovascular events in apparently healthy individuals.[20,21] According to these models, cardiovascular risk categories are defined according to age as follows: low-to-moderate risk (<2.5% for individuals <50 years, <5% for those aged 50–69 years, and <7.5% for those ≥70 years), high risk (2.5–7.5%, 5–10%, and 7.5–15%, respectively), and very high risk (≥7.5%, ≥10%, and ≥15%, respectively).[22]

Despite the availability of several cardiovascular risk prediction models, none directly assesses the extent of arterial wall remodeling or the burden of subclinical atherosclerosis.[23] Consequently, additional imaging techniques have been incorporated into cardiovascular risk assessment to enable a more individualized evaluation. These include carotid intima-media thickness (CIMT), pulse wave velocity (PWV), coronary artery calcium scoring (CACS), and coronary computed tomography angiography (CCTA).

In a population-based cross-sectional study involving 3,087 individuals without established cardiovascular disease or diabetes mellitus, pulse wave velocity (PWV >10 m/s) and coronary artery calcium burden, assessed by computed tomography, were evaluated. Individuals classified as being at high cardiovascular risk exhibited significantly greater coronary calcification, supporting the value of CACS for identifying subclinical vascular disease.[24] Carotid intima-media thickness (CIMT), measured by ultrasonography, represents another important imaging marker of subclinical atherosclerosis. Numerous studies have demonstrated that CIMT independently predicts future cardiovascular events beyond traditional cardiovascular risk factors.[25] Moreover, longitudinal progression of CIMT correlates with the subsequent risk of cardiovascular disease.[26]

Coronary artery calcification constitutes an integral component of the atherosclerotic process, and the coronary artery calcium score reflects the overall atherosclerotic burden within the coronary circulation.[27,28] Coronary artery calcium is currently regarded as the most extensively validated non-invasive imaging biomarker of subclinical coronary atherosclerosis. The presence of coronary calcification strongly correlates with underlying coronary atherosclerosis, whereas its absence substantially reduces—although does not completely exclude—the likelihood of significant obstructive coronary artery disease.[29]

According to the Agatston classification, coronary artery calcium burden is categorized as follows: CACS = 0, no detectable coronary calcification; CACS 1–99 AU, mild coronary calcification; CACS 100–299 AU, moderate coronary calcification; and CACS ≥300 AU, severe coronary calcification associated with a markedly increased cardiovascular risk.[29,30]

Current evidence supports intensification of preventive therapy according to the degree of coronary calcification. Individuals with CACS 1–99 AU generally benefit from moderate-intensity statin therapy, whereas those with a moderate CACS (100–299 AU) should be considered for moderate- to high-intensity statin therapy following an individualized assessment of overall cardiovascular and bleeding risk. Patients with CACS ≥300 AU are usually managed with intensive lipid-lowering therapy because their cardiovascular risk approaches that observed in secondary prevention populations.[30]

The Multi-Ethnic Study of Atherosclerosis (MESA), including 1,391 low-risk individuals, demonstrated that a CACS >100 AU was associated with a substantially increased incidence of cardiovascular events, highlighting its value for cardiovascular risk reclassification.[31] Likewise, in a prospective study of 117 postmenopausal women, CACS values were significantly higher among those with subclinical coronary atherosclerosis, with a considerable proportion exhibiting CACS >100 AU or >400 AU.[32]

Coronary artery calcium scoring has particular clinical value because conventional risk prediction models, including the Framingham Risk Score and SCORE2/SCORE2-OP, do not consistently identify all individuals at increased cardiovascular risk. Furthermore, CACS may modify the diagnostic strategy in patients with a low pre-test probability of obstructive coronary artery disease.[33] Incorporation of CACS into SCORE2/SCORE2-OP has been shown to improve cardiovascular risk classification, reclassifying approximately 48% of individuals initially categorized as high risk into a lower-risk category, while identifying approximately 7% of individuals initially considered low or intermediate risk as being at high cardiovascular risk.[34] Similarly, a study including 1,461 asymptomatic individuals with at least one cardiovascular risk factor demonstrated that combining the Framingham Risk Score with CACS provided superior cardiovascular risk discrimination compared with either method alone.[35]

In adults younger than 45 years, CACS may provide incremental value for cardiovascular risk stratification, particularly in individuals with a family history of premature cardiovascular disease, multiple cardiovascular risk factors, or borderline estimated risk, because conventional 10-year risk prediction models may substantially underestimate lifetime cardiovascular risk.[29]

From a clinical perspective, individuals with a moderate coronary artery calcium score (CACS 100–299 AU) represent an important subgroup in whom therapeutic decision-making remains challenging. Increasing evidence suggests that the actual cardiovascular risk in many of these patients is considerably higher than that estimated by conventional risk prediction models. Consequently, this population may benefit from earlier initiation and more intensive lipid-lowering therapy than would otherwise be recommended based solely on traditional risk calculators.

In conclusion, moderate coronary artery calcium (CACS 100–299 AU) provides incremental prognostic information beyond conventional cardiovascular risk prediction models and represents an important imaging biomarker for identifying asymptomatic individuals who may benefit from earlier and more intensive lipid-lowering therapy.

Lipid-Lowering Therapy

The management of dyslipidemia in patients without established cardiovascular disease is multifaceted and includes lifestyle modification, adherence to a heart-healthy diet, regular physical activity, weight control, and smoking cessation.[36] Contemporary pharmacological treatment includes 3-hydroxy-3-methylglutaryl coenzyme A reductase inhibitors (statins), cholesterol absorption inhibitors (ezetimibe), bile acid sequestrants, proprotein convertase subtilisin/kexin type 9 (PCSK9) inhibitors, microsomal triglyceride transfer protein (MTP) inhibitors, mipomersen, fibrates, omega-3 fatty acids, and cholesteryl ester transfer protein (CETP) inhibitors,[37] as well as emerging targeted therapies and nanoparticle-based drug delivery systems.

Statins

Statins are the first-line pharmacological agents for the treatment of hypercholesterolemia. They reversibly inhibit 3-hydroxy-3-methylglutaryl coenzyme A reductase, thereby reducing serum concentrations of total cholesterol, LDL cholesterol (LDL-C), and, to a lesser extent, triglycerides.[38] A substantial reduction in serum cholesterol levels is usually observed after 4–6 weeks of treatment.[39] Different statins exhibit broadly comparable pleiotropic effects and overall safety profiles.[40] Statin therapy is recommended for primary prevention in patients at moderate, high, or very high cardiovascular risk, as well as for secondary prevention in patients with established cardiovascular disease.[41]

Prospective and observational studies have shown that atorvastatin, simvastatin, and rosuvastatin may reduce LDL-C levels by up to 49% after 12 weeks of treatment and may slow the progression of non-calcified and low-attenuation atherosclerotic plaques. In patients with established atherosclerotic cardiovascular disease, statin therapy has been associated with an increase in calcified plaque volume and a reduction in non-calcified plaque burden, suggesting plaque stabilization and favorable remodeling of atherosclerotic lesions.[42–45] Statin therapy reduces relative cardiovascular risk by approximately 20–30%, largely irrespective of baseline LDL-C levels.[46] Meta-analyses and systematic reviews have demonstrated that statins reduce the risk of myocardial infarction, stroke, major adverse cardiovascular events, and all-cause mortality without a significant increase in myalgia, elevated hepatic transaminases, or diabetes mellitus. In primary prevention among patients with moderate to high cardiovascular risk, statins reduce coronary events by up to 30%, myocardial infarction by up to 31.7%, and cerebrovascular events by up to 14.4%, although a consistent significant reduction in all-cause mortality has not been uniformly demonstrated.[47–49]

The intensity of lipid-lowering therapy in patients at moderate cardiovascular risk should be individualized according to the overall cardiovascular risk profile. High-intensity statin therapy, defined as atorvastatin 40–80 mg or rosuvastatin 20–40 mg, is expected to reduce LDL-C levels by >50%, whereas moderate-intensity statin therapy, such as atorvastatin 10–20 mg or rosuvastatin 5–10 mg, typically achieves an LDL-C reduction of 30–50%.[37] Meta-analyses of large randomized trials have shown that each 1 mmol/L reduction in LDL-C is associated with an approximately 20% reduction in the risk of major vascular events, with an acceptable safety profile for more intensive statin therapy.[50] In patients with acute coronary syndromes, high-intensity statin therapy significantly reduces mortality and recurrent cardiovascular events, whereas the magnitude of benefit appears less pronounced in patients with stable coronary disease.[51–53] The greatest absolute reduction in cardiovascular morbidity and mortality is observed in patients at higher baseline risk, supporting a more intensive lipid-lowering strategy in this population.[54]

Ezetimibe

Ezetimibe, an inhibitor of intestinal cholesterol absorption, lowers LDL-C concentrations by approximately 15–20% when administered either as monotherapy or in combination with statins. The combination of high-intensity statin therapy and ezetimibe is more effective in reducing LDL-C levels than statin monotherapy.[55,56] An observational study including 17,830 patients showed that the addition of ezetimibe was associated with an additional LDL-C reduction of up to 14.8% and tripled the likelihood of achieving guideline-recommended LDL-C targets.[57] This may be particularly relevant in patients with subclinical coronary atherosclerosis and a moderate coronary artery calcium score (CACS 100–299 AU), in whom more intensive LDL-C reduction may help slow the progression of atherosclerotic plaque burden.

PCSK9 Inhibitors

By inhibiting proprotein convertase subtilisin/kexin type 9 (PCSK9), monoclonal antibodies against PCSK9 reduce serum concentrations of total cholesterol, LDL-C, apolipoprotein B, and lipoprotein(a) [Lp(a)].[5] They are indicated in patients who fail to achieve guideline-recommended LDL-C targets despite maximally tolerated conventional lipid-lowering therapy.[59,60] Evolocumab and alirocumab provide additional LDL-C reduction when administered in combination with moderate- or high-intensity statin therapy, as confirmed by a network meta-analysis of randomized clinical trials.[61] These fully human monoclonal antibodies are used in patients with primary hypercholesterolemia who do not achieve LDL-C targets or who are intolerant to statins.[62,63] Oral PCSK9 inhibitors are currently under clinical development and may further expand therapeutic options in the future.[64]

Fibrates

Fibrates exert their lipid-modifying effects through activation of the nuclear peroxisome proliferator-activated receptor alpha (PPAR-α).[65] They reduce endogenous production of very-low-density lipoproteins (VLDL) and enhance their clearance. In addition, fibrates increase serum high-density

lipoprotein cholesterol (HDL-C) concentrations, whereas their effect on LDL-C is comparatively modest.[66] They are primarily indicated in patients with hypertriglyceridemia and mixed dyslipidemia.[67] Combination therapy with a statin and a fibrate produces greater improvement in the lipid profile than statin monotherapy in patients with mixed hyperlipidemia,[68] a finding further supported by meta-analysis.[69] Pemafibrate, a newer selective PPAR-α modulator, has been shown to significantly reduce triglycerides, VLDL cholesterol, and total cholesterol while increasing HDL-C concentrations.[70]

Mipomersen

Mipomersen is an antisense oligonucleotide targeting human apolipoprotein B-100 (apoB-100). By binding directly to hepatic apoB messenger RNA, it inhibits apoB-100 synthesis and thereby reduces plasma concentrations of total cholesterol, LDL-C, and apoB. The drug has been used in patients with homozygous familial hypercholesterolemia or refractory heterozygous familial hypercholesterolemia.[71] A randomized double-blind trial demonstrated that adding mipomersen to maximally tolerated lipid-lowering therapy reduced LDL-C levels by up to 36.9%, together with reductions in apolipoprotein B and Lp(a), markers closely related to atherogenic lipoprotein burden. These effects may contribute to slowing atherosclerosis progression in patients with familial hypercholesterolemia.[72]

Niacin

Niacin reduces serum concentrations of total cholesterol, triglycerides, LDL-C, and Lp(a), while increasing HDL-C levels. These effects have been confirmed in meta-analyses including 30 clinical trials and 9,013 participants, demonstrating reductions in Lp(a) levels of up to 23%.[65,73,74]

Omega-3 Fatty Acids

Omega-3 fatty acids reduce VLDL production, increase lipoprotein lipase activity, and stimulate β-oxidation of fatty acids, which explains their triglyceride-lowering effect and potential relevance in the management of residual lipid risk when used in combination with other lipid-lowering therapies.[75] Observational and clinical studies have shown that higher circulating omega-3 fatty acid levels are associated with a lower incidence of cardiovascular disease[76] and a lower prevalence of high-risk carotid plaques.[77]

Emerging Therapeutic Strategies for Dyslipidemia

Bempedoic acid, an adenosine triphosphate-citrate lyase (ACL) inhibitor, reduces all major atherogenic lipid markers, including LDL cholesterol (LDL-C), non-HDL cholesterol, and apolipoprotein B, while also lowering high-sensitivity C-reactive protein (hsCRP), suggesting additional anti-inflammatory properties.[65] Compared with statins, bempedoic acid has been associated with a lower incidence of muscle-related adverse effects, making it an attractive option for patients with statin intolerance.[78]

Another antisense oligonucleotide, pelacarsen (APO(a)-LRx), targets hepatic LPA messenger RNA, thereby inhibiting apolipoprotein(a) synthesis and reducing lipoprotein(a) [Lp(a)] production.[79] In a phase II randomized placebo-controlled trial, pelacarsen reduced circulating Lp(a) concentrations by up to 80%.[80] The phase III Lp(a) HORIZON trial is expected to determine whether this profound reduction in Lp(a) translates into improved cardiovascular outcome.[81]

Cholesteryl ester transfer protein (CETP) inhibitors interfere with the bidirectional exchange of cholesteryl esters and triglycerides among circulating lipoproteins, resulting in increased HDL cholesterol concentrations and reduced LDL and VLDL cholesterol levels, thereby exhibiting potentially anti-atherogenic properties.[82] Nevertheless, despite favorable effects on lipid profiles, clinical trials have not consistently demonstrated meaningful cardiovascular benefit or convincing effects on the progression of subclinical atherosclerosis.[83] Nanotechnology is emerging as a promising field in preventive cardiology. Nanoparticle-based delivery systems are increasingly being investigated for the targeted administration of statins and RNA-based therapeutics, improving drug bioavailability, enhancing solubility, enabling controlled drug release, and potentially reducing systemic toxicity and adverse effects.[84]

Recently approved lipid-modifying therapies, including APOC3 inhibitors and ANGPTL3 inhibitors, have expanded treatment options for patients with severe or treatment-resistant dyslipidemia and persistent residual atherosclerotic cardiovascular risk.[85,86]

Growing attention has also been directed toward triglyceride-rich lipoprotein (TGRL)-targeted therapies, particularly omega-3 fatty acids, including eicosapentaenoic acid (EPA) and docosahexaenoic acid (DHA). These agents effectively reduce triglyceride concentrations, while cardiovascular outcome benefits have been demonstrated primarily with highly purified EPA formulations in appropriately selected high-risk patients.[87]

Glucagon-like peptide-1 receptor agonists (GLP-1 RAs), widely used in the treatment of type 2 diabetes and obesity, reduce body weight, body mass index (BMI), and glycated hemoglobin (HbA1c), while also producing modest improvements in LDL cholesterol and triglyceride concentrations.[88] A meta-analysis and meta-regression of randomized placebo-controlled trials confirmed their favorable effects on total cholesterol and LDL-C levels.[89] Beyond lipid modification, these agents provide substantial cardiovascular protection through multiple complementary mechanisms.

Muvalaplin is a novel investigational oral agent that selectively inhibits lipoprotein(a) formation. Results from a phase II randomized clinical trial demonstrated a marked reduction in circulating Lp(a) concentrations after 12 weeks of treatment without significant safety concerns.[90]

Despite well-established guideline recommendations for lipid-lowering therapy, initiation and intensification of treatment remain suboptimal in everyday clinical practice, particularly among asymptomatic individuals. This therapeutic inertia is likely attributable to underrecognition of subclinical atherosclerosis and excessive reliance on conventional cardiovascular risk prediction models. In this context, coronary artery calcium scoring (CACS) may play a pivotal role in overcoming therapeutic inertia by identifying patients with a moderate coronary artery calcium score (CACS 100–299 AU) who are likely to benefit from earlier and more intensive lipid-lowering therapy.

Coronary Artery Calcium Score and Therapeutic Recommendations

The 2019 European Society of Cardiology (ESC)/ European Atherosclerosis Society (EAS) Guidelines recommend initiation of high-intensity statin therapy at the maximally tolerated dose to achieve LDL-C targets according to the individual's cardiovascular risk category. If LDL-C goals are not achieved, ezetimibe should be added. Greater treatment intensity results in proportionally larger reductions in LDL-C, and in patients with higher baseline LDL-C concentrations this translates into greater absolute cardiovascular risk reduction. In very-high-risk patients undergoing secondary prevention who fail to achieve LDL-C targets despite maximally tolerated statin therapy combined with ezetimibe, addition of a PCSK9 inhibitor is recommended. Similarly, patients with familial hypercholesterolemia and very high cardiovascular risk may require combination therapy with a maximally tolerated statin and a PCSK9 inhibitor, whereas ezetimibe should be considered in those with statin intolerance.[37]

According to the American Heart Association (AHA)/ American College of Cardiology (ACC) guidelines, adults aged 40–75 years without diabetes mellitus who have LDL-C concentrations ≥70 mg/dL and an estimated 10-year ASCVD risk ≥7.5% should receive moderate- to high-intensity statin therapy. High-intensity statins are recommended when the estimated ASCVD risk is ≥20%, aiming for at least a 50% reduction in LDL-C levels. Additional cardiovascular risk-enhancing factors may further support treatment intensification. Patients at intermediate risk should generally receive moderate-intensity statin therapy, with ezetimibe considered if LDL-C targets are not achieved despite maximally tolerated statin treatment.[91]

Selection of an appropriate cardiovascular risk prediction algorithm remains fundamental to decisions regarding lipid-lowering therapy. A comparative study evaluating recommendations for statin therapy in primary prevention demonstrated considerable disagreement among different cardiovascular risk prediction models, including the Framingham Risk Score, Pooled Cohort Equations (PCE), SCORE2, and MESA. In a simulated population of 7,680 individuals, agreement between these models ranged from only 19% to 85%.[54] These findings underscore the importance of complementary imaging modalities, particularly CACS and coronary computed tomography angiography, for refining cardiovascular risk assessment.

Coronary artery calcium scoring has become an established imaging biomarker of subclinical coronary atherosclerosis and an important tool for cardiovascular risk assessment in primary prevention. Individuals with CACS = 0 AU generally have an excellent prognosis and may often be managed conservatively in the absence of additional major risk factors. Conversely, increasing coronary calcium burden is associated with progressively higher cardiovascular risk, supporting more intensive lipid-lowering therapy and stricter lipid target achievement.[92]

The AHA/ACC Primary Prevention Guidelines emphasize the role of CACS in personalizing statin therapy. In individuals with CACS = 0 AU, statin therapy may be deferred if no major cardiovascular risk-enhancing factors are present. A CACS of 1–99 AU favors statin therapy, particularly in individuals older than 55 years, whereas CACS 100–299 AU strongly supports initiation and intensification of statin treatment. Analysis of more than 16,000 participants demonstrated that CACS-guided decision making may avoid unnecessary statin therapy in 60–80% of middle-aged adults while simultaneously identifying older individuals who are most likely to benefit from treatment.[93]

Increasing evidence suggests that patients with a moderate coronary artery calcium score (CACS 100–299 AU) should not simply be regarded as having intermediate cardiovascular risk. In many of these individuals, the actual cardiovascular risk more closely resembles that observed in high-risk populations, supporting consideration of earlier and more intensive preventive treatment strategies.

Conclusions

Patients with subclinical coronary atherosclerosis and a moderate coronary artery calcium score (CACS 100–299 AU) represent a heterogeneous population in whom conventional cardiovascular risk prediction models frequently underestimate the true burden of disease. Coronary artery calcium scoring provides powerful incremental prognostic information beyond traditional risk algorithms and facilitates earlier identification of individuals who are likely to derive substantial benefit from lipid-lowering therapy.

Current evidence demonstrates that intensive LDL-C reduction with high-intensity statins, supplemented when necessary by ezetimibe or PCSK9 inhibitors, slows the progression of atherosclerotic plaque development and reduces future cardiovascular events. At the same time, the therapeutic landscape continues to evolve with the introduction of novel agents, including bempedoic acid, antisense oligonucleotides, small interfering RNA (siRNA)-based therapies, and other targeted lipid-lowering strategies, allowing increasingly individualized cardiovascular prevention.

Taken together, the available evidence supports considering patients with a moderate coronary artery calcium score (CACS 100–299 AU) as an important subgroup in whom earlier and more intensive lipid-lowering therapy may be justified despite apparently intermediate cardiovascular risk according to conventional prediction models.

Limitations

This narrative review has several limitations. The literature search was restricted to the PubMed/MEDLINE database and English-language publications, which may have resulted in the omission of relevant studies indexed elsewhere or published in other languages. In addition, as a narrative review, the evidence was synthesized descriptively rather than through a formal systematic review methodology, and no standardized assessment of study quality or risk of bias was performed. Finally, the available evidence specifically addressing lipid-lowering strategies in patients with moderate coronary artery calcium scores (CACS 100–299 AU) remains limited,

highlighting the need for further prospective studies to better define optimal therapeutic strategies.

Conflict of Interest

The authors declare that they have no competing interests.

References

1. Kawai K, Finn AV, Virmani R; Subclinical Atherosclerosis Collaborative. Subclinical Atherosclerosis: Part 1: What Is it? Can it Be Defined at the Histological Level? Arterioscler Thromb Vasc Biol. 2024 Jan;44(1):12-23. doi: 10.1161/ATVBAHA.123.319932. Epub 2023 Nov 21. PMID: 38150517.

2. Chong B, Jayabaskaran J, Jauhari SM, Chan SP, Goh R, Kueh MTW, Li H, Chin YH, Kong G, Anand VV, Wang JW, Muthiah M, Jain V, Mehta A, Lim SL, Foo R, Figtree GA, Nicholls SJ, Mamas MA, Januzzi JL, Chew NWS, Richards AM, Chan MY. Global burden of cardiovascular diseases: projections from 2025 to 2050. Eur J Prev Cardiol. 2025 Aug 25;32(11):1001-1015. doi: 10.1093/eurjpc/zwae281. PMID: 39270739.

3. Ralapanawa U, Sivakanesan R. Epidemiology and the Magnitude of Coronary Artery Disease and Acute Coronary Syndrome: A Narrative Review. J Epidemiol Glob Health. 2021 Jun;11(2):169-177. doi: 10.2991/jegh.k.201217.001. Epub 2021 Jan 7. PMID: 33605111; PMCID: PMC8242111.

4. Tsao CW, Vasan RS. Cohort Profile: The Framingham Heart Study (FHS): overview of milestones in cardiovascular epidemiology. Int J Epidemiol. 2015 Dec;44(6):1800-13. doi: 10.1093/ije/dyv337. PMID: 26705418; PMCID: PMC5156338.

5. Yusuf S, Hawken S, Ounpuu S, Dans T, Avezum A, Lanas F, McQueen M, Budaj A, Pais P, Varigos J, Lisheng L; INTERHEART Study Investigators. Effect of potentially modifiable risk factors associated with myocardial infarction in 52 countries (the INTERHEART study): case-control study. Lancet. 2004 Sep 11-17;364(9438):937-52. doi: 10.1016/S0140-6736(04)17018-9. PMID: 15364185.

6. van Trier TJ, Snaterse M, Boekholdt SM, Scholte Op Reimer WJM, Hageman SHJ, Visseren FLJ, Dorresteijn JAN, Peters RJG, Jørstad HT. Validation of Systematic Coronary Risk Evaluation 2 (SCORE2) and SCORE2-Older Persons in the EPIC-Norfolk prospective population cohort. Eur J Prev Cardiol. 2024 Jan 25;31(2):182-189. doi: 10.1093/eurjpc/zwad318. PMID: 37793098; PMCID: PMC10809184.

7. Armstrong AC, Jacobs DR Jr, Gidding SS, Colangelo LA, Gjesdal O, Lewis CE, Bibbins-Domingo K, Sidney S, Schreiner PJ, Williams OD, Goff DC Jr, Liu K, Lima JA. Framingham score and LV mass predict events in young adults: CARDIA study. Int J Cardiol. 2014 Mar 15;172(2):350-5. doi: 10.1016/j.ijcard.2014.01.003. Epub 2014 Jan 16. PMID: 24507735; PMCID: PMC4068332.

8. Michos ED, Nasir K, Braunstein JB, Rumberger JA, Budoff MJ, Post WS, Blumenthal RS. Framingham risk equation underestimates subclinical atherosclerosis risk in asymptomatic women. Atherosclerosis. 2006 Jan;184(1):201-6. doi: 10.1016/j.atherosclerosis.2005.04.004. PMID: 15907856.

9. Matsuzawa Y, Lerman A. Endothelial dysfunction and coronary artery disease: assessment, prognosis, and treatment. Coron Artery Dis. 2014 Dec;25(8):713-24. doi: 10.1097/MCA.0000000000000178. PMID: 25365643; PMCID: PMC4220301.

10. Xu Y, Arora RC, Hiebert BM, Lerner B, Szwajcer A, McDonald K, Rigatto C, Komenda P, Sood MM, Tangri N. Non-invasive endothelial function testing and the risk of adverse outcomes: a systematic review and meta-analysis. Eur Heart J Cardiovasc Imaging. 2014 Jul;15(7):736-46. doi: 10.1093/ehjci/jet256. Epub 2014 Jan 7. PMID: 24399339.

11. Cho YK, Nam CW, Koo BK, Schulman-Marcus J, Hartaigh BÓ, Gransar H, Lu Y, Achenbach S, Al-Mallah M, Andreini D, Bax JJ, Budoff MJ, Cademartiri F, Callister TQ, Chang HJ, Chinnaiyan K, Chow BJW, Cury RC, Delago A, Feuchtner G, Hadamitzky M, Hausleiter J, Kaufmann PA, Kim YJ, Leipsic J, Maffei E, Marques H, Pontone G, Raff GL, Rubinshtein R, Shaw LJ, Villines TC, Berman DS, Jones EC, Peña JM, Lin FY, Min JK. Usefulness of baseline statin therapy in non-obstructive coronary artery disease by coronary computed tomographic angiography: From the CONFIRM (COronary CT Angiography EvaluatioN For Clinical Outcomes: An InteRnational Multicenter) study. PLoS One. 2018 Dec 12;13(12):e0207194. doi: 10.1371/journal.pone.0207194. PMID: 30540755; PMCID: PMC6291090.

12. Waksman R, Merdler I, Case BC, Waksman O, Porto I. Targeting inflammation in atherosclerosis: overview, strategy and directions. EuroIntervention. 2024 Jan 1;20(1):32-44. doi: 10.4244/EIJ-D-23-00606. PMID: 38165117; PMCID: PMC10756224

13. Mehta A, Rigdon J, Tattersall MC, German CA, Barringer TA 3rd, Joshi PH, Sperling LS, Budoff MJ, Bertoni A, Michos ED, Blaha MJ, Stein JH, Shapiro MD. Association of Carotid Artery Plaque With Cardiovascular Events and Incident Coronary Artery Calcium in Individuals With Absent Coronary Calcification: The MESA. Circ Cardiovasc Imaging. 2021 Apr;14(4):e011701. doi: 10.1161/CIRCIMAGING.120.011701. Epub 2021 Apr 8. PMID: 33827231; PMCID: PMC8058258.

14. Morrison AM, Sullivan AE, Aday AW. Atherosclerotic Disease: Pathogenesis and Approaches to Management. Med Clin North Am. 2023 Sep;107(5):793-805. doi: 10.1016/j.mcna.2023.04.004. Epub 2023 Jun 1. PMID: 37541708; PMCID: PMC10547111.

15. Jebari-Benslaiman S, Galicia-García U, Larrea-Sebal A, Olaetxea JR, Alloza I, Vandenbroeck K, Benito-Vicente A, Martín C. Pathophysiology of Atherosclerosis. Int J Mol Sci. 2022 Mar 20;23(6):3346. doi: 10.3390/ijms23063346. PMID: 35328769; PMCID: PMC8954705.

16. Williams MC, Moss AJ, Dweck M, Adamson PD, Alam S, Hunter A, Shah ASV, Pawade T, Weir-McCall JR, Roditi G, van Beek EJR, Newby DE, Nicol ED. Coronary Artery Plaque Characteristics Associated With Adverse Outcomes in the SCOT-HEART Study. J Am Coll Cardiol. 2019 Jan 29;73(3):291-301. doi: 10.1016/j.jacc.2018.10.066. PMID: 30678759; PMCID: PMC6342893.

17. Du Z, Qin Y. Dyslipidemia and Cardiovascular Disease: Current Knowledge, Existing Challenges, and New Opportunities for Management Strategies. J Clin Med. 2023 Jan 3;12(1):363. doi: 10.3390/jcm12010363. PMID: 36615163; PMCID: PMC9820834.

18. Lu J, Zhang H, Chen B, Yang Y, Cui J, Xu W, Song L,

Yang H, He W, Zhang Y, Peng W, Li X. Association and its population heterogeneities between low-density lipoprotein cholesterol and all-cause and cardiovascular mortality: A population-based cohort study. Chin Med J (Engl). 2024 Sep 5;137(17):2075-2083. doi: 10.1097/CM9.0000000000003199. Epub 2024 Jul 30. PMID: 39075633; PMCID: PMC11374287.
19. Peng K, Li X, Wang Z, Li M, Yang Y. Association of low-density lipoprotein cholesterol levels with the risk of mortality and cardiovascular events: A meta-analysis of cohort studies with 1,232,694 participants. Medicine (Baltimore). 2022 Dec 2;101(48):e32003. doi: 10.1097/MD.0000000000032003. PMID: 36482567; PMCID: PMC9726298.
20. SCORE2 working group and ESC Cardiovascular risk collaboration. SCORE2 risk prediction algorithms: new models to estimate 10-year risk of cardiovascular disease in Europe. Eur Heart J. 2021 Jul 1;42(25):2439-2454. doi: 10.1093/eurheartj/ehab309. PMID: 34120177; PMCID: PMC8248998.
21. SCORE2-OP working group and ESC Cardiovascular risk collaboration. SCORE2-OP risk prediction algorithms: estimating incident cardiovascular event risk in older persons in four geographical risk regions. Eur Heart J. 2021 Jul 1;42(25):2455-2467. doi: 10.1093/eurheartj/ehab312. PMID: 34120185; PMCID: PMC8248997.
22. SCORE2 working group and ESC Cardiovascular risk collaboration. SCORE2 risk prediction algorithms: new models to estimate 10-year risk of cardiovascular disease in Europe. Eur Heart J. 2021 Jul 1;42(25):2439-2454. doi: 10.1093/eurheartj/ehab309. PMID: 34120177; PMCID: PMC8248998.
23. Cooney MT, Dudina AL, Graham IM. Value and limitations of existing scores for the assessment of cardiovascular risk: a review for clinicians. J Am Coll Cardiol. 2009 Sep 29;54(14):1209-27. doi: 10.1016/j.jacc.2009.07.020. PMID: 19778661.
24. Strömberg S, Stomby A, Engvall J, Östgren CJ. Systematic Coronary Risk Evaluation 2 (SCORE2), arterial stiffness, and subclinical coronary atherosclerosis in a population-based study. Scand J Prim Health Care. 2025 Jun;43(2):455-462. doi: 10.1080/02813432.2025.2456948. Epub 2025 Jan 24. PMID: 39853091; PMCID: PMC12090275.
25. Bauer M, Caviezel S, Teynor A, Erbel R, Mahabadi AA, Schmidt-Trucksäss A. Carotid intima-media thickness as a biomarker of subclinical atherosclerosis. Swiss Med Wkly. 2012 Oct 25;142:w13705. doi: 10.4414/smw.2012.13705. PMID: 23135891.
26. Touboul PJ, Grobbee DE, den Ruijter H. Assessment of subclinical atherosclerosis by carotid intima media thickness: technical issues. Eur J Prev Cardiol. 2012 Aug;19(2 Suppl):18-24. doi: 10.1177/2047487312448990. PMID: 22801066.
27. Raggi P, Achenbach S. Computed tomography for atherosclerosis and coronary artery disease imaging. Discov Med. 2010 Feb;9(45):98-104. PMID: 20193634.
28. Alexopoulos N, Raggi P. Calcification in atherosclerosis. Nat Rev Cardiol. 2009 Nov;6(11):681-8. doi: 10.1038/nrcardio.2009.165. Epub 2009 Sep 29. PMID: 19786983.
29. Angelov A: Kompyutartomografska diagnostika na koronarnata arterialna bolest [Computed Tomography Diagnosis of Coronary Artery Disease]. Medical University "Prof. Dr. Paraskev Stoyanov", Varna; 2025. (Bulgarian).
30. Gaemperli O, Maurovich-Horvat P, Nieman K, Pontone G, Pugliese F, editors: The EACVI Handbook of Cardiovascular CT. Oxford University Press, Oxford; 2021.
31. Joshi PH, Patel B, Blaha MJ, Berry JD, Blankstein R, Budoff MJ, Wong N, Agatston A, Blumenthal RS, Nasir K. Coronary artery Calcium predicts Cardiovascular events in participants with a low lifetime risk of Cardiovascular disease: The Multi-Ethnic Study of Atherosclerosis (MESA). Atherosclerosis. 2016 Mar;246:367-73. doi: 10.1016/j.atherosclerosis.2016.01.017. Epub 2016 Jan 13. PMID: 26841074.
32. Ismaili J, Ibrahimi P, Berisha-Muharremi V, Karahoda R, Berbatovci-Ukimeraj M, Istrefi N, Gjikolli B, Batalli A, Poniku A, Elezi S, Henein MY, Bajraktari G. Predictors of subclinical atherosclerosis in asymptomatic healthy non-diabetic postmenopausal women. Clin Physiol Funct Imaging. 2025 Jan;45(1):e12920. doi: 10.1111/cpf.12920. PMID: 39688094; PMCID: PMC11650537.
33. Ferrante G, Catapano F, Bacallao B, Romano I, Di Stefano V, Celata A, et al. The role of coronary artery calcium score and european score2 in primary prevention of cardiovascular disease. European Heart Journal. 2024;45 (Supplement_1, ehae666.2720). doi: 10.1093/eurheartj/ehae666.2720
34. Saydam CD. Subclinical cardiovascular disease and utility of coronary artery calcium score. Int J Cardiol Heart Vasc. 2021 Nov 17;37:100909. doi: 10.1016/j.ijcha.2021.100909. Erratum in: Int J Cardiol Heart Vasc. 2023 Apr 21;46:101208. doi: 10.1016/j.ijcha.2023.101208. PMID: 34825047; PMCID: PMC8604741.
35. Greenland P, LaBree L, Azen SP, Doherty TM, Detrano RC. Coronary artery calcium score combined with Framingham score for risk prediction in asymptomatic individuals. JAMA. 2004 Jan 14;291(2):210-5. doi: 10.1001/jama.291.2.210. Erratum in: JAMA. 2004 Feb 4;291(5):563. PMID: 14722147.
36. Pappan N, Awosika AO, Rehman A. Dyslipidemia. In: StatPearls [Internet]. Treasure Island (FL): StatPearls Publishing; 2026 Jan– [cited 2026 Mar 22]. Available from: https://www.ncbi.nlm.nih.gov/books/NBK560891/
37. Mach F, Baigent C, Catapano AL, Koskinas KC, Casula M, Badimon L, Chapman MJ, De Backer GG, Delgado V, Ference BA, Graham IM, Halliday A, Landmesser U, Mihaylova B, Pedersen TR, Riccardi G, Richter DJ, Sabatine MS, Taskinen MR, Tokgozoglu L, Wiklund O; ESC Scientific Document Group. 2019 ESC/EAS Guidelines for the management of dyslipidaemias: lipid modification to reduce cardiovascular risk. Eur Heart J. 2020 Jan 1;41(1):111-188. doi: 10.1093/eurheartj/ehz455. Erratum in: Eur Heart J. 2020 Nov 21;41(44):4255. doi: 10.1093/eurheartj/ehz826. PMID: 31504418.
38. Sizar O, Khare S, Patel P, Talati R. Statin Medications. 2024 Feb 29. In: StatPearls [Internet]. Treasure Island (FL): StatPearls Publishing; 2026 Jan–. PMID: 28613690.
39. Lennernäs H, Fager G. Pharmacodynamics and pharmacokinetics of the HMG-CoA reductase inhibitors. Similarities and differences. Clin Pharmacokinet. 1997 May;32(5):403-25. doi: 10.2165/00003088-199732050-00005. PMID: 9160173.
40. Sadowska A, Osiński P, Roztocka A, Kaczmarz-Chojnacka K, Zapora E, Sawicka D, Car H. Statins-From Fungi to Pharmacy. Int J Mol Sci. 2023 Dec 29;25(1):466.

doi: 10.3390/ijms25010466. PMID: 38203637; PMCID: PMC10779115.
41. Paparodis RD, Bantouna D, Livadas S, Angelopoulos N. Statin therapy in primary and secondary cardiovascular disease prevention. Curr Atheroscler Rep. 2024 Dec 30;27(1):21. doi: 10.1007/s11883-024-01265-9. PMID: 39738779.
42. John LJ, Esheiba EMF, Fathi MAM, Agarwal A, Sreedharan J, Muttappallymyalil J, Shanthakumari N. Efficacy of statins in dyslipidemia: a non-interventional comparative study in a tertiary care hospital, Ajman, UAE. In: Proceedings of the 6th Annual Scientific Meeting of Gulf Medical University; 2014 Nov 5-6; Ajman, UAE. Ajman, UAE: Gulf Medical University; 2014. p. 108–113.
43. Zeb I, Li D, Nasir K, Malpeso J, Batool A, Flores F, Dailing C, Karlsberg RP, Budoff M. Effect of statin treatment on coronary plaque progression - a serial coronary CT angiography study. Atherosclerosis. 2013 Dec;231(2):198-204. doi: 10.1016/j.atherosclerosis.2013.08.019. Epub 2013 Aug 29. PMID: 24267226.
44. Van Rosendael AR, van den Hoogen IJ, Gianni U, Ma X, Tantawy SW, Bax AM, Lu Y, Andreini D, Al-Mallah MH, Budoff MJ, Cademartiri F, Chinnaiyan K, Choi JH, Conte E, Marques H, de Araújo Gonçalves P, Gottlieb I, Hadamitzky M, Leipsic JA, Maffei E, Pontone G, Shin S, Kim YJ, Lee BK, Chun EJ, Sung JM, Lee SE, Virmani R, Samady H, Sato Y, Stone PH, Berman DS, Narula J, Blankstein R, Min JK, Lin FY, Shaw LJ, Bax JJ, Chang HJ. Association of Statin Treatment With Progression of Coronary Atherosclerotic Plaque Composition. JAMA Cardiol. 2021 Nov 1;6(11):1257-1266. doi: 10.1001/jamacardio.2021.3055. PMID: 34406326; PMCID: PMC8374741.
45. Giovannucci J, Shanbhag A, Hong W, Yong Y, PangS, Heanue S, et al. Association of statin therapy with progression of coronary artery calcium composition and density on noncontrast computed tomography. European Heart Journal. 2025;46 (Supplement_1, ehaf784.155). doi: 10.1093/eurheartj/ehaf784.155
46. Gocheva NN, Georgiev B, editors: Statinite v sardechno-sadoviya kontinuum [Statins in the Cardiovascular Continuum]. 2nd ed. Arbilis, Sofia; 2013. (Bulgarian)
47. Chou R, Cantor A, Dana T, Wagner J, Ahmed AY, Fu R, Ferencik M. Statin Use for the Primary Prevention of Cardiovascular Disease in Adults: Updated Evidence Report and Systematic Review for the US Preventive Services Task Force. JAMA. 2022 Aug 23;328(8):754-771. doi: 10.1001/jama.2022.12138. PMID: 35997724.
48. Taylor F, Huffman MD, Macedo AF, Moore TH, Burke M, Davey Smith G, Ward K, Ebrahim S. Statins for the primary prevention of cardiovascular disease. Cochrane Database Syst Rev. 2013 Jan 31;2013(1):CD004816. doi: 10.1002/14651858.CD004816.pub5. PMID: 23440795; PMCID: PMC6481400.
49. Thavendiranathan P, Bagai A, Brookhart MA, Choudhry NK. Primary prevention of cardiovascular diseases with statin therapy: a meta-analysis of randomized controlled trials. Arch Intern Med. 2006 Nov 27;166(21):2307-13. doi: 10.1001/archinte.166.21.2307. PMID: 17130382.
50. Cholesterol Treatment Trialists' (CTT) Collaboration; Baigent C, Blackwell L, Emberson J, Holland LE, Reith C, Bhala N, Peto R, Barnes EH, Keech A, Simes J, Collins R. Efficacy and safety of more intensive lowering of LDL cholesterol: a meta-analysis of data from 170,000 participants in 26 randomised trials. Lancet. 2010 Nov 13;376(9753):1670-81. doi: 10.1016/S0140-6736(10)61350-5. Epub 2010 Nov 8. PMID: 21067804; PMCID: PMC2988224.
51. Afilalo J, Majdan AA, Eisenberg MJ. Intensive statin therapy in acute coronary syndromes and stable coronary heart disease: a comparative meta-analysis of randomised controlled trials. Heart. 2007 Aug;93(8):914-21. doi: 10.1136/hrt.2006.112508. Epub 2007 Feb 3. PMID: 17277349; PMCID: PMC1994400.
52. Cannon CP, Steinberg BA, Murphy SA, Mega JL, Braunwald E. Meta-analysis of cardiovascular outcomes trials comparing intensive versus moderate statin therapy. J Am Coll Cardiol. 2006 Aug 1;48(3):438-45. doi: 10.1016/j.jacc.2006.04.070. Epub 2006 Jul 12. PMID: 16875966.
53. Mills EJ, O'Regan C, Eyawo O, Wu P, Mills F, Berwanger O, Briel M. Intensive statin therapy compared with moderate dosing for prevention of cardiovascular events: a meta-analysis of >40 000 patients. Eur Heart J. 2011 Jun;32(11):1409-15. doi: 10.1093/eurheartj/ehr035. Epub 2011 Mar 8. PMID: 21385791.
54. Stein EA. The power of statins: aggressive lipid lowering. Clin Cardiol. 2003 Apr;26(4 Suppl 3):III25-31. doi: 10.1002/clc.4960261506. PMID: 12708636; PMCID: PMC6654637.
55. Cheng AY, Leiter LA. Clinical use of ezetimibe. Can J Clin Pharmacol. 2003 Winter;10 Suppl A:21A-5A. PMID: 14571302.
56. Ezetimibe: new preparation. A cholesterol-lowering drug with no clinical advantage. Prescrire Int. 2004 Oct;13(73):176-9. PMID: 15499698.
57. Foody JM, Toth PP, Tomassini JE, Sajjan S, Ramey DR, Neff D, Tershakovec AM, Hu H, Tunceli K. Changes in LDL-C levels and goal attainment associated with addition of ezetimibe to simvastatin, atorvastatin, or rosuvastatin compared with titrating statin monotherapy. Vasc Health Risk Manag. 2013;9:719-27. doi: 10.2147/VHRM.S49840. Epub 2013 Nov 15. PMID: 24265554; PMCID: PMC3833706.
58. Wallemacq C. Le médicament du mois. Evolocumab (Repatha®) : Anticorps monoclonal anti-PCSK9 comme nouveau traitement hypocholestérolémiant puissant [Evolocumab (Repatha®) : a human monoclonal antibody against PCSK9 protein as potent cholesterol-lowering therapy]. Rev Med Liege. 2017 Nov;72(11):505-512. French. PMID: 29171950.
59. Schmidt AF, Carter JL, Pearce LS, Wilkins JT, Overington JP, Hingorani AD, Casas JP. PCSK9 monoclonal antibodies for the primary and secondary prevention of cardiovascular disease. Cochrane Database Syst Rev. 2020 Oct 20;10(10):CD011748. doi: 10.1002/14651858.CD011748.pub3. PMID: 33078867; PMCID: PMC8094613.
60. Toth PP, Worthy G, Gandra SR, Sattar N, Bray S, Cheng LI, Bridges I, Worth GM, Dent R, Forbes CA, Deshpande S, Ross J, Kleijnen J, Stroes ESG. Systematic Review and Network Meta-Analysis on the Efficacy of Evolocumab and Other Therapies for the Management of Lipid Levels in Hyperlipidemia. J Am Heart Assoc. 2017 Oct 2;6(10):e005367. doi: 10.1161/JAHA.116.005367. PMID: 28971955; PMCID: PMC5721820.
61. Thavendiranathan P, Bagai A, Brookhart MA, Choudhry NK. Primary prevention of cardiovascular diseases with statin therapy: a meta-analysis of randomized controlled trials. Arch Intern Med. 2006 Nov 27;166(21):2307-13. doi: 10.1001/

archinte.166.21.2307. PMID: 17130382.
62. Mercep I, Strikic D, Hrabac P, Pecin I, Reiner Ž. PCSK9 inhibition: from effectiveness to cost-effectiveness. Front Cardiovasc Med. 2024 Jun 25;11:1339487. doi: 10.3389/fcvm.2024.1339487. PMID: 38988669; PMCID: PMC11234837.
63. Schreml J, Gouni-Berthold I. Role of Anti-PCSK9 Antibodies in the Treatment of Patients with Statin Intolerance. Curr Med Chem. 2018;25(13):1538-1548. doi: 10.2174/0929867324666617061611647. PMID: 28618994.
64. Tokgözoğlu L, Pirillo A, Catapano AL. Oral PCSK9 Inhibitors: Will They Work? Curr Atheroscler Rep. 2025 Apr 30;27(1):53. doi: 10.1007/s11883-025-01299-7. PMID: 40304930.
65. Feingold KR. Triglyceride Lowering Drugs. 2025 Jun 22. In: Feingold KR, Adler RA, Ahmed SF, Anawalt B, Blackman MR, Chrousos G, Corpas E, de Herder WW, Dhatariya K, Dungan K, Hamilton E, Hofland J, Jan de Beur S, Kalra S, Kaltsas G, Kapoor N, Kim M, Koch C, Kopp P, Korbonits M, Kovacs CS, Kuohung W, Laferrère B, Levy M, McGee EA, McLachlan R, Muzumdar R, Purnell J, Rey R, Sahay R, Shah AS, Sperling MA, Stratakis CA, Trence DL, Wilson DP, editors. Endotext [Internet]. South Dartmouth (MA): MDText.com, Inc.; 2000–. PMID: 28402615.
66. Zimetbaum P, Frishman WH, Kahn S. Effects of gemfibrozil and other fibric acid derivatives on blood lipids and lipoproteins. J Clin Pharmacol. 1991 Jan;31(1):25-37. doi: 10.1002/j.1552-4604.1991.tb01883.x. PMID: 2045526.
67. Rosenson RS. Fenofibrate: treatment of hyperlipidemia and beyond. Expert Rev Cardiovasc Ther. 2008 Nov;6(10):1319-30. doi: 10.1586/14779072.6.10.1319. PMID: 19018684.
68. Grundy SM, Vega GL, Yuan Z, Battisti WP, Brady WE, Palmisano J. Effectiveness and tolerability of simvastatin plus fenofibrate for combined hyperlipidemia (the SAFARI trial). Am J Cardiol. 2005 Feb 15;95(4):462-8. doi: 10.1016/j.amjcard.2004.10.012. Erratum in: Am J Cardiol. 2006 Aug 1;98(3):427-8. PMID: 15695129.
69. Choi HD, Shin WG. Safety and efficacy of statin treatment alone and in combination with fibrates in patients with dyslipidemia: a meta-analysis. Curr Med Res Opin. 2014 Jan;30(1):1-10. doi: 10.1185/03007995.2013.842165. Epub 2013 Oct 1. PMID: 24063624.
70. Elbahloul MA, Elgadi A, Ramadan M, Mohamed Amine H, Fayed H, Kasser ME, Hussein A, Labieb F. Efficacy and safety of pemafibrate administration in patients with dyslipidemia: a systematic review and updated meta-analysis of randomized controlled trials. Ann Med Surg (Lond). 2025 Apr 22;87(6):3756-3767. doi: 10.1097/MS9.0000000000003264. PMID: 40486565; PMCID: PMC12140688.
71. Bell DA, Hooper AJ, Watts GF, Burnett JR. Mipomersen and other therapies for the treatment of severe familial hypercholesterolemia. Vasc Health Risk Manag. 2012;8:651-9. doi: 10.2147/VHRM.S28581. Epub 2012 Nov 28. PMID: 23226021; PMCID: PMC3513909.
72. Thomas GS, Cromwell WC, Ali S, Chin W, Flaim JD, Davidson M. Mipomersen, an apolipoprotein B synthesis inhibitor, reduces atherogenic lipoproteins in patients with severe hypercholesterolemia at high cardiovascular risk: a randomized, double-blind, placebo-controlled trial. J Am Coll Cardiol. 2013 Dec 10;62(23):2178-84. doi: 10.1016/j.jacc.2013.07.081. Epub 2013 Sep 4. PMID: 24013058.
73. Birjmohun RS, Hutten BA, Kastelein JJ, Stroes ES. Efficacy and safety of high-density lipoprotein cholesterol-increasing compounds: a meta-analysis of randomized controlled trials. J Am Coll Cardiol. 2005 Jan 18;45(2):185-97. doi: 10.1016/j.jacc.2004.10.031. PMID: 15653014.
74. Sahebkar A, Reiner Ž, Simental-Mendía LE, Ferretti G, Cicero AF. Effect of extended-release niacin on plasma lipoprotein(a) levels: A systematic review and meta-analysis of randomized placebo-controlled trials. Metabolism. 2016 Nov;65(11):1664-1678. doi: 10.1016/j.metabol.2016.08.007. Epub 2016 Aug 31. PMID: 27733255.
75. Oscarsson J, Hurt-Camejo E. Omega-3 fatty acids eicosapentaenoic acid and docosahexaenoic acid and their mechanisms of action on apolipoprotein B-containing lipoproteins in humans: a review. Lipids Health Dis. 2017 Aug 10;16(1):149. doi: 10.1186/s12944-017-0541-3. PMID: 28797250; PMCID: PMC5553798.
76. Alfaddagh A, Kapoor K, Dardari ZA, Bhatt DL, Budoff MJ, Nasir K, Miller M, Welty FK, Miedema MD, Shapiro MD, Tsai MY, Blumenthal RS, Blaha MJ. Omega-3 fatty acids, subclinical atherosclerosis, and cardiovascular events: Implications for primary prevention. Atherosclerosis. 2022 Jul;353:11-19. doi: 10.1016/j.atherosclerosis.2022.06.1018. Epub 2022 Jun 20. PMID: 35759823; PMCID: PMC10961178.
77. Feuchtner G, Langer C, Barbieri F, Beyer C, Dichtl W, Friedrich G, Schgoer W, Widmann G, Plank F. The effect of omega-3 fatty acids on coronary atherosclerosis quantified by coronary computed tomography angiography. Clin Nutr. 2021 Mar;40(3):1123-1129. doi: 10.1016/j.clnu.2020.07.016. Epub 2020 Jul 22. PMID: 32778459.
78. Oscarsson J, Hurt-Camejo E. Omega-3 fatty acids eicosapentaenoic acid and docosahexaenoic acid and their mechanisms of action on apolipoprotein B-containing lipoproteins in humans: a review. Lipids Health Dis. 2017 Aug 10;16(1):149. doi: 10.1186/s12944-017-0541-3. PMID: 28797250; PMCID: PMC5553798.
79. Bhatia HS, Bajaj A, Goonewardena SN, Moriarty PM. Pelacarsen: Mechanism of action and Lp(a)-lowering effect. J Clin Lipidol. 2025 Sep-Oct;19(5):1208-1222. doi: 10.1016/j.jacl.2025.06.004. Epub 2025 Jun 16. PMID: 40781022.
80. Tsimikas S, Karwatowska-Prokopczuk E, Gouni-Berthold I, Tardif JC, Baum SJ, Steinhagen-Thiessen E, Shapiro MD, Stroes ES, Moriarty PM, Nordestgaard BG, Xia S, Guerriero J, Viney NJ, O'Dea L, Witztum JL; AKCEA-APO(a)-LRx Study Investigators. Lipoprotein(a) Reduction in Persons with Cardiovascular Disease. N Engl J Med. 2020 Jan 16;382(3):244-255. doi: 10.1056/NEJMoa1905239. Epub 2020 Jan 1. PMID: 31893580.
81. Formisano P, Vianello E, Dozio E, Tacchini L, Romani L, Frati L, Curcio F, Bellet MM, Corsi-Romanelli MM. Lp(a) in the Horizon of Diagnostics and Therapy. Int J Mol Sci. 2025 Dec 27;27(1):290. doi: 10.3390/ijms27010290. PMID: 41516166; PMCID: PMC12785701.
82. Shrestha S, Wu BJ, Guiney L, Barter PJ, Rye KA. Cholesteryl ester transfer protein and its inhibitors. J Lipid Res. 2018 May;59(5):772-783. doi: 10.1194/jlr.R082735. Epub 2018 Feb 27. PMID: 29487091; PMCID: PMC5928430.
83. Shinkai H. Cholesteryl ester transfer-protein modulator and inhibitors and their potential for the treatment of cardiovascular diseases. Vasc Health Risk Manag. 2012;8:323-31. doi: 10.2147/VHRM.S25238. Epub 2012 May 15. PMID:

22661899; PMCID: PMC3363149.
84. Etemad L, Salmasi Z, Moosavian Kalat SA, Moshiri M, Zamanian J, Kesharwani P, Sahebkar A. An overview on nanoplatforms for statins delivery: Perspectives for safe and effective therapy. Environ Res. 2023 Oct 1;234:116572. doi: 10.1016/j.envres.2023.116572. Epub 2023 Jul 8. PMID: 37429398.
85. Dybiec J, Baran W, Dąbek B, Fularski P, Młynarska E, Radzioch E, Rysz J, Franczyk B. Advances in Treatment of Dyslipidemia. Int J Mol Sci. 2023 Aug 27;24(17):13288. doi: 10.3390/ijms241713288. PMID: 37686091; PMCID: PMC10488025.
86. Balling M, Roepstorff OG, Gerds TA, Varbo A, Mortensen MB, Langsted A, Nordestgaard BG, Afzal S. Risk reduction of ASCVD attributed to lowering of remnant cholesterol from statins, fibrates, APOC3 inhibitors, and ANGPTL3 inhibitors: a cohort study. Atherosclerosis. 2025 Oct;409:120471. doi: 10.1016/j.atherosclerosis.2025.120471. Epub 2025 Aug 6. PMID: 40839980.
87. Khan SU, Lone AN, Khan MS, Virani SS, Blumenthal RS, Nasir K, Miller M, Michos ED, Ballantyne CM, Boden WE, Bhatt DL. Effect of omega-3 fatty acids on cardiovascular outcomes: A systematic review and meta-analysis. EClinicalMedicine. 2021 Jul 8;38:100997. doi: 10.1016/j.eclinm.2021.100997. PMID: 34505026; PMCID: PMC8413259.
88. Albahli OM, Ali S, Alblaihi F, Aljaman AA. The Effect of Glucagon-Like Peptide-1 (GLP-1) Receptor Agonists on the Lipid Profile of Diabetic Patients Using Statins: A Retrospective Cohort Study in the Diabetic Center of King Salman Bin Abdulaziz Hospital, Saudi Arabia. Cureus. 2024 Jul 27;16(7):e65521. doi: 10.7759/cureus.65521. PMID: 39188504; PMCID: PMC11346815.
89. Rivera FB, Chin MNC, Pine PLS, Ruyeras MMJ, Galang DJC, Gandionco KM, Morales BLFD, Climaco ZMV, Bantayan NRB, Magalong JV, Mangubat GF, Ong K. Glucagon-like peptide 1 receptor agonists modestly reduced low-density lipoprotein cholesterol and total cholesterol levels independent of weight reduction: a meta-analysis and meta-regression of placebo controlled randomized controlled trials. Curr Med Res Opin. 2025 Jan;41(1):185-197. doi: 10.1080/03007995.2024.2442027. Epub 2024 Dec 18. PMID: 39666879.
90. Nicholls SJ, Nissen SE, Fleming C, Urva S, Suico J, Berg PH, Linnebjerg H, Ruotolo G, Turner PK, Michael LF. Muvalaplin, an Oral Small Molecule Inhibitor of Lipoprotein(a) Formation: A Randomized Clinical Trial. JAMA. 2023 Sep 19;330(11):1042-1053. doi: 10.1001/jama.2023.16503. PMID: 37638695; PMCID: PMC10463176.
91. Grundy SM, Stone NJ, Bailey AL, Beam C, Birtcher KK, Blumenthal RS, Braun LT, de Ferranti S, Faiella-Tommasino J, Forman DE, Goldberg R, Heidenreich PA, Hlatky MA, Jones DW, Lloyd-Jones D, Lopez-Pajares N, Ndumele CE, Orringer CE, Peralta CA, Saseen JJ, Smith SC Jr, Sperling L, Virani SS, Yeboah J. 2018 AHA/ACC/AACVPR/AAPA/ABC/ACPM/ADA/AGS/APhA/ASPC/NLA/PCNA Guideline on the Management of Blood Cholesterol: A Report of the American College of Cardiology/American Heart Association Task Force on Clinical Practice Guidelines. J Am Coll Cardiol. 2019 Jun 25;73(24):e285-e350. doi: 10.1016/j.jacc.2018.11.003. Epub 2018 Nov 10. Erratum in: J Am Coll Cardiol. 2019 Jun 25;73(24):3237-3241. doi: 10.1016/j.jacc.2019.05.013. Erratum in: J Am Coll Cardiol. 2024 Oct 29;84(18):1772. doi: 10.1016/j.jacc.2024.09.026. PMID: 30423393.
92. Mancini GBJ, Ryomoto A, Yeoh E, Brunham LR, Hegele RA. Recommendations for statin management in primary prevention: disparities among international risk scores. Eur Heart J. 2024 Jan 7;45(2):117-128. doi: 10.1093/eurheartj/ehad539. PMID: 37638490; PMCID: PMC10771376.
93. Keller M, Silber S. Usefulness of the coronary artery calcium (CAC) score for statin prescription in primary prevention: results in over 16.000 assessments. European Heart Journal. 2020;41(Issue Supplement_2, ehaa946.2923) doi:10.1093/ehjci/ehaa946.2923

***Corresponding author:** Georgi Bradov, University Hospital "St. Marina", Varna, Bulgaria. E-mail: g.bradov@gmail.com*

International Journal of Biomedicine 16(4) (2026) 430-441
http://dx.doi.org/10.21103/Article16(4)_RA2

REVIEW ARTICLE

INTERNATIONAL JOURNAL OF BIOMEDICINE

Ex Vivo and In Vivo Gene Therapy Strategies via Viral Vectors: Paving the Way toward a Cure for Hemophilia

Jie Gong[1, 2, *, #], QiuYi Li[1, 2, #], Hong Du[3], Rui Yang[3]

[1]*College of Life Sciences, Inner Mongolia Agricultural University, Hohhot, China*
[2]*Inner Mongolia Key Laboratory of Biomanufacturing, Hohhot, China*
[3]*Chengdu Longyouji Immuno-Biotechnology Co., Ltd. Chengdu, China*
[#]*These authors contributed equally to this work.*

Abstract

Due to the poor quality of life of patients with severe hemophilia, developing a cure method for hemophilia remains pivotal for mitigating associated global health burdens. In the last few years, an increasing number of original research and clinical studies have revealed that gene therapy is a transformative strategy for hemophilia management. Recent advancements in gene therapies, including ex vivo stem cell modification and in vivo viral vector administration, have broadened the scope of gene therapy via viral vectors to address challenges that modulate the specificity of protein expression. This review presents the latest advancements in gene therapy via viral vectors for hemophilia. The vital focus on targeted gene therapy applications for treating hemophilia is not only on exploring administration methods and preconditioning strategies but also on selecting the treatment window and assessing their efficacy. Cell-based therapy offers high specificity and programmability for treating hemophilia A, and in vivo gene therapy provides a safe and straightforward alternative. **(International Journal o Biomedicine. 2026;16(4):430-441.)**

Keywords: gene therapy • hemophilia • stem cells • clinical translation • viral vector

For citation: Gong J, Li QY, Du H, Yang R. Ex Vivo and In Vivo Gene Therapy Strategies via Viral Vectors: Paving the Way toward a Cure for Hemophilia. International Journal of Biomedicine. 2026;16(4):430-441. doi:10.21103/ Article16(4)_RA2

Introduction

Hemophilia is a rare genetic bleeding disorder that occurs more frequently in males. Severe patients have a strong tendency for spontaneous bleeding after injury. Currently, there is no complete cure for this disease. Without proper medical care, the expected lifespan of patients with severe hemophilia is less than 10 years.[1] Therefore, it is urgent to discover more effective treatments.

Hemophilia is usually caused by a mutation in a single gene. The mutated gene could be the factor VIII (FVIII, F8) or the factor IX (FIX, F9). Both of these factors are important components in the coagulation process.[2] Hemophilia can be classified into types A and B. Hemophilia A is caused by a mutation in the F8 gene, leading to low levels of clotting factor VIII. Hemophilia B is caused by a mutation in the F9 gene, leading to low levels of clotting factor IX.

Although protein replacement therapy has constantly evolved, which has made its half-life longer, the long-term economic pressure is also destroying the lives of patients. In the last few years, gene therapy has emerged as a transformative strategy for hemophilia management. Recent advancements in gene therapies, including *ex vivo* stem cell modification and *in vivo* vector administration, have constituted the main focus. This review presents the different delivery strategies in gene therapy for hemophilia (Fig. 1).

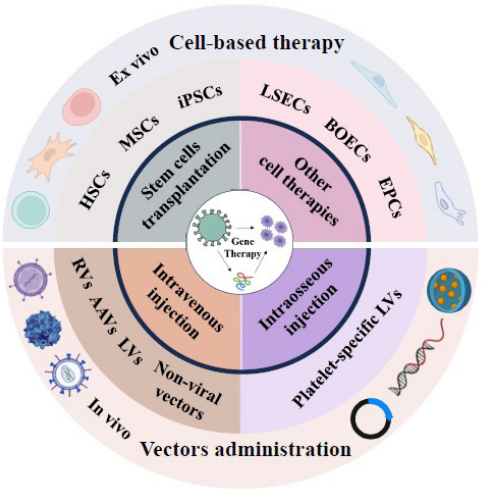

Fig. 1. *Schematic illustration of gene therapies, including stem cell transplantation and in vivo vector administration based on different delivery strategies.*

© 2026 The Author(s). *International Journal of Biomedicine* is published by IMRDC.
This is an open access article under the CC BY-NC-ND 4.0 license.

Treatments in Gene Therapy for Hemophilia

Recent advancements in gene therapy for hemophilia, including cellular therapy and direct vector injection treatments, have broadened the scope of gene therapy to include challenges that modulate the specificity of protein expression.

Ex vivo approach to gene therapy for hemophilia

The use of cell-based gene therapy represents yet another therapeutic option for severe hemophilia.[3] Several candidate cell types can support F8 production: Hematopoietic stem cells (HSCs) derived from BM, mesenchymal stem cells (MSCs), liver sinusoidal endothelial cells (LSECs), blood-outgrowth endothelial cells (BOECs), and endothelial progenitor cells (EPCs) derived from the differentiation of induced pluripotent stem cells (iPSCs).[4] Fig. 2 shows the schematic illustration of implementation procedures for ex vivo approaches.

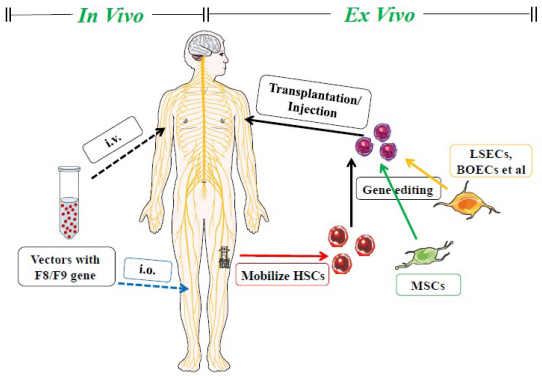

Fig. 2. Schematic illustration of implementation procedures for ex vivo and in vivo gene therapies.

Autologous HSCs transplantation

The most common one is the modified autologous HSC transplantation using vectors carrying the F8 gene. Lentivirus (LV) enables larger gene constructs and, unlike the Adeno-associated Virus (AAV) vector approach, allows the gene of interest to integrate into the host cellular DNA.[5] The latest strategies have leaned towards tissue-specific promoters, especially platelet-specific promoters for HSC transplantation. Most of these strategies were verified in the $F8^{null}$ and $F9^{null}$ mouse model over a decade ago.[6-8] HSCs by LV-F8 led to long-term repopulation of murine recipients with an efficient gene transfer.[9] Shi et al. used a LV-mediated gene transfer system to deliver the human B-domain-deleted F8 (hF8-BDD) expression with platelet-specific αIIb promoter (2bF8) into HSCs, resulting in F8 expression in platelets and sustained therapeutic levels of platelet-F8 with neither inhibitory nor non-inhibitory antibody development.[10]

Recently, a phase 1 trial evaluating the feasibility of HSC gene therapy using platelet F8 in participants with F8 inhibitors, funded by the National Institutes of Health (USA), opened recruitment (NCT03818763). Researchers reported a highly effective case.[11] The participant with a history of F8 inhibitor underwent autologous $CD34^+$ cell transplantation, which was transduced with an LV encoding F8 under the control of the ITGA2B promoter for platelet-specific expression. The level of megakaryocyte FVIII:C was 0.00 mU per 10^6 cells before transduction and 101.32 mU per 10^6 cells after transduction.[12] Also, more clinical studies about HSC transplantation were summarized in Table 1. Other approaches using LVs were under early investigation.[13,14] Merlin et al. used the natural F8 promoter (pF8) to direct gene replacement to F8–secreting cells. This application mediated long-term F8 expression by targeting liver sinusoidal endothelial cells in hemophilic mice, thereby correcting the bleeding phenotype without inhibitor formation.

Other cell therapies

Due to their low immunogenicity, MSCs can be applied without preconditioning before treatment; therefore, numerous immunologic problems have been resolved. Because MSCs can be obtained from the patient's body and reinjected after in vitro modification. Autologous bone-marrow-derived MSCs transduced with an LV expressing coagulation F8 were injected into the left knee joint of cynomolgus monkeys. They confirmed the long-term safety of intra-articular injection of transduced MSCs in non-human primates (NHPs).[15]

Some research on the effectiveness of MSCs for hemophilia was conducted over 10 years ago.[16,17] In animal models, injection of BM-MSC-F8 into HA mice and sheep reduced joint hemorrhage.[18,19] Moreover, Wang et al. generated a transgenic mouse line modified with the hF8-BDD vector, from which hF8-BDD-MSCs were isolated and subsequently transplanted into HA mice. Plasma F8 activities of recipient HA mice increased from 0% to 32%.[20] In a recent study, the protein-coding region of the hF9 gene was inserted to AAVS1. They were transduced into MSCs using the nucleofection method, and high, durable expression of F9 at the protein level was observed both in vivo and in vitro.[21] Also, modified hepatic and pulmonary MSCs capable of secreting coagulation factors could produce endogenous F8.[22,23]

Transplantation of LSECs has been demonstrated in several animal models as a means to treat HA. Kumaran et al. transplanted LSECs into the portal vein and demonstrated liver engraftment and therapeutic correction of HA, with plasma F8 activity exceeding 10% of normal plasma levels.[24]

Blood-derived circulating endothelial cells, referred to as BOECs, represent a clinically promising cell type and exhibit a much higher proliferative potential, which can be expanded in culture for the therapy of HA.[25] BOECs primarily engrafted the spleen and BM after an intravenous (IV) injection. Furthermore, BOECs transfected with F8 can secrete F8 into the plasma, as shown by transplantation into NOD/SCID mice and HA dog.[26,27] F8-transduced BOECs had also been grown into sheets and then transplanted subcutaneously, resulting in partial correction of the disease phenotype in HA mice.[28] It was reported in 2021 that the first preclinical study demonstrated the safety and feasibility of transplantation of GMP-like-produced LV-corrected BOECs within an implantable device for the long-term treatment of HA.[29]

iPSCs are an alternative to embryonic stem cells for HA gene therapy. Firstly, the derivation of iPSCs does not require

Table 1. Clinical trials about HSCs transplantation on hemophilia.

Sponsor	Treatment	N participants enrolled	Dose	Approx. Mean activity	Follow-up (Years) / Durability	ABR	Phase	Status	Clinicaltrials.gov Identifier
Shenzhen Geno-Immune Medical Institute	YUVA-GT-F901 (Lentiviral F9 gene-modified autologous hematopoietic and mesenchymal stem cells)	10 (estimated)	NA	NA	NA	NA	I	Unknown	NCT03961243
Shenzhen Geno-Immune Medical Institute	YUVA-GT-F801 (Lentiviral F8 gene modified autologous hematopoietic stem cells and mesenchymal stem cells)	10 (estimated)	NA	NA	NA	NA	I	Unknown	NCT03217032
Medical College of Wisconsin	Auto CD34+PBSC, transduced with a lentiviral vector encoding ITGA2B-F8-BDD	5 (estimated)	NA	NA	NA	NA	I	Recruiting	NCT03818763
Christian Medical College	Auto CD34+PBSC transduced with a CD68-ET3 lentiviral vector encoding a novel coagulation F8 transgene	6	NA	NA	NA	NA	I	Completed	NCT05265767
Expression Therapeutics	CD34+ hematopoietic stem cells transduced with a CD68-ET3 lentiviral vector (encoding the hFVIII gene)	7 (estimated)	NA	NA	NA	NA	I	Not yet recruiting	NCT04418414

human embryos and thus circumvents the ethical debate and supply constraints associated with their use in research or clinical practice.[30] Secondly, the genetic abnormalities causing HA can be corrected using gene-editing technology, followed by the subsequent selection, expansion, and differentiation of iPSCs into endothelial cell progenitors or fully differentiated LSECs. Partial demonstration of such a therapy had been reported during the past 15 years, in which transplantable EPCs were derived from iPSCs and shown to produce F8 in HA mice.[31-33] There has also been an effort to demonstrate the utility of a combined approach that uses gene therapy to direct expression of an hF8 transgene under a megakaryocyte-specific promoter in iPSC-derived cells.[34,35] Other methods of gene editing have been developed for correcting genetic abnormalities in iPSCs, such as the RNA-guided clustered regularly interspaced short palindromic repeats (CRISPR)-Cas9 system. Such an approach could be used to correct the F8 gene in patient-derived iPSCs.[36-38] That may offer the possibility of an unlimited source of transplantable EPCs for the treatment of hemophilia.

In vivo approach to gene therapy with IB injection for hemophilia

Compared with autologous HSC transplantation, IV injection has simpler operability and higher safety, manifested as mild immunosuppression before vector IV injection (Fig. 2). The key rate-limiting steps in systemic IV delivery include interactions with serum proteins, blood clearance, vascular escape, attachment, endocytosis, intracellular processing, nuclear entry, and vector genome conversion.[39]

AAV-mediated gene transfer approach

An IV injection is currently the predominant method for administering AAV, with most FDA-approved AAV therapies using this route. Both HA and HB have conducted a considerable number of preclinical animal experiments (including mouse models and large animal models) as well as clinical trials.

Early studies for gene therapy for HB with AAV2 focused on delivery to skeletal muscle, both in animal models (mice and dogs) and humans.[40,41] More recent clinical trials of gene transfer to skeletal muscle have used AAV serotype 1 (AAV1) vectors due to their superior transduction capacity in myocytes.[42,43] Potential complications of gene transfer to skeletal muscle from an immune response against hF9 could occur in some situations; thus, more research on HB, including clinical trials, has shifted to hepatic gene transfer.[44,45] This study used an AAV serotype 8 vector (AAV8), a serotype derived from rhesus macaques that has greater liver specificity than AAV2.[46] Additionally, the prevalence of neutralizing antibodies against AAV8 is lower than that against AAV2 in the human population, allowing more patients to be treated with AAV8 potentially.[47,48] Expression of hF9 in mice and NHPs was elevated with self-complementary AAV (scAAV).[49,50] The clinical trial of hepatic gene therapy for HB used a scAAV8 vector delivered via peripheral vein injection, which allowed F9 activity to persist at around 2-5% of normal.[51] The latest clinical trial in China used a novel, engineered, liver-tropic AAV843 expressing a hyperactive Padua F9 protein, which means FIX:C reached a mean of 36.9 IU/dL, demonstrating fairly therapeutic effects.[52,53] and one of the patients underwent

a right total knee arthroplasty successfully on day 479 after vector infusion without F9 concentrate infusion.[54] Another clinical study showed that the phase 3 BENEGENE-2 trial of Fidanacogene Elaparvovec led to reduced bleeding and stable factor IX expression, particularly as it represented an important alternative FIX-R338L/FIX-Padua AAV5 strategy.[55] Great strides have already been made in clinical trials for AAV-mediated gene therapy for HB. Earlier intramuscular studies provided proof of concept and safety data, while liver-directed gene delivery has shown greater success, though it can still be limited by both NAB and anti-capsid CTL responses.

Given the success AAV has shown as a vector for the treatment of HB, it is logical that several approaches have also attempted to use it for HA.[56] When considering AAV-mediated delivery of F8, the most pressing concerns were packaging capacity and AAV immunogenicity. Early studies over the past 10 years on gene therapy for HA with AAV focused on HA animal models (such as mice). At first, 10^{10-11} AAV/BDD-hF8 particles were injected intravenously into C57BL/6 and NOD/scid mice. All C57BL/6 mice tested developed anti-hF8 antibodies. In contrast, NOD/scid mice expressed hF8, reaching 27% of normal human plasma levels.[57] Then, AAV8-β-actin-canine F8 (cF8), AAV-ApoE-hAAT-hF8-BDD and AAV-ApoE-hAAT-rat F8 (rF8)-BDD were developed to express F8 in HA mice achieving therapeutic F8 levels.[58,59] Due to the success of mouse model research, recent studies have focused on preclinical studies in large animals (such as dogs and NHPs) and phase I/II clinical trials. In the NHP experiments, AAVhu37-F8-BDD was administered intravenously at a dose of 1.2×10^{13} genome copy/kg into five macaques; average hF8 expression was 20.2±5.0% of normal.[60] And the AAV integration profiles were polyclonal, evenly distributed across the genome, and showed a slight bias toward regions of open chromatin and actively transcribed genes, with no enrichment in cancer-associated genes.[61] Similar therapeutic effects and integration characteristics were also observed in the AAV gene therapy for hemophilia dogs.[62] Valoctocogene roxaparvovec (AAV5-hF8-SQ) is an adeno-associated virus 5 (AAV5)–based gene-therapy vector containing a coagulation factor VIII (F8) complementary DNA under the control of a liver-selective promoter. The efficacy and safety of the therapy were previously evaluated in men with severe HA in a phase I and II dose-escalation study.[63-65] There was an open-label, single-group, multicenter, phase III study to evaluate the efficacy and safety of Valoctocogene roxaparvovec in men with severe HA, which showed that the mean F8 activity level at weeks 49 through 52 had increased by 41.9 IU per deciliter, with the longest follow-up period up to 261.1 weeks.[66-69] Other important AAV-F8 programs have also undergone multiyear follow-up, including giroctocogene fitelparvovec[70] and multiyear follow-up data for SPK-8011.[71,72] More clinical studies about AAV-mediated IV delivery gene therapy were summarized in Table 2. Numerous clinical studies of AAV-delivered F8 gene therapy have demonstrated therapeutic F8 production and significant reductions in bleeding. We look forward to learning more about the long-term durability and safety of the treatment as we continue to follow the study participants.

LV-mediated gene transfer approach

LV may represent a complementary strategy for IV-directed gene therapy, for the following reasons: (i) low occurrence or feasible overcoming of immune barriers in humans, since the worldwide prevalence of HIV infection is estimated at 0.8%; (ii) efficient integration of LV in the host cells' genome may be preferred for lifelong maintenance of the therapeutic transgene and potentially allows treatment of pediatric patients without the need for vector re-administration; (iii) larger packaging capacity may make LV better suited for transferring F8 expression cassettes. The absence of prior clinical testing of systemic administration, manufacturing hurdles, and concerns about insertional mutagenesis have, until now, hindered preclinical development of in vivo LV gene therapy directed to the liver.

The intravenous gene therapy approach of LV was first validated in HB experiments. Brown et al. had previously shown that IV administration of LV results in efficient, long-term gene transfer to the liver and achieves phenotypic correction of HB in mice and dogs.[3,73,74] More recently, Milani et al. generated allo-antigen-free and phagocytosis-shielded (CD47hi) LV that allowed supra-normal activity of a human coagulation F9 transgene in NHPs, without evidence of acute toxicity and clonal expansion of transduced cells.[75,76] Meanwhile, IV therapy using LV carrying the F8 gene was evaluated in animal models, showing long-term F8 activity and restoration of hemostasis following IV administration to newborn and adult mice, and normal-range human F8 activity in NHPs.[77] Stein et .al. engineered a feline immunodeficiency virus (FIV)-based LV pseudotyped with the baculovirus GP64 envelope glycoprotein to mediate efficient gene transfer to mouse hepatocytes, and reported that LV IV administration conferred sustained F8 expression in HA mice for several months.[78-80] In addition, Staber et .al. demonstrated the development of a vector system for delivery and therapeutic expression of F8 protein from an optimized cF8 cDNA to achieve safe, long-term expression in hepatocytes. This proof-of-principle study in a relevant small-animal model paves the way for preclinical studies in a canine model of HA.[81]Modified F8 gene constructs were described: LV-F8-N6[82] and LV-F8-N6 replacer with a novel 17-aa peptide (LV-F8-V3),[83] carrying the spleen focus-forming virus (SFFV) promoter (equivalent to 4×10^{7}-1×10^{8} transducing units per mouse), injected into the superficial temporal vein. Shorter F8 constructs that can be more readily accommodated in viral vectors may increase therapeutic efficacy and enable effective gene therapy for HA.

It has been shown that the natural source of most F8 production is endothelial cells,[24] Gene transfer of LV expressing F8 from liver endothelial cells has been proposed, and some encouraging results have been reported in HA mice treated as adults,[84,14] Gong et al. developed an LV-mediated F8-BDD transgene with an endothelial-specific promoter to enable F8 protein expression in endothelial cells, especially liver endothelial cells.[85] However, the stability and turnover of these cells, both during postnatal liver growth and in homeostasis in adulthood,, remain only partially understood.[86]

Table 2. Clinical trials about AAV-mediated i.v. gene therapy on hemophilia.

Sponsor	Vector	Manufacturing	N participants enrolled	Dose (vg/kg)	Appox. Mean activity	Follow-up (Years) / Durability	ABR	Phase	Status	Clinicaltrials.gov Identifier
FIX										
St. Jude/ UCL	AAV8-FIX	Mammalian	10	2×10^{11} 6×10^{11} 2×10^{12}	1.9% 2.3% 5.1%	8/stable	2	I/II	Active, not recruiting	NCT00979238
Spark/ Pfizer	SPK-9001 (SPK100-FIX-R338L)	Mammalian	15	5×10^{11}	33.7%	3/stable	0.4	I-III	Completed	NCT02484092
Pfizer	PF-06838435	Mammalian	45	5×10^{11}	26.9%	1.25	1.28	III	Active, not recruiting	NCT03861273
Shire	BAX335 (AAV8-FIX-R338L)	NA	6	2×10^{11} 1×10^{12} 3×10^{12}	3.5% 12% 45% (transient)	1	NA	I/II	Active, not recruiting	NCT01687608
uniQure	AMT-060 (AAV5-FIX)	Insect	10	5×10^{12} 2×10^{13}	4.9% 7.4%	4/stable	0.9	I/II	Completed	NCT02396342
uniQure	AMT-061 (AAV5-FIX-R338L)	Insect	54	2×10^{13}	37%	1.5	0.8	III	Completed	NCT03569891
uniQure	AMT-061 (AAV5-FIX-R338L)	Insect	3	2×10^{13}	31%	6 wk	NA	II	Completed	NCT03489291
Ultragenyx	DTX101 (AAVrh10-FIX)	NA	6	1.6×10^{12} 5×10^{12}	3-8%	1	NA	I/II	Terminated	NCT02618915
Freeline	FLT-180a (AAVS3-FIX-R338L)	Mammalian	6	7.7×10^{11} progressive increased	NA	1	NA	I/II	Terminated	NCT05164471
Freeline	FLT-180a (AAVS3-FIX-R338L)	Mammalian	10	6×10^{11} 1×10^{12} 1.3×10^{12} 2×10^{12}	23-156%	26 wk	0- 2.17 5	I/II	Terminated	NCT03369444 NCT03641703
Sangamo	SB-FIX (AAV6-FIX)	Insect	1	NA	NA	3	NA	I	Terminated	NCT02695160
FVIII										
BioMarin	BMN 270 (AAV5-F8-BDD)	Insect	1 1 6 7	6×10^{12} 2×10^{13} 4×10^{13} 6×10^{13}	<1% 2% 23.2% 52.3%	>1 >1 3/declining expression 4/ declining expression	NA NA 0.5 1.3	I-III	Completed	NCT02576795
BioMarin	BMN 270 (AAV5-F8-BDD)	Insect	144	6×10^{13}	22%	2	NA	III	Completed	NCT03370913
Spark/ Roche	SPK-8016 (AAV-F8-BDD)	Insect	4	5×10^{11}	NA	1	NA	I/II	Completed	NCT03734588
Spark/ Roche	SPK-8011 (AAV-F8-BDD)	Insect	2 3 11 9	5×10^{11} 1×10^{12} 1.5×10^{12} 2×10^{12}	11.5% 20.0% 55.1% 38.7%	1	NA	I/II	Completed	NCT03003533 NCT03876301
Spark/ Roche	SPK-8011 (AAV-F8-BDD)	Insect	12	5×10^{11} 1×10^{12} 2×10^{12}	13% 15% 30%	2.5-3.3/ stable 2-2.5/ stable 1-1.5/ unknown	0.2 1.7 1.7	I/II	Completed	NA
UCL	AAV2/8-HLP-FVIII-V3	Mammalian	3	6×10^{11} 2×10^{12} 6×10^{12}	8-64%	about 1	5	I/II	Active, not recruiting	NCT03001830
Sangamo/ Pfizer	SB-525 (AAV2/6-F8-BDD)	Insect	13	9×10^{11} 2×10^{12} 1×10^{13} 3×10^{13}	NA NA NA 30-250%/ 20-160%	0.6-1.2/un-known	NA	II	Completed	NCT03061201
Sangamo/ Pfizer	SB-525 (AAV2/6-F8-BDD)	Insect	76	NA	NA	>1	NA	III	Active, not recruiting	NCT04370054
Shire	SHP654/BAX88 8 (AAV8-F8-BDD)	Mammalian	21	2×10^{12} 6×10^{12} 1.2×10^{13}	NA	5	NA	I/II	Completed	NCT03370172
Ultragenyx/ Bayer	BAY 2599023/ DTX201 (AAVhu37-F8-BDD)	Mammalian	11	5×10^{12} 1×10^{13} 2×10^{13}	5-20% 8-40% NA	about 1	NA	I/II	Active, not recruiting	NCT03588299

In vivo approach to gene therapy with intraosseous injection for hemophilia

The feasibility of in vivo gene transfer via direct intraosseous (IO) injection of RV and LV into mice was demonstrated ten years ago.[87,88] In addition, in vitro manipulation of stem cells and preconditioning of the subject is not required to achieve a therapeutic benefit. Therefore, this approach may provide a novel treatment for HA. The IO delivery of E-F8-LV using a ubiquitous EF1α promoter initially generated therapeutic levels of F8; however, robust anti-F8 antibody responses ensued, neutralizing functional F8 activity in circulation.[89] Platelets are released from BM megakaryocyte precursors into the circulation, where they play a crucial role in maintaining hemostasis.[90] Platelets may be an ideal vehicle for ectopic F8 expression for several reasons. Miao et al. demonstrated that a single IO injection of LVs can produce long-term stable expression of hF8 in platelets and correct the hemophilia phenotype for at least 5 months after treatment.[91]

Preconditioning before Gene Therapy for Hemophilia

A potential limitation of *in vivo* gene therapy protocols is the induction of virus vector-specific immune responses, which may decrease the vector transduction efficiency and eliminate transduced cells.[92,39,93,94] To reduce immune clearance of viral vectors in the host immune system, researchers have employed various doses and intensities of inhibitors for preconditioning before treatment.

HSC transplantation typically employs relatively intensive immunosuppressive regimens. Cytoreductive therapy can suppress the patient's immune system, reducing the attack on transplanted stem cells and the risk of graft-versus-host disease, and facilitating the implantation of donor cells. The pretreatment protocols for HSC transplantation were classified by the Center for International Blood and Marrow Transplant Research (CIBMTR) as myeloablative conditioning (MAC), nonmyeloablative conditioning (NMAC), and reduced-intensity conditioning (RIC).[95,96] MAC was Alkylating agents (cyclophosphamide, cytarabine, etoposide, and melphalan, et al.) and/or total body irradiation (TBI). The commonly used NMAC regimen consisted of 2 Gy TBI combined with fludarabine or cyclophosphamide, which produced the lowest reduction in blood cell counts. Unlike the MAC regimen, the RIC regimen uses lower doses of the alkylating agents (busulfan, cytarabine, and melphalan) or TBI (usually reduced to less than 70% of the former). The RIC regimen can cause reversible BM suppression (usually within 28 days after HSCT); however, the patient's own hematopoietic function cannot be restored after MAC.

HSC transplantation was mostly used with MAC and high-dose TBI (more than 800 cGy),[7,8,10,97-99,35] which was called the myeloablative regimen, and with NMAC and low-dose TBI (220, 440, 660 cGy),[7,10,99] which was called the nonmyeloablative regimen. There was also the RIC applied with (i) 120 mg/m^2 fludarabine and 120 mg/m^2 melphalan,[11,100] (ii) 30 or 50 mg/kg busulfan via intraperitoneal injection on day -1,[13,14] (iii) 25 or 12.5 mg/kg busulfan per day on days -2 and -1 and 10 mg/kg Anti-(murine)-thymocyte globulin (ATG) on day -2(HSC transplantation occurred at day 0).[98] There was no need for pretreatment in MSC therapy. iPSCs therapy preferred to use cyclosporine A (210 mg/L, in drinking water) starting 3 days before transplantation.[33,38]

In the early years, the AAV IV injection for gene therapy mostly involved the use of low-dose immunosuppressants, like RIC (100 mg/body/day cyclophosphamide and 12.5 mg/body/day tacrolimus after vector injection)[58] and glucocorticoids, such as prophylactic prednisone treatment (1 mg/kg per day sustaining 1 week)[52] or (40 mg per day, tapering from week 3 to week 17 or longer)[63] or rituximab and methylprednisolone without exact dosage.[61] In recent years, both animal experiments and clinical trials have increasingly advocated against pre-treatment with immunosuppressive methods.[64] Per-protocol prophylactic glucocorticoids were administered following ALT elevation.[65] Treatment with oral prednisone or prednisolone was started at a dose of 60 mg per day and was tapered over a period of at least 8 weeks.[66]

The immunosuppression of LV IV injection for gene therapy had various strategies. Firstly, participants were received rituximab and cyclophosphamide with different doses (i) 250 mg/m^2, 2 doses at 3 weekly intervals;[82,101,102] (ii) 250 mg/m^2, intravenously at 4 weekly intervals, total of 4 bolus infusions and 300 mg/m^2 slow intravenous infusions every 15 days, total of 8 doses over 4 months.[83] Secondly, participants were pretreated with a corticosteroid (Prednisone, 1 mg/kg oral, or Dexamethasone, 0.2/0.3 mg/kg IV) and an antihistamine (Benadryl, 1 mg/kg i.m., Famotidine, 0.5 mg/kg i.m., or dexchlorpheniramine, 4 mg/kg IV) before vector infusion.[74,76] Only corticosteroid (methylprednisolone, 10 mg/kg/day) was administered intramuscularly as an immunosuppression regimen from day -1 to day 7 or day -3 to day 9 for NHPs (LV administration occurred at day 0).[77]

Immunosuppression significantly affected the efficacy of stem cell transplantation and direct IV gene therapy. An excessively high dose of TBI increased the risk of severe complications for the participants. The low dose of immunosuppression resulted in poor therapeutic effects of transplanted cells and vector administration. Therefore, the appropriate pretreatment solution remains one of the challenges that need to be addressed in the future.

Selection of the Treatment Window Period on Gene Therapy Applications

Ex vivo manipulation and patient conditioning before transplantation are major hurdles that could be overcome by an in vivo approach. In vivo gene delivery to hematopoietic stem and progenitor cells (HSPCs) after systemic LV administration is enabled by the substantial trafficking of these cells from the liver to the BM in newborn mice. So, it is worth discussing and exploring the treatment window period for in vivo gene therapy.

Milani et al. identified a unique window of opportunity in early postnatal life, when high numbers of circulating HSPCs (cHSPCs) were trafficking from residual hematopoietic niches to the BM. The corresponding results were published in Nature in May 2025.[103] To assess the feasibility of in vivo LV gene transfer into HSPCs, they examined the spatiotemporal evolution of the hematopoietic system in C57BL/6 mice. The findings demonstrated that phagocytosis shielding enhanced LV gene transfer into HSPCs. Given the unique window of opportunity for the genetic engineering of HSCs in newborns, in vivo HSPC gene transfer holds strong translational potential across multiple diseases. However, treating HA at or before birth with cells or viruses lacks a clinical safety record to support this approach.

Conclusions

Collectively, cell-based therapy has attracted considerable attention in HA treatment due to its high specificity and programmability, while *in vivo* gene therapy has attracted attention due to its safety and simple clinical procedures. However, the clinical application of cell-based therapy is limited by several challenges, including rapid degradation due to poor cellular uptake, damage to the body caused by strong immunosuppression, and the persistence of therapeutic effects. The problems with *in vivo* gene therapy that limit its clinical application include potential immunogenicity, off-target toxicity, germline alteration, and persistence of therapeutic effects.

There are several critical obstacles to be overcome to realize their clinical potential fully: (i) Under the condition that ethics permits and the procedures are safe, would the treatments be carried out during the perinatal period or not? Only with sufficient and corresponding data from animal experiments and clinical trials can this question be answered. (ii) Whether cell-based therapy or *in vivo* gene therapy, to probe a 'one-and-done' treatment for hemophilia has always been the vital direction we need to strive for.

Availability of Data and Materials

The datasets used and/or analyzed during the current study are available from the corresponding author on reasonable request.

Competing Interests

The authors declare that they have no competing interests.

Funding

Jie Gong acknowledges support from the Doctoral Start-up Foundation of Inner Mongolia Agricultural University (Grant No. NDYB2024-20) and the Natural Science Foundation of Sichuan Province, China (Grant No.2024NSFSC1667).

Author Contributions

Jie Gong conceptualized and designed the review and acquired the funding.
Jie Gong and QiuYi Li wrote the original draft.
Hong Du and Rui Yang revised the manuscript.
All authors have approved the final article.

References

1. Bhardwaj R, Rath G, Goyal AK. Advancement in the treatment of haemophilia. Int J Biol Macromol. 2018; 118:289-295. doi:10.1016/j.ijbiomac.2018.06.084
2. Marchesini E, Morfini M, Valentino L. Recent Advances in the Treatment of Hemophilia: A Review. Biol: Targets Ther. 2021; 15:221-235. doi:10.2147/btt.S252580
3. Brown BD, Cantore A, Annoni A, Sergi LS, Lombardo A, Della Valle P, D'Angelo A, Naldini L. A microRNA-regulated lentiviral vector mediates stable correction of hemophilia B mice. Blood. 2007;110(13):4144-4152. doi:10.1182/blood-2007-03-078493
4. Fomin ME, Togarrati PP, Muench MO. Progress and challenges in the development of a cell-based therapy for hemophilia A. J Thromb Haemost. 2014;12(12):1954-1965. doi:10.1111/jth.12750
5. Gong J, Wang H-L, Chang L-J. Molecular therapeutics of Hemophilia A and B. Expert Rev Hematol. 2022;431-441. doi :10.1080/17474086.2022.2075339
6. Shi Q. Platelet-Targeted Gene Therapy for Hemophilia. Mol Ther Methods Clin Dev. 2018;9:100-108. doi:10.1016/j.omtm.2018.01.011
7. Zhang G, Shi Q, Fahs SA, Kuether EL, Walsh CE, Montgomery RR. Factor IX ectopically expressed in platelets can be stored in α-granules and corrects the phenotype of hemophilia B mice. Blood. 2010;116 (8):1235-1243. doi:10.1182/blood-2009-11-255612
8. Chen Y, Schroeder JA, Kuether EL, Zhang G, Shi Q. Platelet Gene Therapy by Lentiviral Gene Delivery to Hematopoietic Stem Cells Restores Hemostasis and Induces Humoral Immune Tolerance in FIXnull Mice. Mol Ther. 2014; 22 (1):169-177. doi:10.1038/mt.2013.197
9. Kurre P, Anandakumar P, Kiem HP. Rapid 1-hour transduction of whole bone marrow leads to long-term repopulation of murine recipients with lentivirus-modified hematopoietic stem cells. Gene Therapy. 2006;13(4):369-373. doi:10.1038/sj.gt.3302659
10. Shi Q, Wilcox DA, Fahs SA, Fang J, Johnson BD, Du LM, Desai D, Montgomery RR. Lentivirus-mediated platelet-derived factor VIII gene therapy in murine haemophilia A. J Thromb Haemost. 2007;5(2):352-361. doi:10.1111/j.1538-7836.2007.02346.x
11. Eapen M, Malec LM, Armant MA, Johnson BD, Shi Q, Xu H, Du LM, Jerkins JH, Duffy LJ, Bushman FD, Lee C, Petrichenko A, Hematti P, Brazauskas R, Jobe SM, Hari PN, Wilcox DA. Platelet-Targeted Gene Therapy for Hemophilia A with Inhibitor History. N Engl J Med. 2025;392(4):412-414. doi:10.1056/NEJMc2415164
12. Srivastava A, Abraham A, Aboobacker F, Singh G, Geevar T, Kulkarni U, Selvarajan S, Korula A, Dave RG, Shankar M, Singh AS, Jeba A, Kumaar N, Benjamin C, Lakshmi KM,

Srivastava VM, Shaji RV, Nair SC, Brown HC, Denning G, Lollar P, Doering CB, Spencer T. Lentiviral Gene Therapy with CD34+ Hematopoietic Cells for Hemophilia A. N Engl J Med. 2025;392(5):450-457. doi:doi:10.1056/NEJMoa2410597
13. Doering CB, Denning G, Shields JE, Fine EJ, Parker ET, Srivastava A, Lollar P, Spencer HT. Preclinical development of a hematopoietic stem and progenitor cell bioengineered Factor VIII lentiviral vector gene therapy for Hemophilia A. Hum Gene Ther. 2018;29(10):1183-1201. doi:10.1089/hum.2018.137
14. Merlin S, Fama R, Borroni E, Zanolini D, Bruscaggin V, Zucchelli S, Follenzi A. FVIII expression by its native promoter sustains long-term correction avoiding immune response in hemophilic mice. Blood Adv. 2019;3(5):825-838. doi:10.1182/bloodadvances.2018027979
15. Ohmori T, Mizukami H, Katakai Y, Kawai S, Nakamura H, Inoue M, Shu T, Sugimoto H, Sakata Y. Safety of intra-articular transplantation of lentivirally transduced mesenchymal stromal cells for haemophilic arthropathy in a non-human primate. Int J Hematol. 2018;108(3):239-245. doi:10.1007/s12185-018-2465-8
16. Coutu DL, Cuerquis J, El Ayoubi R, Forner K-A, Roy R, François M, Griffith M, Lillicrap D, Yousefi A-M, Blostein MD, Galipeau J. Hierarchical scaffold design for mesenchymal stem cell-based gene therapy of hemophilia B. Biomaterials. 2011;32(1):295-305. doi:10.1016/j.biomaterials.2010.08.094
17. Dodd M, Marquez-Curtis L, Janowska-Wieczorek A, Hortelano G. Sustained expression of coagulation factor IX by modified cord blood-derived mesenchymal stromal cells. J Gene Med . 2014;16(5-6):131-142. doi:10.1002/jgm.2769
18. Kashiwakura Y, Ohmori T, Mimuro J, Yasumoto A, Ishiwata A, Sakata A, Madoiwa S, Inoue M, Hasegawa M, Ozawa K, Sakata Y. Intra-articular injection of mesenchymal stem cells expressing coagulation factor ameliorates hemophilic arthropathy in factor VIII-deficient mice. J Thromb Haemost. 2012;10(9):1802-1813. doi:10.1111/j.1538-7836.2012.04851.x
19. Porada CD, Sanada C, Kuo C-J, Colletti E, Mandeville W, Hasenau J, Zanjani ED, Moot R, Doering C, Spencer HT, Almeida-Porada G. Phenotypic correction of hemophilia A in sheep by postnatal intraperitoneal transplantation of FVIII-expressing MSC. Exp Hematol. 2011;39(12):1124-1135. doi:10.1016/j.exphem.2011.09.001
20. Wang Q, Gong X, Gong Z, Ren X, Ren Z, Huang S, Zeng Y. The Mesenchymal Stem Cells Derived from Transgenic Mice Carrying Human Coagulation Factor VIII Can Correct Phenotype in Hemophilia A Mice. J Genet Genomics. 2013;40(12):617-628. doi:10.1016/j.jgg.2013.11.002
21. Li S-J, Luo Y, Zhang L-M, Yang W, Zhang G-G. Targeted introduction and effective expression of hFIX at the AAVS1 locus in mesenchymal stem cells. Mol Med Rep. 2017;15(3):1313-1318. doi:10.3892/mmr.2017.6131
22. Sanada C, Kuo CJ, Colletti EJ, Soland M, Mokhtari S, Knovich MA, Owen J, Zanjani ED, Porada CD, Almeida-Porada G. Mesenchymal stem cells contribute to endogenous FVIII:c production. J Cell Physiol. 2013;228 (5):1010-1016. doi:10.1002/jcp.24247
23. Najimi M, Khuu DN, Lysy PA, Jazouli N, Abarca J, Sempoux C, Sokal EM. Adult-Derived Human Liver Mesenchymal-Like Cells as a Potential Progenitor Reservoir of Hepatocytes? Cell Transplant. 2017;16(7):717-728. doi:10.3727/000000007783465154
24. Follenzi A, Benten D, Novikoff P, Faulkner L, Raut S, Gupta S. Transplanted endothelial cells repopulate the liver endothelium and correct the phenotype of hemophilia A mice. J Clin Invest. 2008;8:935-945. doi:10.1172/jci32748
25. Lin Y, Weisdorf DJ, Solovey A, Hebbel RP. Origins of circulating endothelial cells and endothelial outgrowth from blood. J Clin Invest. 2000; 105 (1):71-77. doi:10.1172/jci8071
26. Lin Y, Chang L, Solovey A, Healey JF, Lollar P, Hebbel RP. Use of blood outgrowth endothelial cells for gene therapy for hemophilia A. Blood. 2002;99(2):457-462. doi:10.1182/blood.V99.2.457
27. Ozelo MC, Vidal B, Brown C, Notley C, Hegadorn C, Webster S, Harpell L, Ahlin J, Winterborn A, Handforth J, Arruda VR, Hough C, Lillicrap D. Omental implantation of BOECs in hemophilia dogs results in circulating FVIII antigen and a complex immune response. Blood. 2014;123 (26):4045-4053. doi:10.1182/blood-2013-12-545780
28. Miyata T, Tatsumi K, Sugimoto M, Lillicrap D, Shima M, Ohashi K, Okano T, Matsui H. A novel cell-sheet technology that achieves durable factor VIII delivery in a mouse model of hemophilia A. PLoS ONE. 2013;8(12):e83280. doi:10.1371/journal.pone.0083280
29. Olgasi C, Borsotti C, Merlin S, Bergmann T, Bittorf P, Adewoye AB, Wragg N, Patterson K, Calabria A, Benedicenti F, Cucci A, Borchiellini A, Pollio B, Montini E, Mazzuca DM, Zierau M, Stolzing A, Toleikis PM, Braspenning J, Follenzi A. Efficient and safe correction of hemophilia A by lentiviral vector-transduced BOECs in an implantable device. Mol Ther Methods Clin Dev. 2021;23:551-566. doi:10.1016/j.omtm.2021.10.015
30. Mitani S, Hosoda C, Onodera Y, Takabayashi Y, Sakata A, Shima M, Tatsumi K. Efficient generation of liver sinusoidal endothelial-like cells secreting coagulation factor VIII from human induced pluripotent stem cells. Mol Ther Methods Clin Dev. 2024;32(4):101355. doi:10.1016/j.omtm.2024.101355
31. Xu D, Alipio Z, Fink LM, Adcock DM, Yang J, Ward DC, Ma Y. Phenotypic correction of murine hemophilia A using an iPS cell-based therapy. Proc Natl Acad Sci. 2009; USA 106 (3):808-813. doi:10.1073/pnas.0812090106
32. Gao K, Kumar P, Cortez-Toledo E, Hao D, Reynaga L, Rose M, Wang C, Farmer D, Nolta J, Zhou J, Zhou P, Wang A. Potential long-term treatment of hemophilia A by neonatal co-transplantation of cord blood-derived endothelial colony-forming cells and placental mesenchymal stromal cells. Stem Cell Res Ther. 2019;10(1):34. doi:10.1186/s13287-019-1138-8
33. Rose M, Gao K, Cortez-Toledo E, Agu E, Hyllen AA, Conroy K, Pan G, Nolta JA, Wang A, Zhou P. Endothelial cells derived from patients' induced pluripotent stem cells for sustained factor VIII delivery and the treatment of hemophilia A. Stem Cells Transl Med. 2020;9(6):686-696. doi:10.1002/sctm.19-0261
34. Yakura Y, Ishihara C, Kurosaki H, Kazuki Y, Komatsu N, Okada Y, Doi T, Takeya H, Oshimura M. An induced pluripotent stem cell-mediated and integration-free factor VIII expression system. Biochem Biophys Res Commun. 203; 431(2):336-341. doi:10.1016/j.bbrc.2012.12.096
35. Wang D, Zhang G, Gu J, Shao X, Dai Y, Li J, Pan X, Yao S, Xu A, Jin Y, Huang J, Shi Q, Zhu J, Xi X, Chen Z, Chen S. In vivo generated hematopoietic stem cells from genome

edited induced pluripotent stem cells are functional in platelet-targeted gene therapy of murine hemophilia A. Haematologica. 2020;105 (4):e175-e179. doi:10.3324/haematol.2019.219089
36. Sung JJ, Park CY, Leem JW, Cho MS, Kim DW. Restoration of FVIII expression by targeted gene insertion in the FVIII locus in hemophilia A patient-derived iPSCs. Exp Mol Med. 2019;51(4):1-9. doi:10.1038/s12276-019-0243-1
37. Park CY, Sung JJ, Cho SR, Kim J, Kim DW. Universal Correction of Blood Coagulation Factor VIII in Patient-Derived Induced Pluripotent Stem Cells Using CRISPR/Cas9. Stem Cell Rep. 2019;12(6):1242-1249. doi:10.1016/j.stemcr.2019.04.016
38. Kim DH, Choi SH, Sung JJ, Kim S, Yi H, Park S, Park CW, Oh YW, Lee J, Kim DS, Kim JH, Park CY, Kim DW. Long-term correction of hemophilia A via integration of a functionally enhanced FVIII gene into the AAVS1 locus by nickase in patient-derived iPSCs. Exp Mol Med. 2025;57(1):184-192. doi:10.1038/s12276-024-01375-z
39. Chen Jh, Zhan Lj, Lv Cm, Teng Jb, Cao Cy. Advances and Challenges in Adeno-Associated Virus Gene Therapy Applications of Localized Delivery Strategies. Curr Med Sci. 2025. doi: 10.1007/s11596-025-00084-6
40. Herzog RW, Hagstrom JN, Kung S-H, Tai SJ, Wilson JM, Fisher KJ, High KA. Stable gene transfer and expression of human blood coagulation factor IX after intramuscular injection of recombinant adeno-associated virus. Proc Natl Acad Sci USA. 1997;94(11):5804-5809. doi:10.1073/pnas.94.11.5804
41. Fields PA, Kowalczyk DW, Arruda VR, Armstrong E, McCleland ML, Hagstrom JN, Pasi KJ, Ertl HCJ, Herzog RW, High KA. Role of Vector in Activation of T Cell Subsets in Immune Responses against the Secreted Transgene Product Factor IX. Mol Ther. 2000;1(3):225-235. doi:10.1006/mthe.2000.0032
42. Kay MA, Manno CS, Ragni MV, Larson PJ, Couto LB, McClelland A, Glader B, Chew AJ, J Tai S, Herzog RW, Arruda V, Johnson F, Scallan C, Skarsgard E, Flake AW, High KA. Evidence for gene transfer and expression of factor IX in haemophilia B patients treated with an AAV vector. Nat Genet. 2000;24 (3):257-261. doi:10.1038/73464
43. Flotte TR, Trapnell BC, Humphries M, Carey B, Calcedo R, Rouhani F, Campbell-Thompson M, Yachnis AT, Sandhaus RA, McElvaney NG, Mueller C, Messina LM, Wilson JM, Brantly M, Knop DR, Ye G-j, Chulay JD. Phase 2 Clinical Trial of a Recombinant Adeno-Associated Viral Vector Expressing α1-Antitrypsin: Interim Results. Hum Gene Ther . 2011;22(10):1239-1247. doi:10.1089/hum.2011.053
44. Arruda VR, Stedman HH, Haurigot V, Buchlis G, Baila S, Favaro P, Chen Y, Franck HG, Zhou S, Wright JF, Couto LB, Jiang H, Pierce GF, Bellinger DA, Mingozzi F, Nichols TC, High KA. Peripheral transvenular delivery of adeno-associated viral vectors to skeletal muscle as a novel therapy for hemophilia B. Blood. 2010;115(23):4678-4688. doi:10.1182/blood-2009-12-261156
45. Finn JD, Nichols TC, Svoronos N, Merricks EP, Bellenger DA, Zhou S, Simioni P, High KA, Arruda VR. The efficacy and the risk of immunogenicity of FIX Padua (R338L) in hemophilia B dogs treated by AAV muscle gene therapy. Blood. 2012;120(23):4521-4523. doi:10.1182/blood-2012-06-440123
46. Gao G-P, Alvira MR, Wang L, Calcedo R, Johnston J, Wilson JM. Novel adeno-associated viruses from rhesus monkeys as vectors for human gene therapy. Proc Natl Acad Sci USA. 2002;99(18):11854-11859. doi:10.1073/pnas.182412299
47. Calcedo R, Vandenberghe Luk H, Gao G, Lin J, Wilson James M. Worldwide Epidemiology of Neutralizing Antibodies to Adeno-Associated Viruses. J Infect Dis. 2009;199(3):381-390. doi:10.1086/595830
48. Boutin S, Monteilhet V, Veron P, Leborgne C, Benveniste O, Montus MF, Masurier C. Prevalence of Serum IgG and Neutralizing Factors Against Adeno-Associated Virus (AAV) Types 1, 2, 5, 6, 8, and 9 in the Healthy Population: Implications for Gene Therapy Using AAV Vectors. Hum Gene Ther. 2010;21(6):704-712. doi:10.1089/hum.2009.182
49. Nathwani AC, Rosales C, McIntosh J, Rastegarlari G, Nathwani D, Raj D, Nawathe S, Waddington SN, Bronson R, Jackson S, Donahue RE, High KA, Mingozzi F, Ng CYC, Zhou J, Spence Y, McCarville MB, Valentine M, Allay J, Coleman J, Sleep S, Gray JT, Nienhuis AW, Davidoff AM. Long-term Safety and Efficacy Following Systemic Administration of a Self-complementary AAV Vector Encoding Human FIX Pseudotyped With Serotype 5 and 8 Capsid Proteins. Mol Ther. 2011;19(5):876-885. doi:10.1038/mt.2010.274
50. Chou SC, Huang CP, Su YH, Yu CH, Yang YL, Wang SC, Lin YH, Chen YT, Li JY, Chang YT, Chen SY, Lin SW. Preclinical Evaluation of the Systemic Safety, Efficacy, and Biodistribution of a Recombinant AAV8 Vector Expressing FIX-TripleL in Hemophilia B Mice: Implications for Human Gene Therapy. Int J Mol Sci. 2025;26(13):6073. doi:10.3390/ijms26136073
51. Nathwani AC, Tuddenham EGD, Rangarajan S, Rosales C, McIntosh J, Linch DC, Chowdary P, Riddell A, Pie AJ, Harrington C, O'Beirne J, Smith K, Pasi J, Glader B, Rustagi P, Ng CYC, Kay MA, Zhou J, Spence Y, Morton CL, Allay J, Coleman J, Sleep S, Cunningham JM, Srivastava D, Basner-Tschakarjan E, Mingozzi F, High KA, Gray JT, Reiss UM, Nienhuis AW, Davidoff AM. Adenovirus-Associated Virus Vector–Mediated Gene Transfer in Hemophilia B. N Engl J Med. 2011;365(25):2357-2365. doi:10.1056/NEJMoa1108046
52. Xue F, Li H, Wu X, Liu W, Zhang F, Tang D, Chen Y, Wang W, Chi Y, Zheng J, Du Z, Jiang W, Zhong C, Wei J, Zhu P, Fu R, Liu X, Chen L, Pei X, Sun J, Cheng T, Yang R, Xiao X, Zhang L. Safety and activity of an engineered, liver-tropic adeno-associated virus vector expressing a hyperactive Padua factor IX administered with prophylactic glucocorticoids in patients with haemophilia B: a single-centre, single-arm, phase 1, pilot trial. Lancet Haematol. 2022;9(7):e504-e513. doi:10.1016/s2352-3026(22)00113-2
53. Xue F, Ju M, Zhu T, Zhou Z, Sun J, Yang L, Yan Z, Zhou H, Du X, Zheng C, Zheng J, Wu X, Du Z, Jiang W, Yang C, Xiao X, Liu W, Yang R, Zhang L. Factor IX-Padua AAV gene therapy in hemophilia B: phases 1/2 and 3 trials. Nature Medicine. 2025;32(1):93-102. doi:10.1038/s41591-025-04012-y
54. Xue F, Wang P, Yuan Z, Shi C, Fang Y, Liu W, Wang Y, Xiao X, Yang R, George LA, Zhang L. Total Knee Arthroplasty after Gene Therapy for Hemophilia B. N Engl J Med. 2022;387(17):1622-1624. doi:10.1056/NEJMc2211173
55. Cuker A, Kavakli K, Frenzel L, Wang J-D, Astermark J, Cerqueira MH, Iorio A, Katsarou-Fasouli O, Klamroth R, Shapiro AD, Hermans C, Ishiguro A, Leavitt AD, Oldenburg

JB, Ozelo MC, Teitel J, Biondo F, Fang A, Fuiman J, McKay J, Sun P, Rasko JEJ, Rupon J. Gene Therapy with Fidanacogene Elaparvovec in Adults with Hemophilia B. New England Journal of Medicine. 2024;391(12):1108-1118. doi:10.1056/NEJMoa2302982
56. Herzog RW. Gene therapy for hemophilia. Front Biosci (Landmark Ed). 2015;20(3):556-603. doi:10.2741/4324
57. Chao H, Mao L, Bruce AT, Walsh CE. Sustained expression of human factor VIII in mice using a parvovirus-based vector. Blood. 2000;95(5):1594-1599. doi:10.1182/blood.V95.5.1594.005k34_1594_1599
58. Ishiwata A, Mimuro J, Kashiwakura Y, Niimura M, Takano K, Ohmori T, Madoiwa S, Mizukami H, Okada T, Naka H, Yoshioka A, Ozawa K, Sakata Y. Phenotype correction of hemophilia A mice with adeno-associated virus vectors carrying the B domain-deleted canine factor VIII gene. Thromb Res. 2006;118(5):627-635. doi:10.1016/j.thromres.2005.11.006
59. Zhang W, Mao J, Shen Y, Zhang G, Shao Y, Ruan Z, Wang Y, Wu W, Wang X, Zhu J, Chen S, Xiao W, Xi X. Evaluation of the activity levels of rat FVIII and human FVIII delivered by adeno-associated viral vectors both in vitro and in vivo. Blood Cells Mol Dis. 2018;73:47-54. doi:10.1016/j.bcmd.2018.09.004
60. Greig JA, Nordin JML, White JW, Wang Q, Bote E, Goode T, Calcedo R, Wadsworth S, Wang L, Wilson JM. Optimized Adeno-Associated Viral-Mediated Human Factor VIII Gene Therapy in Cynomolgus Macaques. Hum Gene Ther. 2018. doi: 10.1089/hum.2018.080
61. Russell CB, Vettermann C, Agarwal S, Witt E, Clark W, Arens J, Fronza R, Obrochta Moss KM, Kasprzyk T, Robinson TM, Tran H, Kenet G, Raheja P, Lester W, Eggan K, Zoog S. Recombinant Adeno-Associated Virus Integration Profiles in Nonhuman Primates and Gene Therapy Participants after Treatment with Valoctocogene Roxaparvovec. Hum Gene Ther. 2025;36(13-14):945-955. doi:10.1089/hum.2024.236
62. Nguyen GN, Everett JK, Kafle S, Roche AM, Raymond HE, Leiby J, Wood C, Assenmacher C-A, Merricks EP, Long CT, Kazazian HH, Nichols TC, Bushman FD, Sabatino DE. A long-term study of AAV gene therapy in dogs with hemophilia A identifies clonal expansions of transduced liver cells. Nat Biotechnol. 2020;39(1):47-55. doi:10.1038/s41587-020-0741-7
63. Rangarajan S, Walsh L, Lester W, Perry D, Madan B, Laffan M, Yu H, Vettermann C, Pierce GF, Wong WY, Pasi KJ. AAV5-Factor VIII Gene Transfer in Severe Hemophilia A. N Engl J Med. 2017;377(26):2519-2530. doi:10.1056/NEJMoa1708483
64. Pasi KJ, Rangarajan S, Mitchell N, Lester W, Symington E, Madan B, Laffan M, Russell CB, Li M, Pierce GF, Wong WY. Multiyear Follow-up of AAV5-hFVIII-SQ Gene Therapy for Hemophilia A. N Engl J Med. 2020;382(1):29-40. doi:10.1056/NEJMoa1908490
65. Pasi KJ, Laffan M, Rangarajan S, Robinson TM, Mitchell N, Lester W, Symington E, Madan B, Yang X, Kim B, Pierce GF, Wong WY. Persistence of haemostatic response following gene therapy with valoctocogene roxaparvovec in severe haemophilia A. Haemophilia. 2021;27(6):947-956. doi:10.1111/hae.14391
66. Ozelo MC, Mahlangu J, Pasi KJ, Giermasz A, Leavitt AD, Laffan M, Symington E, Quon DV, Wang J-D, Peerlinck K, Pipe SW, Madan B, Key NS, Pierce GF, O'Mahony B, Kaczmarek R, Henshaw J, Lawal A, Jayaram K, Huang M, Yang X, Wong WY, Kim B. Valoctocogene Roxaparvovec Gene Therapy for Hemophilia A. N Engl J Med. 2022;386(11):1013-1025. doi:10.1056/NEJMoa2113708
67. O'Mahony B, Dunn AL, Leavitt AD, Peyvandi F, Ozelo MC, Mahlangu J, Peerlinck K, Wang J-D, Lowe GC, Tan CW, Giermasz A, Tran H, Khoo T-L, Cockrell E, Pepperell D, Chambost H, López Fernández MF, Kazmi R, Majerus E, Skinner MW, Klamroth R, Quinn J, Yu H, Wong WY, Robinson TM, Pipe SW. Health-related quality of life following valoctocogene roxaparvovec gene therapy for severe hemophilia A in the phase 3 trial GENEr8-1. Journal of Thrombosis and Haemostasis. 2023;21(12):3450-3462. doi:10.1016/j.jtha.2023.08.032
68. Leavitt AD, Mahlangu J, Raheja P, Symington E, Quon DV, Giermasz A, López Fernández MF, Kenet G, Lowe G, Key NS, Millar CM, Pipe SW, Madan B, Chou S-C, Klamroth R, Mason J, Chambost H, Peyvandi F, Majerus E, Pepperell D, Rivat C, Yu H, Robinson TM, Ozelo MC. Efficacy, safety, and quality of life 4 years after valoctocogene roxaparvovec gene transfer for severe hemophilia A in the phase 3 GENEr8-1 trial. Research and Practice in Thrombosis and Haemostasis. 2024;8(8). doi:10.1016/j.rpth.2024.102615
69. Leavitt AD, Mahlangu J, Raheja P, Symington E, Quon DV, Giermasz A, Kenet G, Lowe G, Key NS, Millar CM, Pipe SW, Chou S-C, Klamroth R, Mason J, Chambost H, Peyvandi F, Majerus E, Pepperell D, Tan CW, Yu H, Chavele K-M, Ozelo MC. Durability of efficacy, safety, and quality of life 5 years after valoctocogene roxaparvovec gene transfer for severe hemophilia A: final phase 3 GENEr8-1 trial results. Research and Practice in Thrombosis and Haemostasis. 2026;10(3). doi:10.1016/j.rpth.2026.103416
70. Leavitt AD, Konkle BA, Stine KC, Visweshwar N, Harrington TJ, Giermasz A, Arkin S, Fang A, Plonski F, Yver A, Ganne F, Agathon D, Resa MdlA, Tseng L-J, Di Russo G, Cockroft BM, Cao L, Rupon J. Giroctocogene fitelparvovec gene therapy for severe hemophilia A: 104-week analysis of the phase 1/2 Alta study. Blood. 2024;143(9):796-806. doi:10.1182/blood.2022018971
71. Elkouby L, Armour SM, Toso R, DiPietro M, Davidson RJ, Nguyen GN, Willet M, Kutza S, Silverberg J, Frick J, Crosariol M, Wang Y, Wang C, High KA, Sabatino DE, Anguela XM. Preclinical assessment of an optimized AAV-FVIII vector in mice and non-human primates for the treatment of hemophilia A. Molecular Therapy - Methods & Clinical Development . 2022;24:20-29. doi:10.1016/j.omtm.2021.11.005
72. George LA, Monahan PE, Eyster ME, Sullivan SK, Ragni MV, Croteau SE, Rasko JEJ, Recht M, Samelson-Jones BJ, MacDougall A, Jaworski K, Noble R, Curran M, Kuranda K, Mingozzi F, Chang T, Reape KZ, Anguela XM, High KA. Multiyear Factor VIII Expression after AAV Gene Transfer for Hemophilia A. New England Journal of Medicine. 2021;385(21):1961-1973. doi:10.1056/NEJMoa2104205
73. Cantore A, Nair N, Della Valle P, Di Matteo M, Màtrai J, Sanvito F, Brombin C, Di Serio C, D'Angelo A, Chuah M, Naldini L, VandenDriessche T. Hyperfunctional coagulation factor IX improves the efficacy of gene therapy in hemophilic mice. Blood. 2021;120(23):4517-4520. doi:10.1182/blood-2012-05-432591
74. Cantore A, Ranzani M, Bartholomae CC, Volpin M, Valle

PD, Sanvito F, Sergi LS, Gallina P, Benedicenti F, Bellinger D, Raymer R, Merricks E, Bellintani F, Martin S, Doglioni C, D'Angelo A, VandenDriessche T, Chuah MK, Schmidt M, Nichols T, Montini E, Naldini L. Liver-directed lentiviral gene therapy in a dog model of hemophilia B. Sci Transl Med. 2015;7 (277):277ra228. doi:10.1126/scitranslmed.aaa1405
75. Milani M, Annoni A, Bartolaccini S, Biffi M, Russo F, Di Tomaso T, Raimondi A, Lengler J, Holmes MC, Scheiflinger F, Lombardo A, Cantore A, Naldini L. Genome editing for scalable production of alloantigen-free lentiviral vectors for in vivo gene therapy. EMBO Mol Med. 2017;9(11):1558-1573. doi:10.15252/emmm.201708148
76. Milani M, Annoni A, Moalli F, Liu T, Cesana D, Calabria A, Bartolaccini S, Biffi M, Russo F, Visigalli I, Raimondi A, Patarroyo-White S, Drager D, Cristofori P, Ayuso E, Montini E, Peters R, Iannacone M, Cantore A, Naldini L. Phagocytosis-shielded lentiviral vectors improve liver gene therapy in nonhuman primates. Sci Transl Med. 2019;11 (493):eaav7325. doi:10.1126/scitranslmed.aav7325
77. Milani M, Canepari C, Liu T, Biffi M, Russo F, Plati T, Curto R, Patarroyo-White S, Drager D, Visigalli I, Brombin C, Albertini P, Follenzi A, Ayuso E, Mueller C, Annoni A, Naldini L, Cantore A. Liver-directed lentiviral gene therapy corrects hemophilia A mice and achieves normal-range factor VIII activity in non-human primates. Nat Commun. 2022;13(1):2454. doi:10.1038/s41467-022-30102-3
78. Stein CS, Kang Y, Sauter SL, Townsend K, Staber P, Derksen TA, Martins I, Qian J, Davidson BL, McCray PB. In Vivo Treatment of Hemophilia A and Mucopolysaccharidosis Type VII Using Nonprimate Lentiviral Vectors. Mol Ther. 2001;3(6):850-856. doi:10.1006/mthe.2001.0325
79. Kang Y, Xie L, Tran DT, Stein CS, Hickey M, Davidson BL, McCray PB. Persistent expression of factor VIII in vivo following nonprimate lentiviral gene transfer. Blood. 2005;106(5):1552-1558. doi:10.1182/blood-2004-11-4358
80. Sinn PL, Goreham-Voss JD, Arias AC, Hickey MA, Maury W, Chikkanna-Gowda CP, McCray JPB. Enhanced Gene Expression Conferred by Stepwise Modification of a Nonprimate Lentiviral Vector. Hum Gene Ther. 2007;18(12):1244-1252. doi:10.1089/hum.2006.127
81. Staber JM, Pollpeter MJ, Anderson CG, Burrascano M, Cooney AL, Sinn PL, Rutkowski DT, Raschke WC, McCray PB. Long-term correction of hemophilia A mice following lentiviral mediated delivery of an optimized canine factor VIII gene. Gene Ther. 2017;24(11):742-748. doi:10.1038/gt.2017.67
82. Ward NJ, Buckley SM, Waddington SN, Vandendriessche T, Chuah MK, Nathwani AC, McIntosh J, Tuddenham EG, Kinnon C, Thrasher AJ, McVey JH. Codon optimization of human factor VIII cDNAs leads to high-level expression. Blood. 2011;117(3):798-807. doi:10.1182/blood-2010-05-282707
83. McIntosh J, Lenting PJ, Rosales C, Lee D, Rabbanian S, Raj D, Patel N, Tuddenham EG, Christophe OD, McVey JH, Waddington S, Nienhuis AW, Gray JT, Fagone P, Mingozzi F, Zhou SZ, High KA, Cancio M, Ng CY, Zhou J, Morton CL, Davidoff AM, Nathwani AC. Therapeutic levels of FVIII following a single peripheral vein administration of rAAV vector encoding a novel human factor VIII variant. Blood. 2013;121(17):3335-3344. doi:10.1182/blood-2012-10-462200
84. Merlin S, Cannizzo ES, Borroni E, Bruscaggin V, Schinco P, Tulalamba W, Chuah MK, Arruda VR, VandenDriessche T, Prat M, Valente G, Follenzi A. A novel platform for immune tolerance induction in hemophilia A mice. Mol Ther. 2017;25(8):1815-1830. doi:10.1016/j.ymthe.2017.04.029
85. Gong J, Yang R, Zhou M, Chang L-J. Improved intravenous lentiviral gene therapy based on endothelial-specific promoter-driven factor VIII expression for hemophilia A. Mol Med. 2023;29(1):74. doi:10.1186/s10020-023-00680-z
86. Suzuki Y, Kakisaka K, Matsumoto T, Nogami K, Katagiri H, Takahara T, Takikawa Y. Orthotopic liver transplantation for haemophilia A may not always lead to a phenotypic cure of haemophilia A: A case report. Haemophilia. 2018;24(6):e420-e422. doi:10.1111/hae.13604
87. McCauslin CS, Wine J, Cheng L, Klarmann KD, Candotti F, Clausen PA, Spence SE, Keller JR. In vivo retroviral gene transfer by direct intrafemoral injection results in correction of the SCID phenotype in Jak3 knock-out animals. Blood. 2003;102(3):843-848. doi:10.1182/blood-2002-12-3859
88. Worsham DN, Schuesler T, von Kalle C, Pan D. In Vivo Gene Transfer into Adult Stem Cells in Unconditioned Mice by in Situ Delivery of a Lentiviral Vector. Mol Ther. 2006;14 (4):514-524. doi:10.1016/j.ymthe.2006.05.014
89. Miao CH. Hemophilia A gene therapy via intraosseous delivery of factor VIII-lentiviral vectors. Thromb J. 2016;14(S1):41. doi:10.1186/s12959-016-0105-1
90. Michelson AD. How Platelets Work: Platelet Function and Dysfunction. J Thromb Thrombolys. 2003;16(1/2):7-12. doi:10.1023/b:Thro.0000014586.77684.82
91. Wang X, Shin SC, Chiang AFJ, Khan I, Pan D, Rawlings DJ, Miao CH. Intraosseous Delivery of Lentiviral Vectors Targeting Factor VIII Expression in Platelets Corrects Murine Hemophilia A. Mol Ther. 2015;23(4):617-626. doi:10.1038/mt.2015.20
92. Nayak S, Herzog RW. Progress and prospects: immune responses to viral vectors. Gene Ther. 2009;17(3):295-304. doi:10.1038/gt.2009.148
93. Mingozzi F, High KA. Immune responses to AAV vectors: overcoming barriers to successful gene therapy. Blood. 2013;122(1):23-36. doi:10.1182/blood-2013-01-306647
94. Yin L, He H, Zhang H, Shang Y, Fu C, Wu S, Jin T. Revolution of AAV in Drug Discovery: From Delivery System to Clinical Application. J Med Virol. 2025;97(6):e70447. doi:10.1002/jmv.70447
95. Gyurkocza B, Sandmaier BM. Conditioning regimens for hematopoietic cell transplantation: one size does not fit all. Blood. 2014;124(3):344-353. doi:10.1182/blood-2014-02-514778
96. Chaudhry M, Ali N. Reduced-intensity conditioning hematopoietic stem cell transplantation: looking forward to an international consensus. Blood Res. 2015;50(2):69-70. doi:10.5045/br.2015.50.2.69
97. Gong J, Chung TH, Zheng J, Zheng H, Chang LJ. Transduction of modified factor VIII gene improves lentiviral gene therapy efficacy for hemophilia A. J Biol Chem. 2021;297 (6):1-13. doi:10.1016/j.jbc.2021.101397
98. Journal of Clinical InvestigationShi Q, Wilcox DA, Fahs SA, Weiler H, Wells CW, Cooley BC, Desai D, Morateck PA, Gorski J, Montgomery RR. Factor VIII ectopically targeted to platelets is therapeutic in hemophilia A with high-titer inhibitory antibodies. J Clin Invest. 2006;116(7):1974-1982. doi:10.1172/JCI28416

99. Kuether EL, Schroeder JA, Fahs SA, Cooley BC, Chen Y, Montgomery RR, Wilcox DA, Shi Q. Lentivirus-mediated platelet gene therapy of murine hemophilia A with pre-existing anti-factor VIII immunity. J Thromb Haemost. 2012;10 (8):1570-1580. doi:10.1111/j.1538-7836.2012.04791.x
100. Bacigalupo A, Ballen K, Rizzo D, Giralt S, Lazarus H, Ho V, Apperley J, Slavin S, Pasquini M, Sandmaier BM, Barrett J, Blaise D, Lowski R, Horowitz M. Defining the Intensity of Conditioning Regimens: Working Definitions. Biol Blood Marrow Transplant. 2009;15(12):1628-1633. doi:10.1016/j.bbmt.2009.07.004
101. Nathwani AC, Gray JT, McIntosh J, Ng CYC, Zhou J, Spence Y, Cochrane M, Gray E, Tuddenham EGD, Davidoff AM. Safe and efficient transduction of the liver after peripheral vein infusion of self-complementary AAV vector results in stable therapeutic expression of human FIX in nonhuman primates. Blood. 2006;109(4):1414-1421. doi:10.1182/blood-2006-03-010181
102. Nathwani AC, Gray JT, Ng CY, Zhou J, Spence Y, Waddington SN, Tuddenham EG, Kemball-Cook G, McIntosh J, Boon-Spijker M, Mertens K, Davidoff AM. Self-complementary adeno-associated virus vectors containing a novel liver-specific human factor IX expression cassette enable highly efficient transduction of murine and nonhuman primate liver. Blood. 2006;107(7):2653-2661. doi:10.1182/blood-2005-10-4035
103. Milani M, Fabiano A, Perez-Rodriguez M, Hernandez RJ, Zecchillo A, Zonari E, Ottonello S, Basso-Ricci L, Canepari C, Volpin M, Iannello V, Capo V, Quaranta P, Seffin L, Russo F, Biffi M, Ormoli L, Brombin C, Carlucci F, Forlino A, Filibian M, Montini E, Scala S, Villa A, Bueren JA, Rio P, Aiuti A, Cantore A, Naldini L. In vivo haemopoietic stem cell gene therapy enabled by postnatal trafficking. Nature. 2025; 643(8073):1097-1106. doi:10.1038/s41586-025-09070-3

***Corresponding author:** *Jie Gong. E-mail: 18647442552@163.com*

International Journal of Biomedicine 16(4) (2026) 442-454
http://dx.doi.org/10.21103/Article16(4)_RA3

REVIEW ARTICLE

INTERNATIONAL JOURNAL OF BIOMEDICINE

The Clinical Application of AI in Advanced Medical Imaging and Image Processing in Diagnostic Radiology

Rowa Aljondi[1*]

[1]*Department of Applied Radiologic Technology, College of Applied Medical Sciences, University of Jeddah, Jeddah, Saudi Arabia*

Abstract

Background: Artificial intelligence (AI), particularly deep learning (DL), now interacts with every part of the imaging chain, from raw data acquisition and image reconstruction to segmentation, diagnosis, prognosis, and follow-up. Evidence has grown rapidly, but it is spread across modalities, tasks, and reporting standards, making it difficult to assess for clinical translation.
Objective: To provide an integrated, clinically focused overview of AI in advanced medical imaging and image processing, with particular emphasis on the imaging modalities magnetic resonance imaging (MRI), computed tomography (CT), and positron emission tomography (PET).
Methods and Results: Structured narrative review using the PRISMA-ScR principles. We searched PubMed/MEDLINE, Embase, Web of Science, Scopus, and IEEE Xplore for papers from January 2015 to June 2026. The two anchor reviews were Wang et al. (2021) on DL-based reconstruction and Obuchowicz et al. (2024) on clinical image-processing applications.
Deep learning reconstruction is the most advanced clinical application. Commercial and regulator-cleared products reduce MRI acquisition time by approximately 60–80%, reduce the CT dose without compromising low-contrast detectability, and reduce PET acquisition or tracer dose by 50%-75%. Self-configuring segmentation networks (such as nnU-Net) achieve Dice coefficients ≥0.90 for many downstream organs; prospective randomized trials in breast screening show that AI-dependent reading can maintain or increase cancer detection rates while reducing radiologists' workload by approximately 44%. A multimodal approach extends imaging by incorporating radiomics to predict treatment response and enable long-term monitoring. Challenges remain: lack of external validation, data shift, algorithmic bias, hallucination in generative reconstruction, poor interpretability, and fragmented regulation.
Conclusion: AI is moving from proof of concept to clinical infrastructure. Safe scale-up requires physics-informed, uncertainty-aware models; multicentre, federated validation; adherence to CLAIM, TRIPOD+AI, and DECIDE-AI; and post-deployment monitoring. **(International Journal of Biomedicine. 2026;16(4):442-454.)**

Keywords: deep learning, magnetic resonance imaging, computed tomography, positron emission tomography, clinical translation

For citation: Aljondi R. The Clinical Application of AI in Advanced Medical Imaging and Image Processing in Diagnostic Radiology. International Journal of Biomedicine. 2026;16(4):442-454. doi:10.21103/Article16(4)_RA3

Introduction

In modern medicine, medical imaging is the primary non-invasive means of accessing anatomy, physiology, and molecular function and underpins most diagnostic and therapeutic decisions. MRI provides unmatched soft-tissue contrast without ionizing radiation, CT provides fast, high-resolution attenuation maps, and PET quantifies metabolic and receptor-level processes. However, each modality has a structural trade-off: MRI has slow acquisition times, CT and PET involve radiation exposure, and the data generated by each modality is too large for clinicians to review thoroughly. However, a family of representation learning methods known as deep learning (DL), based on multilayer neural networks, has revolutionized how these trade-offs are managed. Convolutional architectures, and more recently transformer and diffusion models,[1-3] have penetrated all layers of the imaging pipeline since 2015. Early surveys identified hundreds of proof-of-concept studies in classification, detection, and segmentation,[2] and later reviews framed AI as a pathway to "high-performance medicine," where algorithms support, but do not supplant, clinical practice.[4,5] By 2023, the field had advanced to the point that a key question was whether regulators would approve and reimburse a product.[6]

© 2026 The Author(s). *International Journal of Biomedicine* is published by IMRDC.
This is an open access article under the CC BY-NC-ND 4.0 license.

There has been a parallel evolution of two strands of literature. The first is image formation: how DL reconstructs diagnostic images from undersampled MRI k-space, Low-dose CT sinograms, or Low-count PET data. Wang et al. provided a thorough overview of this strand for MRI, CT, and PET, covering model-based and data-driven perspectives, as well as early commercial products with FDA 510(k) clearance.[7] The second strand focuses on image analysis: segmentation, detection, classification, prediction, and quality control. Obuchowicz et al. compiled 34 recent studies from a variety of modalities including X-ray, MRI, CT, SPECT, ultrasonography, mammography, and histopathology, and divided clinical applications into seven categories: segmentation, detection and diagnosis, pre-processing, personalized treatment planning, predictive analytics, quality control, and monitoring and follow-up.[8]

The two strands cannot be separated in the clinic. Noise texture changes due to reconstruction decisions, which in turn affect segmentation accuracy and radiomic feature values, ultimately influencing prognosis prediction.[9–11] When evaluating a DL reconstruction product, a radiology department should first consider its impact on each downstream task, not just perceived image quality.

This review bridges the two strands. It makes specific contributions to:

1. Summarize the fundamental DL architectures and learning paradigms to be mapped by the clinical reader to imaging physics.

2. Summarize the evidence of DL reconstruction in MRI, CT, and PET, including commercial products and reported performance.

3. Map the clinical applications to the seven categories of Obuchowicz et al., including some representative quantitative results and the best available evidence (randomized trials).

4. Summarize modality-specific evidence and the regulatory landscape.

5. Discuss the technical, clinical, ethical and regulatory challenges to adoption and propose a research agenda.

Review Methodology

This is a structured narrative review. It follows the PRISMA 2020 reporting guidelines[12] and, where applicable, the PRISMA-ScR extension for scoping reviews,[13] as appropriate for a non-systematic synthesis. It was not registered and does not pool effect sizes.

Anchor sources. We used two peer-reviewed reviews to set the conceptual boundaries: Wang et al.[7] for the DL-based reconstruction of medical images, MRI/CT/PET, and Obuchowicz et al.[8] for clinical applications of image processing. They asked us to trace the primary studies back to their origins and follow articles backward.

Databases and period. We searched PubMed/MEDLINE, Embase, Web of Science Core Collection, Scopus, and IEEE Xplore for English-language articles published from 1 January 2015 to 30 June 2026. We used pre-2015 landmark papers in the methodological field (such as compressed sensing, ML-EM, and OSEM reconstruction) as background.

Search concepts. Three blocks were combined with AND: (i) *"artificial intelligence" OR "deep learning" OR "machine learning" OR "neural network" OR "transformer" OR "diffusion model" OR "foundation model"*; (ii) *"magnetic resonance imaging" OR "computed tomography" OR "positron emission tomography" OR "mammography" OR "radiography" OR "ultrasonography"*; (iii) *"reconstruction" OR "segmentation" OR "detection" OR "diagnosis" OR "radiomics" OR "prognosis" OR "treatment planning" OR "quality control"*.

Selection. We prioritized randomized controlled trials and prospective studies over other study designs, followed by multicentre or externally validated retrospective studies, systematic reviews and meta-analyses, seminal method papers that established an architecture or paradigm, and reporting guidelines and regulatory analyses and included only single-centre studies without external validation in the absence of external validation when they depicted a distinct clinical task. We excluded editorials, conference abstracts without full text, and non-imaging AI.

Fundamentals of AI for Medical Imaging

From handcrafted features to learned representations

There are two families of AI-based imaging methods.[8] Classical machine learning (ML) relies on a priori features, including intensity statistics, shape descriptors, and texture. Radiomics formalizes this by viewing images as 'minable data' rather than just pictures.[14,15] Later, the Image Biomarker Standardization Initiative (IBSI) standardized 169 feature definitions, improving feature reproducibility across software and centers.[16,17]

Deep learning, in contrast, extracts hierarchical features directly from pixels or raw signals: low-level layers find edges and textures, whereas higher levels find semantic structure.[1,3] Deep learning scores are now higher on most tasks, but not on every task. In fact, Nurzynska et al. showed that, despite using a small dataset, a handcrafted feature based on texture analysis of vertebral bodies on CT predicted patient age better than DL, [18] suggesting that small datasets and well-known physics can still favor handcrafted features.

Learning paradigms

Three paradigms are relevant.[7] *Supervised learning* minimizes the loss between predictions and paired ground truth (i.e., low-dose and full-dose CT pairs). When full-dose references or fully sampled data are unavailable, *unsupervised and self-supervised learning* leverage data structure. *Reinforcement learning* provides a reward signal to train an agent; it is seldom used, for example, to tune iterative reconstruction parameters automatically. Most reconstruction/analysis models used in the clinic are supervised, with self-supervised pre-training emerging as a possibility.

Core architectures

Table 1 summarizes the architectures that recur throughout this review. There are two trends here. First, self-configuring frameworks like nnU-Net show that an effective pipeline can matter more than innovative architecture, as nnU-Net matched or surpassed most specialized approaches

Table 1.
Core deep learning architectures in medical imaging and their main clinical roles.

Architecture	Key idea	Main imaging roles	References
Convolutional neural network (CNN)	Local, weight-shared filters learn spatial features hierarchically	Classification, detection, denoising	[1,2]
U-Net	Encoder–decoder with skip connections preserves spatial detail	Segmentation; image-to-image reconstruction	[19]
Residual network (ResNet)	Identity shortcuts let very deep networks train stably	Backbone for classification; residual denoising	[20]
Generative adversarial network (GAN)	Generator and discriminator compete, producing realistic images	Low-dose denoising, super-resolution, cross-modality synthesis	[21]
nnU-Net	Self-configuring U-Net pipeline adapts preprocessing, architecture and training to each dataset	Out-of-the-box segmentation across organs and modalities	[22]
Vision transformer / UNETR	Self-attention models long-range context	3D segmentation, multimodal fusion	[23,24]
Diffusion model	Learns to reverse a gradual noising process	Reconstruction, synthesis, data augmentation	[25]
Foundation model	Large model pre-trained on broad data, adapted to many tasks	Promptable segmentation (SAM, MedSAM); generalist diagnosis	[26–30]

on 23 public datasets.[22] Second, foundation models trained on billions of images guarantee label-efficient adaptation. For example, MedSAM, trained on over 1.5 million image–mask pairs, segments structures from a simple prompt,2[7]and a self-supervised retinal model, RETFound, generalizes to predicting both ocular and systemic disease.[29] A new trend is the development of generalist medical AI models that integrate images, text, and other information.[28,30]

Training and evaluation essentials

Good models require a training, validation, and test set, preferably collected from a different institution or scanner.[7] To avoid overfitting, data is enhanced using techniques such as data augmentation (affine transforms, noise injection). Typically, reconstruction models are trained using mean squared error (L2) or mean absolute error (L1), or a combination of structural similarity (SSIM), perceptual, or adversarial loss.[7] Performance measurement should not be limited to pixel measures such as peak signal-to-noise ratio (PSNR) and SSIM but should also include task-based measures such as lesion detectability, segmentation agreement, and reader studies.

AI in Image Reconstruction: MRI, CT, and PET

Reconstruction is the first step in the clinical workflow, and its quality carries over to all subsequent steps in the computational pipeline.[7] Acquisition time limits MRI; radiation dose or counting statistics limit CT and PET. DL methods are tackling these challenges in three ways: (i) image domain post-processing – a network refines the initial analytic reconstruction; (ii) model-based (unrolled) networks – iterations of a physics-based optimization are unfolded into network layers with data-consistency steps; and (iii) direct (end-to-end) mapping from raw data to image.

Magnetic resonance imaging

Classical MRI must obey the Nyquist sampling in k-space, slowing dynamic and high-resolution protocols. Parallel imaging and compressed sensing (CS) relax this requirement; CS relies on image sparsity in a transform domain[31] but requires handcrafted priors and long iterative solvers. In MR reconstruction, Wang et al. first applied DL to map undersampled data to fully sampled images in 2016.[32] AUTOMAP then showed that a network could learn the domain transform directly from raw sensor data to image.[33]

Model-based networks soon became the dominant design because they contained the MR forward model. These works all involved unrolling a gradient-descent scheme as a variational network: Hammernik et al.[34] for multi-coil knee MRI;Schlemper et al.[35] for a deep cascade of CNN blocks combined with data-consistency layers for dynamic cardiac MRI; MoDL used a learned denoiser and data-consistency step based on the conjugate gradient algorithm for dynamic cardiac MRI.[36] Data-driven GANs enhanced perceptual sharpness in CS-MRI.[37]

The key was publicly available raw data. The fastMRI dataset was released with raw k-space and DICOM images of the knee and, later, the brain,[38] and the 2020 fastMRI challenge showed that the best models produced high-radiological-quality images at 4-fold acceleration, whereas subtle pathology was lost at 8-fold acceleration,[39] For fully sampled references, self-supervised physics-guided training eliminates the need for a reference,[40] Comprehensive surveys of parallel imaging summarize these trends,[41] and distribution-based diffusion models are increasingly used as powerful imaging-acceleration priors in MRI.[42]

A growing body of clinical evidence supports this. A prospective interchangeability study found 4-fold DL-accelerated knee MRI at 3 T to be diagnostically interchangeable with conventional imaging for diagnosing internal derangement.[43] A commercial DL product achieved 60% faster volumetric brain MRI without compromising automated volumetric measurements.[44] Failure monitoring and radiologist training are important translation issues that must be addressed, along with protocol harmonization.[45]

Computed tomography

The CT reconstruction has progressed from Filtered back-projection (FBP) to Statistical iterative reconstruction and model-based iterative reconstruction and now to DL reconstruction (DL reconstruction).[46,47] Iterative methods suppress noise at low dose, but may create a "plastic" noise texture and are often computationally expensive.

This field was sparked by the 2016 AAPM Low-Dose CT Grand Challenge.[48] Some initial networks included the residual encoder–decoder CNN (RED-CNN),[49] a directional-wavelet CNN,5[1] and FBPConvNet (residual U-Net),[51] which corrected FBP images. The sparse-view CT was solved using the framelet-based U-Net[52] and the DD-Net.[53] Adversarial and perceptual losses preserved the texture better than pixel-wise losses for GANs.[54,55] A modularized deep net (MDN) achieved results comparable to or better than those of commercial iterative reconstruction (IR) in a blinded reader study.[56] Theories are reviewed, and the trend toward physics-integrated designs [57,58] is summarized.

DLR has been commercialized, and clinical studies support this. DLR has been shown to enhance the image quality of ultra-high-resolution abdominal CT compared with hybrid and model-based iterative reconstruction,[59] and phantom studies have measured the potential for dose reduction using a DL algorithm.[60] In head CT, the SNR improved by up to 54% in grey matter and 60% in white matter, and the CNR improved by up to 58% compared with adaptive statistical iterative reconstruction (ASIR-V).[61] Lower noise levels and higher CNR in unenhanced brain CT images were achieved using DL-based reconstruction compared with hybrid iterative reconstruction.[62] Research algorithms have continued to expand the range: the use of shape priors for GAN-based sinogram inpainting boosted PSNR for limited-angle CT by 7 dB,[63] and an approximation to iterative reconstruction (UnetU) for photon-counting micro-CT enabled a much faster material decomposition.[64]

Positron emission tomography

Analytic FBP, iterative maximum-likelihood expectation-maximization (MLEM),[65] and accelerated iterative ordered-subsets EM (OSEM)[66] have been used for PET reconstruction. The clinical drivers for AI are shorter acquisition times (to minimize motion and increase throughput) and a lower tracer dose (to minimize radiation, particularly in children and with repeated exams).

In 2017, Xiang et al.[67] combined DL with PET to estimate standard-dose images from low-dose PET and to co-register MRI and PET using a deep auto-context CNN. Gong et al. incorporated a CNN representation into iterative reconstruction,[68] while DeepPET reconstructed images directly from sinograms using an encoder–decoder network, a much faster approach than OSEM.[69] A 3D conditional GAN generated full-dose PET images from one-quarter-dose PET.[70] The DL with multi-contrast MRI inputs yielded diagnostic-quality images from ultra-low-dose (around 1%) 18F-florbetaben PET for amyloid imaging,[71] and a GAN with task-specific perceptual loss was able to do the same without MRI.[72]These methods are discussed in detail by Reader et al.[73]

In clinical applications, this enabled a 2-fold reduction in 18F-FDG acquisition time without sacrificing diagnostic performance when using the digital PET/CT platform for DL denoising,[74] and a positive business case was generated for real-world implementation of AI-based reduced-dose FDG PET.[75]

Cross-modality synthesis and attenuation correction

PET/MRI does not have a direct measure of photon attenuation. For brain PET/MRI, pseudo-CT generated by DL showed better performance than the atlas and Dixon methods in achieving correct attenuation correction,[76] and zero-echo-time and Dixon inputs also showed good performance for correct attenuation correction in the pelvis.[77] This synthesis principle applies to MR-only radiotherapy planning.[78]

Commercial products and reported performance

Not every vendor-reported gain is replicated independently, and there are differences between jurisdictions in what indications are considered "cleared" (Table 2).

Dose and scan time should be reduced only after confirming performance locally with phantom and patient studies.

Stability, hallucination and trust

The reconstructed DL is unstable: very small changes in the input produce large artifacts, and adding more training

Table 2.

Representative regulator-cleared DL reconstruction products and reported benefits, as summarised by Wang et al. [7] and subsequent clinical studies.

Product (vendor)	Modality	Reported benefit	References
AI-assisted compressed sensing, ACS (United Imaging)	MRI	About 80% scan-time reduction for most fast spin-echo sequences; most body-part protocols under 100 s	[7]
SubtleMR (Subtle Medical)	MRI	About 60% scan-time reduction; volumetric measures preserved	[7,44]
AiCE (Canon Medical)	CT	Lower noise, higher signal and contrast-to-noise ratio than hybrid iterative reconstruction	[7,59,62]
TrueFidelity (GE HealthCare)	CT	Improved image quality and dose-reduction potential at low dose	[7,60,61]
DELTA (United Imaging)	CT	Up to 80% dose reduction; low-contrast detectability improved by up to 157%	[7]
HYPER DLR (United Imaging)	PET	Acquisition shortened from 3 to under 1 min per bed position; SNR improved by 42%	[7]
SubtlePET (Subtle Medical)	PET	Diagnostic images from 25–50% of the standard acquisition time	[7,74,75]

samples does not necessarily improve the result.[79] Hallucination maps and uncertainty estimates motivate generative models to hallucinate realistic but false structures. These risks can be mitigated with data consistency layers, physics-based unrolling, and task-based evaluation (lesion detectability and not PSNR only).

Clinical Applications Across the Imaging Pathway

Obuchowicz et al. categorized clinical AI apps into seven categories.[8] The same structure is used, with each category linked to the best available evidence. In the following, these categories are located along the patient's imaging pathway in Figure 1.

Figure 1. The seven application categories of Obuchowicz et al.[8] and the reconstruction framework of Wang et al.[7] are incorporated into the clinical imaging pathway to formulate AI applications. Later steps have varying levels of evidence, with the most clinically mature step being reconstruction.

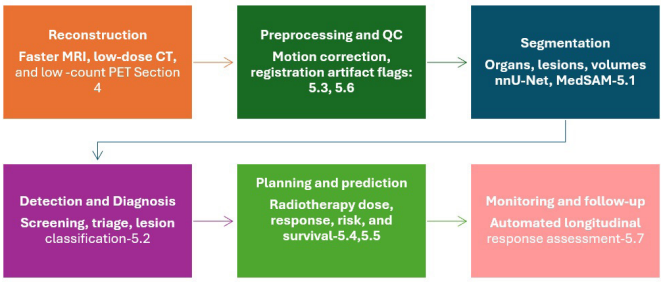

Highlighted: the most clinically mature step, with regulator – cleared products in MRI, CT, and PET

Fig. 1. *AI applications along the imaging pathway · 6 stages.*

Image segmentation

Segmentation, which is the delineation of organs, lesions, or tissue classes, is the basis for the following: volumetry, radiotherapy planning, radiomics, and surgical navigation. Considerable progress has been made in recent years through public challenges such as the Brain Tumor Segmentation (BraTS) challenge[81] and the Medical Segmentation Decathlon (MSD), which includes 10 CT and MRI tasks.[82] nnU-Net is the winner of the Decathlon and is still a good baseline.[22,82] TotalSegmentator achieved a high Dice coefficient of 0.943 on routine CT, and a fully convolutional network for cardiac MRI was evaluated with human-level accuracy in nearly 5,000 participants from the UK Biobank.[84]

In oncology, nnU-Net was found to outperform other architectures for prostate gland and zonal segmentation on MRI[85] and to segment pediatric Wilms tumor with a median Dice of 0.90 and a median Hausdorff distance of 7.2 mm compared to manual segmentation.[86] Model-based segmentation can be extended to new structures with only limited annotations, called promptable foundation models.[27] The choice of metric is important: Boundary errors or missed small lesions can be covered up by dice alone, and the Metrics Reloaded framework supplies task-specific advice.[87] In radiotherapy, the segmentation of 21 organs at risk was at the expert level for the head and neck.[88]

Disease detection and diagnosis

Detection and diagnosis are the most researched applications. A meta-analysis of 24 studies showed a mean sensitivity of 89% for brain metastases on an MRI scan; however, there was a lack of homogeneity with respect to false-positive reports, which prevented a consolidated analysis.[89]

Breast imaging is evidence-based to the highest degree. A DL system decreased the number of false positives (FP) by 1.2% and 5.7% and the number of false negatives (FN) by 2.7% and 9.4%, respectively, in retrospective UK and US data.[90] Stand-alone AI was comparable to the average of 101 radiologists[91] and, in an external evaluation, the top three commercially available algorithms showed improved sensitivity over the first-reader radiologists.[92] Prospective evidence followed. In the MASAI trial (over 80,000 women), AI-assisted screening was found not to affect screening workload or false-positive rates adversely and led to a 44% reduction in cancer detection.[93] The nationwide implementation study PRAIM in Germany (463,094 women) with AI-supported double reading confirmed a higher detection rate compared to standard double reading, with no increase in the recall rate.[95] In the ScreenTrustCAD study, AI plus 1 radiologist was proven to be non-inferior to standard double reading.[94] DL also has the potential to enhance the interpretation of digital breast tomosynthesis (DBT):[96] a single-slice DBT classifier achieved an accuracy of 93.2%,[97] and an MRI model, when applied to BRCA carriers, was able to retrospectively identify 65% of cancers earlier than radiologists.[98]

Thoracic imaging: an end-to-end model for low-dose CT lung screening achieved an AUC of 0.944 and, when applied to nontraining scans, reduced false positives by 11% and false negatives by 5% compared with six radiologists.[99] CheXNeXt identified 14 pathologies on chest radiographs, achieving a 100% match rate with the radiologists.[100] A YOLO-based detector on chest radiographs has achieved an average precision of 0.815[101] in detecting foreign objects.

Focused abdominal ultrasound is used for emergency and abdominal imaging, and automated ML is used to classify haemoperitoneum, achieving sensitivity and specificity greater than 94% and an AUROC of 0.97 on external validation.[102] AI tools that facilitate large-vessel occlusion diagnosis on CT angiography reduce stroke workflow,[103] and multinational CT models have achieved approximately 90% accuracy for COVID-19 pneumonia.[104] CNN has classified liver masses on multiphase CT,[105] and a multiparametric MRI pipeline has distinguished healthy livers from livers with lesions, with an AUC of 0.85.[106] An MRI of the prostate can be used to identify clinically significant cancer with a multiple-instance support vector machine (SVM) with a 92% accuracy rate.[107]

In addition to radiology, the diabetic retinopathy study,[108] dermatology,[109] and lung histopathology[110] demonstrated the performance of specialists and provided methodological models that the radiology community has adopted.

Image preprocessing and enhancement

Preprocessing enhances the data fed into human readers and subsequent algorithms. In addition to the reconstruction methods presented in Section 4, applications include unsupervised

deformable registration (VoxelMorph) that registers volumes in under a minute, versus under an hour for classical methods,[112] and retrospective correction of the signal loss caused by motion in diffusion-weighted MRI of the liver, which improved ADC accuracy in the left lobe.[111] Scan times are also shortened by using synthetic contrast generation and super-resolution, provided the outputs are validated against acquired images.

Personalized treatment planning

Automatic contouring is now routinely used in many radiotherapy centers, and has been shown to limit planning time and inter-observer variability.[113] For prostate intensity-modulated radiotherapy[114] and glioblastoma volumetric modulated arc therapy, DL models have been applied directly to the anatomy to predict 3D dose distributions, showing sensitivity to anatomical variations and even supporting quality assurance of automatic contouring[115] in glioblastoma. Image-based DL has also been applied to individualize radiotherapy dose for lung cancer,[116] and MR-only planning is also supported by MR-derived synthetic CT.[78]

Predictive analytics

Predictive models integrate imaging with clinical data to predict prognosis, treatment response/likelihood of future complications. A DL network was able to predict survival in non-small-cell lung cancer (NSCLC) from routine computed tomography (CT) across multiple cohorts.[117] Another study of locally advanced cervical cancer showed that a DL model using multiparametric MRI outperformed clinical models when predicting response to neoadjuvant chemotherapy.[118] DL risk models based on mammography were superior to the Tyrer–Cuzick model,[119] and Sybil predicted future lung cancer from a single low-dose CT with an AUC of up to 0.92 over 1 year,[120] and chest radiographs alone predicted long-term mortality.[121] In general, fusion of imaging with electronic health records and molecular data significantly outperforms the single-modality models.[122-124]

Quality control

Before the image is presented to the reader or an algorithm, the automated quality control checks the image first. A DL model agreed with radiologists in its assessment of the diagnostic quality of liver MRI on T2-weighted images, [125] and reference-free networks have been developed to detect motion artifacts in MRI, thereby allowing repeated sequences. At the same time, the patient remains on the table.[126] Quality control also involves identifying out-of-distribution input on which an AI model is likely to fail.

Monitoring and follow-up

Automated and repeatable measurement is a benefit of longitudinal assessment. An artificial neural network was used in a multicentre neuro-oncology study to quantify tumor response on MRI and to predict overall survival more accurately than the central neuro-oncology radiological assessment, based on the Response Assessment in Neuro-Oncology (RANO) criteria[127] (Table 3). Pathological complete response in rectal cancer was predicted using multi-task DL on serial MRI.[128] The same applies to pediatric follow-up, e.g., through automated volumetry using nnU-Net-based Wilms tumor measurement.[86]

Modality-Specific Evidence and the Regulatory Landscape

Maturity by modality

The evidence base is uneven across modalities. Table 4 summarises where AI has reached routine practice and where it remains investigational.

Regulatory clearance and evidence gaps

Regulatory approval has clinical trial results. Many of the AI devices that make their way to the European market do so before the US market, with the largest proportion of cleared devices in radiology.[129] Retrospective evaluation was used by nearly all of the 130 FDA-cleared AI devices, and

Table 3.

Representative clinical applications and quantitative results.

Category	Task (modality)	Method	Key result	References
Segmentation	104 structures (CT)	nnU-Net-based	Mean Dice 0.943	[83]
Segmentation	Wilms tumor (MRI)	nnU-Net	Median Dice 0.90; HD95 7.2 mm	[86]
Detection	Brain metastases (MRI)	DL meta-analysis	Pooled sensitivity 89%	[89]
Detection	Breast screening (mammography)	AI-supported reading, RCT	Detection maintained or increased; workload −44%	[93]
Detection	Breast screening (mammography)	AI-supported double reading	Detection +17.6%; recall not increased	[95]
Detection	Lung screening (LDCT)	3D CNN	AUC 0.944	[99]
Diagnosis	Hemoperitoneum (US)	AutoML	AUROC 0.97 (external)	[102]
Diagnosis	Prostate cancer (MRI)	Texture + MIL-SVM	Accuracy 92%	[107]
Preprocessing	Low-dose CT	GAN inpainting	PSNR +7 dB	[63]
Treatment planning	Glioblastoma dose (CT)	Cascaded 3D U-Net	Contour-sensitive dose prediction	[115]
Prediction	Future lung cancer (LDCT)	Sybil	1-year AUC up to 0.92	[120]
Monitoring	Glioma response (MRI)	ANN	Better survival prediction than central RANO assessment	[127]

Table 4.
Maturity of AI applications by modality.

Modality	Most mature applications	Highest level of evidence	Main open problems	References
MRI	DL reconstruction for accelerated scans; brain, prostate and cardiac segmentation	Prospective interchangeability studies; regulator-cleared products	Hallucination at high acceleration; vendor- and field-strength dependence	[33–45,84,85]
CT	DL reconstruction for low dose; whole-body segmentation; lung nodule and stroke triage	Reader studies; multicenter retrospective validation	Noise-texture shift affects radiomics; generalization across scanners	[48–64,83,99]
PET and PET/MRI	Low-count denoising; fast acquisition; MR-based attenuation correction	Clinical non-inferiority studies; real-world deployments	Quantitative bias in standardized uptake values; tracer diversity	[67–77]
Mammography and DBT	Screening support; triage; workload reduction	Randomized and nationwide prospective studies	Interval-cancer outcomes; equity across populations	[90–98]
Radiography	Chest radiograph triage; foreign-body and fracture detection	Multireader retrospective studies	Label noise; shortcut learning	[100,101,121]
Ultrasound	Focused emergency examinations; automated measurements	Multicenter retrospective validation	Operator dependence; video-level analysis	[102]
SPECT and nuclear medicine	Dementia staging; denoising	Single-center studies	Small datasets	[8]

most were not assessed across multiple sites.[130] Sixty-four of 100 commercially available CE-marked radiology products had no peer-reviewed evidence of efficacy, and only a minority had evidence of clinical impact beyond diagnostic accuracy.[131]

Now the regulations are becoming stricter. To guide post-clearance adaptive AI devices, the FDA has established predetermined change-control plans in the U.S. On top of the Medical Device Regulation, obligations for data governance, transparency, and human oversight have been introduced, and most medical AI is classified as high-risk under the European Union's Artificial Intelligence Act. The Saudi Food and Drug Authority (SFDA) has published specific guidance for the review and approval of AI- and ML-based medical devices, aligning with the Saudi Vision 2030 digital health objectives. The reality for departments is that it is important to start, rather than finish, the evaluation process—in addition to clearance, prospective monitoring and periodic revalidation are required.

Challenges, Limitations and Future Directions

Evidence quality and generalizability

One of the main flaws in the field is the disconnect between retrospective accuracy and real-world benefit.[132] Of the 516 published imaging AI studies, only 6% performed external validation.[133] When external validation does occur, it is usually accompanied by a drop in algorithm performance, with approximately a quarter of studies showing a significant decline.[134] There are shortcuts that models can learn: pneumonia detectors trained on chest radiographs learned to detect the hospital of origin rather than the disease.[135]

Data: quantity, quality, shift and privacy

There is limited, curated, well-labeled, and representative data.[136] Domain shift arises from variations in scanners, protocols, reconstruction kernels, and populations. It can be alleviated by domain adaptation,[137] synthetic data generated by generative models,[138] and harmonization, but these methods are not a substitute for training data with diversity. Federated learning is a way to train models across institutions without moving patient data. It achieved 99% of the performance of a centralized model for brain tumor segmentation,[139] and a 20-institution federated model for predicting COVID-19 outcomes showed significant improvement in generalisability.[140] The scalability of this approach relies on privacy-preserving computation, secure aggregation, and governance mechanisms.[141,142] In the Gulf region, especially in Saudi Arabia, federated and regionally curated datasets are particularly significant, as most public training data come from North American, European, and East Asian populations.

Bias and equity

AI can embed and exacerbate health inequities. Systematic underdiagnosis of disease was observed using state-of-the-art chest radiograph classifiers in female, Black, Hispanic, and younger patients, as well as in patients with Medicaid insurance.[143] DL models have also been shown to predict a patient's race from medical images, even for degraded images, which experts cannot.[144] Subgroup performance reporting and fairness audits should therefore be standard.

Interpretability and trust

Many models of reconstruction and analysis of DLs are black boxes.[7] The instability of saliency methods like Grad-CAM, which produce heat maps to pinpoint parts of an image that influence a prediction,[145] and their inability to explain their importance are well known. Radiology-specific reviews emphasize the need to appraise explanations with clinical users.[146,147] The physics-based unrolled networks, along with the data-consistency layers and pixel-wise uncertainty maps, provide more meaningful transparency into reconstruction than post hoc saliency.[79,80]

Reporting standards and evaluation frameworks

There are guidelines for the AI life cycle now: CLAIM for imaging studies in AI [148] (updated 2024[149]); TRIPOD+AI for prediction models;[150] CONSORT-AI for randomized trials;[151] and an international consensus on trustworthy and deployable medical AI (FUTURE-AI).[153] Journals and funders should

insist on compliance, and departments should consider these structures when purchasing commercial tools. The need is obvious: systematic reviews have shown that DL can achieve accuracy comparable to clinicians on internal test sets, while prospective studies are limited and many are at high risk of bias.[154–156] Authors, reviewers, and readers have practical appraisal guides to use.[157]

Workflow integration, regulation and liability

Regardless of the tools' accuracy, they can fail if they generate clicks or alerts, or cause delays. For successful deployment, these elements must be integrated with PACS and RIS; there must be clear guidelines on who is responsible for taking action on AI output; and there must be ongoing monitoring for any performance drift.[45] Issues of liability (manufacturer, institution or radiologist) and reimbursement are not fully clear.[6]

Future directions

Five directions appear most promising:

1. Physics-informed and self-supervised reconstruction that maintains data consistency, quantifies uncertainty, and requires no fully sampled or full-dose references.[40,42,58] Foundational and generalist models that can be adapted to new tasks, modalities, and institutions with few labels, and that combine images with reports and clinical data.[26-30,123]

3. Integrated pipelines from acquisition to decision that optimize the reconstruction process for subsequent tasks, such as detection or quantification, not just visual quality.[7,60]

4. Studies that have followed the MASAI and PRAIM models[93,95] in measuring patient outcomes, cost-effectiveness, and equity.

5. Fairness audits and post-market surveillance for federated, regionally representative data

Conclusions

AI, an integral part of the clinical infrastructure, now enhances medical imaging. It is most developed for reconstruction – MRI acquisitions are shortened, CT dose is reduced, and PET is accelerated, while maintaining diagnostic information, using DL methods approved by regulators. Self-configuring segmentation systems, validated in randomized breast-screening trials; predictive models based on imaging and clinical data; and automated quality control and monitoring now cover the entire imaging pathway outlined by Wang et al.[7] and Obuchowicz et al.[8]

The primary constraints have become ones other than algorithmic accuracy on curated test sets. They are generalizations across scanners and populations, not subject to hallucination or instability, fair, interpretable, and limited to prospective outcome data. To close these gaps, there is a need for physics-informed and uncertainty-aware models; for multicenter and federated validation, including under-represented populations (such as Saudi Arabia and the Gulf region); for consistent use of CLAIM, TRIPOD+AI, CONSORT-AI, and DECIDE-AI; and for ongoing post-deployment monitoring. When these conditions are met, AI can provide faster, safer, more accurate and more equitable imaging for patients.

Conflicts of Interest

The author declares no conflicts of interest.

References

1. LeCun Y, Bengio Y, Hinton G. Deep learning. Nature 2015;52:436–444. doi: 10.1038/nature14539
2. Litjens G, Kooi T, Ehteshami Bejnordi B, Setio AAA, Ciompi F, Ghafoorian M, et al. A survey on deep learning in medical image analysis. Med Image Anal 2017;42:60–88. doi: 10.1016/j.media.2017.07.005
3. Shen D, Wu G, Suk HI. Deep learning in medical image analysis. Annu Rev Biomed Eng 2017;19:221–248. doi:10.1146/annurev-bioeng-071516-044442
4. Hosny A, Parmar C, Quackenbush J, Schwartz LH, Aerts HJWL. Artificial intelligence in radiology. Nat Rev Cancer 2018;18(8):500–510. doi: 10.1038/s41568-018-0016-5
5. Topol EJ. High-performance medicine: the convergence of human and artificial intelligence. Nat Med 2019;25:44–56. doi: 10.1038/s41591-018-0300-7
6. Rajpurkar P, Lungren MP. The current and future state of AI interpretation of medical images. N Engl J Med 2023;388(21):1981–1990. doi: 10.1056/NEJMra2301725
7. Wang S, Cao G, Wang Y, Liao S, Wang Q, Shi J, Li C, Shen D. Review and prospect: artificial intelligence in advanced medical imaging. Front Radiol 2021;1:781868. doi: 10.3389/fradi.2021.781868
8. Obuchowicz R, Strzelecki M, Piórkowski A. Clinical applications of artificial intelligence in medical imaging and image processing—a review. Cancers 2024;16(10):1870. doi: 10.3390/cancers16101870
9. Esteva A, Chou K, Yeung S, Naik N, Madani A, Mottaghi A, et al. Deep learning-enabled medical computer vision. NPJ Digit Med 2021;4:5. doi: 10.1038/s41746-020-00376-2
10. Bi WL, Hosny A, Schabath MB, Giger ML, Birkbak NJ, Mehrtash A, et al. Artificial intelligence in cancer imaging: clinical challenges and applications. CA: Cancer J Clin 2019;69(2):127–157. doi:10.3322/caac.21552
11. Sahiner B, Pezeshk A, Hadjiiski LM, Wang X, Drukker K, Cha KH, et al. Deep learning in medical imaging and radiation therapy. Med Phys 2019;46(1):e1–e36. doi: 10.1002/mp.13264
12. Page MJ, McKenzie JE, Bossuyt PM, Boutron I, Hoffmann TC, Mulrow CD, et al. The PRISMA 2020 statement: an updated guideline for reporting systematic reviews. BMJ 2021;372:n71. doi: 10.1136/bmj.n71
13. Tricco AC, Lillie E, Zarin W, O'Brien KK, Colquhoun H, Levac D, et al. PRISMA extension for scoping reviews (PRISMA-ScR): checklist and explanation. Ann Intern Med 2018;169(7):467–473. doi:10.7326/M18-0850
14. Gillies RJ, Kinahan PE, Hricak H. Radiomics: images are more than pictures, they are data. Radiology 2016;278(2):563–577. doi: 10.1148/radiol.2015151169
15. Lambin P, Leijenaar RTH, Deist TM, Peerlings J, de Jong EEC, van Timmeren J, et al. Radiomics: the bridge between medical imaging and personalized medicine. Nat Rev Clin Oncol 2017;14:749–762. doi: 10.1038/nrclinonc.2017.141
16. Zwanenburg A, Vallières M, Abdalah MA, Aerts HJWL, Andrearczyk V, Apte A, et al. The Image Biomarker Standardization Initiative: standardized quantitative radiomics for high-throughput image-based phenotyping. Radiology 2020;295(2):328–338. https://doi.org/10.1148/radiol.2020191145

17. Mayerhoefer ME, Materka A, Langs G, Häggström I, Szczypiński P, Gibbs P, et al. Introduction to radiomics. J Nucl Med 2020;61(4):488–495. doi: 10.2967/jnumed.118.222893
18. Nurzynska K, Piórkowski A, Strzelecki M, Kociołek M, Banyś RP, Obuchowicz R. Differentiating age and sex in vertebral body CT scans – texture analysis versus deep learning approach. Biocybern Biomed Eng 2024;44(1):20–30. doi: 10.1016/j.bbe.2023.11.002
19. Ronneberger O, Fischer P, Brox T. U-Net: convolutional networks for biomedical image segmentation. In: Medical Image Computing and Computer-Assisted Intervention - MICCAI 2015. Lecture Notes in Computer Science, vol. 9351. Cham: Springer; 2015. p. 234–241. doi: 10.1007/978-3-319-24574-4_28
20. He K, Zhang X, Ren S, Sun J. Deep residual learning for image recognition. In: Proceedings of the IEEE Conference on Computer Vision and Pattern Recognition (CVPR); 2016. p. 770–778. doi: 10.1109/CVPR.2016.90
21. Goodfellow I, Pouget-Abadie J, Mirza M, Xu B, Warde-Farley D, Ozair S, et al. Generative adversarial networks. Commun ACM 2020;63(11):139–144. doi: 10.1145/3422622
22. Isensee F, Jaeger PF, Kohl SAA, Petersen J, Maier-Hein KH. nnU-Net: a self-configuring method for deep learning-based biomedical image segmentation. Nat Methods 2021;18:203–211. doi: 10.1038/s41592-020-01008-z
23. Hatamizadeh A, Tang Y, Nath V, Yang D, Myronenko A, Landman B, et al. UNETR: transformers for 3D medical image segmentation. In: Proceedings of the IEEE/CVF Winter Conference on Applications of Computer Vision (WACV); 2022. p. 1748–1758. doi: 10.1109/WACV51458.2022.00181
24. Shamshad F, Khan S, Zamir SW, Khan MH, Hayat M, Khan FS, et al. Transformers in medical imaging: a survey. Med Image Anal 2023;88:102802. doi: 10.1016/j.media.2023.102802
25. Kazerouni A, Aghdam EK, Heidari M, Azad R, Fayyaz M, Hacihaliloglu I, et al. Diffusion models in medical imaging: a comprehensive survey. Med Image Anal 2023;88:102846. doi: 10.1016/j.media.2023.102846
26. Kirillov A, Mintun E, Ravi N, Mao H, Rolland C, Gustafson L, et al. Segment anything. In: Proceedings of the IEEE/CVF International Conference on Computer Vision (ICCV); 2023. p. 3992–4003. doi: 10.1109/ICCV51070.2023.00371
27. Ma J, He Y, Li F, Han L, You C, Wang B. Segment anything in medical images. Nat Commun 2024;15:654. doi: 10.1038/s41467-024-44824-z
28. Moor M, Banerjee O, Abad ZSH, Krumholz HM, Leskovec J, Topol EJ, Rajpurkar P. Foundation models for generalist medical artificial intelligence. Nature 2023;616:259–265. doi: 10.1038/s41586-023-05881-4
29. Zhou Y, Chia MA, Wagner SK, Ayhan MS, Williamson DJ, Struyven RR, et al. A foundation model for generalizable disease detection from retinal images. Nature 2023;622:156–163. doi: 10.1038/s41586-023-06555-x
30. Tu T, Azizi S, Driess D, Schaekermann M, Amin M, Chang PC, et al. Towards generalist biomedical AI. NEJM AI 2024;1(3):AIoa2300138. https://doi.org/10.1056/AIoa2300138
31. Villota S, Inga E. Sparse Transform and Compressed Sensing Methods to Improve Efficiency and Quality in Magnetic Resonance Medical Imaging. Sensors 2025. 25(16):5137. doi: 10.3390/s25165137
32. Wang S, Su Z, Ying L, Peng X, Zhu S, Liang F, et al. Accelerating magnetic resonance imaging via deep learning. In: Proceedings of the IEEE 13th International Symposium on Biomedical Imaging (ISBI); 2016:514–517. doi: 10.1109/ISBI.2016.7493320
33. Zhu B, Liu JZ, Cauley SF, Rosen BR, Rosen MS. Image reconstruction by domain-transform manifold learning. Nature 2018;555:487–492. doi: 10.1038/nature25988
34. Hammernik K, Klatzer T, Kobler E, Recht MP, Sodickson DK, Pock T, et al. Learning a variational network for reconstruction of accelerated MRI data. Magn Reson Med 2018;79(6):3055–3071. doi: 10.1002/mrm.26977
35. Schlemper J, Caballero J, Hajnal JV, Price AN, Rueckert D. A deep cascade of convolutional neural networks for dynamic MR image reconstruction. IEEE Trans Med Imaging 2018;37(2):491–503. doi: 10.1109/TMI.2017.2760978
36. Aggarwal HK, Mani MP, Jacob M. MoDL: model-based deep learning architecture for inverse problems. IEEE Trans Med Imaging 2019;38(2):394–405. doi: 10.1109/TMI.2018.2865356
37. Yang G, Yu S, Dong H, Slabaugh G, Dragotti PL, Ye X, et al. DAGAN: deep de-aliasing generative adversarial networks for fast compressed sensing MRI reconstruction. IEEE Trans Med Imaging 2018;37(6):1310–1321. doi: 10.1109/TMI.2017.2785879
38. Knoll F, Zbontar J, Sriram A, Muckley MJ, Bruno M, Defazio A, et al. fastMRI: A publicly available raw k-space and DICOM dataset of knee images for accelerated MR image reconstruction using machine learning. Radiol Artif Intell 2020;2(1):e190007. doi: 10.1148/ryai.2020190007
39. Muckley MJ, Riemenschneider B, Radmanesh A, Kim S, Jeong G, Ko J, et al. Results of the 2020 fastMRI challenge for machine learning MR image reconstruction. IEEE Trans Med Imaging 2021;40(9):2306–2317. doi: 10.1109/TMI.2021.3075856
40. Yaman B, Hosseini SAH, Moeller S, Ellermann J, Uğurbil K, Akçakaya M. Self-supervised learning of physics-guided reconstruction neural networks without fully sampled reference data. Magn Reson Med 2020;84(6):3172–3191. doi: 10.1002/mrm.28378
41. Knoll F, Hammernik K, Zhang C, Moeller S, Pock T, Sodickson DK, et al. Deep-learning methods for parallel magnetic resonance imaging reconstruction: a survey of the current approaches, trends, and issues. IEEE Signal Process Mag 2020;37(1):128–140. doi: 10.1109/MSP.2019.2950640
42. Chung H, Ye JC. Score-based diffusion models for accelerated MRI. Med Image Anal 2022;80:102479. doi: 10.1016/j.media.2022.102479
43. Recht MP, Zbontar J, Sodickson DK, Knoll F, Yakubova N, Sriram A, et al. Using deep learning to accelerate knee MRI at 3 T: results of an interchangeability study. AJR Am J Roentgenol 2020;215(6):1421–1429. doi: 10.2214/AJR.20.23313
44. Bash S, Wang L, Airriess C, Zaharchuk G, Gong E, Shankaranarayanan A, et al. Deep learning enables 60% accelerated volumetric brain MRI while preserving quantitative performance: a prospective, multicenter, multireader trial. AJNR Am J Neuroradiol 2021;42(12):2130–2137. doi: 10.3174/ajnr.A7358
45. Chaudhari AS, Sandino CM, Cole EK, Larson DB, Gold GE, Vasanawala SS, et al. Prospective deployment of deep learning in MRI: a framework for important considerations, challenges, and recommendations for best practices. J Magn Reson Imaging 2021;54(2):357–371. doi: 10.1002/jmri.27331
46. Willemink MJ, Noël PB. The evolution of image

reconstruction for CT-from filtered back projection to artificial intelligence. Eur Radiol 2019;29(5):2185–2195. doi: 10.1007/s00330-018-5810-7
47. Wang G. A perspective on deep imaging. IEEE Access 2016;4:8914–8924. doi: 10.1109/ACCESS.2016.2624938
48. McCollough CH, Bartley AC, Carter RE, Chen B, Drees TA, Edwards P, et al. Low-dose CT for the detection and classification of metastatic liver lesions: results of the 2016 Low Dose CT Grand Challenge. Med Phys 2017;44(10):e339–e352. doi: 10.1002/mp.12345
49. Chen H, Zhang Y, Kalra MK, Lin F, Chen Y, Liao P, et al. Low-dose CT with a residual encoder-decoder convolutional neural network. IEEE Trans Med Imaging 2017;36(12):2524–2535. doi: 10.1109/TMI.2017.2715284
50. Kang E, Min J, Ye JC. A deep convolutional neural network using directional wavelets for low-dose X-ray CT reconstruction. Med Phys 2017;44(10):e360–e375. doi: 10.1002/mp.12344
51. Jin KH, McCann MT, Froustey E, Unser M. Deep convolutional neural network for inverse problems in imaging. IEEE Trans Image Process 2017;26(9):4509–4522. doi: 10.1109/TIP.2017.2713099
52. Han Y, Ye JC. Framing U-Net via deep convolutional framelets: application to sparse-view CT. IEEE Trans Med Imaging 2018;37(6):1418–1429. doi: 10.1109/TMI.2018.2823768
53. Zhang Z, Liang X, Dong X, Xie Y, Cao G. A sparse-view CT reconstruction method based on combination of DenseNet and deconvolution. IEEE Trans Med Imaging 2018;37(6):1407–1417. doi: 10.1109/TMI.2018.2823338
54. Wolterink JM, Leiner T, Viergever MA, Išgum I. Generative adversarial networks for noise reduction in low-dose CT. IEEE Trans Med Imaging 2017;36(12):2536–2545. doi: 10.1109/TMI.2017.2708987
55. Yang Q, Yan P, Zhang Y, Yu H, Shi Y, Mou X, et al. Low-dose CT image denoising using a generative adversarial network with Wasserstein distance and perceptual loss. IEEE Trans Med Imaging 2018;37(6):1348–1357. doi: 10.1109/TMI.2018.2827462
56. Shan H, Padole A, Homayounieh F, Kruger U, Khera RD, Nitiwarangkul C, et al. Competitive performance of a modularized deep neural network compared to commercial algorithms for low-dose CT image reconstruction. Nat Mach Intell 2019;1:269–276. doi: 10.1038/s42256-019-0057-9
57. Koetzier LR, Mastrodicasa D, Szczykutowicz TP, van der Werf NR, Wang AS, Sandfort V, et al. Deep learning image reconstruction for CT: technical principles and clinical prospects. Radiology 2023;306(3):e221257. doi: 10.1148/radiol.221257
58. Wang G, Ye JC, De Man B. Deep learning for tomographic image reconstruction. Nat Mach Intell 2020;2(12):737–748. doi: 10.1038/s42256-020-00273-z
59. Akagi M, Nakamura Y, Higaki T, Narita K, Honda Y, Zhou J, et al. Deep learning reconstruction improves image quality of abdominal ultra-high-resolution CT. Eur Radiol 2019;29(11):6163–6171. doi: 10.1007/s00330-019-06170-3
60. Greffier J, Hamard A, Pereira F, Barrau C, Pasquier H, Beregi JP, et al. Image quality and dose reduction opportunity of deep learning image reconstruction algorithm for CT: a phantom study. Eur Radiol 2020;30:3951–3959. doi: 10.1007/s00330-020-06724-w
61. Pula M, Kucharczyk E, Zdanowicz A, Guzinski M. Image quality improvement in deep learning image reconstruction of head computed tomography examination. Tomography 2023;9(4):1485–1493. doi: 10.3390/tomography9040118
62. Cozzi A, Cè M, De Padova G, Libri D, Caldarelli N, Zucconi F, et al. Deep learning-based versus iterative image reconstruction for unenhanced brain CT: a quantitative comparison of image quality. Tomography 2023;9(5):1629–1637. doi: 10.3390/tomography9050130
63. Valat E, Farrahi K, Blumensath T. Sinogram inpainting with generative adversarial networks and shape priors. Tomography 2023;9(3):1137–1152. doi: 10.3390/tomography9030094
64. Nadkarni R, Clark DP, Allphin AJ, Badea CT. A deep learning approach for rapid and generalizable denoising of photon-counting micro-CT images. Tomography 2023;9(4):1286–1302. doi: 10.3390/tomography9040102
65. Kasai R, Otsuka, H. Graph-Enhanced Expectation Maximization for Emission Tomography. Journal of Imaging 2026;12(1):48. doi: 10.3390/jimaging12010048
66. Huang H-M, Hsiao I-T (2016). Accelerating an Ordered-Subset Low-Dose X-Ray Cone Beam Computed Tomography Image Reconstruction with a Power Factor and Total Variation Minimization. PLoS ONE 11(4): e0153421. doi: 10.1371/journal.pone.0153421
67. Xiang L, Qiao Y, Nie D, An L, Lin W, Wang Q, Shen D. Deep auto-context convolutional neural networks for standard-dose PET image estimation from low-dose PET/MRI. Neurocomputing 2017;267:406–416. doi: 10.1016/j.neucom.2017.06.048
68. Gong K, Guan J, Kim K, Zhang X, Yang J, Seo Y, et al. Iterative PET image reconstruction using convolutional neural network representation. IEEE Trans Med Imaging 2019;38(3):675–685. doi: 10.1109/TMI.2018.2869871
69. Häggström I, Schmidtlein CR, Campanella G, Fuchs TJ. DeepPET: a deep encoder–decoder network for directly solving the PET image reconstruction inverse problem. Med Image Anal 2019;54:253–262. doi: 10.1016/j.media.2019.03.013
70. Wang Y, Yu B, Wang L, Zu C, Lalush DS, Lin W, et al. 3D conditional generative adversarial networks for high-quality PET image estimation at low dose. NeuroImage 2018;174:550–562. doi: 10.1016/j.neuroimage.2018.03.045
71. Chen KT, Gong E, de Carvalho Macruz FB, Xu J, Boumis A, Khalighi M, et al. Ultra–low-dose ^{18}F-florbetaben amyloid PET imaging using deep learning with multi-contrast MRI inputs. Radiology 2019;290(3):649–656. doi: 10.1148/radiol.2018180940
72. Ouyang J, Chen KT, Gong E, Pauly J, Zaharchuk G. Ultra-low-dose PET reconstruction using generative adversarial network with feature matching and task-specific perceptual loss. Med Phys 2019;46(8):3555–3564. doi: 10.1002/mp.13626
73. Reader AJ, Corda G, Mehranian A, da Costa-Luis C, Ellis S, Schnabel JA. Deep learning for PET image reconstruction. IEEE Trans Radiat Plasma Med Sci 2021;5(1):1–25. doi: 10.1109/TRPMS.2020.3014786
74. Weyts K, Lasnon C, Ciappuccini R, Lequesne J, Corroyer-Dulmont A, Quak E, et al. Artificial intelligence-based PET denoising could allow a two-fold reduction in [^{18}F]FDG PET acquisition time in digital PET/CT. Eur J Nucl Med Mol Imaging 2022;49(11):3750–3760. doi: 10.1007/s00259-022-05800-1
75. Katsari K, Penna D, Arena V, Polverari G, Ianniello A, Italiano D, et al. Artificial intelligence for reduced dose 18F-FDG PET examinations: a real-world deployment through a standardized framework and business case assessment.

EJNMMI Phys 2021;8:25. doi: 10.1186/s40658-021-00374-7
76. Liu F, Jang H, Kijowski R, Bradshaw T, McMillan AB. Deep learning MR imaging–based attenuation correction for PET/MR imaging. Radiology 2018;286(2):676–684. doi: 10.1148/radiol.2017170700
77. Leynes AP, Yang J, Wiesinger F, Kaushik SS, Shanbhag DD, Seo Y, et al. Zero-echo-time and Dixon deep pseudo-CT (ZeDD CT): direct generation of pseudo-CT images for pelvic PET/MRI attenuation correction using deep convolutional neural networks with multiparametric MRI. J Nucl Med 2018;59(5):852–858. doi: 10.2967/jnumed.117.198051
78. Han X. MR-based synthetic CT generation using a deep convolutional neural network method. Med Phys 2017;44(4):1408–1419. doi: 10.1002/mp.12155
79. Antun V, Renna F, Poon C, Adcock B, Hansen AC. On instabilities of deep learning in image reconstruction and the potential costs of AI. Proc Natl Acad Sci U.S.A 2020;117(48):30088–30095. doi: 10.1073/pnas.1907377117
80. Bhadra S, Kelkar VA, Brooks FJ, Anastasio MA. On hallucinations in tomographic image reconstruction. IEEE Trans Med Imaging 2021;40(11):3249–3260. doi: 10.1109/TMI.2021.3077857
81. Menze BH, Jakab A, Bauer S, Kalpathy-Cramer J, Farahani K, Kirby J, et al. The multimodal brain tumor image segmentation benchmark (BRATS). IEEE Trans Med Imaging 2015;34(10):1993–2024. doi: 10.1109/TMI.2014.2377694
82. Antonelli M, Reinke A, Bakas S, Farahani K, Kopp-Schneider A, Landman BA, et al. The Medical Segmentation Decathlon. Nat Commun 2022;13:4128. doi: 10.1038/s41467-022-30695-9
83. Wasserthal J, Breit HC, Meyer MT, Pradella M, Hinck D, Sauter AW, et al. TotalSegmentator: robust segmentation of 104 anatomic structures in CT images. Radiol Artif Intell 2023;5(5):e230024. doi: 10.1148/ryai.230024
84. Bai W, Sinclair M, Tarroni G, Oktay O, Rajchl M, Vaillant G, et al. Automated cardiovascular magnetic resonance image analysis with fully convolutional networks. J Cardiovasc Magn Reson 2018;20(1):65. doi: 10.1186/s12968-018-0471-x
85. Rodrigues NM, Silva S, Vanneschi L, Papanikolaou N. A comparative study of automated deep learning segmentation models for prostate MRI. Cancers 2023;15(5):1467. doi: 10.3390/cancers15051467
86. Buser MAD, van der Steeg AFW, Wijnen MHWA, Fitski M, van Tinteren H, van den Heuvel-Eibrink MM, et al. Radiologic versus segmentation measurements to quantify Wilms tumor volume on MRI in pediatric patients. Cancers 2023;15(7):2115. doi: 10.3390/cancers15072115
87. Maier-Hein L, Reinke A, Godau P, Tizabi MD, Buettner F, Christodoulou E, et al. Metrics reloaded: recommendations for image analysis validation. Nat Methods 2024;21:195–212. doi: 10.1038/s41592-023-02151-z
88. Nikolov S, Blackwell S, Zverovitch A, Mendes R, Livne M, De Fauw J, et al. Clinically applicable segmentation of head and neck anatomy for radiotherapy: deep learning algorithm development and validation study. J Med Internet Res 2021;23(7):e26151. doi: 10.2196/26151
89. Ozkara BB, Chen MM, Federau C, Karabacak M, Briere TM, Li J, Wintermark M. Deep learning for detecting brain metastases on MRI: a systematic review and meta-analysis. Cancers 2023;15(2):334. doi: 10.3390/cancers15020334
90. McKinney SM, Sieniek M, Godbole V, Godwin J, Antropova N, Ashrafian H, et al. International evaluation of an AI system for breast cancer screening. Nature 2020;577:89–94. doi: 10.1038/s41586-019-1799-6
91. Rodriguez-Ruiz A, Lång K, Gubern-Merida A, Broeders M, Gennaro G, Clauser P, et al. Stand-alone artificial intelligence for breast cancer detection in mammography: comparison with 101 radiologists. J Natl Cancer Inst 2019;111(9):916–922. doi: 10.1093/jnci/djy222
92. Salim M, Wåhlin E, Dembrower K, Azavedo E, Foukakis T, Liu Y, et al. External evaluation of 3 commercial artificial intelligence algorithms for independent assessment of screening mammograms. JAMA Oncol 2020;6(10):1581–1588. doi: 10.1001/jamaoncol.2020.3321
93. Lång K, Josefsson V, Larsson AM, Larsson S, Högberg C, Sartor H, et al. Artificial intelligence-supported screen reading versus standard double reading in the Mammography Screening with Artificial Intelligence trial (MASAI): a clinical safety analysis of a randomised, controlled, non-inferiority, single-blinded, screening accuracy study. Lancet Oncol 2023;24(8):936–944. doi: 10.1016/S1470-2045(23)00298-X
94. Dembrower K, Crippa A, Colón E, Eklund M, Strand F; ScreenTrustCAD Trial Consortium. Artificial intelligence for breast cancer detection in screening mammography in Sweden: a prospective, population-based, paired-reader, non-inferiority study. Lancet Digit Health 2023;5(10):e703–e711. doi: 10.1016/S2589-7500(23)00153-X
95. Eisemann N, Bunk S, Mukama T, Baltus H, Elsner SA, Gomille T, et al. Nationwide real-world implementation of AI for cancer detection in population-based mammography screening. Nat Med 2025;31:917–924. doi: 10.1038/s41591-024-03408-6
96. Lotter W, Diab AR, Haslam B, Kim JG, Grisot G, Wu E, et al. Robust breast cancer detection in mammography and digital breast tomosynthesis using an annotation-efficient deep learning approach. Nat Med 2021;27:244–249. doi: 10.1038/s41591-020-01174-9
97. Mendes J, Matela N, Garcia N. Avoiding tissue overlap in 2D images: single-slice DBT classification using convolutional neural networks. Tomography 2023;9(1):398–412. doi: 10.3390/tomography9010032
98. Anaby D, Shavin D, Zimmerman-Moreno G, Nissan N, Friedman E, Sklair-Levy M. 'Earlier than early' detection of breast cancer in Israeli BRCA mutation carriers applying AI-based analysis to consecutive MRI scans. Cancers 2023;15(12):3120. doi: 10.3390/cancers15123120
99. Ardila D, Kiraly AP, Bharadwaj S, Choi B, Reicher JJ, Peng L, et al. End-to-end lung cancer screening with three-dimensional deep learning on low-dose chest computed tomography. Nat Med 2019;25:954–961. doi: 10.1038/s41591-019-0447-x
100. Rajpurkar P, Irvin J, Ball RL, Zhu K, Yang B, Mehta H, et al. Deep learning for chest radiograph diagnosis: a retrospective comparison of the CheXNeXt algorithm to practicing radiologists. PLoS Med 2018;15(11):e1002686. doi: 10.1371/journal.pmed.1002686
101. Kufel J, Bargieł-Łączek K, Koźlik M, Czogalik Ł, Dudek P, Magiera M, et al. Chest X-ray foreign objects detection using artificial intelligence. J Clin Med 2023;12(18):5841. doi: 10.3390/jcm12185841
102. Jeong D, Jeong W, Lee JH, Park SY. Use of automated machine learning for classifying hemoperitoneum on ultrasonographic images of Morrison's pouch: a multicenter retrospective study. J Clin Med 2023;12(12):4043. doi: 10.3390/jcm12124043
103. Murray NM, Unberath M, Hager GD, Hui FK.

Artificial intelligence to diagnose ischemic stroke and identify large vessel occlusions: a systematic review. J Neurointerv Surg 2020;12(2):156–164. doi:10.1136/neurintsurg-2019-015135
104. Harmon SA, Sanford TH, Xu S, Turkbey EB, Roth H, Xu Z, et al. Artificial intelligence for the detection of COVID-19 pneumonia on chest CT using multinational datasets. Nat Commun 2020;11:4080. doi: 10.1038/s41467-020-17971-2
105. Yasaka K, Akai H, Abe O, Kiryu S. Deep learning with convolutional neural network for differentiation of liver masses at dynamic contrast-enhanced CT: a preliminary study. Radiology 2018;286(3):887–896. doi: 10.1148/radiol.2017170706
106. Skwirczyński M, Tabor Z, Lasek J, Schneider Z, Gibała S, Kucybała I, et al. Deep learning algorithm for differentiating patients with a healthy liver from patients with liver lesions based on MR images. Cancers 2023;15(12):3142. doi: 10.3390/cancers15123142
107. Gibala S, Obuchowicz R, Lasek J, Schneider Z, Piórkowski A, Pociask E, Nurzynska K. Textural features of MR images correlate with an increased risk of clinically significant cancer in patients with high PSA levels. J Clin Med 2023;12(8):2836. doi: 10.3390/jcm12082836
108. Gulshan V, Peng L, Coram M, Stumpe MC, Wu D, Narayanaswamy A, et al. Development and validation of a deep learning algorithm for detection of diabetic retinopathy in retinal fundus photographs. JAMA 2016;316(22):2402–2410. doi: 10.1001/jama.2016.17216
109. Esteva A, Kuprel B, Novoa RA, Ko J, Swetter SM, Blau HM, Thrun S. Dermatologist-level classification of skin cancer with deep neural networks. Nature 2017;542:115–118. doi: 10.1038/nature21056
110.Coudray N, Ocampo PS, Sakellaropoulos T, Narula N, Snuderl M, Fenyö D, et al. Classification and mutation prediction from non–small cell lung cancer histopathology images using deep learning. Nat Med 2018;24:1559–1567. doi: 10.1038/s41591-018-0177-5
111.Raspe J, Harder FN, Rupp S, McTavish S, Peeters JM, Weiss K, et al. Retrospective motion artifact reduction by spatial scaling of liver diffusion-weighted images. Tomography 2023;9(5):1839–1856. doi: 10.3390/tomography9050146
112.Balakrishnan G, Zhao A, Sabuncu MR, Guttag J, Dalca AV. VoxelMorph: a learning framework for deformable medical image registration. IEEE Trans Med Imaging 2019;38(8):1788–1800. doi: 10.1109/TMI.2019.2897538
113.Cardenas CE, Yang J, Anderson BM, Court LE, Brock KB. Advances in auto-segmentation. Semin Radiat Oncol 2019;29(3):185–197. doi: 10.1016/j.semradonc.2019.02.001
114.Nguyen D, Long T, Jia X, Lu W, Gu X, Iqbal Z, Jiang S. A feasibility study for predicting optimal radiation therapy dose distributions of prostate cancer patients from patient anatomy using deep learning. Sci Rep 2019;9:1076. doi: 10.1038/s41598-018-37741-x
115.Poel R, Kamath AJ, Willmann J, Andratschke N, Ermiş E, Aebersold DM, et al. Deep-learning-based dose predictor for glioblastoma–assessing the sensitivity and robustness for dose awareness in contouring. Cancers 2023;15(17):4226. doi: 10.3390/cancers15174226
116.Lou B, Doken S, Zhuang T, Wingerter D, Gidwani M, Mistry N, et al. An image-based deep learning framework for individualising radiotherapy dose: a retrospective analysis of outcome prediction. Lancet Digit Health 2019;1(3):e136–e147. doi: 10.1016/S2589-7500(19)30058-5
117.Hosny A, Parmar C, Coroller TP, Grossmann P, Zeleznik R, Kumar A, et al. Deep learning for lung cancer prognostication: a retrospective multi-cohort radiomics study. PLoS Med 2018;15(11):e1002711. doi: 10.1371/journal.pmed.1002711
118.Zhang Y, Wu C, Xiao Z, Lv F, Liu Y. A deep learning radiomics nomogram to predict response to neoadjuvant chemotherapy for locally advanced cervical cancer: a two-center study. Diagnostics 2023;13(6):1073. doi: 10.3390/diagnostics13061073
119.Yala A, Lehman C, Schuster T, Portnoi T, Barzilay R. A deep learning mammography-based model for improved breast cancer risk prediction. Radiology 2019;292(1):60–66. doi: 10.1148/radiol.2019182716
120. Mikhael PG, Wohlwend J, Yala A, Karstens L, Xiang J, Takigami AK, et al. Sybil: a validated deep learning model to predict future lung cancer risk from a single low-dose chest computed tomography. J Clin Oncol 2023;41(12):2191–2200. doi: 10.1200/JCO.22.01345
121. Lu MT, Ivanov A, Mayrhofer T, Hosny A, Aerts HJWL, Hoffmann U. Deep learning to assess long-term mortality from chest radiographs. JAMA Netw Open 2019;2(7):e197416. doi: 10.1001/jamanetworkopen.2019.7416
122. Huang SC, Pareek A, Seyyedi S, Banerjee I, Lungren MP. Fusion of medical imaging and electronic health records using deep learning: a systematic review and implementation guidelines. NPJ Digit Med 2020;3:136. doi: 10.1038/s41746-020-00341-z
123. Acosta JN, Falcone GJ, Rajpurkar P, Topol EJ. Multimodal biomedical AI. Nat Med 2022;28:1773–1784. doi: 10.1038/s41591-022-01981-2
124. Lipkova J, Chen RJ, Chen B, Lu MY, Barbieri M, Shao D, et al. Artificial intelligence for multimodal data integration in oncology. Cancer Cell 2022;40(10):1095–1110. doi: 10.1016/j.ccell.2022.09.012
125. Esses SJ, Lu X, Zhao T, Shanbhogue K, Dane B, Bruno M, Chandarana H. Automated image quality evaluation of T_2-weighted liver MRI utilizing deep learning architecture. J Magn Reson Imaging 2018;47(3):723–728. doi: 10.1002/jmri.25779
126. Küstner T, Liebgott A, Mauch L, Martirosian P, Bamberg F, Nikolaou K, et al. Automated reference-free detection of motion artifacts in magnetic resonance images. Magn Reson Mater Phy 2018;31:243–256. doi: 10.1007/s10334-017-0650-z
127. Kickingereder P, Isensee F, Tursunova I, Petersen J, Neuberger U, Bonekamp D, et al. Automated quantitative tumour response assessment of MRI in neuro-oncology with artificial neural networks: a multicentre, retrospective study. Lancet Oncol 2019;20(5):728–740. doi: 10.1016/S1470-2045(19)30098-1
128. Jin C, Yu H, Ke J, Ding P, Yi Y, Jiang X, et al. Predicting treatment response from longitudinal images using multi-task deep learning. Nat Commun 2021;12:1851. doi: 10.1038/s41467-021-22188-y
129. Muehlematter UJ, Daniore P, Vokinger KN. Approval of artificial intelligence and machine learning-based medical devices in the USA and Europe (2015–20): a comparative analysis. Lancet Digit Health 2021;3(3):e195–e203. doi: 10.1016/S2589-7500(20)30292-2
130. Wu E, Wu K, Daneshjou R, Ouyang D, Ho DE, Zou J. How medical AI devices are evaluated: limitations and recommendations from an analysis of FDA approvals. Nat Med 2021;27:582–584. doi: 10.1038/s41591-021-01312-x
131. van Leeuwen KG, Schalekamp S, Rutten MJCM, van Ginneken B, de Rooij M. Artificial intelligence in radiology: 100 commercially available products and their scientific evidence.

Eur Radiol 2021;31:3797–3804. doi: 10.1007/s00330-021-07892-z
132. Kelly CJ, Karthikesalingam A, Suleyman M, Corrado G, King D. Key challenges for delivering clinical impact with artificial intelligence. BMC Med 2019;17:195. doi: 10.1186/s12916-019-1426-2
133. Kim DW, Jang HY, Kim KW, Shin Y, Park SH. Design characteristics of studies reporting the performance of artificial intelligence algorithms for diagnostic analysis of medical images: results from recently published papers. Korean J Radiol 2019;20(3):405–410. doi: 10.3348/kjr.2019.0025
134. Yu AC, Mohajer B, Eng J. External validation of deep learning algorithms for radiologic diagnosis: a systematic review. Radiol Artif Intell 2022;4(3):e210064. doi: 10.1148/ryai.210064
135. Zech JR, Badgeley MA, Liu M, Costa AB, Titano JJ, Oermann EK. Variable generalization performance of a deep learning model to detect pneumonia in chest radiographs: a cross-sectional study. PLoS Med 2018;15(11):e1002683. doi: 10.1371/journal.pmed.1002683
136. Willemink MJ, Koszek WA, Hardell C, Wu J, Fleischmann D, Harvey H, et al. Preparing medical imaging data for machine learning. Radiology 2020;295(1):4–15. doi: 10.1148/radiol.2020192224
137. Guan H, Liu M. Domain adaptation for medical image analysis: a survey. IEEE Trans Biomed Eng 2022;69(3):1173–1185. doi: 10.1109/TBME.2021.3117407
138. Chen RJ, Lu MY, Chen TY, Williamson DFK, Mahmood F. Synthetic data in machine learning for medicine and healthcare. Nat Biomed Eng 2021;5:493–497. doi: 10.1038/s41551-021-00751-8
139. Sheller MJ, Edwards B, Reina GA, Martin J, Pati S, Kotrotsou A, et al. Federated learning in medicine: facilitating multi-institutional collaborations without sharing patient data. Sci Rep 2020;10:12598. doi: 10.1038/s41598-020-69250-1
140. Dayan I, Roth HR, Zhong A, Harouni A, Gentili A, Abidin AZ, et al. Federated learning for predicting clinical outcomes in patients with COVID-19. Nat Med 2021;27:1735–1743. doi: 10.1038/s41591-021-01506-3
141. Rieke N, Hancox J, Li W, Milletarì F, Roth HR, Albarqouni S, et al. The future of digital health with federated learning. NPJ Digit Med 2020;3:119. doi: 10.1038/s41746-020-00323-1
142. Kaissis GA, Makowski MR, Rückert D, Braren RF. Secure, privacy-preserving and federated machine learning in medical imaging. Nat Mach Intell 2020;2:305–311. doi: 10.1038/s42256-020-0186-1
143. Seyyed-Kalantari L, Zhang H, McDermott MBA, Chen IY, Ghassemi M. Underdiagnosis bias of artificial intelligence algorithms applied to chest radiographs in under-served patient populations. Nat Med 2021;27:2176–2182. doi: 10.1038/s41591-021-01595-0
144. Gichoya JW, Banerjee I, Bhimireddy AR, Burns JL, Celi LA, Chen LC, et al. AI recognition of patient race in medical imaging: a modelling study. Lancet Digit Health 2022;4(6):e406–e414. doi: 10.1016/S2589-7500(22)00063-2
145. Selvaraju RR, Cogswell M, Das A, Vedantam R, Parikh D, Batra D. Grad-CAM: visual explanations from deep networks via gradient-based localization. In: Proceedings of the IEEE International Conference on Computer Vision (ICCV); 2017. p. 618–626. doi: 10.1109/ICCV.2017.74
146. Reyes M, Meier R, Pereira S, Silva CA, Dahlweid FM, von Tengg-Kobligk H, et al. On the interpretability of artificial intelligence in radiology: challenges and opportunities. Radiol Artif Intell 2020;2(3):e190043. doi: 10.1148/ryai.2020190043
147. van der Velden BHM, Kuijf HJ, Gilhuijs KGA, Viergever MA. Explainable artificial intelligence (XAI) in deep learning-based medical image analysis. Med Image Anal 2022;79:102470. doi: 10.1016/j.media.2022.102470
148. Mongan J, Moy L, Kahn CE Jr. Checklist for Artificial Intelligence in Medical Imaging (CLAIM): a guide for authors and reviewers. Radiol Artif Intell 2020;2(2):e200029. doi: 10.1148/ryai.2020200029
149. Tejani AS, Klontzas ME, Gatti AA, Mongan JT, Moy L, Park SH, et al. Checklist for Artificial Intelligence in Medical Imaging (CLAIM): 2024 update. Radiol Artif Intell 2024;6(4):e240300. doi: 10.1148/ryai.240300
150. Collins GS, Moons KGM, Dhiman P, Riley RD, Beam AL, Van Calster B, et al. TRIPOD+AI statement: updated guidance for reporting clinical prediction models that use regression or machine learning methods. BMJ 2024;385:e078378. doi: 10.1136/bmj-2023-078378
151. Liu X, Cruz Rivera S, Moher D, Calvert MJ, Denniston AK; SPIRIT-AI and CONSORT-AI Working Group. Reporting guidelines for clinical trial reports for interventions involving artificial intelligence: the CONSORT-AI extension. Nat Med 2020;26:1364–1374. doi: 10.1038/s41591-020-1034-x
152. Vasey B, Nagendran M, Campbell B, Clifton DA, Collins GS, Denaxas S, et al. Reporting guideline for the early-stage clinical evaluation of decision support systems driven by artificial intelligence: DECIDE-AI. Nat Med 2022;28:924–933. doi: 10.1038/s41591-022-01772-9
153. Lekadir K, Frangi AF, Porras AR, Glocker B, Cintas C, Langlotz CP, et al. FUTURE-AI: international consensus guideline for trustworthy and deployable artificial intelligence in healthcare. BMJ 2025;388:e081554. doi: 10.1136/bmj-2024-081554
154. Liu X, Faes L, Kale AU, Wagner SK, Fu DJ, Bruynseels A, et al. A comparison of deep learning performance against health-care professionals in detecting diseases from medical imaging: a systematic review and meta-analysis. Lancet Digit Health 2019;1(6):e271–e297. doi: 10.1016/S2589-7500(19)30123-2
155. Aggarwal R, Sounderajah V, Martin G, Ting DSW, Karthikesalingam A, King D, et al. Diagnostic accuracy of deep learning in medical imaging: a systematic review and meta-analysis. NPJ Digit Med 2021;4:65. doi:10.1038/s41746-021-00438-z
156. Nagendran M, Chen Y, Lovejoy CA, Gordon AC, Komorowski M, Harvey H, et al. Artificial intelligence versus clinicians: systematic review of design, reporting standards, and claims of deep learning studies. BMJ 2020;368:m689. doi: 10.1136/bmj.m689
157. Bluemke DA, Moy L, Bredella MA, Ertl-Wagner BB, Fowler KJ, Goh VJ, et al. Assessing radiology research on artificial intelligence: a brief guide for authors, reviewers, and readers-from the Radiology Editorial Board. Radiology 2020;294(3):487–489. doi: 10.1148/radiol.2019192515

***Corresponding author**: Dr. Rowa Aljondi. E-mail: rmaljondi@uj.edu.sa*

International Journal of Biomedicine 16(4) (2026) 455-461
http://dx.doi.org/10.21103/Article16(4)_RA4

REVIEW ARTICLE

INTERNATIONAL JOURNAL OF BIOMEDICINE

Microtubular Organization and Dynamics: Synthetic Chemistry, Chemical Biology, Biotechnology, Medicine and Biomedicine Perspectives

Zahir Hussain[1*]

[1]*Department of Physiology, Faculty of Medicine, Umm Al-Qura University, Makkah 21955, Saudi Arabia*

Abstract

Microtubules are important cytoskeletal structures that provide mechanical support, motility, intracellular transport, chromosome segregation, and cytoplasmic organization. They participate in several cellular processes related to intracellular transport, including the movement of organelles, mRNA, secretory vesicles, and macromolecular assemblies within the cell. The structure and organization of microtubules have been elaborated in the present article with illustrations of tubulin heterodimers, protofilaments forming a single linear chain, a longitudinal side view showing a stable structural lattice, seam, and the cross-sectional view of parallel protofilaments. The structure and organization of microtubules have been described using information on structural polarity, nucleation, polymerization, and dynamics. Furthermore, some basic concepts regarding the interaction between microtubules and ion channels and biochemicals have also been included. Some of the unsolved issues about the basic concepts have been pointed out. The present review, in general, provides information on microtubular organization and dynamics from the perspectives of synthetic chemistry, chemical biology, synthetic biology, biotechnology, and medicine/biomedicine. Future studies will clarify the unresolved issues related to microtubular structure, organization, dynamics, and interactions with ion channels and biochemical/physiological/pathophysiological factors. **(International Journal of Biomedicine. 2026;16(4):455-461.)**

Keywords: microtubular structure • organization and dynamics • nucleation • polymerization • ion-channels • biochemicals

For citation: Hussain Z. Microtubular Organization and Dynamics: Synthetic Chemistry, Chemical Biology, Biotechnology, Medicine and Biomedicine Perspectives. International Journal of Biomedicine. 2026;16(4):455-461. doi:10.21103/Article16(4)_RA4

Abbreviations

CS, chitosan; **GDP,** guanosine diphosphate; **GTP,** guanosine triphosphate; **γ-TuRC,** γ-tubulin ring complex; **Hcy,** homocysteine; **ILs,** interleukins; **ITZ,** itraconazole; **MTOC,** m**icrotubule organizing center; PLEKHA7,** pleckstrin homology domain-containing family-A member-7; **ST-CS,** N-stearoyl chitosan; **TRP channels,** transient receptor potential channels; **TRPM8:** transient receptor potential melastatin-8; **VitD,** vitamin D.

Introduction

The cytoskeleton is a structural network in the cell's cytoplasm, and microtubules are part of it. Microtubules are important cytoskeletal structures that provide mechanical support, motility, intracellular transport, chromosome segregation, and cytoplasmic organization.[1] These structures are present in cilia and flagella.[2] Microtubules are rigid filaments, but hollow tube-like cylinders made up of biopolymers of globular tubulin proteins. They form the internal structural framework of eukaryotic cells. They serve as microscopic roadways for intracellular transport and are involved in structural support, maintaining the shape of the cell, and separating the chromosomes into two daughter cells during cell division by forming the mitotic spindle.[3] They are considered the tracks for the walk of motor proteins kinesin and dynein for the transport of materials, including the movement of the organelles and vesicles in the cell. Growth and shrinkage of microtubules generate force.

Microtubules bind to many proteins, including the motor proteins (dynein and kinesin), the microtubule-binding protein katanin, and a variety of proteins involved in regulating microtubular dynamics.[4] They take part in several cellular processes related to intracellular transport,

© 2026 The Author(s). *International Journal of Biomedicine* is published by IMRDC.
This is an open access article under the CC BY-NC-ND 4.0 license.

including the movement of organelles, mRNA, secretory vesicles, and macromolecular assemblies in the cell.[3,5,6]Their mechanics influence cellular and molecular processes, as well as cell morphology.[7] The cell locomotion associated with microtubule-like processes observed quite early was confirmed later with biochemical techniques and electron microscopy.[8] Microtubules are termed neurotubules during the development of neurons, and they can control the dynamics of actin, which is another cytoskeletal component.[9]

The cell types have variations in microtubular organization. Sites of cell-cell contacts and their organization along the apical-basal axis for microtubular minus ends in epithelia, and, after nucleation, the release of minus-end re-anchoring in peripheral areas by ninein, PLEKHA7 (Pleckstrin homology domain-containing family-A member-7), etc.,[10]help transport vesicles, organelles, proteins, etc., along the apical-basal axis. Microtubules in fibroblasts and mesenchymal cells anchor at the centrosome and spread with plus ends towards the periphery of the cell, helping in cell migration.

There is a significant role for membrane potentials,[11-18] membrane interactions,[19,20] ion channels,[21-25] and a variety of physiological/biochemical factors in various diseases/disease conditions.[26-33] Interaction of the ion channels occurs with the microtubules for transport and other functions. At the same time, the physiological/pathophysiological variables influence the structure, organization, dynamics, and activity of microtubules. The present review provides important information on microtubular organization and dynamics, employing concepts and modern techniques and methods from synthetic chemistry, chemical biology, synthetic biology, biotechnology, medicine, and biomedicine.

Structure and Organization of Microtubules

Microtubules are long, rigid, and hollow cylinders composed of α- and β-tubulin dimers. The microtubules have a lumen or inner hollow space. Almost 50% of the amino acids are identical in the α and β types of tubulins. The molecular weight of each of them is about 50 kDa. The fundamental microtubular subunit is a dimer composed of two globular proteins (alpha-tubulin and beta-tubulin) that are tightly bound to each other (Fig. 1). In other words, tubulin heterodimers are fundamental building blocks of microtubules, composed of alpha- and beta-tubulin polypeptides linked noncovalently.[34-36]

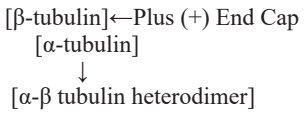

Fig. 1. *Tubulin heterodimers.*

Each heterodimer weighs 55 kDa and consists of closely related globular alpha and beta monomers. They have asymmetric nucleotide-binding protein surface pockets: alpha tubulin on the N-site (tightly and non-exchangeably/non-hydrolyzably binds GTP (guanosine triphosphate)), and beta tubulin on the E-site (reversibly binds GTP for hydrolyzing it to GDP exchangeably).[36]

The protofilament is a linear chain of repeating tubulin heterodimers end-to-end, forming a long string; the linear protofilaments are formed by polymerization of α/β-tubulin dimers, forming a single microtubule. The addition of further α/β-tubulin dimers may then extend this microtubule. Their stacking is always in the same direction: alpha matches up with beta, and the directional orientation or polarity is established by the filament (Fig. 2). When viewed from the side, a stable structural lattice is observed, formed by the hollow interior and the repeating dimers (Fig. 3).

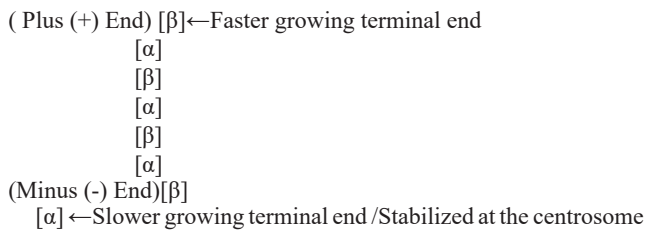

Fig. 2. *Protofilaments forming single linear chain.*

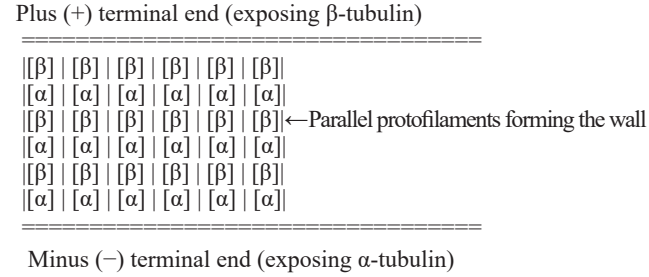

Fig. 3. *Longitudinal side view showing a stable structural lattice*

The microtubule, forming a hollow cylinder of protofilaments in cross section, is seen as a ring structure of 13 protofilaments (1-13 linear protofilaments forming the tube wall), containing alpha- and beta-tubulins alternatively in a circular geometry. Instead of the perfect alternation, the alpha subunits touch the alpha subunits laterally between the 7th and 8th protofilaments, creating a seam (Fig. 4).

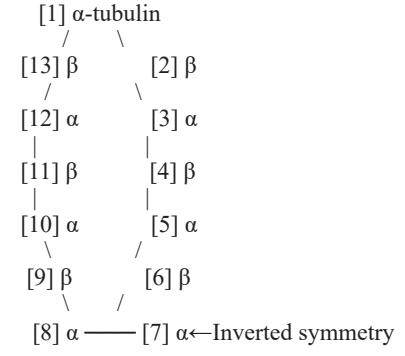

Fig. 4. *Seam-a ring containing a standard 13-protofilament microtubule.*

To form the hollow wall of a microtubule, 13 protofilaments, aligned in parallel, typically align side by side, representing alternative alpha and beta subunits (Fig. 5).

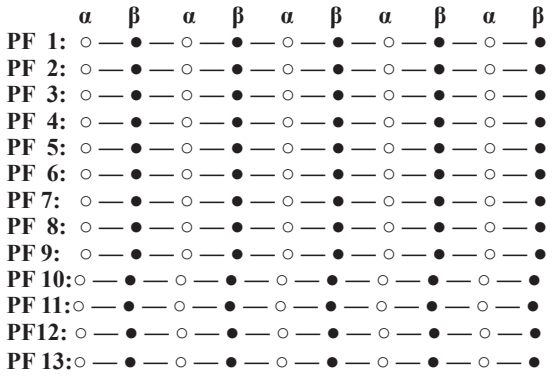

Fig. 5. *Cross-sectional view of parallel protofilaments.*

Each protofilament is made of a string of α-tubulin and β-tubulin. Thirteen parallel protofilaments, aligned side by side, wrap around each other and form a hollow, straw-like tube or standard microtubule, though fewer or more protofilaments in microtubules have been observed.[37]

The elongation at the plus (+) end (with exposed β-subunits of a tubulin dimer) is rapid compared with that at the minus (-) end (with exposed α-subunits of a tubulin dimer). In other words, α-subunits are exposed in one end, whereas β-subunits are exposed in the other end in a protofilament. Furthermore, protofilaments bundle in parallel with the same polarity.[38]

Side-by-side or lateral association or bonding of protofilaments forms a sheet that rolls up to assemble a cylindrical microtubule wall.[37] Resultantly, the association between adjacent protofilaments provides the required structural rigidity and strength to the microtubules.

Table 1.

Structure and organization of microtubules.

Structures/ structural features	Specific characteristics/structural organization
Subunits	Alpha and beta tubulins; they bind together non-covalently and form the building block of microtubules
Protofilaments	Head-to-tail assembly of the tubulin dimers forming thirteen linear/ parallel protofilaments that associate linearly and make a hollow wall of the tube of each microtubule
Associated regulatory motors	Kinesins and dyneins are associated regulatory motor proteins that move along microtubules using ATP hydrolysis to transport vesicles and organelles. Kinesins (anterograde motors) move to the plus (+) terminal end, and the dyneins (retrograde) move to the minus (-) terminal end
Structural polarity	Fast growing/dynamic plus (+) end is terminated by beta-tubulin, whereas the anchored, stabilized, and slow-growing minus (-) end is terminated by alpha-tubulin
Tube dimension	Length may vary from a few hundred nanometers to several micrometers, whereas the inner lumen diameter is around 15 nanometers and the outer diameter is about 25 nanometers
Dynamics of assembly (instability)	Rapid growth or polymerization and sudden shrinkage or depolymerization, in a continuous cycle, are driven by GTP (guanosine triphosphate) binding and hydrolysis on beta-tubulin, manifesting dynamic instability. Catastrophe is the rapid disassembly.
Nucleation and anchoring	The minus (-) ends are anchored, e.g., at the centrosome (microtubule organizing center) by gamma-tubulin ring complexes, which serve as templates for assembly.

Table 2.

Structural polarity.

Structure/related features	Minus (-) terminal end	Positive (+) terminal end
Terminal subunits	Alpha-tubulin exposed	Beta-tubulin exposed
Anchor	At MTOC in centrosome	Cell periphery/ outward
Growth rate	Stable, slow growing	Rapidly grows and shrinks/dynamic
GTP cap	Locked/protected from disassembly	Active growth present stabilizing GTP cap
Instability	Low level of activity as it is stable/dormant	Constant transitions showing high activity in sudden catastrophe & rescue periods
Motor proteins	Dyneins (retrograde)	Kinesins (anterograde)
Nucleation	Capped/stabilized by gamma-tubulin ring complexes	Freely performs rapid elongation

The Pseudo-helical structure forms via lateral bonding of protofilaments, in which one turn of the helix contains 13 tubulin dimers from different protofilaments.[39] However, the microfilaments can have other forms, e.g., helical filaments in protists.[40]

Two types of lattices can appear in the subunits of the lateral protofilaments in a microtubule. These are A-type and B-type. If protofilaments bond between adjacent α and β-subunits of tubulin, this constitutes an A-type lattice. If the α and β subunits from one protofilament associate with the α and β subunits from another adjacent protofilament, it is a type-2 lattice, the primary microtubular arrangement.[41] Nucleation and Polymerization

The critical, rate-limiting first step in the formation of microtubules, when α- and β-tubulin dimers aggregate into a nucleus or initial seed that supports rapid filament polymerization, is called microtubule nucleation.[42] Microtubule nucleation starts the formation of microtubules under the well-organized system- microtubule organizing centers (MTOCs) that contain another tubulin-γ-tubulin (different from α- and β-tubulin subunits), which forms a structure called the γ-tubulin ring complex (γ-TuRC) for starting the polymerization by acting as a template for α/β-tubulin dimers and serving as a cap at the minus end where the growth of microtubules continues on the plus side and away from the MTOC.

The Golgi bodies can also act as a nucleation platform for microtubules.[43] However, centrosomes are considered the primary MIOC in most cells; e.g., MTOCs for cilia and flagella are located at their bases, called basal bodies. Centrosome nucleation is symmetrical inherently. However, the Golgi-related nucleation presents asymmetry. Furthermore, augmin, a protein complex, is an important factor in centrosome-associated microtubule formation and binds γ-TuRC to increase microtubule density around the mitotic spindle origin.[44] Interaction of α- and β-tubulin dimers occurs during the microtubular nucleation process, forming a stable seed (the start of microtubule polymerization via elongation, enabling the rapid attachment of additional dimers to form the hollow, cylindrical microtubules).

Dynamics of Microtubules

To exhibit the dynamics, the ends of a microtubule rapidly switch back and forth dynamically between growing (assembly) and shrinking (disassembly).[45] Tubulin dimers bind two GTP molecules (non-exchangeable alpha-tubulin site and exchangeable beta -tubulin site). Still, the GDP on the beta-tubulin subunit is hydrolyzed after the dimer joins the growing microtubule.

During polymerization, tubulin dimers are GTP (guanosine-5'-triphosphate)-bound to the beta-tubulin subunit, enabling the stable addition and growth of microtubular structures with dynamic instability.[46] The GTP bound to α-tubulin serves as a non-exchangeable, permanent, and non-hydrolyzable structure, and is stable, playing a structural role (maintaining the proper shape/integrity of the tubulin heterodimer) in this bound state. The assembly properties of GDP-tubulin differ from those of GTP-tubulin: GDP-tubulin falls apart, shrinking the cell's internal skeleton; in other words, it is more prone to depolymerization. In contrast, GTP-tubulin is involved in its assembly and growth.[47]

A catastrophe, or the switch from growth to shrinkage, is a sudden moment when a growing skeletal tube or microtubule stops elongating and begins to fall apart. Whereas the rescue is a process when GTP-bound tubulin begins adding again to the tip of the microtubule and a sudden transition of the microtubule occurs from shrinking to a growing state again.[48] Interactions of Microtubules with Ion Channels and Biochemicals

The microtubules and transient receptor potential (TRP) channels exhibit and maintain a bidirectional physical and functional interaction that controls cellular signaling, channel gating, and cytoskeletal dynamic properties. [21-23,49-53] Microtubules interact with the inner surface of the membrane and help in the regulation of membrane potentials.[25 The interaction among] microtubules, transient receptor potential melastatin-8 (TRPM8) ion channels, and testosterone is involved in regulating sensory transduction, non-genomic hormonal signaling, and cell trafficking.[54-59]

Voltage-gated sodium channels are regulated by microtubules, which serve as intracellular tracks for channel trafficking and anchor them to specific domains of the cell membrane.[60] It was found that the tracking proteins of the plus end of microtubules are important modulators for cardiac sodium channels/ arrhythmogenesis.[60] Regarding the association of voltage-gated sodium channels with microtubules, the electrostatic forces and hydrogen bonding were found to be significantly involved in several medical disorders.[61-63]

Various biochemical factors in medical disorders are associated with structural changes, organization, and dynamics. Some of those are, insulin in diabetes (Shiels et al., 2007),[26] adipokines in diabetes (Kim et al., 2023),[30] interleukins (ILs),[64,65] homocysteine (Hcy),[66-67] vitamin D (VitD),[68,69] cholesterol,[70] adipokines in various medical disorders,[71,72] hepcidin and iron,[73,74] and steroid hormones.[75]

Itraconazole (ITZ) therapy significantly reduces microtubule formation in endothelial cells, which contributes to its efficacy in anti-cancer and anti-angiogenic activities.[76-78] The intersection of itraconazole with N-stearoyl chitosan (ST-CS) was revealed, with the purpose of using chitosan (CS) polymers pharmaceutically as a coating for liposomes for drug delivery of the anti-microtubule agent ITZ for cellular delivery and oncological purposes.[78]

Conclusion

Despite the well-established fundamental concepts regarding the importance of alpha and beta tubulins and how GTP controls dynamic instability, it is still not known how these microtubular subunits regulate complex cellular processes. Furthermore, the structural modifications and alterations at the atomic level occurring in response to physical forces that change the activity of GTPase or the conformation of the lattice are not yet resolved.

In connection with the structural seam, it is not yet clear how the structural discontinuity of the seam occurs and how it is involved in the binding and signaling of certain proteins. As concerns tissue development, the non-centrosomal regulation, along with the exact mechanism by which centrosomes are downregulated, is also not clearly known. Which rules govern the tubulin code have not yet been explored. In vitro 2D cell culture studies of microtubular functions have been conducted. Still, the alterations in microtubular dynamics that occur in 3D tissues in real time, and in 'in vivo' processes/differentiation are largely unexplored. The self-organizational/self-assembly principles governing microtubular linkages under changing stress conditions are not well understood.

A crucial question remains to be solved: how the mechanical load in growing or shrinking microtubules directly influences the conformation of ion channels. Furthermore, there are several other issues in the interaction between microtubules and ion channels. Another complexity is accurately simulating dynamic transitions in multi-subunit ion channels while they interact with the array of non-centrosome microtubules.

The present review provides information on microtubular organization and dynamics from the perspectives of synthetic chemistry, chemical biology, synthetic biology, biotechnology, and medicine/biomedicine. Hopefully, future studies will clarify the unresolved issues related to microtubular structure, organization, dynamics, and dynamic interactions with ion channels, as well as biochemical/physiological-pathophysiological variations.

Sources of Funding

This research received no external funding.

Conflicts of Interest

The author declares no conflicts of interest.

Author Contribution Statement

The author confirms responsibility for the conceptualization, design, review, editing, and final writing of the present manuscript.

Acknowledgements

The author expresses sincere appreciation to his students who gathered the lecture records and helped compile this article.

Dedication

The author dedicates this article to the loving memory of his mentor and first postdoctoral advisor, Dr. W. McIntyre (Mac) Burnham, Professor Emeritus in the Department of Pharmacology and Toxicology, Temerty Faculty of Medicine, University of Toronto. The author had the privilege of conducting research and collaborating on several funded programs in Dr. Burnham's laboratory, beginning with a postdoctoral fellowship from January 10 to December 31, 1995.

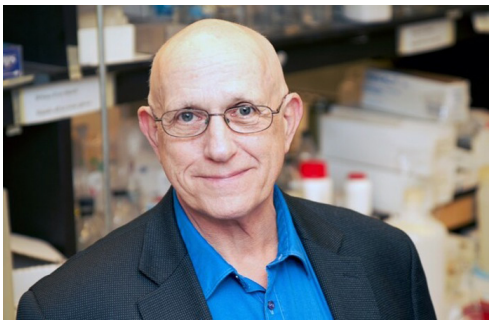

Professor Willets McIntyre (Mac) Burnham (Chicago, 1939 – Toronto, 2024), B.A., Ph.D. Renowned neuropharmacologist, electrophysiologist, neuropsychopharmacologist, epileptologist, and Professor Emeritus, Department of Pharmacology & Toxicology, Temerty Faculty of Medicine, University of Toronto

References

1. Logan CM, Menko AS. Microtubules: Evolving roles and critical cellular interactions. Exp Biol Med (Maywood). 2019;244(15):1240-54.
2. Owa M, Uchihashi T, Yanagisawa HA, Yamano T, Iguchi H, Fukuzawa H, et al. Inner lumen proteins stabilize doublet microtubules in cilia and flagella. Nat Commun. 2019;10(1):1143.
3. Vale RD. The molecular motor toolbox for intracellular transport. Cell. 2003;112(4):467-80.
4. Howard J, Hyman AA. Microtubule polymerases and depolymerases. Curr Opin Cell Biol. 2007;19(1):31-5.
5. Barlan K, Gelfand VI. Microtubule-Based Transport and the Distribution, Tethering, and Organization of Organelles. Cold Spring Harb Perspect Biol. 2017;9(5):a025817.
6. Yildiz A. Sorting out microtubule-based transport. Nat Rev Mol Cell Biol. 2021;22(2):73.
7. Hawkins T, Mirigian M, Selcuk Yasar M, Ross JL. Mechanics of microtubules. J Biomech. 2010;43(1):23-30. Erratum in: J Biomech. 2011;44(9):1829-30.
8. Wayne R. Plant Cell Biology: From Astronomy to Zoology Archived 2024-02-21 at the Wayback Machine. Amsterdam: Elsevier/Academic Press, p. 165. 2009.
9. Zhao B, Meka DP, Scharrenberg R, König T, Schwanke B, Kobler O, et al. Microtubules Modulate F-actin Dynamics during Neuronal Polarization. Sci Rep. 2017;7(1):9583.
10. Bartolini F, Gundersen GG. Generation of noncentrosomal microtubule arrays. J Cell Sci. 2006;119(Pt 20):4155-63.
11. Hussain Z, Cottrell GA, Burnham WM. Determination of after-discharge threshold elicited by amygdala stimulation. The Aga Khan University Fourth Annual National symposium on Role of Neurosciences in Health, Education and research, Karachi. 1997.
12. Ratushnyak AS, Zapara TA, Zharkikh AA, Ratushnyak OA. Effects of changes in dynamic equilibrium in microtubule and microfilament systems on the plastic responses of neurons. Neurosci Behav Physiol. 1997;27(4):353-9.
13. Rutherford LC, DeWan A, Lauer HM, Turrigiano GG. Brain-derived neurotrophic factor mediates the activity-dependent regulation of inhibition in neocortical cultures. J Neurosci. 1997;17(12):4527-35.
14. Hussain Z, Backx PH. Effects of lidocaine on sodium

channels with altered inactivation properties.34th Annual Medical Symposium, JPMC, Karachi. 1997.
15. Abdul Kadir L, Stacey M, Barrett-Jolley R. Emerging Roles of the Membrane Potential: Action Beyond the Action Potential. Front Physiol. 2018;9:1661.
16. Pokorný J, Pokorný J, Vrba J. Generation of Electromagnetic Field by Microtubules. Int J Mol Sci. 2021;22(15):8215.
17. Hussain Z. Electrophysiology of membrane potentials: mathematical physiology and mathematical medicine perspectives. Int J Biol Biotech. 2022; 19 (2): 161-70.
18. Nasilli G, Lin X, Swiatlowska P, Meraviglia V, Pérez-Hernández M, Zhang M, et al. Decreasing Microtubule Detyrosination Improves Cardiac Mechanics and Sodium Channel Function in Arrhythmogenic Cardiomyopathy. Circ Arrhythm Electrophysiol. 2026;19(7):e014354.
19. Matias C, Hussain MH, Hussain Z. Lipid membrane-estrogen interaction: molecular and biophysical perspective: A mini overview. International Journal of Biology Research. 2017; 5 (2): 35-42.
20. Hussain Z. Membrane lipid-estrogen interaction and management of medical disorders: biophysical medicine. Gomal Journal of Medical Sciences. 2025a; 23 (1 Special), 181-86.
21. Wu Y, Dai X-Q, Li Q, Chen CX, Mai W, Hussain Z, et al. Kinesin-2 mediates physical and functional interactions between polycystin-2 and fibrocystin. Hum Mol Genet. 2006;15(22):3280-92.
22. Li Q, Dai XQ, Shen PY, Wu Y, Long W, Chen CX, et al. Direct binding of alpha-actinin enhances TRPP3 channel activity J Neurochem. 2007;103(6):2391-2400.
23. Goswami C, Hucho T. Submembraneous microtubule cytoskeleton: biochemical and functional interplay of TRP channels with the cytoskeleton. FEBS J. 2008;275(19):4684-99.
24. Hussain Z, Zahir H. Sodium channels, neurosteroid receptors and physiochemical and ischemic changes in a kindling model of epilepsy in rat. Symposium JPMC, Karachi. 2012.
25. Cantero MDR, Villa Etchegoyen C, Perez PL, Scarinci N, Cantiello HF. Bundles of Brain Microtubules Generate Electrical Oscillations. Sci Rep. 2018;8(1):11899.
26. Shiels H, O'Connell A, Qureshi MA, Howarth FC, White E, Calaghan S. Stable microtubules contribute to cardiac dysfunction in the streptozotocin-induced model of type 1 diabetes in the rat. Mol Cell Biochem. 2007;294(1-2):173-80.
27. Sohail S, Hussain Z. Electrolyte and cholesterol variations in patients with diabetes mellitus.. 35th All Pak Sc Conf, Genomics for Health and Prosperity, University of Karachi. 2008.
28. Naz L, Hussain Z, Husain T. Risk factors and biochemical variations in patients with ischemic stroke. Int J Biol Biotech. 2009;6 (1-2):83-87.
29. Sohail S, Javaid A, Khan TA, Zahir H, Hussain Z. Diabetes mellitus, obesity and adipocytokines: Pathophysiological perspectives. Int J Biol Biotech. 2019;16 (2): 325-39.
30. Kim J, Oh CM, Kim H. The Interplay of Adipokines and Pancreatic Beta Cells in Metabolic Regulation and Diabetes. Biomedicines. 2023;11(9):2589.
31. Hussain Z. Correlation of Serum Homocysteine, Interleukin-6 and Cholesterol in Overweight Women of Reproductive Age Group with Type 2 Diabetes Mellitus: A Case-control Study. Journal of Clinical and Diagnostic Research. 2025b;19 (4):CC06-CC12.
32. Hussain Z. Comparative analysis of IL-6, hepcidin, homocysteine and cholesterol in normal-weight and overweight diabetic and non-diabetic adult men. Rawal Medical Journal. 2026a; 51 (2):374-78.
33. Malki MS, Babateen O, Hussain Z, Tawakul A, Subahi A, Obaid AA, et al. Low-Frequency Episodic Migraine with Aura and Associated Hypertension in Overweight Postmenopausal Women: Interplay of Serum Interleukin-6 and Vitamin D. Medicina-Lithuania. (Preprints) 2026; 2026011619.
34. Tian G, Cowan NJ. Tubulin-specific chaperones: components of a molecular machine that assembles the α/β heterodimer. Methods Cell Biol. 2013;115:155-71.
35. Montecinos-Franjola F, Chaturvedi SK, Schuck P, Sackett DL. All tubulins are not alike: Heterodimer dissociation differs among different biological sources. J Biol Chem. 2019;294(26):10315-324.
36. Wethekam LC, Moore JK. αβ-tubulin heterodimers: Origins and regulation of microtubule building blocks. Mol Biol Cell. 2026;37(1):re1.
37. Chaaban S, Brouhard GJ. A microtubule bestiary: structural diversity in tubulin polymers. Mol Biol Cell. 2017;28(22):2924-31.
38. Goodson HV, Jonasson EM. Microtubules and Microtubule-Associated Proteins. Cold Spring Harb Perspect Biol. 2018;10(6):a022608.
39. Sui H, Downing KH. Structural basis of interprotofilament interaction and lateral deformation of microtubules. Structure. 2010;18(8):1022-31.
40. Bassen DM, Hou Y, Bowser SS, Banavali NK. Maintenance of electrostatic stabilization in altered tubulin lateral contacts may facilitate formation of helical filaments in foraminifera. Sci Rep. 2016;6:31723.
41. Nogales E. Structural insights into microtubule function. Annu Rev Biochem. 2000; 69:277-302.
42. Roostalu J, Surrey T. Microtubule nucleation: beyond the template. Nat Rev Mol Cell Biol. 2017;18(11):702-10.
43. Vinogradova T, Miller PM, Kaverina I. Microtubule network asymmetry in motile cells: role of Golgi-derived array. Cell Cycle. 2009;8(14):2168-74.
44. Uehara R, Nozawa RS, Tomioka A, Petry S, Vale RD, Obuse C, et al. The augmin complex plays a critical role in spindle microtubule generation for mitotic progression and cytokinesis in human cells. Proc Natl Acad Sci U S A. 2009;106(17):6998-7003.
45. Karp G. Cell and Molecular Biology: Concepts and Experiments. USA: John Wiley & Sons. p. 355. ISBN 978-0-471-46580-5. 2005.
46. Weisenberg RC. Microtubule formation in vitro in solutions containing low calcium concentrations. Science. 1972;177(4054):1104-5.
47. Weisenberg RC, Deery WJ, Dickinson PJ. Tubulin-nucleotide interactions during the polymerization and depolymerization of microtubules. Biochemistry. 1976;15(19):4248-54.
48. Mitchison T, Kirschner M. Dynamic instability of microtubule growth. Nature. 1984;312(5991):237-42.
49. Smani T, Dionisio N, López JJ, Berna-Erro A, Rosado JA. Cytoskeletal and scaffolding proteins as structural and functional determinants of TRP channels. Biochim Biophys

Acta. 2014;1838(2):658-64.
50. Hussain Z. Protein-protein interaction for the activity of TRPP2 channels and membrane and cytoskeletal regulation: physiological and mathematical medicine. Int J Biol Biotech. 2025c;22 (4): 901-08.
51. Hussain Z. Polycystin-2 ion-channels: structure and functions in primary cilia. Int J Biol Biotech. 2026b;23 (2): 217-24.
52. Wang Q, Wan W, Zhang H, Zhou T, Shen HM, Huang P, et al. Deacetylation of ATG16L1 is required for LC3-associated lysosomal microautophagy. Autophagy. 2025;21(12):2948-62.
53. Hussain Z, Gondi CS, Demirkhanyan L. Protein-protein interaction between TRPP2 channels and the linking proteins for Ca^{+} regulation: molecular, patch-clamp and planar lipid bilayer electrophysiological and biophysical studies. Int J Biol Biotech. 2025; 22 (3): 483-89.
54. Asuthkar S, Elustondo PA, Demirkhanyan L, Sun X, Baskaran P, Velpula KK, et al. The TRPM8 protein is a testosterone receptor: I. Biochemical evidence for direct TRPM8-testosterone interactions. J Biol Chem. 2015a;290(5):2659-69.
55. Asuthkar S, Demirkhanyan L, Sun X, Elustondo PA, Krishnan V, Baskaran P, et al. The TRPM8 protein is a testosterone receptor: II. Functional evidence for an ionotropic effect of testosterone on TRPM8. J Biol Chem. 2015b;290(5):2670-88.
56. Hussain Z, Demirkhanyan L, Asuthkar S, Zakharian E. Testosterone is a Highly Potent and Specific Agonist of TRPM8. Biophysical Journal. 2017; 110 (3, Supplement 1): p613a.
57. Demirkhanyan L, Krishnan V, Asuthkar S, Alexander B, Hussain Z, Baskaran P, et al. (2018). TRPM8 Regulates Sexual Desire and Satiety. Biophysical Journal. 2018; 114 (3, Supplement 1): p643a.
58. Mohandass A, Krishnan V, Gribkova ED, Asuthkar S, Baskaran P, Nersesyan Y, et al. TRPM8 as the rapid testosterone signaling receptor: Implications in the regulation of dimorphic sexual and social behaviors. FASEB J. 2020;34(8):10887-906.
59. Muthu SJ, Lakshmanan G, Shimray KW, Kaliyappan K, Sathyanathan SB, Seppan P. Testosterone Influence on Microtubule-Associated Proteins and Spine Density in Hippocampus: Implications on Learning and Memory. Dev Neurosci. 2022;44(6):498-507.
60. Marchal GA, Galjart N, Portero V, Remme CA. Microtubule plus-end tracking proteins: novel modulators of cardiac sodium channels and arrhythmogenesis. Cardiovasc Res. 2023;119(7):1461-79.
61. O'Brien JE, Sharkey LM, Vallianatos CN, Han C, Blossom JC, Yu T, et al. Interaction of voltage-gated sodium channel Nav1.6 (SCN8A) with microtubule-associated protein Map1b. J Biol Chem. 2012;287(22):18459-66.
62. Ahmadi S, Achari VM, Hussainb Z, Hashim R. Epimeric and anomeric relationship of octyl- α -D-gluco/galactosides: insight from density functional theory and atom in molecules studies. Computational and Theoretical Chemistry (Amsterdam: Elsevier). 2017; 1108: 93–102.
63. Hussain Z. Sodium channel hydrogen bonding in epilepsy: molecular physiology and biophysics. International Journal of Biology and Biotechnology. 2024a; 21 (1): 45-52.
64. Wareham LK, Echevarria FD, Sousa JL, Konlian DO, Dallas G, Formichella CR, et al. Interleukin-6 promotes microtubule stability in axons via Stat3 protein-protein interactions. iScience. 2021;24(10):103141.
65. Noorwali AA, Hussain Z. Interplay of serum IL-6 and vitamin D in overweight non-anemic reproductive age women with systemic lupus erythematosus. International Journal of Biomedicine. 2026; 16(1): 26-32.
66. Kang YJ. Copper and homocysteine in cardiovascular diseases. Pharmacol Ther. 2011;129(3):321-31.
67. Javaid A, Sohail S, Khan TA, Zahir H, Hussain Z. Ischemic disease and obesity: Plasma Lipids, Homocysteine and Hematological studies. Intern J Biol Biotech. 2019;16 (1): 49-58.
68. Kamimura S, Gallieni M, Zhong M, Beron W, Slatopolsky E, Dusso A. Microtubules mediate cellular 25-hydroxyvitamin D3 trafficking and the genomic response to 1,25-dihydroxyvitamin D3 in normal human monocytes. J Biol Chem. 1995;270(38):22160-6.
69. Hussain Z, Babateen O. Serum Vitamin D and Proinflammatory Markers Correlate Inversely in Overweight Postmenopausal Women with Type-2 Diabetes Mellitus. Pathophysiology. 2025; 32 (2).
70. Li Q, Ferrare JT, Silver J, Wilson JO, Arteaga-Castaneda L, Qiu W, et al. Cholesterol in the cargo membrane amplifies tau inhibition of kinesin-1-based transport. Proc Natl Acad Sci U S A. 2023;120(3):e2212507120.
71. Sohail S, Hussain Z. Pathophysiology of ischemic disorders- Ischemia, adipocytokines and diabetes mellitus. Int J Biol Biotech. 2013; 10 (2): 155-66.
72. Sasankan D, Mohan R. The Mechanobiology of Adipocyte Hypertrophy: Cytoskeletal Remodelling as a Driver of Insulin Resistance in Obesity. Cell Biochem Funct. 2026;44(8):e70283.
73. Goldfarb AN, Freeman KC, Sahu RK, Elagib KE, Holy M, Arneja A, et al. Iron control of erythroid microtubule cytoskeleton as a potential target in treatment of iron-restricted anemia. Nat Commun. 2021;12(1):1645.
74. Hussain Z. Investigating the role of serum hepcidin and interleukin-6 in non-anemic women with acute ischemic stroke. International Journal of Biomedicine. 2024b;14(2):260-64.
75. Sewer MB, Li D. Regulation of steroid hormone biosynthesis by the cytoskeleton. Lipids. 2008;43(12):1109-15.
76. Del Carratore R, Carpi A, Beffy P, Lubrano V, Giorgetti L, Maserti BE, et al. Itraconazole inhibits HMEC-1 angiogenesis. Biomed Pharmacother. 2012;66(4):312-7.
77. Liu R, Li J, Zhang T, Zou L, Chen Y, Wang K, et al. Itraconazole suppresses the growth of glioblastoma through induction of autophagy: involvement of abnormal cholesterol trafficking. Autophagy. 2014;10(7):1241-55.
78. Eh Suk VR, Marlina A, Hussain Z, Misran M. N-Stearoyl Chitosan as a Coating Material for Liposomes Encapsulating Itraconazole. Arabian Journal for Science and Engineering, 2021; 46 (6): 5645-53.

***Corresponding author:** Prof. Dr. Zahir Hussain, PhD. Department of Physiology, Faculty of Medicine, Umm Al-Qura University, Makkah 21955, Saudi Arabia. E-mail: zahirhussa@gmail.com*

International Journal of Biomedicine 16(4) (2026) 462-468
http://dx.doi.org/10.21103/Article16(4)_OA1

ORIGINAL ARTICLE

INTERNATIONAL JOURNAL OF BIOMEDICINE

Clinical and Pathological Characteristics Associated with *BRAF* V600E Mutation in Vietnamese Patients with Papillary Thyroid Carcinoma

Nguyen Thanh Hai[1], Tran Quang Phuc[2], Nguyen Huu Le[3], Nguyen Van Chuyen[4], Nguyen Thi Thu Trang[4], Cao Ba Loi[2*]

[1]*Nghe An Lung Hospital, Nghe An, Vietnam*
[2]*The National Institute of Malariology, Parasitology and Entomology, Hanoi, Vietnam*
[3]*Nghe An Department of Health, Nghe An. Vietnam*
[4]*Department of Military Hygiene, Vietnam Military Medical University, Hanoi, Vietnam*

Abstract

Background: Papillary thyroid carcinoma is the most common type of malignant thyroid tumor. A mutation frequently found in papillary thyroid carcinoma is *BRAF* V600E. This study aimed to determine the prevalence of the *BRAF* V600E mutation and to analyze the association between the *BRAF* V600E mutation and clinicopathological parameters in patients with papillary thyroid carcinoma.

Methods and Results*:* An analytical descriptive study was conducted in 88 patients with thyroid cancer at Nghe An Provincial Endocrinology Hospital. All patients were tested for the *BRAF* V600E mutation using polymerase chain reaction. Clinical and pathological variables, including age, sex, tumor size, multifocality, lymph node metastasis, and thyroid cancer stage, were compared between the *BRAF* V600E (+) and *BRAF* V600E (-) patient groups.

The *BRAF* V600E mutation was detected in 23 cases, accounting for 26.2%. Our study showed that the *BRAF* V600E mutation was statistically associated with tumor size, lymph node metastasis, N stage, and more advanced TNM stage.

Conclusion*:* The *BRAF* V600E mutation is common in papillary thyroid carcinoma and is associated with clinical and pathological factors such as tumor size, lymph node metastasis, N stage, and more advanced TNM stage of papillary thyroid carcinoma. **(International Journal of Biomedicine. 2026;16(4):462-468.)**

Keywords: papillary thyroid carcinoma • mutation • lymph node metastasis • thyroid cancer

For citation: Hai NT, Phuc TQ, Le LH, Chuyen NV, Trang NTT, Loi CB. Clinical and Pathological Characteristics Associated with *BRAF* V600E Mutation in Vietnamese Patients with Papillary Thyroid Carcinoma. International Journal of Biomedicine. 2026;16(4):462-468. doi:10.21103/ Article16(4) OA1

Introduction

Thyroid cancer is the most common endocrine malignancy, and its incidence has increased rapidly worldwide over the past several decades. The incidence of thyroid cancer increased threefold from 4.9 to 14.3 per 100,000 persons during the period from 1975 to 2009.[1] Thyroid cancer includes three main pathological types: differentiated thyroid cancer (DTC), anaplastic thyroid cancer (ATC), and medullary thyroid cancer (MTC). More than 90% of thyroid cancers are DTC. DTC is further divided into two types: papillary thyroid carcinoma (PTC) and follicular thyroid cancer (FTC). Among the four pathological types, papillary thyroid carcinoma is the most common, accounting for 89-90% of all thyroid malignancies.[2] Thyroid cancer has a good prognosis, with a 10-year survival rate of 80-95%. However, 10-20% of thyroid cancer cases develop more severe disease, leading to frequent recurrence and higher mortality rates.[3]

Currently, clinical guidelines have been developed to classify patients into different risk groups. This allows clinicians to adjust treatment more aggressively and to monitor more closely patients considered at high risk. Clinical guidelines are based on pathological risk factors including patient age, sex, comorbidities, tumor size, histological type, lymph node invasion, and extrathyroidal metastasis.[4]

However, risk stratification is often inaccurate, with 15% of tumor recurrences and 10% of thyroid cancer deaths occurring in patients considered to be at low risk. Therefore,

© 2026 The Author(s). *International Journal of Biomedicine* is published by IMRDC.
This is an open access article under the CC BY-NC-ND 4.0 license.

clinicians have attempted to develop better prognostic algorithms, and recently molecular tumor biomarkers have received widespread attention.[5]

Many studies have demonstrated a strong association between the *BRAF* V600E mutation (B-Raf proto-oncogene serine/threonine kinase) and advanced tumor characteristics, extrathyroidal extension, lymph node metastasis, and advanced disease stage (III and IV) in papillary thyroid carcinoma.[6] In contrast, some studies have not demonstrated a significant association between the *BRAF* V600E mutation and clinicopathological characteristics.[7] This controversy has been addressed by larger studies with meta-analyses. These studies have confirmed the association between *BRAF* V600E and advanced tumor characteristics, particularly extrathyroidal extension, lymph node involvement, advanced TNM stages (III and IV), and a higher risk of recurrence.[8,9]

However, the question of whether the *BRAF* V600E mutation represents a poorer prognosis for papillary thyroid carcinoma patients in all regions of the world remains unanswered. This issue has been investigated by only a few authors and with very short follow-up periods. Therefore, the purpose of our study was to analyze *BRAF* V600E mutation status and clarify the association between the *BRAF* V600E mutation and clinicopathological parameters in patients with papillary thyroid carcinoma in Nghe An, Vietnam.

Materials and Methods

Study Design

The study design was analytical and descriptive, and included patients with thyroid cancer from Nghe An Endocrinology Hospital, Vietnam. Data on patient characteristics were collected from individuals undergoing thyroid cancer screening who were subsequently confirmed to have thyroid cancer.

This study was conducted from September 2023 to September 2025. This study was approved by the Ethics Committee of the Institute of Malariology and Parasitology (approval number 1178/QD-VSR dated day 8 month 12 year 2023). All patients provided written consent for all surgical procedures and mutation analyses.

Study Participants

Inclusion criteria: All individuals who attended thyroid disease screening at Nghe An Provincial Endocrinology Hospital, totaling 2,164 patients. Patients were confirmed to have thyroid cancer after clinical examination, diagnostic imaging, preoperative thyroid ultrasonography (US), fine needle aspiration biopsy (FNAB), and other tests. When preoperative findings suggested lymph node metastasis, computed tomography (CT) was performed. The location of the thyroid tumor was divided into four regions: upper third, middle third, lower third, or thyroid isthmus according to ultrasonographic findings.

From the initial group of patients attending thyroid cancer examination and screening, we selected 88 patients who were confirmed to have thyroid cancer. A total of 88 patients with a confirmed diagnosis of thyroid cancer were included in the study based on the following criteria: (1) postoperative gene analysis: *BRAF* V600E mutation; (2) preoperative ultrasonography: ultrasonography was performed at the hospital's ultrasonography department within 1 month before surgery, with complete ultrasonographic descriptions and clear images; and (3) tumor characteristics: diameter ≤ 10 mm and > 10-40 mm. Patients with thyroid cancer agreed to participate in the study and had complete medical records.

Exclusion criteria: Patients were excluded if they refused mutation analysis, had missing clinical data, or had a previous history of another cancer.

Study Variables

Demographic factors (age, sex) and clinicopathological parameters, including tumor size, tumor multifocality, unifocality, lymph node metastasis, location of lymph node metastasis, thyroid cancer stage, and the presence of the *BRAF* V600E mutation, were included in the analysis.

Data Collection

DNA extraction

Tumor tissue and corresponding adjacent normal tissue from thyroid cancer specimens were obtained by thyroidectomy. Tumor DNA was extracted from sections of formalin-fixed paraffin-embedded tissue. DNA purification was performed using the QIAamp DNA Mini Kit (Qiagen, Hilden, Germany) according to the manufacturer's instructions. Tumor areas were manually dissected with a DNA-free scalpel under a microscope to obtain the important portion of the tumor. DNA extraction for PCR analysis was completed.

Detection of the BRAF V600E mutation

BRAF gene mutation analysis was performed on thyroid tumors from paraffin-embedded tissue blocks. Tissue samples were obtained from surgical cases at the Department of Pathology, Nghe An Provincial Endocrinology Hospital.

In cases of unilateral multifocal papillary thyroid carcinoma, analysis was performed on the tumor with the largest diameter, defined as the primary lesion. In patients with bilateral nodules classified as Bethesda V (suspicious for malignancy) or VI (malignant), mutation analysis was performed on tumors from both lobes. The larger tumor was designated as the primary lesion, and the remaining tumor in the contralateral lobe was referred to as the contralateral tumor.

Quantitative real-time PCR technique for BRAF mutation analysis

BRAF V600E mutation analyses were performed by pathologists after surgical treatments of patients. The primers used were: 5'-TCATAATGCTTGCTCTGATAGGA-3' (forward primer) and 5'-GGCCAAAAATTT-ATCAGTGGA-3' (reverse primer). The following steps were performed in the amplification reaction: (1) initial denaturation for 15 seconds at 95°C, (2) annealing for 30 seconds at 57°C, (3) extension for 30 seconds at 72°C, and (4) holding at 4°C. A 2 µL aliquot of the PCR product was electrophoresed on 1% Tris-borate-EDTA (TBE) agarose. The appearance of a band indicated the presence of *BRAF* amplification.

Histopathological diagnosis

The histopathological diagnosis of thyroid cancer was confirmed by experienced physicians based on the current diagnostic criteria of the World Health Organization.[10]

Tumor-node-metastasis (TNM) staging was performed using the eighth edition of the American Joint Committee on Cancer (AJCC) staging system.[11]

Data Analysis

For qualitative variables, data were presented as frequencies and percentages (%).To evaluate associations between variables, bivariate analysis was performed using the Chi-square test when its conditions were met or Fisher's exact test as an alternative. Data analysis was performed using SPSS version 20. Results were presented as p-values. A p-value of less than 0.05 for each test was considered statistically significant. Logistic regression analysis was used to determine whether clinicopathological and ultrasonographic characteristics were independent variables.

Results

Patient Demographic Information

A total of 8 (9%) patients were male, and 80 (91%) patients were female. Age is considered a risk factor in the prognosis of patients with thyroid cancer. According to the TNM staging criteria of the American Thyroid Association, patients were divided at the age of 55 years. Of the 88 patients, 61 (70%) were younger than 55 years, and 27 (30%) were 55 years or older. While 73% of patients had a tumor size ≤ 10 mm, 27% had a tumor size of 10-40 mm. Our study showed that 23 patients with thyroid cancer had the *BRAF* gene mutation, whereas 65 patients were negative for the mutated gene.

Among the 88 patients with thyroid cancer, 35 patients were confirmed to have lymph node metastasis by histopathological results, giving a lymph node metastasis rate of 40%. The status of lymph node metastasis in the central compartment, lateral neck, or both was confirmed by postoperative histopathological results for each patient.

Nineteen patients underwent thyroid lobectomy. While 13 patients underwent total thyroidectomy, 56 patients underwent total thyroidectomy with lymph node dissection.

There were 49 (56%) patients classified as stage I. The remaining patients were classified as stage II and stage III, accounting for 41% and 3%, respectively. Most patients were diagnosed with papillary thyroid carcinoma (94%; 83/88), while the remaining patients were diagnosed with the follicular variant of papillary thyroid carcinoma (5%; 4/88) and follicular thyroid carcinoma (1%; 1/88). Clinical and pathological information from the 88 patients was collected and is presented in Table 1.

Association between the *BRAF* V600E Mutation and Clinicopathological Characteristics in Papillary Thyroid Carcinoma

The clinical and pathological characteristics of thyroid cancers with the *BRAF* mutation were separately compared with those without the mutation (Table 2).

There were 23 cases of the *BRAF* V600E gene mutation in the specimens, yielding a mutation rate of 26.2%. Among patients carrying gene mutation, 18 patients were younger than 55 years, and 5 patients were aged ≥ 55 years. Among

Table 1.

Demographic and clinicopathological characteristics of patients with thyroid cancer.

Variables	Patients' parameters	Total n (%)	Variables	Patients' parameters	Total n (%)
Sex	Male	8 (9)	T stage	T1	68 (77)
	Female	80 (91)		T2	3 (3)
Age	< 55 years	61 (70)		T3b	14 (16)
	≥ 55 years	27 (30)		T4a	3 (3)
Tumor size	≤ 10 mm	64 (73)	N stage	N0	50 (57)
	10-40 mm	24 (27)		N1	35 (40)
Histological variant	Papillary thyroid carcinoma	83 (94)		Nx	3 (3)
	Follicular thyroid carcinoma	1 (1)	M stage	M0	88 (100)
	Follicular variant of papillary thyroid carcinoma	4 (5)		M1	
Lymph node metastasis	Yes	35 (40)	AJCC stage	I	49 (56)
	No	53 (60)		II	36 (41)
Location of lymph node metastasis	Central compartment	25 (67)		III	3 (3)
	Lateral neck	1 (4)	Type of surgery	Thyroid lobectomy	19 (22)
	Both	9 (29)		Total thyroidectomy	13 (15)
Tumor focality	Unifocal	67 (76)		Total thyroidectomy with lymph node dissection	56 (63)
	Multifocal	21 (23)	BRAF V600E	Yes	23 (26)
				No	65 (74)

these patients, 52% had a tumor size ≤ 10 mm and 48% had a tumor size of 10-40 mm. Among the 23 cases with the *BRAF* V600E gene mutation, 91% had lymph node metastasis, with central, lateral neck, and both locations accounting for 67%, 4%, and 29%, respectively. Among the 23 patients, 17 had a single focus, and the remainder had multifocal disease.

Regarding tumor staging, among the 23 patients with the gene mutation, 2 were stage I, 19 were stage II, and 2 were stage III.

Gene sequence data were collected from 88 thyroid tissue samples; we identified *BRAF* V600E mutation status in 22 (96%) patients with papillary thyroid carcinoma and 1 (4%) patient with the follicular variant of papillary thyroid carcinoma.

There was no significant association between *BRAF* V600E positivity and multifocality. Multifocality was slightly higher in the *BRAF* (+) group than in the *BRAF* (-) group; however, the difference was not statistically significant (p=0.771). In our study, females accounted for the majority (91%); however, there was no statistically significant difference between males and females in relation to the *BRAF* V600E mutation.

A notable finding in our study was that the *BRAF* V600E mutation was significantly associated with tumor size, lymph node metastasis, N stage, and a more advanced stage of papillary thyroid carcinoma.

The proportion of *BRAF* V600E-positive patients with tumor sizes of 10-40 mm was higher than that in the negative

Table 2.

Comparison of clinical and pathological parameters according to detection of the BRAF V600E mutation in patients with papillary thyroid carcinoma.

Patients' parameters		BRAF V600E positive n=23 (%)	BRAF V600E negative n=65 (%)	p-value
Sex	Male	3 (13)	5 (8)	0.426
	Female	20 (87)	60 (92)	
Age	< 55 years	18 (78)	43 (66)	0.279
	≥ 55 years	5 (22)	22 (34)	
Tumor size	≤ 10 mm	12 (53)	52 (80)	0.010
	10-40 mm	11 (47)	13 (20)	
Histological variant	Papillary thyroid carcinoma	22 (96)	61 (94)	1.000
	Follicular thyroid carcinoma	0 ()	1 (2)	
	Follicular variant of papillary thyroid carcinoma	1 (4)	3 (4)	
Lymph node metastasis	Yes	21 (91)	14 (22)	<0.001
	No	2 (9)	51 (78)	
Location of lymph node metastasis	Central compartment	14 (67)	11 (79)	0.822
	Lateral neck	1 (4)	0 (0)	
	Both	6 (29)	3 (21)	
Tumor focality	Unifocal	17 (74)	50 (77)	0.771
	Multifocal	6 (26)	15 (23)	
T stage	T1	16 (70)	52 (80)	0.192
	T2	0 (0)	3 (5)	
	T3b	5 (22)	9 (14)	
	T4a	2 (8)	1 (1)	
N stage	N0	2 (9)	48 (74)	<0.001
	N1	21 (91)	14 (22)	
	Nx	0 (0)	3 (4)	
M stage	M0	23 (100)	65 (100)	—
	M1			
AJCC stage	I	2 (9)	47 (72)	<0.001
	II	19 (83)	17 (26)	
	III	2 (8)	1 (1)	
Type of surgery	Thyroid lobectomy	4 (17)	15 (23)	0.882
	Total thyroidectomy	3 (13)	10 (15)	
	Total thyroidectomy with lymph node dissection	16 (70)	40 (62)	

group (p=0.01). Among 24 patients with tumor sizes of 10-40 mm, the *BRAF* V600E gene mutation occurred in 47% of patients, whereas patients without the mutation accounted for only 20%. *BRAF* V600E positivity was associated with lymph node metastasis (p<0.001). Specifically, among 35 patients with lymph node metastasis, 21 (91%) carried the *BRAF* V600E mutation, and 14 (22%) did not.

TNM staging was performed in 88 patients. Among 49 patients with stage I disease, the gene mutation was detected in 2 (9%) patients, and no mutation was detected in 47 (72%) patients. The proportion of *BRAF* V600E-positive patients with stage II and III papillary thyroid carcinoma was higher than that in the negative group (p<0.001). Among 36 patients with stage II disease, the gene mutation was detected in 19 (83%), and no mutation was detected in 17 (26%). Among 3 patients with stage III disease, 2 had the *BRAF* V600E mutation.

In addition, in our study, the *BRAF* V600E mutation was associated with the extent of cancer spread (N stage) to regional lymph nodes (p<0.001).

Discussion

In Vietnam, in recent years thyroid cancer has increased markedly and has become one of the 10 most common cancers.[12] Recent studies have shown that gene mutations are important factors in tumorigenesis. In 2002, Davies et al. first reported the *BRAF* V600E mutation in the MEK-ERK pathway in human malignancies. The *BRAF* V600E mutation is considered one of the key genes in papillary thyroid carcinoma and initiates the process of tumor formation. Recent studies have found that the frequency of the *BRAF* mutation ranges from 25-83% of papillary thyroid carcinoma cases, depending on the study population and geographic region.[13] Furthermore, the association between the *BRAF* V600E mutation and clinical prognostic factors of papillary thyroid carcinoma remains controversial. Some authors have demonstrated an association between the *BRAF* V600E mutation and poor prognostic factors such as advanced TNM stage, bilaterality, multifocality, extrathyroidal tumor invasion and lymph node metastasis, distant metastasis, higher tumor stage, and recurrence of papillary thyroid carcinoma.[8,9] On the other hand, some other studies have not confirmed the prognostic value of the *BRAF* V600E mutation in PTC.[7] To clarify these apparently contradictory results, we evaluated the association between the gene mutation and clinical factors of papillary thyroid carcinoma.

According to these results, among 88 patients with thyroid cancer, the mutation prevalence was 26%, whereas no mutation was detected in 74%. The results of this study are consistent with several previous reports from Italy, Korea, and Singapore.[14-16] In contrast, a recent study in Korea reported the *BRAF* V600E mutation in 60% of patients with small papillary thyroid carcinoma, and two studies in China reported mutation rates of 83.33% and 82.28%.[17-18] The reason that the *BRAF* V600E mutation rates in China and Korea were higher than in our study may be that access to health examination services is easier, providing more opportunities for mutation testing. Furthermore, mutation analysis in our study was performed in a relatively small number of patients (88 patients); therefore, the mutation prevalence may have been underestimated. In addition, differences in mutation prevalence may be due to differences in study populations, geographic regions, and racial factors.

In our study, papillary thyroid carcinoma accounted for the majority of thyroid cancer cases. PTC is a slowly progressing cancer with favorable long-term survival with standard treatments such as total thyroidectomy and radioactive iodine-131 treatment for residual thyroid tissue after surgery.

In our study, thyroid cancer occurred more frequently in women than in men. This result is also consistent with several previous studies; Changjiao Yan et al. reported that papillary thyroid carcinoma frequently occurs in women at a ratio of 3:1.[19] In our study, we found that the gene mutation was more common in female patients, but the difference was not statistically significant (p=0.426).

Lymph node metastasis was confirmed histopathologically in 35 patients, representing 40% of patients. Because lymph node metastasis is a risk factor for local recurrence and increases the mortality rate in papillary thyroid carcinoma,[20] these patients need to be stratified by lymph node metastasis and evaluated for its association with the *BRAF* V600E mutation. It has been reported that the rate of lymph node metastasis ranges from 24.1% to 64.1% in papillary thyroid carcinoma.[21] The lymph node metastasis results in our study were like those reported in the literature.

In our study population, we found that the age distribution, sex ratio, multifocality, and T stage of thyroid cancer did not differ significantly between patients with and without the *BRAF* V600E mutation. These findings indicate that the presence of the mutation was not associated with age, sex, multifocality, or T stage among patients with papillary thyroid carcinoma in our study population.

The prevalence of the *BRAF* V600E mutation was higher in the group of patients with multifocal tumors confirmed by postoperative histopathology, but the difference was not statistically significant (p=0.771). This differs from the meta-analysis by Li et al., which reported that the *BRAF* V600E mutation was significantly associated with multifocality, cervical lymph node metastasis, and higher TNM stage. They demonstrated that the *BRAF* V600E mutation leads to more aggressive characteristics.[22]

The results of our study showed an association between the *BRAF* V600E mutation and tumor size > 10-40 mm in patients with papillary thyroid carcinoma (p=0.01). This means that the proportion of patients positive for the mutated gene with tumor size > 10-40 mm was higher than that in the negative group. Virk et al. reported results similar to those of our study. They demonstrated that tumor size greater than 5 mm was associated with papillary thyroid microcarcinoma.[23] In contrast, another study demonstrated no association between the mutation and large tumor size.[24] Therefore, the association between the BRAF V600E mutation and tumor size remains controversial.

According to the Eighth Edition of the American Joint Committee on Cancer (AJCC) staging system, patients with stage II and III disease accounted for 44% and 4%, respectively.

Our study showed that the *BRAF* V600E mutation was highly associated with more advanced disease stages II and III ($p<0.001$). The proportion of patients positive for the mutated gene at stages II and III was higher than that in the negative group. Furthermore, we found that the rate of lymph node metastasis in patients with the *BRAF* V600E mutation was significantly higher than in those without the mutation. We found that the *BRAF* V600E mutation was associated with lymph node metastasis ($p<0.001$). Several studies have reported that lymph node metastasis was significantly higher in patients with papillary thyroid carcinoma carrying the mutation.[25]

Our analyses showed a significant association between the presence of *BRAF* V600E and tumor size, lymph node metastasis, N stage, and more advanced TNM stage ($p<0.05$). Our analysis is consistent with previous reports. Liu et al. demonstrated that the mutation was associated with advanced TNM stage (III/IV), lymph node metastasis, and tumor recurrence.[26] In contrast, Mai Trong Khoa reported in a study of Vietnamese patients with differentiated thyroid cancer that 75.8% had the *BRAF* V600E mutation. The authors also reported that the mutated gene was not associated with age, sex, histopathological characteristics, disease stage, T classification, lymph node metastasis, or distant metastasis.2[7]However, the sample size in our study was relatively small. Therefore, the sample size should be expanded to further study the association between the *BRAF* V600E mutation and clinicopathological parameters in papillary thyroid carcinoma.

The present study has several limitations. First, the sample size was relatively small, with 2,164 patients screened for thyroid cancer, after which 88 cases were diagnosed with thyroid cancer and included in our study. The results showed that the *BRAF* V600E gene mutation is common in papillary thyroid carcinoma and is associated with tumor size, lymph node metastasis, and thyroid cancer stage. A larger number of patients in our study could help confirm our findings. Second, these results are due to the short follow-up period. Therefore, oncological outcomes such as recurrence, metastasis, and survival could not yet be observed. Future studies with larger patient groups and longer follow-up periods are needed to evaluate oncological outcomes.

Conclusion

This study showed that the prevalence of the *BRAF* V600E mutation was 26% among 88 patients with thyroid cancer at Nghe An Provincial Endocrinology Hospital. Furthermore, our study initially demonstrated the relationship between the *BRAF* V600E gene mutation and clinical and pathological characteristics in patients with papillary thyroid carcinoma. The results showed that the *BRAF* V600E gene mutation is common in papillary thyroid carcinoma. Our study showed that the gene mutation was associated with tumor size ($p=0.01$), lymph node metastasis ($p<0.001$), N stage ($p<0.001$), and more advanced TNM stage ($p<0.001$) in patients with papillary thyroid carcinoma.

Ethical Considerations

This study was approved by the Ethics Committee under Decision No 1178/QD-VSR of the National Institute of Malariology, Parasitology and Entomology.

Authorship Contributions

Conceptualization: Nguyen Thanh Hai, Tran Quang Phuc; Data curation: Cao Ba Loi. Formal analysis: Nguyen Thanh Hai, Nguyen Van Chuyen; Nguyen Thi Thu Trang; Methodology and Research: Cao Ba Loi, Nguyen Huu Le, Tran Quang Phuc; Supervision: Cao Ba Loi. Drafting - Revision and editing: Cao Ba Loi, Nguyen Van Chuyen.

Disclosure and Conflicts of Interest

The authors declare that they have no potential conflicts of interest relevant to this article.

References

1. Davies L, Welch HG. Current thyroid cancer trends in the United States. JAMA Otolaryngol Head Neck Surg. 140: 317-322, 2014. doi: 10.1001/jamaoto.2014 Feb. PMID: 24557566
2. Alzahrani AS, Xing M. Impact of Iymph node metastases identified on central neck dissection (CND) on the recurrence of papillary thyroid cancer: Potential role of *BRAF*V600E mutation in defining CND. Endocr Relat Cancer 20: 1322, 2013 Feb . doi: 10.1530/ERC-12-0309. PMID: 23132792; PMCID : PMC3779438.
3. Coca-Pelaz, A, Shah J.P, Hernandez-PreraJ.C, Ghossein R.A, Rodrigo J.P, Hartl D.M, et al. Papillary Thyroid Cancer—Aggressive Variants and Impact on Management: A Narrative Review. Adv. Ther. 2020 June, 37, 3112–3128. doi: 10.1007/s12325-020-01391-1. PMID: 32488657; PMCID: PMC7467416.
4. Cooper DS, Doherty GM, Haugen BR, Kloos RT, Lee SL, Mandel SJ et al. Revised American Thyroid Association management guidelines for patients with thyroid nodules and differentiated thyroid cancer. Thyroid (2009) Oct 19(11):1167–1214. doi: 10.1089/thy.2015.0020. PMID: 26462967; PMCID: PMC4739132.
5. Ringel Matthew D, Julie Ann Sosa, Zubair Baloch. American Thyroid Association Management Guidelines for Adult Patients with Differentiated Thyroid Cancer. Thyroid 2025 Aug; 35(8): 841-985. doi: 10.1177/10507256251363120. PMID: 40844370; PMCID: PMC13090833.
6. Kebebew E, Weng J, Bauer J, Ranvier G, Clark OH, Duh QY, et al. The prevalence and prognostic value of *BRAF* mutation in thyroid cancer. Ann Surg 2007 Sep;246:466–70. doi: 10.1097/SLA.0b013e318148563d. PMID: 17717450; PMCID: PMC1959359.
7. Lai Hon-Fan, Jen-Fan Hang, Po-Chung Kuo. BRAF V600E Mutation Lacks Association with Poorer Clinical Prognosis in Papillary Thyroid Carcinoma. Annals of Surgical Oncology 2024 Feb; 31(5): 3495-501. doi: 10.1245/s10434-024-14935-4. PMID: 38300401
8. Gatta Elisa, Ilenia Pirola, Elena Gandossi. Prognostic Value of BRAF V600E Mutation in Papillary Thyroid Carcinoma: A Meta-Analysis of Nodal Involvement, Distant Metastases, Recurrence, and Mortality. Endocrine Practice 2026 Mar; 32(3): 416-26. doi: 10.1016/j.eprac.2025.12.003. PMID : 41419184

9. Fu Tao, Jiahao Chen, Xiaxia Jin. Association between Clinicopathological Features and BRAF V600E Mutation in Papillary Thyroid Carcinoma: A Meta-Analysis and Systematic Review. Oncology 2026 May; 1-14. doi: 10.1210/jc.2012-2104. PMID: 23055546; PMCID: PMC3513529.
10. Lloyd R, Osamura R, Klöppel G, Rosai J. WHO Classification of Tumours of Endocrine Organs, 4th ed.; IARC Press: Lyon, France, 2017.
11. Tuttle R.M, Haugen B, Perrier N.D. Updated American Joint Committee on Cancer/Tumor-Node-Metastasis Staging System for Differentiated and Anaplastic Thyroid Cancer (Eighth Edition): What Changed and Why? Thyroid 2018 Jan, 27, 751–756. doi: 10.1089/thy.2017.0102. PMID: 28463585; PMCID: PMC5467103.
12. Global Cancer Observatory. Accessed March 10, 2020. doi: 10.3322/caac.21660. PMID: 33538338.
13. Liu CP, Chen TW, Liu ZM. Associations between *BRAF*V600E and prognostic factors and poor outcomes in papillary thyroid carcinoma: a meta-analysis. World Journal of Surgical Oncology 2016 Sep; 14: 241. doi: 10.1007/s12020-016-1101-7. PMID: 27600854; PMCID: PMC5012084.
14. Frasca F, Nucera C, Pellegriti G, Gangemi P, Attard M, Stella, M, et al. *BRAF*(V600E) mutation and the biology of papillary thyroid cancer. Endocrine-Related Cancer 2008 Mar, 15, 191–205. doi: 10.1677/ERC-07-0212. PMID (: 18310287.
15. Chung S.Y, Lee J.S, Lee H.; Park, S.H, Kim S.J, Ryu H.S. Cytomorphological Factors and *BRAF* Mutation Predicting Risk of Lymph Node Metastasis in Preoperative Liquid-Based Fine Needle Aspirations of Papillary Thyroid Carcinoma. Acta Cytol. 2013 Apr, 57, 252–258. doi: 10.1159/000350438. PMID: 23636013.
16. Goh X, Lum J, Yang S.P, Chionh S.B, Koay E, Chiu L et al. *BRAF* mutation in papillary thyroid cancer-Prevalence and clinical correlation in a South-East Asian cohort. Clin. Otolaryngol. 2019 Mar, 44, 114–123. doi: 10.1111/coa.13238. PMID: 30294871.
17. Zhou C, Li J, Wang Y, Xue S, Zhang, Y. Association of *BRAF* gene and TSHR with cervical lymph node metastasis of papillary thyroid microcarcinoma. Oncol. Lett. 2018 Oct, 17, 183–194. doi: 10.3892/ol.2018.9715. PMID: 30655754; PMCID: PMC6313165.
18. Xiangqian Z, Chen P, Ming G, Jingtai Z, Xiukun H, Jingzhu Z, et al. Risk factors for cervical lymph node metastasis in papillary thyroid microcarcinoma: A study of 1,587 patients. Cancer Biol. Med. 2019 Feb, 16, 121–130. doi: 10.20892/j.issn.2095-3941.2018.0125. PMID: 31119052; PMCID: PMC6528461.
19. Changjiao Yan, Meiling Huang, Xin Li, Ting Wang. Relationship between *BRAF* V600E and clinical features in papillary thyroid carcinoma. Endocr Connect. 2019 Jun 17;8(7):988–996. doi: 10.1530/EC-19-0210. PMID: 31252408; PMCID: PMC6652244.
20. Ruan Jiaying, Zhendong Chen, Shitu Chen, et al. Lateral lymph node metastasis in papillary thyroid microcarcinoma: a study of 5241 follow-up patients. Endocrine Clinicopathological features and risk factors of lymph node metastasis in central region of 1433 cases of thyroid micropapillary carcinoma; 83(2): 414-21. doi: 10.1007/s12020-023-03486-5. PMID: 37596455.
21. Peng C, Wei SF, Zheng XQ, Yu Y, Zhang Y, Cheng WY, et al. Clinicopathological features and risk factors of lymph node metastasis in central region of 1433 cases of thyroid micropapillary carcinoma. J Clin Oncol 2016; 43: 95-99. doi: 10.5114/pjp.2022.124486. PMID: 36734433
22. Li F, Chen G, Sheng C, Gusdon AM, Huang Y, Lv Z et al. *BRAF*V66E mutation in papillary thyroid microcarcinoma: a meta-analysis. Endocr Relat Cancer 2015 Nov; 22: 159-168. doi:10.1530/ERC-14-0531. PMID: 25593071; PMCID: PMC4629836.
23. Virk RK, Van Dyke AL, Finkelstein A, Prasad A, Gibson J, Hui P, et al. *BRAF*V600E mutation in papillary thyroid microcarcinoma: a genotypephenotype correlation. Mod Pathol 2013 Jan;26:62–70. doi: 10.1038/modpathol.2012.152. PMID: 22918165.
24. Miccoli P, Minuto MN, Ugolini C, Panicucci E, Berti P, Massi M, et al. Intrathyroidal differentiated thyroid carcinoma: tumor size-based surgical concepts. World J Surg 2007;31:888–94. doi: 10.1007/s00268-006-0795-9. PMID: 17426903.
25. Lim JY, Hong SW, Lee YS, Kim BW, Park CS, Chang HS, et al. Clinicopathologic implications of the *BRAF*(V600E) mutation in papillary thyroid cancer; a subgroup analysis of 3130 cases in a single center. Thyroid Clinicopathologic implications of the BRAF(V600E) mutation in papillary thyroid cancer; a subgroup analysis of 3130 cases in a single center, 23(11):1423–1430. doi: 10.1007/s00268-006-0795-9. PMID: 17426903.
26. Liu C, Chen T, Liu Z. Associations between *BRAF* and Prognostic Factors and Poor Outcomes in Papillary Thyroid Carcinoma: A Meta-Analysis. World J. Surg. Oncol. 2016, 14, 241. doi: 10.1007/s12020-011-9519-7. PMID: 27600854; PMCID: PMC5012084.
27. Mai Trong Khoa, Pham Cam Phuong, Nguyen Thanh Trung. The Relationship Between the *BRAF*V600E Mutation in Differentiated Thyroid Cancer and Clinicopathologic Factors in Vietnam. Biomedical Journal of Scientific & Technical Research. Volume 9- Issue 1: 2018 Sep. doi: 10.26717/BJSTR.2018.09.001748.

***Corresponding author:** *Cao Ba Loi, MD, PhD. Department of Science and Training. The National Institute of Malariology, Parasitology and Entomology. E-mail: caoloi28111964@gmail.com*

International Journal of Biomedicine 16(4) (2026) 469-476
http://dx.doi.org/10.21103/Article16(4)_OA2

ORIGINAL ARTICLE

INTERNATIONAL JOURNAL OF BIOMEDICINE

Short-Term Cancer Trends in Tabuk City, Saudi Arabia: A Retrospective Study (2023–2025)

Khalid Alhazmi[1*]

[1]*Department of Pathology, Faculty of Medicine, University of Tabuk, Tabuk, Saudi Arabia*

Abstract

Background: Cancer is the commonest cause of death in people over 70 years of age. Importantly, the global cancer trends have shifted in recent years; research regarding cancer in Tabuk City, Saudi Arabia, is scarce. We aimed to assess the patterns and trends of cancer in Tabuk, Saudi Arabia, from January 2023 to December 2025.

Methods and Results: A retrospective study was conducted at King Fahd Specialist Hospital, Tabuk, Saudi Arabia. The patients' records during the stated period were reviewed. A checklist was used to collect sociodemographic factors, tumor stage, histological subtypes, laterality, extent, and diagnostic methods for cancers. The most prevalent cancer was breast cancer (25.4% to 36.7%), followed by colorectal (14.7% to 19.9%) and thyroid (2% to 12.2%); 54.2% to 63.5% were women, and the mean age was 53.0±16.6 years. Only thyroid cancer demonstrated a significant decreasing trend (χ^2=21.98, P<0.001), whereas no significant trends were observed for the remaining major cancer types. The diagnosis was histopathological in the majority of cases, and regional lymph node involvement was the most common extent of disease at diagnosis.

Conclusion: Breast cancer was the most prevalent cancer in Tabuk City, Saudi Arabia, followed by colorectal and thyroid cancers; females were more affected. The cancer trend was stable in the short term, except for thyroid cancer, which showed a decreasing trend. The diagnosis was histopathological in the majority of cases, and the local lymph nodes were commonly involved at the time of diagnosis. (**International Journal of Biomedicine. 2026;16(4):469-476.**)

Keywords: cancer • prevalence • trends • Tabuk • Saudi Arabia

For citation: Alhazmi K. Short-Term Cancer Trends in Tabuk City, Saudi Arabia: A Retrospective Study (2023–2025). International Journal of Biomedicine. 2026;16(4):469-476. doi:10.21103/ Article16(4)_OA2

Introduction

Worldwide, 19.3 million new cancer cases and 10 million new cancer deaths were reported globally in 2020, according to the GLOBOCAN 2020 data on cancer incidence and mortality compiled by the International Agency for Research on Cancer.[1] The most common malignancy was breast cancer in females (2.3 million new cases and 11.7% of all cancers), followed by lung cancer (11.4%), colorectal cancer (10%), prostate cancer (7.3%), and stomach cancer (5.6%).[2]

Cancer is the first or second leading cause of death in the age group >70 years worldwide, with an increasing burden on the patients, community, and healthcare systems, and is a significant cause of poor quality of life.[3]

Importantly, the global cancer trends have shifted in recent years, with breast cancer overtaking lung cancer to become the most commonly diagnosed cancer worldwide in 2020. Despite this change in incidence, lung, liver, stomach, breast, and colorectal cancers remained the five leading causes of cancer-related mortality. Notably, liver cancer showed a significant change in mortality ranking, rising from the third leading cause of cancer death in 2018 to the second leading cause in 2020, highlighting evolving patterns in the global cancer burden.[4]

Cancer incidence in Saudi Arabia has increased over the last two decades, ratcheting up to global levels. There is a marked upsurge of cancer burden in terms of incidence and the potential economic burden, which may inform cancer control measures.[5,6] Cancer incidence was slightly higher among Saudi nationals than among non-Saudi residents, with crude incidence rates of 66.86 and 66.28 per 100,000 population, respectively, during 2021–2022. Saudi women had higher crude and age-standardized incidence rates than men, although cancer rates in men surpassed those of women in people aged >70 years.

Among the Saudi population, the most frequently diagnosed cancers were breast, colorectal, and thyroid cancers.[7] A study published in Saudi Arabia showed that the risk factors for breast cancer are obesity, family history, and use of oral contraceptives; most cases originated in the central region (80.1%), with the southern regions accounting for 12.7%. Hypertension and diabetes mellitus were the

© 2026 The Author(s). *International Journal of Biomedicine* is published by IMRDC.
This is an open access article under the CC BY-NC-ND 4.0 license.

predominant coexisting conditions. Invasive ductal carcinoma was identified as the most common histological subtype (89.7%). Most patients were diagnosed at TNM stages II and III (55.2%), and metastases were present in 27.7% of cases.[8]

A sustainable increasing trend was observed in breast cancer in Saudi Arabia during the past 20 years, with a 151.7% surge, accounting for 30.9% of cancer in Saudi women. Although the increasing trend is universal, the Eastern region recorded the highest rate, and the Al-Jouf region showed the highest increasing trend. The steepest rise was observed in the age group 70 to 74 years.[9]

Breast cancer in the Eastern Province of Saudi Arabia showed a relatively young mean age at diagnosis (49 years), with two-thirds locally advanced disease. The invasive ductal carcinoma was reported in four out of five women, along with a predominance of hormone receptor-positive disease. Importantly, an 80% rise in new cases is predicted by 2028, so there is an urgent need to strengthen screening programs for earlier detection.[10] Yanbu authorities in Saudi Arabia implemented a quality improvement strategy that led to a substantial increase in screening attendance and a marked improvement in diagnostic efficiency. This success could be replicated in other regions.[11]

Alshamsan et al.[12] highlighted the rapid increase of breast cancer in Saudi Arabia during the period from 2002 to 2020 and stressed the need to expand mammography screening coverage and strengthen breast cancer care capacity in Saudi Arabia.

Regarding cancer of the gastrointestinal tract, an increasing trend was observed, mirroring changes in socioeconomic factors with the adoption of sedentary lifestyles and Westernized unhealthy diets. The increasing rates of obesity and diabetes, hepatitis, and Helicobacter pylori are other plausible explanations.[13] Alyami and colleagues[14] conducted a study in the South Region of Saudi Arabia and observed that GIT cancer was the commonest, with colon and liver cancers identified as the most common specific cancer types. These findings highlight the burden of GIT cancer and emphasize the need for interventions targeting modifiable risk factors in Saudi Arabia.

Colorectal cancer (cancer of the colon and rectum) in Saudi Arabia presents in the advanced stage in 29% and at a younger age. KRAS mutations are observed in 49.6%, while BRAF mutations are found in only 0.4%. Survival outcomes were affected by age at diagnosis, highlighting the importance of demographic rather than molecular predictors in survival.[15,16]

Colorectal cancer is on the rise and varies significantly by geographical region. It is the fourth leading cause of death in some areas and is ranked third after breast and bronchial cancer in some regions.[17] Colorectal cancer is the third leading cause of cancer death globally. A recent survey found that the prevalence of this cancer increased with age, and 12.9% were suffering from polyps.[18] In Saudi Arabia, colorectal cancer is the second leading cause of death in men and third in women. Importantly, the disease usually presents with lymph node involvement and distant metastasis.[19]

Although lung cancer in Saudi Arabia demonstrates a relatively low crude incidence, there is an increasing trend with a higher frequency of aggressive histological subtypes. Males are more affected due to the high tobacco exposure and environmental risks. Regionally, the Eastern region recorded the highest prevalence, followed by Tabuk, Riyadh, and the Northern regions. These findings highlight clear regional and demographic disparities, along with an overall increasing burden of lung cancer in Saudi Arabia. These findings highlight the need for targeted tobacco control policies, earlier detection strategies, and region-specific cancer prevention programs to reduce the lung cancer burden in Saudi Arabia.[20,21]

Regarding thyroid cancer, nodules may be present in nearly two-thirds of the population, depending on age. However, only 20% of those cases are clinically significant (cancer, pressure symptoms, and thyroid dysfunction in 10%, 5%, and 5%, respectively). Thyroid nodules are common, and thyroid cancer occurs in 7%-15% of them.[22]

Thyroid carcinoma is the most common endocrine malignancy among Saudi women and the ninth most common among men; the incidence increased twenty-twofold among men and fifteenfold in females. Furthermore, the mortality increased threefold and sixfold among women and men, respectively.[23] Thyroid cancer in Saudi Arabia is diagnosed at a younger age and with larger sizes; in addition, persistence and recurrence were high.[24,25] Most cases were benign, and papillary neoplasms were the commonest.[26] The incidence is controversial in the Northern region of Saudi Arabia, including Tabuk.[27,28]

The International Agency for Research reported one million new cases of gynecological cancer in 2020, accounting for nearly one in five of all cancers,[1,29] of them, 13,000 cases were reported in Saudi Arabia. The literature on gynecological cancer in Saudi Arabia is scarce and has been limited by the small sample sizes and short durations of the published studies.[30] Gynecological cancer is ranked fourth in Saudi Arabia, after breast, thyroid, and colorectal cancers. There is significant variation in gynecological cancer by geographic regions. Plausible explanations could be the interaction of genetics and environmental factors.[31]

The situation is not different in the Gulf countries (GCC): an emerging trend and shifting epidemiological pattern have been observed due to changing lifestyle factors (obesity and physical inactivity), with breast, colorectal, and thyroid cancers being the most prevalent. Historically, cancer has been lower in the GCC than in many countries in the West. However, a rising trend was observed over the last two decades, with projections suggesting a substantial increase in both incidence and mortality; the aging population and modifiable risk factors are to blame.[32-35] Breast cancer remains the most common cancer among women in the GCC, mainly due to BRCA1/2 mutations, lifestyle, and reproductive factors.[36,37] Lung cancer and thyroid cancer showed rising trends. Plausible explanations could include increased smoking and improved diagnostic practices.[38,39] Prostate cancer is also emerging as an increasingly important malignancy in the region, and many cases are diagnosed at advanced stages due to limited early detection practices.[40]

In our study, we aimed to assess the cancer incidence

pattern in Tabuk City, Saudi Arabia, from January 2023 to December 2025. Investigating the pattern of cancer in Saudi Arabia is justifiable due to the rising rate and changing pattern of cancers both worldwide and in Saudi Arabia. In addition, research on this important disease is scarce in the Tabuk Region. For that reason, it is important to provide readily accessible data to inform the scientific community, healthcare providers, and policymakers. Current data will help determine the best treatment option and guide preventive measures. The Kingdom of Saudi Arabia is a large country with significant geographical diversity.[41,42] Therefore, studies assessing the patterns and trends of cancer across different regions are justified. The current data will provide a baseline for cancer in Tabuk City and inform policymakers for future planning on intervention and prevention.

Patients and Methods

A retrospective study was conducted in King Fahd Specialist Hospital, and the patients' records from January 2023 to December 2025 were reviewed.

Inclusion Criteria

• Age: ≥18 years

• Diagnosis: Adult patients with malignant or in situ neoplasms confirmed histopathologically or through accepted clinical and imaging criteria.

Exclusion Criteria

Cancer in children < 18 years, histologically/imaging not confirmed.

Data Collection Procedure

A checklist was used to collect age, gender, residence, nationality, marital status, cancer type, tumor stage, histological subtypes, laterality, extent, and the diagnostic methods (histology versus clinical diagnostic methods, including imaging).

Sample Size

Patients who were confirmed to have cancer in King Fahd Specialist Hospital during the years 2023 and 2025

Sampling Technique

All patients who were diagnosed with cancer during the stated period (2023-2025).

Ethical Consideration

With strict adherence to the Declaration of Helsinki, no patient's details were recorded. The data collected were stored by the first author in a dedicated encrypted file and used only for this research. Ethical approval was obtained from the ethics committee of the University of Tabuk (Ref. UT-831-378-2026, dated February 16, 2026).

Statistical Analysis

The Statistical Package for the Social Sciences (IBM SPSS, Version 29, New York) was used for data analysis, and the data were presented as mean ± SD. Descriptive statistics will summarize demographic and baseline characteristics. The association between cancer type and demographic factors was assessed using the Chi-Square test. The cancer trends were assessed using the Cochran–Armitage test for linear trend.

Results

A total of 684 cancer cases were recorded in Tabuk City between 2023 and 2025 (Table 1).

Table 1.

Frequency of different types of cancer in Tabuk City during the period from January 2023 to December 2025.

Cancer type	2023 (n = 197), n (%)	2024 (n = 236), n (%)	2025 (n = 251), n (%)
Colorectal	31 (15.7%)	47 (19.9%)	37 (14.7%)
Small intestine	3 (1.5%)	4 (1.7%)	5 (2.0%)
Stomach	3 (1.5%)	8 (3.4%)	8 (3.2%)
Esophagus	3 (1.5%)	3 (1.3%)	3 (1.2%)
Liver	8 (4.1%)	8 (3.4%)	14 (5.6%)
Pancreas	1 (0.5%)	5 (2.1%)	3 (1.2%)
Lung	14 (7.1%)	12 (5.1%)	8 (3.2%)
Breast	58 (29.4%)	60 (25.4%)	92 (36.7%)
Thyroid	24 (12.2%)	6 (2.5%)	5 (2.0%)
Urinary bladder	3 (1.5%)	5 (2.1%)	7 (2.8%)
Lymphomas	14 (7.1%)	32 (13.6%)	22 (8.8%)
Kidney	4 (2.0%)	6 (2.5%)	9 (3.6%)
Oropharyngeal	11 (5.6%)	12 (5.1%)	7 (2.8%)
Endometrium	5 (2.5%)	2 (0.8%)	5 (2.0%)
Skin	4 (2.0%)	6 (2.5%)	9 (3.6%)
Testis	1 (0.5%)	4 (1.7%)	2 (0.8%)
Prostate	4 (2.0%)	2 (0.8%)	2 (0.8%)
Cervix	0 (0.0%)	1 (0.4%)	1 (0.4%)
Mandible	1 (0.5%)	2 (0.8%)	1 (0.4%)
Gallbladder	0 (0.0%)	1 (0.4%)	1 (0.4%)
Soft tissue	0 (0.0%)	7 (3.0%)	0 (0.0%)
Ovary	0 (0.0%)	1 (0.4%)	0 (0.0%)
Parotid	1 (0.5%)	1 (0.4%)	1 (0.5%)
Aorta	1 (0.5%)	0 (0.0%)	1 (0.4%)
Lip	1 (0.5%)	0 (0.0%)	1 (0.4%)
Adrenal gland	1 (0.5%)	0 (0.0%)	0 (0.0%)
Other/unknown	1 (0.5%)	1 (0.4%)	7 (2.8%)

The mean age of patients was 52.97±16.56 years; 58.3% were women, 41.7% were men (Table 2). Most patients were Saudi nationals (79.4%), whereas non-Saudi patients represented 20.6%. Regarding marital status, the data were incomplete: unknown status accounted for the largest proportion (65.4%), followed by married (19.0%) and single (14.9%). Divorced and widowed patients represented only a small fraction of cases. Regional lymph node involvement (61.3%) was the most common presentation, followed by in situ tumors (19.3%).

Interestingly, the most frequent category of tumors was paired site with unspecified laterality (39.2%), followed

by right-sided (30.5%) and left-sided tumors (23.9%), while bilateral tumors accounted for 6.6%. The majority of cases had unknown grade (74.3%), whereas grade II tumors accounted for 16.1%, grade I (4.8%), and grade III (4.8%). Regarding diagnostic methods, histological confirmation was the predominant method (94.6%), while clinical or imaging methods were used in 5.4% of cases (Table 2).

There were 197 cancer cases in Tabuk City, Saudi Arabia, in the year 2023. The distribution of malignancies was not uniform, with breast cancer constituting the most prevalent malignancy of the total reported cancers (29.4%), followed by colorectal cancer (15.7%), thyroid cancer (12.2%), lymphomas (7.1%), and lung cancer (5.1%) (Table 3).

In the current data, the highest number of cancer cases was reported in 2024 (236 cases). The distribution was like that observed in 2023, with breast cancer remaining the most prevalent malignancy (25.4%) of the total reported cases, followed by colorectal cancer (19.9%), lymphomas (13.6%), and lung cancer (5.1%). A higher prevalence of breast cancer was observed in the year 2025 (36.7%) of the total malignancies, followed by colorectal cancer (14.7%), lymphomas (8.8%), and liver cancer (5.6%).

Regarding the temporal profile of cancer in Tabuk City from 2023 to 2025, there was an increasing trend, with 197, 236, and 251 cases reported in 2023, 2024, and 2025, respectively.

Table 2 presents demographic and clinical characteristics of cancer patients in Tabuk City, Saudi Arabia, 2023–2025.

Table 2.

Demographic and clinical characteristics of cancer patients in Tabuk City, Saudi Arabia, 2023–2025.

Characteristic	2023	2024	2025	Overall
Age (years), mean ± SD	52.58 ±16.42	52.65 ±16.4	53.59 ±16.88	52.97 ±16.56
Gender				
Women	125 (63.5%)	137 (58.1%)	137 (54.2%)	399 (58.3%)
Men	72 (36.5%)	99 (41.9%)	114 (45.8%)	285 (41.7%)
Nationality				
Saudi	151 (76.6%)	194 (82.2%)	198 (78.9%)	543 (79.4%)
Non-Saudi	46 (23.4%)	42 (17.8%)	53 (21.1%)	141 (20.6%)
Marital status				
Single	32 (16.2%)	32 (13.6%)	38 (15.1%)	102 (14.9%)
Married	36 (18.3%)	43 (18.2%)	51 (20.3%)	130 (19.0%)
Divorced	0 (0.0%)	2 (0.8%)	0 (0.0%)	2 (0.3%)
Widowed	1 (0.5%)	1 (0.4%)	1 (0.4%)	3 (0.4%)
Unknown	128 (65.0%)	158 (66.9%)	161 (64.1%)	447 (65.4%)
Extent of disease				
In situ	41 (20.8%)	40 (16.9%)	51 (20.3%)	132 (19.3%)
Regional direct extension	0 (0.0%)	0 (0.0%)	1 (0.4%)	1 (0.1%)
Regional lymph nodes	126 (64.0%)	149 (63.1%)	144 (57.4%)	419 (61.3%)
Regional NOS	0 (0.0%)	0 (0.0%)	0 (0.0%)	0 (0.0%)
Distant metastasis	28 (14.2%)	15 (6.4%)	20 (8.0%)	63 (9.2%)
Regional lymph nodes and distant metastasis	2 (1.0%)	32 (13.6%)	35 (13.9%)	69 (10.1%)
Laterality				
Right	64 (32.5%)	64 (27.1%)	80 (31.9%)	208 (30.5%)
Left	47 (23.9%)	55 (23.3%)	61 (24.3%)	163 (23.9%)
Bilateral	22 (11.2%)	17 (7.2%)	6 (2.4%)	45 (6.6%)
Paired site, laterality not stated	64 (32.5%)	100 (42.4%)	104 (41.4%)	268 (39.2%)
Grade				
I	6 (3.0%)	15 (6.3%)	12 (4.8%)	33 (4.8%)
II	34 (17.2%)	41 (17.4%)	35 (13.9%)	110 (16.1%)
III	6 (3.0%)	10 (4.2%)	17 (6.8%)	33 (4.8%)
Unknown	151 (76.6%)	170 (72.0%)	187 (74.5%)	508 (74.3%)
Method of diagnosis				
Histology	195 (99.0%)	221 (93.6%)	231 (92.0%)	647 (94.6%)
Clinical methods/imaging	2 (1.0%)	15 (6.4%)	20 (8.0%)	37 (5.4%)

Table 3.

Cancer trends in Tabuk City, Saudi Arabia, during the period from January 2023 to December 2025.

Cancer type	2023 n (%)	2024 n (%)	2025 n (%)	χ^2	P-value	Trend interpretation
Breast	58 (29.4)	60 (25.4)	92 (36.7)	3.12	0.073	No significant trend
Colorectal	31 (15.7)	47 (19.9)	37 (14.7)	0.15	0.696	No significant trend / fluctuating
Lymphomas	14 (7.1)	32 (13.6)	22 (8.8)	0.17	0.676	No significant trend
Lung	14 (7.1)	12 (5.1)	8 (3.2)	3.60	0.058	No significant trend
Liver	8 (4.1)	8 (3.4)	14 (5.6)	0.71	0.400	No significant trend
Thyroid	24 (12.2)	6 (2.5)	5 (2.0)	21.98	0.001	Significant decreasing trend
Kidney	4 (2.0)	6 (2.5)	9 (3.6)	1.02	0.312	No significant trend
Skin	4 (2.0)	6 (2.5)	9 (3.6)	1.02	0.312	No significant trend

Notes: Percentages were calculated using the total number of cancer cases diagnosed in each year as the denominator. Trends were assessed using the Cochran–Armitage test for linear trend.

Table 3 presents the overall trends in cancer types in Tabuk City, Saudi Arabia, from January 2023 to December 2025. No significant trend was observed for lung cancer from 2023 to 2025 (7.1%, 5.1%, and 3.2%, respectively; χ^2=3.60, P=0.058). A significant decreasing trend was observed in thyroid cancer over the same period (12.2%, 2.5%, and 2.0%, respectively; χ^2=21.98, P<0.001). Regarding breast cancer, the rate increased from 29.4% in 2023 to 36.7% in 2025. No significant trend was observed for colorectal cancer (15.7%, 19.9%, and 14.7%, respectively; χ^2=0.15, P=0.696), lymphomas (7.1%, 13.6%, and 8.8%; χ^2=0.17, P=0.676), liver cancer (4.1%, 3.4%, and 5.6%; χ^2=0.71, P=0.400), kidney cancer (2.0%, 2.5%, and 3.6%; χ^2=1.02, P=0.312), or skin cancer (2.0%, 2.5%, and 3.6%; χ^2=1.02, P=0.312).

Short-term cancer trends were stable across nationality, marital status, grade, and laterality. However, we found significant differences across the study years for extent of disease (P=0.010) and method of diagnosis (P=0.016) (Table 4).

Table 4.

Chi-Square Test for Selected Variables by Year (2023–2025).

Variable	χ^2-value	df	P-value	Interpretation
Gender vs Year	3.42	2	0.181	Not significant
Nationality vs Year	2.96	2	0.227	Not significant
Marital status vs Year	5.88	8	0.661	Not significant
Extent of disease vs Year	16.74	6	0.010	Significant
Laterality vs Year	9.52	6	0.146	Not significant
Tumor grade vs Year	7.88	6	0.247	Not significant
Method of diagnosis vs Year	8.21	2	0.016	Significant

Discussion

A total of 684 cases were recorded during the period (from January 2023 to December 2025) in Tabuk City, Saudi Arabia, with a gradual increase in the number of cases from 197 in 2023 to 251 in 2025. The increase in the number of registered cancer cases may reflect population growth, improved access to healthcare, expansion of screening services, enhanced diagnostic capacity, or changes in referral patterns. Our findings are in line with previous global findings and those in the Middle East, the increasing trends in cancer could be due to improvements in diagnostic methods and demographic changes.[5,6,43]

Similarly, shifting epidemiological patterns and rising cancer burden were observed in the Gulf Cooperation Council countries. The most prevalent cancers in the GCC countries were breast, colorectal, and thyroid. Importantly, there were 42,475 new cancer cases and 19,895 cancer-related deaths in the year 2020, and the projections for the year 2040 could be more than double the current rate.[32-35] Lifestyle factors, a high body mass index, and shifting demographic factors are the major determinants of the increasing cancer rate. Early detection and obesity prevention to reduce the increasing cancer rate are highly needed. The mean age of patients was 52.97±16.56 years. This finding is consistent with reports from the Saudi Cancer Registry, which show that the majority of cancer cases occur in individuals older than 45 years.[44,45] Age is a well-established risk factor for cancer due to cumulative exposure to environmental carcinogens and genetic mutations over time.[1]

Females accounted for 58.3% of all cancer cases. A plausible explanation might be the high prevalence of breast cancer among women in Saudi Arabia. Breast cancer remained the most common cancer throughout the study period. Although a higher proportion was observed in 2025, no statistically significant temporal trend was detected. Breast cancer contributes significantly to the national cancer burden.[8,9,44,46] Similarly, Cao et al.[4] found that breast cancer displaced lung cancer globally and in China; the increasing rate of breast cancer could be explained by declining fertility rates,[47] and shorter breastfeeding duration. Obesity and rapid societal and economic development are further plausible explanations.[34,48-50]

The predominance of breast cancer observed in the present study is similar to regional trends in GCC countries. Breast cancer in the GCC occurs at younger ages and advanced stages compared to Western countries.[8,9] Lifestyles, reproductive factors, and genetic susceptibility are significant,

with studies identifying non-BRCA and BRCA-related variants. Breast cancer screening programs, promoting early detection, and expanding genetic counseling are recommended.

In this study, colorectal cancer was the second most common cancer in Tabuk City, followed by lymphomas, lung, and thyroid cancer. Our findings were similar to those of Elwali et al.,[19] who conducted a study in Saudi Arabia and found that colorectal cancer is the leading cause of cancer in men and the second in women. Regarding lung cancer, our findings were similar to a study published in Almadinah Almunawara,[51] which found a rate of 13 cases/year, like the current observed annual cases ranging from 8 to 14. In this study, thyroid cancer was the third most common cancer, accounting for 2.0%–12.2% of all cancers during the study period, in line with a recently published study that found that the commonest cancer was breast, followed by colorectal, and thyroid cancer.[52] The observed decline may reflect changes in referral patterns, diagnostic practices, case ascertainment, or true disease occurrence. Further studies are required to clarify this finding.

The proportion of lung cancer varied from 3.2% to 7.1% of all cancers and was higher than in previous studies.[20,21,51,53] Saudi nationals constitute the majority of cases (79.5%), while non-Saudi residents account for approximately one-fifth of cases. The current findings were like previous studies published in Saudi Arabia,[25,43,50] which reported a higher prevalence of cancer in Saudi nationals.

In the current study, regional lymph node involvement was the most common extent of disease, accounting for 61.3%. Our findings were in line with Leong et al.[54] This pattern may reflect delayed diagnosis, referral pathways, differences in screening practices, or variations in case mix.

In this study, in 39.2% of cases, the laterality was not specified,, which may reflect incomplete documentation or recording of laterality in the cancer registry. Laterality reporting is vital for clinical decision-making and epidemiological monitoring. The current data showed that 94.6% of cancers were diagnosed by histopathology; these findings were consistent with international oncology guidelines, which consider histopathology the gold standard for cancer diagnosis.

Study Limitations

The results of this study should be viewed in the presence of the following limitations: the retrospective nature of the study and the missing or unknown data observed in a significant proportion (the histological grade is unknown in 74.3% of cases, and marital status was unknown in 65.4%) may have affected the accuracy of certain estimates. The study was retrospective and had a single-center design. Therefore, generalization to the whole Tabuk Region cannot be ensured. Improving the reporting methods for Registry data is highly recommended, particularly for histological grading, given its importance for prognosis estimation and treatment planning.

Conclusion

The most common cancer in Tabuk, Saudi Arabia, was breast cancer, followed by colorectal and thyroid cancer. Most patients were middle-aged or older adults, and females accounted for a greater proportion of cases. Breast cancer remained the most common malignancy throughout the study period, although no statistically significant temporal trend was observed. No statistically significant temporal trends were observed for the major cancer types except thyroid cancer, which demonstrated a significant decreasing trend; regional lymph node involvement was common at the time of diagnosis. The diagnosis was made by histopathology in the majority of cases. Future studies focusing on specific cancer types and associated risk factors are highly recommended in the Tabuk region.

References

1. Sung H, Ferlay J, Siegel RL, Laversanne M, Soerjomataram I, Jemal A, Bray F. Global Cancer Statistics 2020: GLOBOCAN Estimates of Incidence and Mortality Worldwide for 36 Cancers in 185 Countries. CA Cancer J Clin. 2021 May;71(3):209-249. doi: 10.3322/caac.21660. Epub 2021 Feb 4. PMID: 33538338.

2. Ferlay J, Colombet M, Soerjomataram I, Siegel R, Torre L, Jemal A. Global and regional estimates of the incidence and mortality for 38 cancers: GLOBOCAN 2018. Lyon: International Agency for Research on Cancer. World Health Organization. 2018; 394:424.

3. World Health Organization (WHO). Global Health Estimates 2020: Deaths by Cause, Age, Sex, by Country and by Region, 2000-2019. WHO; 2020. Accessed January 25, 2026. who.int/data/gho/data/themes/mortality-and-global-health-estimates/ghe-leading-causes-of-death

4. Cao W, Chen HD, Yu YW, Li N, Chen WQ. Changing profiles of cancer burden worldwide and in China: a secondary analysis of the global cancer statistics 2020. Chin Med J (Engl). 2021 Mar 17;134(7):783-791. doi: 10.1097/CM9.0000000000001474. PMID: 33734139; PMCID: PMC8104205.

5. Jazieh AR, Da'ar OB, Alkaiyat M, Zaatreh YA, Saad AA, Bustami R, Alrujaib M, Alkattan K. Cancer Incidence Trends From 1999 to 2015 And Contributions Of Various Cancer Types To The Overall Burden: Projections To 2030 And Extrapolation Of Economic Burden In Saudi Arabia. Cancer Manag Res. 2019 Nov 14;11:9665-9674. doi: 10.2147/CMAR.S222667. PMID: 32009819; PMCID: PMC6861167.

6. Althubiti MA, Nour Eldein MM. Trends in the incidence and mortality of cancer in Saudi Arabia. Saudi Med J. 2018 Dec;39(12):1259-1262. doi: 10.15537/smj.2018.12.23348. PMID: 30520511; PMCID: PMC6344657.

7. Alqahtani WS, Almufareh NA, Domiaty DM, Albasher G, Alduwish MA, Alkhalaf H, Almuzzaini B, Al-Marshidy SS, Alfraihi R, Elasbali AM, Ahmed HG, Almutlaq BA. Epidemiology of cancer in Saudi Arabia thru 2010-2019: a systematic review with constrained meta-analysis. AIMS Public Health. 2020 Sep 11;7(3):679-696. doi: 10.3934/publichealth.2020053. PMID: 32968686; PMCID: PMC7505779.

8. Omer AA, Bin Dayel SA, Hummedi AS, Almuhaimed NI. The epidemiological and clinicopathological features of breast cancer in Riyadh, Saudi Arabia. Saudi Med J. 2024 Mar;45(3):288-294. doi: 10.15537/smj.2024.45.3.20230656. PMID: 38438204; PMCID: PMC11115392.

9. Basudan AM. Breast Cancer Incidence Patterns in

the Saudi Female Population: A 17-Year Retrospective Analysis. Medicina (Kaunas). 2022 Nov 9;58(11):1617. doi: 10.3390/medicina58111617. PMID: 36363574; PMCID: PMC9697748.
10. Almohanna H, Almsned F, Alharbi H, Al Dossary N, Alrasheed A, Alzayer R, Alwosaibai K. A comprehensive epidemiological analysis of breast cancer in the Eastern Province of Saudi Arabia. Sci Rep. 2025 Jul 1;15(1):20816. doi: 10.1038/s41598-025-05276-7. PMID: 40592998; PMCID: PMC12216766.
11. Ibrahim HS, Albeshan SM, ElRefaei MA. Transforming Breast Cancer Care and Clinical Outcomes: Local Experience in Yanbu Industrial City, Saudi Arabia. Clin Breast Cancer. 2025 Apr;25(3):e240-e248.e2. doi: 10.1016/j.clbc.2024.10.011. Epub 2024 Oct 26. PMID: 39567338.
12. Alshamsan B. Trends in breast cancer incidence, age at diagnosis, and stage in Saudi Arabia, 2002-2022: a population-based study. Cancer Treat Res Commun. 2026;46:101077. doi: 10.1016/j.ctarc.2025.101077. Epub 2025 Dec 13. PMID: 41411719.
13. Alreshidi FS. Epidemiology and patterns of GI tract cancers in Saudi Arabia: benefit of prompt lifestyle changes. Int J Clin Exp Pathol. 2025 Jun 15;18(6):222-232. doi: 10.62347/OLDP2841. PMID: 40642397; PMCID: PMC12238797.
14. Alyami HS, Naser AY, Dahmash EZ, Alyami MH, Belali OM, Assiri AM, Rehman A, Alsaleh AM, Alsaleh HA, Hussein SH, Amer SM, Asiri SA, Almuadi AI. Clinical and Therapeutic Characteristics of Cancer Patients in the Southern Region of Saudi Arabia: A Cross-Sectional Study. Int J Environ Res Public Health. 2021 Jun 21;18(12):6654. doi: 10.3390/ijerph18126654. PMID: 34205637; PMCID: PMC8296400.
15. Alsadhan N, Alhurishi SA, Pujades-Rodriguez M, Shuweihdi F, Brennan C, West RM. Demographic and clinical characteristics associated with advanced stage colorectal cancer: a registry-based cohort study in Saudi Arabia. BMC Cancer. 2024 Apr 26;24(1):533. doi: 10.1186/s12885-024-12270-1. PMID: 38671382; PMCID: PMC11055310.
16. Alharbi A, Bin Dokhi H, Almuhaini G, Alomran F, Masuadi E, Alomran N. Prevalence of colorectal cancer biomarkers and their impact on clinical outcomes in Riyadh, Saudi Arabia. PLoS One. 2021 May 12;16(5):e0249590. doi: 10.1371/journal.pone.0249590. PMID: 33979337; PMCID: PMC8116043.
17. Sindhu CK, Nijar AK, Leong PY, Li ZQ, Hong CY, Malar L, Lee PY, Kwa SK. Awareness of Colorectal Cancer among the Urban Population in the Klang Valley. Malays Fam Physician. 2019 Dec 31;14(3):18-27. PMID: 32175037; PMCID: PMC7067497.
18. Koirala D, Pathak R, Kafle Bhandari B, Jha A, Hamal R, Gnawali A, Pandey R, Bhusal M. Detection of Colonic Polyps During Colonoscopy in a Tertiary Care Center of Nepal. J Nepal Health Res Counc. 2021 Dec 15;19(3):596-602. doi: 10.33314/jnhrc.v19i3.3678. PMID: 35140437.
19. Elwali NE, Jarrah O, Alzahrani SG, Alharbi MB, Alhejaily AG, Alsharm AA, Elhassan MMA. Colorectal Cancer in Saudi Arabia: The Way Forward. Asian Pac J Cancer Prev. 2023 Jan 1;24(1):13-19. doi: 10.31557/APJCP.2023.24.1.13. PMID: 36708547; PMCID: PMC10152865.
20. AlOmar RS, AlAbdulKader AM. Epidemiology of Lung Cancer in Saudi Arabia, Saudi Cancer Registry, 2015-2020. J Epidemiol Glob Health. 2025 Dec 4;15(1):143. doi: 10.1007/s44197-025-00491-x. PMID: 41340013; PMCID: PMC12678664.
21. Almatroudi A. A Retrospective Cohort Study of Lung Cancer Incidences and Epidemiological Analysis in Saudi Arabian Population from 2006-2016. Int J Environ Res Public Health. 2021 Nov 11;18(22):11827. doi: 10.3390/ijerph182211827. PMID: 34831584; PMCID: PMC8622663.
22. Durante C, Grani G, Lamartina L, Filetti S, Mandel SJ, Cooper DS. The Diagnosis and Management of Thyroid Nodules: A Review. JAMA. 2018 Mar 6;319(9):914-924. doi: 10.1001/jama.2018.0898. Erratum in: JAMA. 2018 Apr 17;319(15):1622. doi: 10.1001/jama.2018.3696. PMID: 29509871.
23. Flemban AF, Kabrah S, Alahmadi H, Alqurashi RK, Turaes AS, Almaghrabi R, Al Harbi S, Khogeer AA. Patterns of Thyroid Cancer Mortality and Incidence in Saudi Arabia: A 30-Year Study. Diagnostics (Basel). 2022 Nov 7;12(11):2716. doi: 10.3390/diagnostics12112716. PMID: 36359559; PMCID: PMC9689402.
24. Samargandy S, Qari R, Aljadani A, Assaqaf D Sr, Etaiwi A, Alghamdi D, Marzouki H, Alhozali A, Merdad M, Al-Hajeili M. Clinicopathological Characteristics of Thyroid Cancer in a Saudi Academic Hospital. Cureus. 2020 May 10;12(5):e8044. doi: 10.7759/cureus.8044. PMID: 32528780; PMCID: PMC7282375.
25. Alqahtani SM. Cytological patterns of thyroid lesions in Najran, Saudi Arabia: A 5-year retrospective study. Saudi Med J. 2022 Jul;43(7):735-742. doi: 10.15537/smj.2022.43.7.20220223. PMID: 35830995; PMCID: PMC9749690.
26. Alzahrani AS, Alomar H, Alzahrani N. Thyroid Cancer in Saudi Arabia: A Histopathological and Outcome Study. Int J Endocrinol. 2017;2017:8423147. doi: 10.1155/2017/8423147. Epub 2017 Feb 27. PMID: 28348588; PMCID: PMC5350345.
27. Alshehri B. Descriptive Epidemiological Analysis of Thyroid Cancer in the Saudi Population (2001-2013). Asian Pac J Cancer Prev. 2017 May 1;18(5):1445-1451. doi: 10.22034/APJCP.2017.18.5.1445. PMID: 28612600; PMCID: PMC5555560.
28. Alghamdi IG, Hussain II, Alghamdi MS, Dohal AA, Almalki SS, El-Sheemy MA. The incidence rate of thyroid cancer among women in Saudi Arabia: an observational descriptive epidemiological analysis of data from Saudi Cancer Registry 2001-2008. J Immigr Minor Health. 2015 Jun;17(3):638-43. doi: 10.1007/s10903-014-0044-5. PMID: 24859807.
29. Sankaranarayanan R, Ferlay J. Worldwide burden of gynaecological cancer: the size of the problem. Best Pract Res Clin Obstet Gynaecol. 2006 Apr;20(2):207-25. doi: 10.1016/j.bpobgyn.2005.10.007. Epub 2005 Dec 13. PMID: 16359925.
30. Makoha FW, Raheem MA. Gynecological cancer incidence in a hospital population in Saudi Arabia: the effect of foreign immigration over two decades. J Obstet Gynaecol Res. 2008 Aug;34(4):538-42. doi: 10.1111/j.1447-0756.2008.00735.x. PMID: 18937706.
31. Manzoor H, Naheed H, Ahmad K, Iftikhar S, Asif M, Shuja J, Sultan N, Ali I, Inayatullah S, Khan YH. Pattern of gynaecological malignancies in south western region of Pakistan: An overview of 12 years. Biomed Rep. 2017 Nov;7(5):487-491. doi: 10.3892/br.2017.993. Epub 2017 Sep 28. PMID: 29109863; PMCID: PMC5663976.

32. Al-Othman S, Haoudi A, Alhomoud S, Alkhenizan A, Khoja T, Al-Zahrani A. Tackling cancer control in the Gulf Cooperation Council Countries. Lancet Oncol. 2015 May;16(5):e246-57. doi: 10.1016/S1470-2045(15)70034-3. PMID: 25943069.
33. Alessy SA, Alqahtani SA, Vignat J, Abuhmaidan A, Basmi AEL, Al Lawati N, Ali A-Nooh A, Shelpai W, Alhomoud S, Al-Zahrani A, Bray F, Znaor A. The current and future cancer burden in the Gulf Cooperation Council (GCC) countries. Cancer Med. 2024 Sep;13(17):e70141. doi: 10.1002/cam4.70141. PMID: 39279725; PMCID: PMC11403302.
34. Gaskell C, Lutimba S, Bendriss G, Aleem E. Obesity, Physical Activity, and Cancer Incidence in Two Geographically Distinct Populations; The Gulf Cooperation Council Countries and the United Kingdom-A Systematic Review and Meta-Analysis. Cancers (Basel). 2024 Dec 17;16(24):4205. doi: 10.3390/cancers16244205. PMID: 39766104; PMCID: PMC11674634.
35. Ramadan M. Assessing the contribution of nine preventable risk factors attributed to the burden of early onset colorectal cancer in Gulf Cooperation Council (GCC) countries. Prev Med Rep. 2023 Aug 28;35:102389. doi: 10.1016/j.pmedr.2023.102389. PMID: 37691888; PMCID: PMC10483048.
36. Ravichandran K, Al-Zahrani AS. Association of reproductive factors with the incidence of breast cancer in Gulf Cooperation Council countries. East Mediterr Health J. 2009 May-Jun;15(3):612-21. PMID: 19731777.
37. Bukamal Z, AlRayes A. Prevalence of BRCA1 and BRCA2 Mutations Among High-risk Bahraini Patients with Breast Cancer. Gulf J Oncolog. 2023 May;1(42):22-25. PMID: 37283256.
38. Ramadan MM, Alkhatabi HA, Aboalola D, Alaa S, Alsiary RA. Burden, and trends of breast cancer along with attributable risk factors in Gulf Cooperation Council countries from 1990 to 2019 and its projections. PLoS One. 2025 Oct 6;20(10):e0331198. doi: 10.1371/journal.pone.0331198. PMID: 41052148; PMCID: PMC12500115.
39. Ibrahim WH, Rasul KI, Khinji A, Ahmed MS, Bener A. Clinical and epidemiological characteristics of lung cancer cases in Qatar. East Mediterr Health J. 2010 Feb;16(2):166-70. PMID: 20799569.
40. El-Karak F, Shamseddine A, Omar A, Haddad I, Abdelgawad M, Naqqash MA, Kaddour MA, Sharaf M, Abdo E. Prostate cancer across four countries in the Middle East: a multi-centre, observational, retrospective and prognostic study. Ecancermedicalscience. 2024 Apr 16;18:1695. doi: 10.3332/ecancer.2024.1695. PMID: 38774566; PMCID: PMC11108050.
41. Radi SM. Breast Cancer awareness among Saudi females in Jeddah. Asian Pac J Cancer Prev. 2013;14(7):4307-12. doi: 10.7314/apjcp.2013.14.7.4307. PMID: 23991994.
42. Midhet FM, Sharaf FK. Impact of health education on lifestyles in central Saudi Arabia. Saudi Med J. 2011 Jan;32(1):71-6. PMID: 21212921.
43. Bray F, Jemal A, Grey N, Ferlay J, Forman D. Global cancer transitions according to the Human Development Index (2008-2030): a population-based study. Lancet Oncol. 2012 Aug;13(8):790-801. doi: 10.1016/S1470-2045(12)70211-5. Epub 2012 Jun 1. PMID: 22658655.
44. Saudi Health Council. Saudi Cancer Registry Annual Report. Riyadh; 2023. Available from https://shc.gov.sa/Arabic/NewNCC/Activities/AnnualReports/Cancer%20Incidence%20Report%202023.pdf . last accessed, March 16, 2026
45. Alzahrani HA. Rising cancer burden among older adults in Saudi Arabia: A longitudinal analysis of incidence rates by demographics, 2013-2022. Saudi Med J. 2025 Dec;46(12):1463-1471. doi: 10.15537/smj.2025.46.12.20250569. PMID: 41402089; PMCID: PMC12707041.
46. Chaabna K, Ladumor H, Cheema S. Ecological study of breast cancer incidence among nationals and nonnationals in the Gulf Cooperation Council countries. East Mediterr Health J. 2023 Jan 19;29(1):40-48. doi: 10.26719/emhj.23.005. PMID: 36710613
47. Admoun C, Mayrovitz HN. The Etiology of Breast Cancer. In: Mayrovitz HN, editor. Breast Cancer [Internet]. Brisbane (AU): Exon Publications; 2022 Aug 6. Chapter 2. PMID: 36122154.
48. Wilkinson L, Gathani T. Understanding breast cancer as a global health concern. Br J Radiol. 2022 Feb 1;95(1130):20211033. doi: 10.1259/bjr.20211033. Epub 2021 Dec 14. PMID: 34905391; PMCID: PMC8822551.
49. DeSantis CE, Bray F, Ferlay J, Lortet-Tieulent J, Anderson BO, Jemal A. International Variation in Female Breast Cancer Incidence and Mortality Rates. Cancer Epidemiol Biomarkers Prev. 2015 Oct;24(10):1495-506. doi: 10.1158/1055-9965.EPI-15-0535. Epub 2015 Sep 10. PMID: 26359465.
50. Pfeiffer RM, Webb-Vargas Y, Wheeler W, Gail MH. Proportion of U.S. Trends in Breast Cancer Incidence Attributable to Long-term Changes in Risk Factor Distributions. Cancer Epidemiol Biomarkers Prev. 2018 Oct;27(10):1214-1222. doi: 10.1158/1055-9965.EPI-18-0098. Epub 2018 Aug 1. PMID: 30068516; PMCID: PMC8423092.
51. Katib Y, Mulla N. Epidemiological and clinical characteristics of lung cancer in Saudi Arabia: a retrospective study in single oncology center. Oncol Res. 2024 Oct 16;32(11):1803-1809. doi: 10.32604/or.2024.052358. PMID: 39449814; PMCID: PMC11497172.
52. Aljurf M, Al-Azemi N, Al-Zahrani AS, Altwaijri Y, Aleid M, Alrawaji A, Nasiri A, Alotiby M, Al-Nemari A, Al-Alyani S, Al-Zamzami A, Al-Juhani A, Mellgren A, Almashhadi S, Fakih RE, Al-Asiri MA. Cancer epidemiology in the Kingdom of Saudi Arabia, 2024. Hematol Oncol Stem Cell Ther. 2026 Jan-Mar 01;19(1):27-36. doi: 10.4103/hemoncstem.HEMONCSTEM-D-26-00008. Epub 2026 Jun 23. PMID: 42333072.
53. Da'ar OB, Zaatreh YA, Saad AA, Alkaiyat M, Pasha T, Ahmed AE, Bustami R, Alkattan K, Jazieh AR. The Burden, Future Trends, And Economic Impact Of Lung Cancer In Saudi Arabia. Clinicoecon Outcomes Res. 2019 Nov 19;11:703-712. doi: 10.2147/CEOR.S224444. PMID: 31819562; PMCID: PMC6875252.
54. Leong SP, Witte MH. Cancer metastasis through the lymphatic versus blood vessels. Clin Exp Metastasis. 2024 Aug;41(4):387-402. doi: 10.1007/s10585-024-10288-0. Epub 2024 Jun 28. PMID: 38940900; PMCID: PMC11374872.

***Corresponding author:** *Khalid Alhazmi, Department of Pathology, Faculty of Medicine, University of Tabuk, Tabuk, Saudi Arabia. E-mail: kalhazmi@ut.edu.sa*

International Journal of Biomedicine 16(4) (2026) 477-485
http://dx.doi.org/10.21103/Article16(4)_OA3

ORIGINAL ARTICLE

INTERNATIONAL JOURNAL OF BIOMEDICINE

Enhanced Oxidative Phosphorylation Induces Autophagy in Prolactinomas

Yutao Shen[1*]

[1]*School of Nursing, Zhejiang Changzheng Vocational & Technical College, Hangzhou, Zhejiang, China*

Abstract

Background: Currently, there is limited understanding of the relationship between oxidative phosphorylation and autophagy. The microarray data we obtained from prolactinoma samples and normal pituitary samples have revealed enhanced oxidative phosphorylation and autophagy activation in prolactinomas. However, whether autophagy is activated by enhanced oxidative phosphorylation remains unknown.

Methods and Results: Rat prolactinoma MMQ cells were treated with triiodothyronine (T_3) to enhance oxidative phosphorylation, and then autophagy, intracellular reactive oxygen species (ROS), and the expression of RSK1 and its active form, phospho-RSK1, ATG7, and ATG101 were detected. Next, intracellular ROS were eliminated with N-Acetyl-L-cysteine (NAC), and then autophagy and the expression of RSK1, phospho-RSK1, ATG7, and ATG101 were detected. Enhancing oxidative phosphorylation in MMQ cells increased ROS levels, and this accumulation activated autophagy by suppressing RSK1 activation and increasing ATG7 and ATG101 expression.

Conclusion: These findings provide a novel perspective that couples oxidative phosphorylation with autophagy, in which ROS play a pivotal role in linking these two biological functions in prolactinomas. **(International Journal of Biomedicine. 2026;16(4):477-485.)**

Keywords: pituitary adenoma, oxygen consumption rate, reactive oxygen species

For citation: Shen Y. Enhanced Oxidative Phosphorylation Induces Autophagy in Prolactinomas. International Journal of Biomedicine. 2026;16(4):477-485. doi:10.21103/Article16(4)_OA3

Introduction

Pituitary adenoma is a common intracranial tumor, accounting for approximately 25% of all intracranial tumors, and approximately 40% of all pituitary adenomas are prolactinomas.[1] Treating these tumors remains a great clinical challenge, especially for drug-resistant prolactinomas and refractory pituitary tumors[1] due to the lack of effective treatment targets and the complicated mechanism of pituitary tumorigenesis. Autophagy has been reported to be involved in tumorigenesis[2] and is considered a treatment target;[3] however, whether and how autophagy affects pituitary tumorigenesis remain to be fully elucidated.

Autophagy is a significant mechanism for maintaining cellular homeostasis by recycling intracellular nutrients and quality-controlling proteins. Tumor cells rely on autophagy for survival because of their active proliferation, altered metabolism, and nutrient-deprived environment.[4] In tumor cells, autophagy can facilitate tumorigenesis by promoting cell proliferation, but it can also suppress tumorigenesis by inhibiting cell survival and inducing cell death.[5,6] ATG7 and ATG101 have been considered as essential molecules for autophagy.[7,8] ATG7 is an E1-like enzyme that activates ATG12; it functions as an E1 enzyme for ATG5-ATG12 conjugation.[9] ATG101 interacts with ULK1 in an ATG13-dependent manner; ATG101 stabilizes ATG13 expression and contributes to ATG13 function by protecting it from proteasomal degradation.[10]

Abnormal metabolism is a hallmark of cancer.[11-13] Although aerobic glycolysis is commonly regarded as the dominant metabolic pathway in cancer cells,(14) recent research suggests that oxidative phosphorylation (OXPHOS) is also utilized by cancer cells.[15-18] Additionally, the effects of mitochondria on cancer cells are well documented,[19-25] suggesting that mitochondria function actively in cancer cells. Studies have shown that respiratory chain complexes I and III in mitochondria are the primary sources of reactive oxygen species (ROS);[26] therefore, actively functioning mitochondria and enhanced OXPHOS usually lead to increased ROS generation, and excess ROS cause many physiological and pathological changes in cells. However, it is unclear whether mitochondrial activity is increased and ROS influence autophagy in human prolactinoma cells.

© 2026 The Author(s). *International Journal of Biomedicine* is published by IMRDC.
This is an open access article under the CC BY-NC-ND 4.0 license.

In this study, we investigated prolactinomas using a microarray and found abnormalities in the autophagy and oxidative phosphorylation pathways. We found that autophagy was activated and that oxidative phosphorylation was enhanced in prolactinomas. Hence, this project was designed to determine the relevance of activated autophagy and enhanced oxidative phosphorylation in prolactinomas.

Materials and Methods

Tissue Samples and Histology

All prolactinoma samples were obtained from the Department of Neurosurgery, Beijing Tiantan Hospital. Fresh tumor tissue samples were immediately snap-frozen in liquid nitrogen and stored at -80°C. All normal pituitary samples were obtained from Tianjin First Central Hospital by organ donation. Fresh normal pituitary samples were also immediately snap-frozen in liquid nitrogen and stored at -80°C. A total of 31 prolactinoma samples and 25 normal pituitary samples were included in the present study, of which 7 frozen prolactinoma samples and 6 frozen normal pituitary samples were subjected to microarray, 15 paraffin-embedded prolactinoma samples and 10 paraffin-embedded normal pituitary samples were subjected to immunohistochemistry, 4 frozen prolactinoma samples and 4 frozen normal pituitary samples were subjected to Western blot, and 5 frozen prolactinoma samples and 5 frozen normal pituitary samples were subjected to respiratory chain complexes I, III and IV activity assays. Informed consent was obtained from all enrolled subjects, and the study was conducted in accordance with the principles of the Declaration of Helsinki.

Total RNA Extraction

Total RNA was extracted and purified using a mirVana™ miRNA Isolation Kit (AM1561, Ambion, USA) following the manufacturer's instructions. An Agilent Bioanalyzer 2100 (Agilent Technologies, USA) was used to obtain an RNA integrity number (RIN) and assess RNA integrity. Only those samples that showed no degradation (2100 RIN $\geq$ 7.0 and 28S/18S $\geq$ 0.7) were used to generate labeled targets.

Microarray Hybridization

Total RNA was amplified and labeled using a Low Input Quick Amp Labeling Kit, One-Color (5190-2305, Agilent Technologies, USA), following the manufacturer's instructions. Labeled cRNA was purified with an RNeasy Mini Kit (74106, QIAGEN, Germany). Each slide was hybridized with 1.65 **µg** of Cy3-labeled cRNA using a Gene Expression Hybridization Kit (5188-5242, Agilent Technologies, USA) in a hybridization oven (G2545A, Agilent Technologies, USA), according to the manufacturer's instructions. After 17 hours of hybridization, slides were washed in staining dishes (121, Thermo Shandon, USA) with a Gene Expression Wash Buffer Kit (5188-5327, Agilent Technologies, USA), following the manufacturer's instructions. Slides were scanned with an Agilent Microarray Scanner (G2565CA, Agilent Technologies, USA) using the default settings (dye channel: green, scan resolution: 5 µm, PMT: 100, 10%, 16 bit). Data were extracted with Feature Extraction software 10.7 (Agilent Technologies, USA). Raw data were normalized by the Quantile algorithm using GeneSpring Software 11.0 (Agilent Technologies, USA).

Bioinformatics Analysis

The Ingenuity Pathway Analysis (IPA) software package (version 9.0, USA; http://www.ingenuity.com) and the Kyoto Encyclopedia of Genes and Genomes (KEGG) were used to identify predominant canonical pathways in prolactinomas.

Immunohistochemistry (IHC)

Fifteen prolactinoma samples and 10 normal pituitary samples were fixed in 10% paraformaldehyde, decalcified in formic acid, and embedded in paraffin. All samples were sectioned at 5 µM and then processed for IHC staining with an anti-LC3B (1:100, 3868, CST, USA) antibody. The slides were placed in a BOND-III apparatus manufactured by Leica Biosystems, a fully automated, random-access, continuous-access slide-staining system that processes IHC tests simultaneously. IHC protocol F was selected on the machine, and 20 min with epitope retrieval was set as the heat-induced epitope retrieval (HIER) parameter. The Bond™ Polymer Refine Detection (DS9800, Leica Biosystems, Germany) was used to detect the primary antibody. The slides were scanned as digital pictures, and the expression was examined using Aperio AT2 (Leica Biosystems, Germany). The results were calculated using Aperio AT2 (Leica Biosystems, Germany) with digital slide viewing software. The staining intensity was stratified on a scale of 0-3 (0 = no staining, 1 = weak, 2 = moderate, and 3 = strong). An H-score was obtained by multiplying the staining intensity with a constant to adjust the mean to the strongest staining [H-score = 3 * (percentage of strong staining); 1.0 (% weak), 2.0 (% moderate), 3.0 (% strong)] to give a score ranging from 0-300.

Respiratory Chain Complex I, III, and IV Activity Assay

Complex I activity was detected using a Complex I Enzyme Activity Microplate Assay Kit (ab109721, Abcam, UK) according to the manufacturer's instructions. Proteins were isolated from 100 mg of fresh tissue and were diluted to the desired concentration. In total, 200 µl of the diluted sample was used. The absorbance was detected at 450 nm using a multimode microplate reader (Tecan, Männedorf, Switzerland). Complex III activity was detected using a Mitochondrial Complex III Activity Assay Kit (K520, BioVision, USA) according to the manufacturer's instructions. Proteins were isolated from 100 mg of fresh tissue and were diluted to the desired concentration. In total, 200 µl of the diluted sample was used. The absorbance was detected at 550 nm using a multimode microplate reader (Tecan, Männedorf, Switzerland). Complex IV activity was detected using a Complex IV Human Enzyme Activity Microplate Assay Kit (ab109909, Abcam, UK) according to the manufacturer's instructions. Proteins were isolated from 100 mg of fresh tissue and were diluted to the desired concentration. In total, 200 µl of the diluted sample was used. The absorbance was

detected at 550 nm using a multimode microplate reader (Tecan, Männedorf, Switzerland).

Cell Culture

The rat pituitary MMQ cell line was purchased from the American Type Culture Collection (ATCC, USA), whose commercial designation is CRL-10609™, and were cultured in F-12K Medium (30-2004, ATCC, USA) supplemented with 15% (v/v) horse serum (16050-122, Gibco, USA) and 2.5% (v/v) fetal bovine serum (10099-141, Gibco, USA) in a humidified incubator at 37°C in 5% (v/v) CO_2. The culture medium was replaced every other day. For triiodothyronine (T_3) stimulation, MMQ cells were treated with 1 nM or 10 nM, or 100 nM T_3 (T2877, Sigma-Aldrich, USA) for 24 hours. For ROS stimulation, MMQ cells were treated with 100 nM T_3 (T2877, Sigma-Aldrich, USA) and 300 μM pyocyanin (ab141099, Abcam, UK) for 24 hours and 1 hour, respectively. One group of MMQ cells was pretreated with 5 mM N-Acetyl-L-cysteine (NAC) (A105422, Aladdin, China) for 2 hours to eliminate intracellular ROS, and the other group of MMQ cells was not treated with NAC. To activate autophagy, MMQ cells were treated with 100 nM rapamycin (ab120224, Abcam, UK) or 10 mM LiCl (C8381, Solarbio, China) for 24 hours. For autophagy inhibition, MMQ cells were treated with 30 μM chloroquine (C193834, Aladdin, China) or 2.5 mM 3-methyladenine (ab120841, Abcam, UK) for 24 hours. For bromocriptine treatment after autophagy activation or inhibition, MMQ cells were treated with 50 μM bromocriptine (S84497, Yuanye Bio-Technology, China) for 48 hours.

Autophagy Detection

MMQ cells were collected by centrifugation and then resuspended to a density of 1 x 10^6/ml. Autophagy in MMQ cells was detected using an Autophagy Detection Kit (ab139484, Abcam, UK) according to the manufacturer's instructions. The fluorescence images were observed and photographed using a fluorescence microscope (Axio Observer. Z1, Zeiss, Germany). The autophagic signal was imaged using a standard FITC filter set, and the nucleus was imaged using a DAPI filter set.

Measurement of Intracellular ROS

After MMQ cells were treated with 1 nM, 10 nM, or 100 nM T_3 for 24 hours, intracellular ROS were monitored using a Cellular Reactive Oxygen Species Detection Assay Kit (ab186029, Abcam, UK) according to the manufacturer's instructions. The fluorescence intensity was detected at E_x/E_m = 650/675 nm using a multimode microplate reader (Tecan, Männedorf, Switzerland).

Mitochondrial Superoxide Detection

After MMQ cells were treated with 1 nM, 10 nM, or 100 nM T_3 for 24 hours, mitochondrial superoxide was detected using a MitoSOX™ Red Mitochondrial Superoxide Indicator (M36008, ThermoFisher, USA) according to the manufacturer's instructions. The fluorescence intensity was detected at E_x/E_m = 510/580 nm using a multimode microplate reader (Tecan, Männedorf, Switzerland).

Oxygen Consumption Assessment

The oxygen consumption rate (OCR) was assessed using an Oxygen Consumption Rate Assay Kit (600800, Cayman Chemical, USA) according to the manufacturer's instructions. The fluorescence intensity was detected at E_x/E_m = 380/650 nm using a multimode microplate reader (Tecan, Männedorf, Zürich, Switzerland). The OCR is the slope of the curve obtained by plotting fluorescence intensity over time.

Protein Extraction and Western Blot Assay

Tissue samples or cells were lysed using RIPA lysis buffer (C1050, Applygen, China) with a protease inhibitor cocktail (P1265, Applygen, China) and a phosphatase inhibitor cocktail (P1260, Applygen, China). The total protein concentration was determined using a BCA Protein Assay Kit (SK258437, ThermoFisher, USA). Equal amounts of total proteins were separated by SDS-PAGE (10% gels) for SQSTM1 (1:1000, 39749, CST, USA), RSK1 (1:1000, 8408, CST, USA), phospho-RSK1 (1:1000, 9335, CST, USA), ATG7 (1:1000, 8558, CST, USA) and ATG101 (1:1000, 13492, CST, USA) detection, and 15% gels were used for LC3B (1:500, 3868, CST, USA) detection. GAPDH was used as the protein loading control. After SDS-PAGE, the proteins on the gels were transferred to BioTrace nitrocellulose membranes (66485, Pall, USA), blocked with 5% skim milk in Tris-buffered saline (TBS, pH 7.4; 20 mM Tris-HCl, 150 mM NaCl), and then incubated with different primary antibodies overnight at 4°C. The following day, the membranes were incubated with IRDye-labeled goat anti-mouse or goat anti-rabbit IgG at room temperature for 1 hour. Finally, the protein bands were scanned using a LI-COR Odyssey system (LI-COR Biosciences, USA). At least 3 independent experiments were performed, and a representative result is shown.

Cell Viability Assay

Cell viability was determined using a Cell Counting Kit-8 (CK04, Dojindo, Japan) according to the manufacturer's instructions. MMQ cells were plated in 96-well plates at approximately 1×10^4 cells per well. After addition of the CCK-8 solution, the plate was incubated at 37°C for 4 hours, and absorbance was measured at 450 nm using a multimode microplate reader (Tecan, Männedorf, Switzerland).

Cell Proliferation Assay

Cell proliferation was determined using a BrdU Cell Proliferation ELISA (11647229001, Roche, Switzerland) according to the manufacturer's instructions. MMQ cells were plated in 96-well plates at approximately 1×10^4 cells per well. After addition the BrdU solution, the plate was incubated at 37°C for 2 hours, and the cells were then fixed for 30 minutes at room temperature. Next, after adding the anti-BrdU-POD solution, the plate was incubated at room temperature for 90 minutes. After Substrate solution and 1 M H_2SO_4 were added to the wells, absorbance was measured at 450 nm using a multimode microplate reader (Tecan, Männedorf, Switzerland).

Measurement of Prolactin Production

The concentration of prolactin in the culture supernatant was measured using a Prolactin ELISA Kit (K4688, BioVision,

USA) according to the manufacturer's instructions. The supernatant was collected from the culture medium. In total, 50 µl of the supernatant was used. The absorbance was detected at 450 nm using a multimode microplate reader (Tecan, Männedorf, Switzerland).

Statistical Analysis

Statistical analyses were performed using GraphPad Prism 7 (San Diego, USA). The data are presented as the mean ± standard error of the mean (SEM). Variables were analyzed using an unpaired Student's t-test to compare two groups, unless indicated otherwise. For all statistical analyses, a p-value < 0.05 was considered statistically significant.

Results

Differentially Expressed Genes are Enriched in the Autophagy and Oxidative Phosphorylation Pathways in Prolactinomas

We observed significant differences in expression between prolactinoma and normal pituitary samples by gene expression microarray analysis. A total of 2,481 genes were significantly differentially expressed in the prolactinoma and normal pituitary samples ($p < 0.05$, fold change > 2). Among these 2,481 genes, 1,001 were upregulated, and 1,480 were downregulated in prolactinoma samples (Supplementary Table 1).

Based on the results of the IPA and KEGG pathway analyses, we found that the genes upregulated in prolactinomas were enriched in the regulation of the autophagy (Figure 1A) and oxidative phosphorylation (Figure 1B) pathways.



Figure 1. *Ingenuity pathway analysis of differentially expressed genes in prolactinomas.*

(A) The genes with upregulated expression are enriched in the regulation of the autophagy pathway. (B) The genes with upregulated expression are enriched in the oxidative phosphorylation pathway. Pink represents most genes with upregulated expression in the pathway, while green represents most genes with downregulated expression in the pathway. The more up- or downregulated genes enriched in the pathway there are, the darker the pink or green color in the grid.

We speculated that autophagy was activated and that oxidative phosphorylation was enhanced in prolactinomas because the genes with upregulated expression directly or indirectly participate in both processes. There were two genes with upregulated expression in the regulation of the autophagy pathway: ATG7 and ATG101 (Supplementary Table 2). We speculated that ATG7 and ATG101 were relevant to the autophagy activation in prolactinomas. We further analyzed the KEGG data and found that the expression of RPS6KA1, also known as RSK1 and involved in the mTOR signaling pathway, was downregulated in prolactinomas (Supplementary Table 1 and Supplementary Table 2). RSK1 functions in the mTOR pathway by directly phosphorylating TSC2, thereby potently inhibiting TSC2's ability to suppress mTOR signaling. (27) We speculated that RSK1 was also relevant to the autophagy activation in prolactinomas.

Autophagy Activation in Prolactinomas

LC3B and SQSTM1 were selected to verify the autophagy activation in prolactinomas. Compared with normal pituitaries, prolactinomas had increased LC3B expression (Figure 2A, 2B) and reduced SQSTM1 expression (Figure 2B). Then, we detected the expression of ATG7, ATG101, RSK1, and its active form, phospho-RSK1, in prolactinomas and normal pituitaries. The results showed that the expression of ATG7 and ATG101 was higher in prolactinomas than in normal pituitaries (Figure 2C), and the expression of RSK1 and phospho-RSK1 was lower in prolactinomas than in normal pituitaries (Figure 2C). These results indicated that autophagy was activated in prolactinomas, and the expression of ATG7, ATG101, and RSK1 was consistent with microarray data.

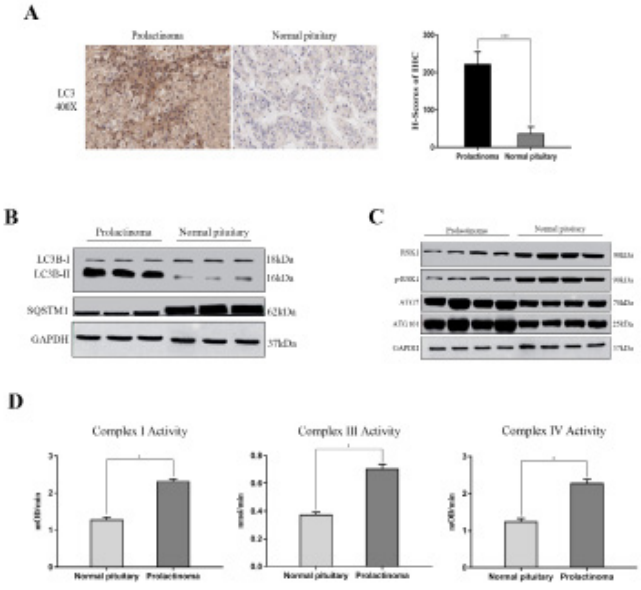

Figure 2. *Validation of microarray data in tissue samples.*

*(A) Immunohistochemistry showed that the expression of LC3 in prolactinomas was higher than that in normal pituitaries (n = 15 for prolactinomas, n = 10 for normal pituitaries). (B) The expression of LC3B-II in prolactinomas was higher than in normal pituitaries. The expression of SQSTM1 in prolactinomas was lower than in normal pituitaries (n = 3 for prolactinomas, n = 3 for normal pituitaries). (C) The expression of RSK1 and phospho-RSK1 in prolactinomas was lower than in normal pituitaries. The expression of ATG7 and ATG101 in prolactinomas was higher than in normal pituitaries (n = 4 for prolactinomas, n = 4 for normal pituitaries). (D) The activity of respiratory chain complexes I, III and IV was higher in prolactinomas than in normal pituitaries (n = 5 for prolactinomas, n = 5 for normal pituitaries). Bars represent the mean of the respective individual ratios ± SEM. *- p<0.05; ***- p<0.001.*

The Increased Activity of Respiratory Chain Complexes I, III, and IV in Prolactinomas

To verify that oxidative phosphorylation is enhanced in prolactinomas, we assessed mitochondrial function by measuring the activities of respiratory chain complexes I, III, and IV. The results showed that the activities of respiratory chain complexes I, III, and IV were higher in prolactinomas than in normal pituitaries (Figure 2D). These results indicated that oxidative phosphorylation was enhanced in prolactinomas.

Enhanced Oxidative Phosphorylation Induces Autophagy and Increases the Expression of ATG7 and ATG101, and Suppresses the Activation of RSK1 in MMQ Cells

To study whether enhanced oxidative phosphorylation induces autophagy in prolactinomas, we used triiodothyronine (T_3) to enhance oxidative phosphorylation and then detected autophagy in MMQ cells. First, to verify that T_3 enhances oxidative phosphorylation in MMQ cells, we measured OCR after treatment with different concentrations of T_3. The results showed that T_3 treatment increases OCR in a dose-dependent manner, suggesting enhanced oxidative phosphorylation in MMQ cells (Figure 3A, 3B). After MMQ cells were treated with 1 nM, 10 nM, or 100 nM T_3 for 24 hours, we directly detected autophagy using an Autophagy Detection Kit. As shown in Figure 3C, the LC3 fluorescence intensity increased with increasing T_3 concentration. Additionally, total protein was extracted from MMQ cells after 24 hours of treatment with different concentrations of T_3, and the expression of LC3B-II and SQSTM1 was detected by Western blot. As shown in Figure 3D, LC3B-II expression increased, while SQSTM1 expression decreased as T3 concentration increased. These results indicated that enhanced oxidative phosphorylation induced autophagy in MMQ cells.

We further assessed the expression of ATG7, ATG101, RSK1, and phospho-RSK1 in MMQ cells after treatment with 1 nM, 10 nM, or 100 nM T_3 for 24 hours. The results showed that the expression of ATG7 and ATG101 increased with increasing T_3 concentration; there was no significant difference in RSK1 expression between groups; and the expression of phospho-RSK1 decreased with increasing T_3 concentration (Figure 3E). These results indicated that enhanced oxidative phosphorylation increased the expression of ATG7 and ATG101 and suppressed RSK1 activation in MMQ cells.

Enhanced Oxidative Phosphorylation Stimulates ROS Generation in MMQ Cells

Electron leakage during electron flow through the electron transport chain produces ROS.(26) To investigate whether ROS production in MMQ cells increases when oxidative phosphorylation is enhanced, we measured cellular ROS levels after cells were treated with 1 nM, 10 nM, or 100 nM T_3 for 24 hours. Compared with cells not treated with T_3, cells treated with T_3 showed increased ROS production, which increased with increasing T_3 concentration (Figure 4A). We also used MitoSOX, a fluorophore that is activated by mitochondrial superoxide oxidation to assess mitochondrial ROS formation, and confirmed that enhanced oxidative phosphorylation led to mitochondrial-mediated ROS production (Figure 4B).

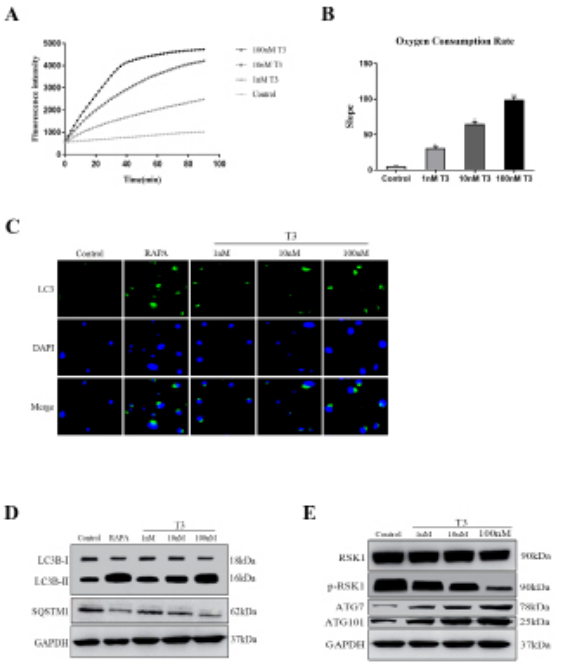

Figure 3. *Enhanced oxidative phosphorylation induces autophagy and the increased expression of ATG7 and ATG101, suppressing the activation of RSK1.*

*(A and B) Assessment of oxygen consumption rate (OCR) in T_3-treated MMQ cells at different doses for 24 hours. (C) MMQ cells were treated with different doses of T_3 for 24 hours. An Autophagy Detection Kit was used to detect autophagy in MMQ cells. Rapamycin-treated MMQ cells were used as a positive control. (D) After extraction of the proteins from MMQ cells treated with different doses of T_3 for 24 hours, Western blotting was performed using an anti-LC3B antibody and an anti-SQSTM1 antibody. Rapamycin-treated MMQ cells were used as a positive control. (E) After extraction of the proteins from MMQ cells treated with different doses of T_3 for 24 hours, Western blotting was performed using anti-RSK1, anti-phospho-RSK1, anti-ATG7, and anti-ATG101 antibodies. Bars represent the mean of the respective individual ratios ± SEM. n = 3. **- p<0.01; ***- p<0.001.*

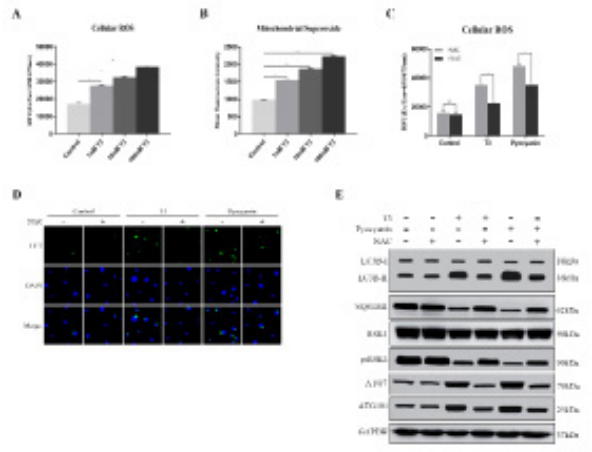

Figure 4. *Enhanced oxidative phosphorylation stimulates ROS generation, and ROS induces autophagy and the increased expression of ATG7 and ATG101, suppressing the activation of RSK1.*

*(A) Intracellular ROS generation in T_3-treated MMQ cells. (B) Mitochondrial superoxide generation in T_3-treated MMQ cells measured by MitoSOX. (C) NAC eliminated a portion of ROS in T_3 (100nM/24 h)-treated and pyocyanin-treated MMQ cells. (D) An Autophagy Detection Kit was used to detect autophagy in each group of MMQ cells. Pyocyanin-treated MMQ cells were used as a positive control. (E) After ROS were partially eliminated by NAC treatment, autophagy was decreased, the expression of ATG7 and ATG101 was decreased, and the activation of RSK1 was increased. Bars represent the mean of the respective individual ratios ± SEM. n = 3. *- p<0.05; **- p<0.01; ns - not significant.*

ROS Induce Autophagy and Increase the Expression of ATG7 and ATG101, thereby Suppressing RSK1 Activation in MMQ Cells

We next sought to verify that ROS induce autophagy and increase the expression of ATG7 and ATG101, and to suppress the activation of RSK1. We speculated that the elimination of ROS would suppress autophagy and the expression of ATG7 and ATG101, and promote RSK1 phosphorylation. The ROS scavenger NAC was used to eliminate ROS in MMQ cells, and pyocyanin, a compound known to rapidly stimulate ROS production in cells, was used as a positive control. The results in Figure 4C showed that pyocyanin stimulated MMQ cells to produce substantial amounts of ROS, and NAC treatment reduced the ROS. The results in Figure 4D showed that NAC treatment reduced LC3 fluorescence intensity in the T3- and pyocyanin-treated groups. Additionally, NAC treatment decreased LC3B-II expression and increased SQSTM1 expression in the T_3-treated and pyocyanin-treated groups (Figure 4E). In addition, NAC treatment decreased the expression of ATG7 and ATG101 and increased the expression of phospho-RSK1 in the T_3-treated and pyocyanin-treated groups (Figure 4E). Thus, NAC-mediated elimination of ROS suppressed autophagy and the expression of ATG7 and ATG101, and promoted RSK1 phosphorylation in MMQ cells. These results suggested that enhanced oxidative phosphorylation induced autophagy and increased the expression of ATG7 and ATG101, thereby suppressing the activation of RSK1 by stimulating ROS generation in MMQ cells.

The Role of Autophagy in MMQ Cells

We further investigated the role of autophagy in MMQ cells. We divided the MMQ cells into two groups: a bromocriptine-treated group and a bromocriptine-untreated group. Bromocriptine is a kind of dopamine agonist that can suppress tumor cells of prolactinoma. For each group, we chose two autophagy activators, rapamycin and LiCl, to activate autophagy in the cells, and two autophagy inhibitors, chloroquine and 3-methyladenine, to inhibit autophagy in the cells. The results of the CCK-8 assay showed that in the bromocriptine-untreated group, cell viability increased after autophagy activation; after autophagy inhibition, cell viability decreased (Figure 5A), and the results were identical in the bromocriptine-treated group (Figure 5B). The results of the BrdU assay showed that in the bromocriptine-untreated group, proliferation increased after autophagy activation; after autophagy inhibition, proliferation decreased (Figure 5C), and the results were identical in the bromocriptine-treated group (Figure 5D). We also measured prolactin production in the supernatant of MMQ cells. The results showed that in the bromocriptine-untreated group, prolactin concentration increased after autophagy activation; after autophagy inhibition, it decreased (Figure 5E), and the results were identical in the bromocriptine-treated group (Figure 5F). Based on these results, we discovered that autophagy played a protective role in MMQ cells, enhancing cell viability and proliferation and increasing prolactin secretion under both normal and pharmacological inhibition conditions.

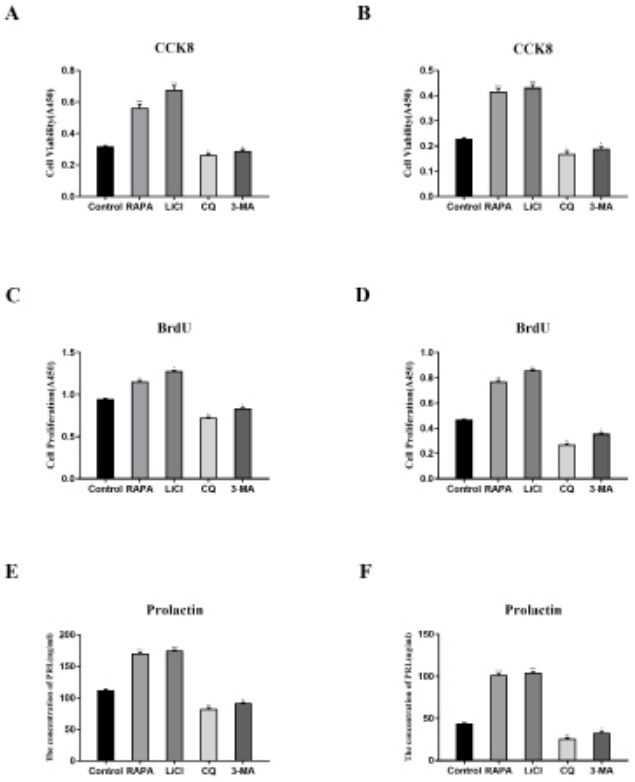

Figure 5. *The role of autophagy in MMQ cells.*

*(A) In the bromocriptine-untreated group, cell viability was enhanced after autophagy was activated by rapamycin and LiCl treatment, and the cell viability was reduced after autophagy was inhibited by chloroquine and 3-methyladenine treatment. (B) In the bromocriptine-treated group, cell viability was enhanced after autophagy was activated by rapamycin and LiCl treatment, and cell viability was reduced after autophagy was inhibited by chloroquine and 3-methyladenine treatment. (C) In the bromocriptine-untreated group, proliferation was enhanced after autophagy was activated by rapamycin and LiCl treatment, and proliferation was reduced after autophagy was inhibited by chloroquine and 3-methyladenine treatment. (D) In the bromocriptine-treated group, proliferation was enhanced after autophagy was activated by rapamycin and LiCl treatment, and proliferation was reduced after autophagy was inhibited by chloroquine and 3-methyladenine treatment. (E) In the bromocriptine-untreated group, the concentration of prolactin was increased after autophagy was activated by rapamycin and LiCl treatment, and the concentration of prolactin was decreased after autophagy was inhibited by chloroquine and 3-methyladenine treatment. (F) In the bromocriptine-treated group, the concentration of prolactin was increased after autophagy was activated by rapamycin and LiCl treatment, and the concentration of prolactin was decreased after autophagy was inhibited by chloroquine and 3-methyladenine treatment. Bars represent the mean of the respective individual ratios ± SEM. n = 3. *- p<0.05; **- p<0.01; ***- p<0.001.*

Discussion

The study of autophagy is extensive and in-depth, and a key aspect of autophagy research is the study of regulatory mechanisms.[28] Oxidative phosphorylation is a vital process in the energy production of aerobic cells, accounting for approximately 90% of adenosine triphosphate (ATP) generation during catabolism.[29] Bartolomé A et al. reported that autophagy is induced after uncoupling of oxidative phosphorylation in MEFs.[30] However, whether changes in

oxidative phosphorylation in prolactinomas induce autophagy is unclear.

In this study, we show that prolactinomas exhibit increased LC3-II expression and reduced SQSTM1 expression, indicating autophagy activation. Additionally, we show that prolactinomas have increased activity of respiratory chain complexes I, III, and IV. These results indicate that oxidative phosphorylation is enhanced in prolactinomas due to active mitochondrial function. The respiratory chain complexes I and III are the primary sources of ROS.[26] Thus, the active respiratory chain complexes I and III may cause ROS accumulation in tumor cells. Furthermore, we detected upregulation of ATG7 and ATG101 and downregulation of RSK1, according to the microarray results. The Western blot assay demonstrated that the expression of ATG7 and ATG101 was upregulated, and that the expression of RSK1 was downregulated, in prolactinomas. Next, we artificially enhanced oxidative phosphorylation in MMQ cells using T_3 and found that autophagy was activated and ROS generation increased accordingly. We also found that after oxidative phosphorylation was enhanced, the expression of ATG7 and ATG101 increased; the expression of RSK1 did not change; however, the expression of phospho-RSK1, the active form of RSK1, decreased, suggesting that RSK1 activation was suppressed. Then, we used NAC to reduce ROS levels in MMQ cells and found that, compared with the NAC-untreated group, autophagy was suppressed, and the expression of ATG7 and ATG101 was decreased in the NAC-treated group. In addition, RSK1 expression did not change significantly, whereas phospho-RSK1 expression increased, suggesting that RSK1 was activated in the NAC-treated group.

mTOR is a downstream effector molecule regulated by many signaling pathways, such as PI3K/Akt, AMPK, MAPK, and P53, and plays a significant regulatory role in tumor cells. The mTOR pathway is a common signaling pathway in autophagy, and extensive reports indicate that mTORC1, one of the mTOR complexes, is a major negative regulator of autophagy.[31-33] TSC2 is involved in the mTOR pathway and negatively regulates mTORC1,[34] and RSK1 directly phosphorylates TSC2 and potently inhibits its activity.[27] In summary, RSK1 is a negative regulator of autophagy. In prolactinomas, our results show that RSK1 and its active form, phospho-RSK1, are downregulated. In MMQ cells, although RSK1 expression is not markedly altered, its activation is suppressed.

ATG7 and ATG101 are essential molecules for autophagy; their roles in the process of autophagy have been clearly described.[7-10] Zhu J et al. reported that ATG7-mediated autophagy is a key player in regulating bladder cancer invasion,[35] and Lévy J et al. reported that the inactivation of ATG7 in intestinal epithelial cells inhibits the formation of precancerous lesions.[36] Additionally, Wei H et al. reported that knockout of FIP200, a component of the ULK1-ATG13-FIP200-ATG101 complex, significantly suppresses mammary tumorigenesis and progression in a mouse model of human breast cancer.[37] Our results show that the expression of ATG7 and ATG101 is upregulated in prolactinomas, and that their expression is increased while oxidative phosphorylation is enhanced in MMQ cells. We think that the increased expression of ATG7 and ATG101 is due to RSK1 suppression and leads to autophagy activation in prolactinomas; the underlying mechanism remains to be further explored.

ROS are a group of molecules including superoxide anions ($O_2^{\cdot-}$), hydroxyl radicals ($OH\cdot$), and hydrogen peroxide (H_2O_2). These molecules are synthesized within cells through oxygen metabolism and serve as important signaling molecules at low levels.[38] Mitochondria produce the majority of intracellular ROS through electron leakage from the electron transport chain during oxidative phosphorylation.[39,40] It is generally accepted that ROS induce autophagy.[41,42] Our findings demonstrate that ROS induce autophagy and suppress RSK1 activation in MMQ cells. However, we have not identified the relationship between ROS accumulation and RSK1 suppression in this study, and we need to conduct further research into the specific mechanism.

We further explored the role of autophagy in MMQ cells. Interestingly, we discovered that in both the bromocriptine-untreated and bromocriptine-treated groups, autophagy enhanced cell viability and proliferation and increased prolactin secretion. Recent studies have demonstrated that tumor resistance to anticancer therapies, including chemotherapy, radiation therapy, and targeted therapy, can be enhanced by upregulation of autophagy in various tumor cell lines.[43,44] Furthermore, growing evidence indicates that autophagy inhibition augments cytotoxicity when combined with several anticancer drugs in preclinical models.[45-47] Dopamine agonists have become the initial therapy for most patients with prolactinomas since they are found to be successful in reducing prolactin levels and reducing the tumor size. However, there are still some patients who do not respond to dopamine agonists satisfactorily even at considerably high doses; in other words, they display a pharmacological resistance to the function of these drugs.[48,49] Although resistant tumors appear to have fewer D_2 receptors, based on our experimental results, we speculate that the activation of autophagy in prolactinomas contributes to resistance to dopamine agonists. Furthermore, the recurrence rate of pituitary adenomas differs between subtypes, being highest in prolactinomas, with the highest incidence of recurrence occurring between 1 and 5 years after surgery.[50] We speculate that the activation of autophagy in prolactinomas is also associated with the high recurrence rate since autophagy plays a protective role in MMQ cells.

In conclusion, our findings provide a novel perspective that couples oxidative phosphorylation with autophagy, in which ROS play a pivotal role in linking these two biological functions in prolactinomas.

Acknowledgments

The author deeply and sincerely appreciates Beijing Tiantan Hospital and Tianjin First Central Hospital for providing prolactinoma and normal pituitary tissue samples.

Sources of Funding

This research received no specific grant from any funding agency in the public, commercial, or not-for-profit sectors.

Disclosure and Conflicts of Interest

The author declares no conflicts of interest.

References

1. Gillam MP, Molitch ME, Lombardi G, Colao A. Advances in the treatment of prolactinomas. Endocr Rev. 2006;27(5):485-534.
2. White E, Mehnert JM, Chan CS. Autophagy, Metabolism, and Cancer. Clin Cancer Res. 2015;21(22):5037-46.
3. Sui X, Chen R, Wang Z, Huang Z, Kong N, Zhang M, et al. Autophagy and chemotherapy resistance: a promising therapeutic target for cancer treatment. Cell Death Dis. 2013;4:e838.
4. Mowers EE, Sharifi MN, Macleod KF. Functions of autophagy in the tumor microenvironment and cancer metastasis. FEBS J. 2018;285(10):1751-66.
5. Lim KH, Staudt LM. Toll-like receptor signaling. Cold Spring Harb Perspect Biol. 2013;5(1):a011247.
6. Salminen A, Kaarniranta K, Kauppinen A. Beclin 1 interactome controls the crosstalk between apoptosis, autophagy and inflammasome activation: impact on the aging process. Ageing Res Rev. 2013;12(2):520-34.
7. Xiong J. Atg7 in development and disease: panacea or Pandora's Box? Protein Cell. 2015;6(10):722-34.
8. Noda NN, Mizushima N. Atg101: Not Just an Accessory Subunit in the Autophagy-initiation Complex. Cell Struct Funct. 2016;41(1):13-20.
9. Tanida I, Mizushima N, Kiyooka M, Ohsumi M, Ueno T, Ohsumi Y, et al. Apg7p/Cvt2p: A novel protein-activating enzyme essential for autophagy. Mol Biol Cell. 1999;10(5):1367-79.
10. Mercer CA, Kaliappan A, Dennis PB. A novel, human Atg13 binding protein, Atg101, interacts with ULK1 and is essential for macroautophagy. Autophagy. 2014;5(5):649-62.
11. Hanahan D, Weinberg RA. Hallmarks of cancer: the next generation. Cell. 2011;144(5):646-74.
12. Boroughs LK, DeBerardinis RJ. Metabolic pathways promoting cancer cell survival and growth. Nat Cell Biol. 2015;17(4):351-9.
13. Pavlova NN, Thompson CB. The Emerging Hallmarks of Cancer Metabolism. Cell Metab. 2016;23(1):27-47.
14. Hsu PP, Sabatini DM. Cancer cell metabolism: Warburg and beyond. Cell. 2008;134(5):703-7.
15. Mathupala SP, Ko YH, Pedersen PL. The pivotal roles of mitochondria in cancer: Warburg and beyond and encouraging prospects for effective therapies. Biochim Biophys Acta. 2010;1797(6-7):1225-30.
16. LeBleu VS, O'Connell JT, Gonzalez Herrera KN, Wikman H, Pantel K, Haigis MC, et al. PGC-1alpha mediates mitochondrial biogenesis and oxidative phosphorylation in cancer cells to promote metastasis. Nat Cell Biol. 2014;16(10):992-1003, 1-15.
17. Jiang L, Xiao L, Sugiura H, Huang X, Ali A, Kuro-o M, et al. Metabolic reprogramming during TGFbeta1-induced epithelial-to-mesenchymal transition. Oncogene. 2015;34(30):3908-16.
18. Viale A, Corti D, Draetta GF. Tumors and mitochondrial respiration: a neglected connection. Cancer Res. 2015;75(18):3685-6.
19. Viale A, Pettazzoni P, Lyssiotis CA, Ying H, Sanchez N, Marchesini M, et al. Oncogene ablation-resistant pancreatic cancer cells depend on mitochondrial function. Nature. 2014;514(7524):628-32.
20. Roesch A, Vultur A, Bogeski I, Wang H, Zimmermann Katharina M, Speicher D, et al. Overcoming Intrinsic Multidrug Resistance in Melanoma by Blocking the Mitochondrial Respiratory Chain of Slow-Cycling JARID1Bhigh Cells. Cancer Cell. 2013;23(6):811-25.
21. Strohecker AM, White E. Targeting mitochondrial metabolism by inhibiting autophagy in BRAF-driven cancers. Cancer Discov. 2014;4(7):766-72.
22. Lu CL, Qin L, Liu HC, Candas D, Fan M, Li JJ. Tumor cells switch to mitochondrial oxidative phosphorylation under radiation via mTOR-mediated hexokinase II inhibition--a Warburg-reversing effect. PLoS One. 2015;10(3):e0121046.
23. Maiuri MC, Kroemer G. Essential role for oxidative phosphorylation in cancer progression. Cell Metab. 2015;21(1):11-2.
24. Tan AS, Baty JW, Dong LF, Bezawork-Geleta A, Endaya B, Goodwin J, et al. Mitochondrial genome acquisition restores respiratory function and tumorigenic potential of cancer cells without mitochondrial DNA. Cell Metab. 2015;21(1):81-94.
25. Xu Q, Biener-Ramanujan E, Yang W, Ramanujan VK. Targeting metabolic plasticity in breast cancer cells via mitochondrial complex I modulation. Breast Cancer Res Treat. 2015;150(1):43-56.
26. Turrens JF. Mitochondrial formation of reactive oxygen species. J Physiol. 2003;552(Pt 2):335-44.
27. Roux PP, Ballif BA, Anjum R, Gygi SP, Blenis J. Tumor-promoting phorbol esters and activated Ras inactivate the tuberous sclerosis tumor suppressor complex via p90 ribosomal S6 kinase. Proc Natl Acad Sci U S A. 2004;101(37):13489-94.
28. Abada A, Elazar Z. Getting ready for building: signaling and autophagosome biogenesis. EMBO Rep. 2014;15(8):839-52.
29. Lehninger AL, Wadkins CL, Cooper C, Devlin TM, Gamble JL. Oxidative phosphorylation. Science. 1958;128(3322):450-6.
30. Bartolomé A, García-Aguilar A, Asahara SI, Kido Y, Guillén C, Pajvani UB, et al. MTORC1 Regulates both General Autophagy and Mitophagy Induction after Oxidative Phosphorylation Uncoupling. Molecular and cellular biology. 2017;37(23).
31. Yorimitsu T, Klionsky DJ. Autophagy: molecular machinery for self-eating. Cell Death Differ. 2005;12 Suppl 2:1542-52.
32. Rubinsztein DC, Gestwicki JE, Murphy LO, Klionsky DJ. Potential therapeutic applications of autophagy. Nat Rev Drug Discov. 2007;6(4):304-12.
33. Pattingre S, Espert L, Biard-Piechaczyk M, Codogno P. Regulation of macroautophagy by mTOR and Beclin 1 complexes. Biochimie. 2008;90(2):313-23.
34. Tee AR, Fingar DC, Manning BD, Kwiatkowski DJ, Cantley LC, Blenis J. Tuberous sclerosis complex-1 and -2 gene products function together to inhibit mammalian target of rapamycin (mTOR)-mediated downstream signaling. Proc Natl Acad Sci U S A. 2002;99(21):13571-6.
35. Zhu J, Tian Z, Li Y, Hua X, Zhang D, Li J, et al. ATG7 Promotes Bladder Cancer Invasion via Autophagy-Mediated Increased ARHGDIB mRNA Stability. Adv Sci (Weinh). 2019;6(8):1801927.

36. Levy J, Cacheux W, Bara MA, L'Hermitte A, Lepage P, Fraudeau M, et al. Intestinal inhibition of Atg7 prevents tumour initiation through a microbiome-influenced immune response and suppresses tumour growth. Nat Cell Biol. 2015;17(8):1062-73.
37. Wei H, Guan JL. Pro-tumorigenic function of autophagy in mammary oncogenesis. Autophagy. 2012;8(1):129-31.
38. Gough DR, Cotter TG. Hydrogen peroxide: a Jekyll and Hyde signalling molecule. Cell Death Dis. 2011;2:e213.
39. St-Pierre J, Buckingham JA, Roebuck SJ, Brand MD. Topology of superoxide production from different sites in the mitochondrial electron transport chain. J Biol Chem. 2002;277(47):44784-90.
40. Murphy MP. How mitochondria produce reactive oxygen species. Biochem J. 2009;417(1):1-13.
41. Azad MB, Chen Y, Gibson SB. Regulation of autophagy by reactive oxygen species (ROS): implications for cancer progression and treatment. Antioxid Redox Signal. 2009;11(4):777-90.
42. Moore MN. Autophagy as a second level protective process in conferring resistance to environmentally-induced oxidative stress. Autophagy. 2008;4(2):254-6.
43. Hu YL, Jahangiri A, Delay M, Aghi MK. Tumor cell autophagy as an adaptive response mediating resistance to treatments such as antiangiogenic therapy. Cancer Res. 2012;72(17):4294-9.
44. Zou Z, Yuan Z, Zhang Q, Long Z, Chen J, Tang Z, et al. Aurora kinase A inhibition-induced autophagy triggers drug resistance in breast cancer cells. Autophagy. 2012;8(12):1798-810.
45. Firat E, Weyerbrock A, Gaedicke S, Grosu AL, Niedermann GJPO. Chloroquine or Chloroquine-PI3K/Akt Pathway Inhibitor Combinations Strongly Promote γ-Irradiation-Induced Cell Death in Primary Stem-Like Glioma Cells. 2012;7(10):e47357.
46. Carew JS, Nawrocki ST, Kahue CN, Zhang H, Yang C, Chung L, et al. Targeting autophagy augments the anticancer activity of the histone deacetylase inhibitor SAHA to overcome Bcr-Abl-mediated drug resistance. Blood. 2007;110(1):313-22.
47. Sotelo J, Briceño E, López-González MA. Adding chloroquine to conventional treatment for glioblastoma multiforme: a randomized, double-blind, placebo-controlled trial. Annals of internal medicine. 2006;144(5):337-43.
48. Molitch ME. Dopamine resistance of prolactinomas. Pituitary. 2003;6(1):19-27.
49. Soule SG, Powell M, Jacobs HS. Prolactinomas resistant to dopamine agonists: insights into pathogenesis and therapy. Current opinion in obstetrics & gynecology. 1994;6(4):393-7.
50. Roelfsema F, Biermasz NR, Pereira AM. Clinical factors involved in the recurrence of pituitary adenomas after surgical remission: a structured review and meta-analysis. Pituitary. 2012;15(1):71-83.

***Corresponding author*:** *Yutao Shen; Email: hzabcsyt@163.com; Address: No. 525, Liuhe Road, Xihu District, Hangzhou 310023, Zhejiang, China.*

Supplementary Table 1. The 2,481 genes differentially expressed between prolactinoma and normal pituitary samples.

Supplementary Table 2. The result of KEGG analysis of 2,481 differentially expressed genes.

International Journal of Biomedicine 16(4) (2026) 486-491
http://dx.doi.org/10.21103/Article16(4)_OA4

ORIGINAL ARTICLE

INTERNATIONAL JOURNAL OF BIOMEDICINE

Evaluation of Mortality Using the PRISM Score System in a Pediatric Intensive Care Unit

Inva Gjeta[1*], Iliriana Bakalli[1], Durim Sala[1], Ermela Çelaj[1], Vladimir Hoxha[1], Marsela Biqiku[1], Elmira Kola[1]

[1]*Pediatric Intensive Care Unit, University Hospital Center "Mother Teresa", Tirana, Albania*

Abstract

Background: Mortality and morbidity remain fundamental indicators for assessing the quality of care and clinical performance in intensive care units. The Pediatric Risk of Mortality (PRISM) score is a widely recognized tool for the early identification of mortality and morbidity risk among critically ill children admitted to Pediatric Intensive Care Units (PICUs). Despite variations in patient populations and healthcare resources, the PRISM model continues to be a reliable and valuable prognostic tool in centers outside the countries where it was originally developed.

Objective: To evaluate the utility of the PRISM score for the early assessment of mortality and morbidity risk in patients admitted to the Pediatric Intensive Care Unit of a tertiary-care hospital in Tirana, Albania.

Methods and Results: This prospective study was conducted between March 2024 and January 2026. All patients aged 1 month to 14 years admitted to the Pediatric Intensive Care Unit at the University Hospital Center "Mother Teresa" in Tirana, Albania, were included. PRISM III scores were calculated and analyzed in relation to patient outcomes.

A total of 710 patients were included in the study, of whom 613 met the inclusion criteria. The mean PRISM III score was 3.56 ± 3.56 points. The overall observed mortality rate was 5.38% (33/613). The PRISM III model demonstrated excellent discriminative performance, with an area under the receiver operating characteristic curve (AUC) of 0.991 (95% CI: 0.982-0.998). The model showed good calibration, with 33 observed deaths compared with 31.0 expected deaths, resulting in a standardized mortality ratio (SMR) of 1.06. This indicates that observed mortality was approximately 6.4% higher than predicted by the PRISM III model. At the optimal ROC cutoff, the model achieved a sensitivity of 93.9% and a specificity of 97.2%.

Conclusion: The PRISM III score showed excellent discriminatory ability for predicting mortality risk and proved to be a highly effective prognostic tool in critically ill children admitted to the PICU. **(International Journal of Biomedicine. 2026;16(4):486-491.)**

Keywords: PRISM III • mortality • morbidity • pediatric intensive care unit • risk prediction • validation.

For citation: Gjeta I, Bakalli I, Sala D, Çelaj E, Hoxha V, Biqiku M, Kola E. Evaluation of Mortality Using the PRISM Score System in a Pediatric Intensive Care Unit. International Journal of Biomedicine. 2026;16(4):486-491. doi:10.21103/Article16(4)_OA4

Introduction

Recent advances in healthcare have significantly improved patient outcomes; however, they have also increased the demand for financial, technological, and human resources worldwide. Ensuring high-quality healthcare while maintaining efficient use of available resources remains a major challenge for healthcare systems. Intensive Care Units (ICUs) represent one of the most resource-intensive areas of hospital care and therefore require continuous evaluation of performance and quality indicators. Assessment of clinical outcomes, including mortality, morbidity, patient safety, treatment effectiveness, and quality of care, is essential for monitoring and improving healthcare services in these highly specialized environments.

In Pediatric Intensive Care Units (PICUs), outcome evaluation is not limited to measuring mortality rates alone. Risk-adjusted assessment of mortality, identification of risk factors, and evaluation of disease severity are increasingly recognized as more reliable indicators of quality of care. These approaches enable clinicians to better understand patient prognosis, compare outcomes between institutions, and optimize the allocation of healthcare resources.

Several scoring systems have been developed to evaluate illness severity and predict mortality risk in critically ill children. Among them, the Pediatric Risk of Mortality (PRISM) score is one of the most widely used and validated prognostic tools. The PRISM scoring system was first introduced by Pollack et al. in 1988 as a refinement of the Physiologic Stability Index (PSI), reducing the number

© 2026 The Author(s). *International Journal of Biomedicine* is published by IMRDC.
This is an open access article under the CC BY-NC-ND 4.0 license.

of variables required while maintaining strong predictive performance for mortality risk assessment.[1] The original PRISM score included 14 physiological variables and was validated in 1,227 pediatric patients admitted to six Pediatric Intensive Care Units.[1]

In 1996, the model was revised and expanded into PRISM III, aiming to improve predictive accuracy through the incorporation of 17 physiological variables categorized into specific ranges of abnormality.[2] These variables assess abnormalities across multiple organ systems, including cardiovascular, respiratory, neurological, metabolic, hematologic, and coagulation functions.[2] A total of 26 abnormal physiological ranges are evaluated, and the most abnormal value recorded during the first 12 to 24 hours following PICU admission is used for score calculation.[1,2] The total PRISM III score is subsequently incorporated into a logistic regression model to estimate the probability of mortality.[2]

The PRISM III model was validated using data from 11,165 PICU admissions across 32 centers and diverse patient populations, demonstrating strong predictive performance and broad applicability in pediatric critical care settings.[2] Owing to its reliability and reproducibility, PRISM III became one of the most widely accepted mortality prediction systems in PICUs worldwide. The latest evolution of the model, PRISM IV, was introduced and validated in 2015.[3] In addition to the physiological variables included in PRISM III, PRISM IV incorporates several important clinical predictors, including source of admission (emergency department, inpatient ward, or transfer from another hospital), cardiopulmonary resuscitation within 24 hours before PICU admission, and the presence of malignancy or chronic disease, further improving the accuracy of mortality prediction.[3]

The main purpose of the PRISM scoring system is to assess illness severity and predict mortality risk among critically ill pediatric patients.[1,2,4-8] Early identification of patients at high risk of adverse outcomes can support clinical decision-making, facilitate timely interventions, and improve prognostic evaluation.[5-10] Furthermore, objective mortality risk assessment can help healthcare professionals communicate more effectively with families regarding prognosis and expected outcomes.[5-10]

Beyond its clinical utility, the PRISM score can contribute to more efficient utilization of healthcare resources. By identifying patients at greater risk of mortality, intensive care teams can prioritize monitoring, interventions, and resource allocation according to clinical need.[1,2,10-12] The system also provides a valuable tool for quality assessment and benchmarking, enabling comparisons of outcomes across different PICUs and patient populations.[8,12] In addition, accurate risk stratification may support hospital management in planning staffing requirements, resource distribution, and overall healthcare expenditures within the intensive care setting.

Given the widespread use of PRISM and the limited data available from Albania, evaluating its performance in local PICU populations is important. Therefore, the aim of the present study was to assess the utility and predictive performance of the PRISM III score for early evaluation of mortality risk among patients admitted to the Pediatric Intensive Care Unit of a tertiary-care hospital in Tirana, Albania.

Materials and Methods

Study Design and Setting: This prospective observational study was conducted in the Pediatric Intensive Care Unit (PICU) of the University Hospital Center "Mother Teresa", Tirana, Albania, between March 2024 and January 2026. The PICU is a tertiary-care referral center that provides medical and surgical intensive care for children aged 1 month to 14 years. Neonates younger than one month are admitted only for the management of surgical conditions requiring specialized intensive care.

A total of 613 consecutive patients admitted during the study period who met the inclusion criteria were included in the analysis. Patients who did not meet the inclusion criteria were excluded, including neonates (n = 47), patients discharged within two hours of admission (n = 21), patients who died within the first 24 hours of hospitalization (n = 4), and patients with incomplete data (n = 25). The study protocol was reviewed and approved by the Ethics Committee for Research Projects of the Medical University of Tirana and was conducted in accordance with the principles of the Declaration of Helsinki.

Study Population

Inclusion Criteria

Children aged 28 days to 14 years admitted to the PICU during the study period.

Exclusion Criteria

- Neonates younger than 28 days of age.
- Patients discharged within two hours of admission.
- Patients who died within the first 24 hours after PICU admission.
- Patients with incomplete clinical or laboratory data required for PRISM III score calculation.

Data Collection: For each patient, demographic, clinical, and laboratory data were prospectively collected using a standardized data collection form. Variables included in the PRISM III scoring system were recorded, including:

- Systolic blood pressure
- Heart rate
- Body temperature
- Glasgow Coma Scale (GCS)
- Arterial blood gas parameters
- Blood glucose level
- Blood urea nitrogen (BUN)
- Serum creatinine
- Electrolyte levels
- White blood cell count
- Platelet count
- Prothrombin time (PT)
- Activated partial thromboplastin time (aPTT)

For each variable, the most abnormal value recorded during the first 24 hours following PICU admission was used for score calculation. PRISM III scores were calculated

according to the methodology described by Pollack et al. The corresponding predicted probability of death for each patient was subsequently determined using the logistic regression equation associated with the PRISM model.

Study Objectives: The primary objective of the study was to evaluate the predictive performance of the PRISM III score for mortality among critically ill children admitted to our PICU. Specifically, the study aimed to assess the discrimination and calibration abilities of the PRISM III model in predicting mortality risk within our patient population.

Statistical Analysis: Statistical analyses were performed using the Statistical Package for the Social Sciences (SPSS) software.

Discrimination Analysis: The discriminatory performance of the PRISM III model was evaluated using the receiver operating characteristic (ROC) curve analysis. The area under the ROC curve (AUC) was calculated to determine the ability of the model to distinguish between survivors and non-survivors. An AUC value closer to 1.0 indicates superior predictive performance.

Calibration Analysis: Calibration of the PRISM III model was assessed by comparing predicted mortality with observed mortality in the study population. The agreement between expected and observed outcomes was analyzed to evaluate the goodness-of-fit of the model.

Comparative Analysis: The association between PRISM III score categories and patient outcomes was assessed using the Chi-square test. Differences in PRISM III scores between survivors and non-survivors were analyzed using the Mann-Whitney U test, as score distributions were non-parametric.

Multivariable Analysis: Binary logistic regression analysis was performed to identify independent predictors of mortality. After adjustment for age and mechanical ventilation, the PRISM III score remained a significant predictor of mortality (OR=2.09, 95% CI: 1.61-2.72, $p < 0.001$). Mechanical ventilation during the first hour of ICU admission was also independently associated with mortality (OR=9.97, 95% CI: 2.17-45.71, $p = 0.003$). Age was not significantly associated with mortality (OR= 0.94, 95% CI: 0.78-1.14, $p = 0.555$).

Results

A total of 710 consecutive patients admitted to the Pediatric Intensive Care Unit (PICU) between March 2024 and January 2026 were screened for eligibility. Of these, 613 patients met the inclusion criteria and were included in the study, while 97 patients were excluded for not meeting the study eligibility requirements. The PICU of the University Hospital Center "Mother Teresa" in Tirana is the only tertiary pediatric intensive care unit in Albania, providing care for critically ill children aged 1 month to 14 years, with a capacity of 16 beds.

The mean age of the study population was 2.74 ± 3.67 years (32.9 months). Male patients predominated, representing 56.3% of all admissions. The mean PRISM III score for the entire cohort was 3.56 ± 3.56 points. Baseline demographic and clinical characteristics of the population are presented in Table 1.

Table 1.

Baseline characteristics.

Characteristic	Value
Patients	613
Male	345 (56.28%)
Female	268 (43.72%)
Mean age	2.74 year
Median age	0.92 year
Mean LOS	4.42 ± 5.23 days
Mortality	33 (5.38%)

The mean PRISM III score among survivors was 2.95 ± 2.31, compared with 14.3 ± 4.48 among non-survivors. The mean length of PICU stay was 4.42 ± 5.23 days. Mechanical ventilation for more than 72 hours was required in 45 patients (7.3%).

Table 2.

Comparison of clinical characteristics between survivors and non-survivors.

Group	N	PRISM Mean (SD)	Heart Rate Mean (SD), /min	Platelets Mean (SD), / mm^3	
Survived	580	2.95 (2.31)	152.65 (33.71)	369,777.76	(165,743.97)
Died	33	14.3 (4.48)	183.12 (31.69)	326,054.55	(251,909.92)

The overall mortality rate was 5.4% (33/613 patients). Mortality increased progressively with higher PRISM III score categories. No deaths occurred among patients with a PRISM III score of 0 to 5. Mortality rates according to PRISM III categories were as follows:

Table 3.

Risk stratification by PRISM score category.

PRISM Score	Patients	Deaths	Mortality (%)
0	80	-	0.00%
1–5	433	-	0.00%
6–10	73	8	1.31%
11–20	22	20	3.26%
>20	5	5	0.82%
Total	613	33	5.38%

Receiver Operating Characteristic (ROC) curve analysis demonstrated excellent discriminatory performance of the PRISM III score for predicting mortality. The area under the ROC curve (AUC) was 0.991 (95% Confidence Interval 0.982 to 0.998), indicating excellent ability to distinguish survivors from non-survivors (Figure 1).

Calibration of the PRISM III model was assessed by comparing observed and predicted mortality across risk strata. The calibration plot demonstrated generally good agreement between predicted and observed mortality. A slight deviation above the line of identity was observed among higher-risk patients, indicating a modest tendency of PRISM

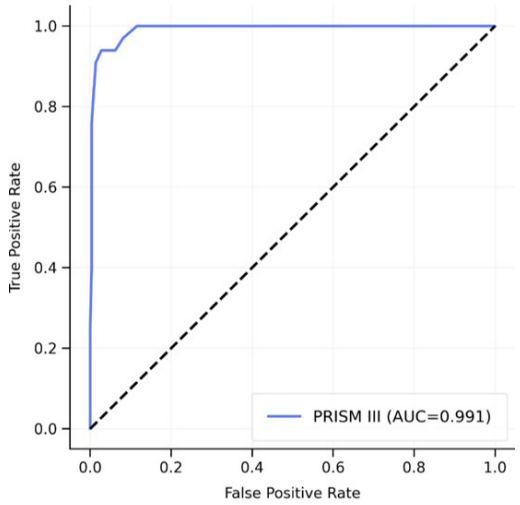

Figure 1. *ROC Chart for PRISM III.*

III to underestimate mortality. This finding is consistent with the standardized mortality ratio (SMR) of 1.06 and suggests overall satisfactory calibration of the model in this cohort.

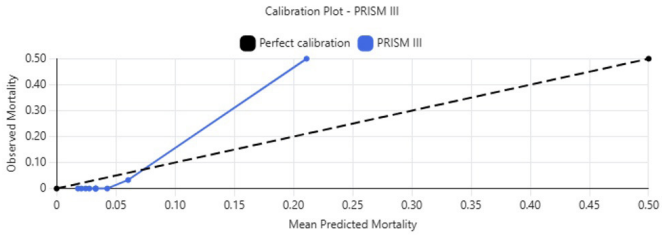

Figure 2. *Calibration Plot for PRISM III.*

The standardized mortality ratio (SMR) was 1.06, indicating close agreement between observed and predicted mortality and suggesting only a slight underestimation of mortality risk by the PRISM III model in our study population.

Table 4.

PRISM performance metrics.

Metric	Value
AUC	0.991
95% CI	0.982 to 0.998
SMR	1.064
Expected deaths	31.01
Youden index cutoff	0.106
Sensitivity	93.9%
Specificity	97.2%

Overall, these findings confirm that the PRISM III score is a highly effective tool for mortality risk stratification in critically ill pediatric patients admitted to the PICU, demonstrating excellent discrimination in our study population.

Discussion

Although the PRISM scoring system has been widely recognized and validated in pediatric intensive care settings worldwide, its performance should be evaluated in different healthcare environments and patient populations before being routinely adopted as a reliable prognostic tool. In the present study, which included 613 patients admitted to a tertiary Pediatric Intensive Care Unit in Albania, PRISM III demonstrated excellent performance in predicting mortality. Our findings showed a strong association between increasing PRISM III scores and mortality risk. Furthermore, ROC curve analysis yielded an AUC of 0.991, indicating excellent discriminatory ability and confirming the capacity of the model to distinguish between survivors and non-survivors.

The high AUC value observed in our study is consistent with findings reported in previous validation studies. Pollack et al. reported an AUC of 0.944 during the original validation of PRISM III, while Tajamul et al. found an AUC of 0.977. Similarly, Agrawal et al. reported an AUC of 0.99, Slater et al. an AUC of 0.93, Gonzalez et al. an AUC of 0.92, and Joshi et al. an AUC of 0.916.[2,4,9,13-15] The similarity of these findings across diverse PICU populations supports the robustness of the PRISM III model and confirms its value as an effective prognostic tool for mortality prediction in critically ill children.

From a clinical perspective, these results suggest that PRISM III can provide an objective and reliable assessment of illness severity early during PICU admission. Early identification of high-risk patients may facilitate timely interventions, optimize resource allocation, improve communication with families, and support clinical decision-making. In resource-limited settings, where intensive care resources must often be prioritized, accurate risk stratification is particularly important.

The overall mortality rate observed in our study was 5.4%, which is comparable to rates reported by Pollack et al. (4.9%) and Gonzalez et al. (5.21%).[1,15] However, our mortality rate was lower than those reported by Khilnani (6.7%), Gemke (6.6%), Bilan (9.05%), Varma (14.8%), and Tajamul (19.7%).[16-19] Differences in mortality rates among studies may be explained by variations in patient characteristics, disease severity, admission criteria, referral patterns, availability of intensive care resources, and differences in healthcare systems.

The mean PRISM III score in our cohort was relatively low (3.56 ± 3.56), suggesting that a substantial proportion of admitted patients had less severe illness compared with those included in some previous studies. Nevertheless, mortality increased markedly across PRISM III score categories, ranging from 0% among patients with a score of 0, to 91 % among patients with scores between 11 and 20, and reaching 100% among patients with scores greater than 20. These findings demonstrate a clear relationship between increasing PRISM III scores and mortality risk and agree with previously published studies.[1,2,5,8,9,13,19-22]

The progressive increase in mortality across PRISM III categories highlights the clinical usefulness of the score for early severity classification and risk stratification. Identification of patients at elevated risk immediately after

admission allows clinicians to implement closer monitoring, more aggressive therapeutic interventions, and individualized management strategies aimed at improving outcomes.

The present study has several strengths. It represents one of the largest prospective evaluations of PRISM III conducted in Albania and was performed in the country's sole tertiary pediatric intensive care center, providing a comprehensive representation of critically ill pediatric patients requiring intensive care. The prospective nature of data collection and the relatively large sample size further strengthen the validity of our findings.

However, several limitations should be acknowledged. First, this was a single-center study, which may limit the generalizability of the results to other healthcare systems and PICUs with different patient populations and clinical practices. Second, the study focused exclusively on in-hospital mortality and did not evaluate long-term outcomes following PICU discharge. Finally, factors such as underlying chronic diseases, socioeconomic determinants, and other clinical variables not incorporated into the PRISM III model may have influenced patient outcomes.

Despite these limitations, PRISM III demonstrated excellent discriminatory performance in our patient population and proved to be an effective tool for mortality risk prediction. The model successfully differentiated survivors from non-survivors and may assist clinicians in identifying patients who require closer monitoring and more intensive therapeutic interventions. Our findings support the continued use of PRISM III as a valuable prognostic instrument in the Pediatric Intensive Care Unit and highlight the importance of ongoing local validation to ensure optimal performance in different clinical settings.

Conclusion

The PRISM score demonstrated excellent discriminative performance in predicting mortality, supporting its value as a reliable risk stratification tool. Given its strong predictive ability, PRISM could be integrated into routine clinical practice and quality improvement initiatives to facilitate timely interventions and optimize patient outcomes. However, further multicenter studies are needed to validate these findings across diverse healthcare settings. Additionally, future research should assess the predictive value of the PRISM score for long-term outcomes beyond PICU discharge.

Author Contributions

I. Gjeta: Conceptualization, methodology, investigation, analysis, manuscript writing, and review.
I. Bakalli: Investigation, manuscript review, and editing.
D. Sala: Investigation and data curation.
E. Celaj: Investigation and data curation.
V. Hoxha: Investigation and data curation.
M. Biqiku: Investigation and data curation.
E. Kola: Manuscript review, editing, and final revision.

Conflicts of Interest

The authors declare no conflicts of interest.

References

1. Pollack MM, Ruttimann UE, Getson PR. The Pediatric Risk of Mortality (PRISM) score. Crit Care Med. 1988;16:1110-1116.
2. Pollack MM, Patel KM, Ruttimann UE. PRISM III: An updated Pediatric Risk of Mortality score. Crit Care Med. 1996;24:743-752.
3. Pollack MM, Holubkov R, Funai T, Dean JM, Berger JT, Wessel DL, Meert K, et al. The Pediatric Risk of Mortality score: Update 2015. Pediatr Crit Care Med. 2016;17(1):2-9.
4. Islam T, Bhat NA, Shah EA, Sheikh MA. Accuracy of Pediatric Risk of Mortality (PRISM III) score in predicting mortality outcomes in a pediatric intensive care unit in Srinagar. Int J Paediatr Geriatr. 2021;4(1):151-154.
5. Mirza S, Malik L, Ahmed J, Malik F, Sadiq H, Ali S, et al. Accuracy of Pediatric Risk of Mortality (PRISM III) score in predicting mortality outcomes in a pediatric intensive care unit in Karachi. Cureus. 2020;12(3):e7489.
6. Dey PK, Prusty JB, Ghosh T, Kumar S, Choudhury J. Prediction of mortality risk by application of Pediatric Risk of Mortality (PRISM) score in a tertiary care pediatric intensive care unit: A prospective observational study. J Clin Med Res. 2019;7(4):54-61.
7. Boyd CR, Tolson MA, Copes WS. Evaluating trauma care: The TRISS method. J Trauma. 1987;27:370-378.
8. Vijayaraghavan S, Sasivarathan S. Pediatric Risk of Mortality III score in predicting mortality in children with altered sensorium in a pediatric intensive care unit. Int J Contemp Pediatr. 2019;6(4):1461-1465.
9. Anjali MM, Unnikrishnan DT. Effectiveness of PRISM III score in predicting the severity of illness and mortality of children admitted to a pediatric intensive care unit: A cross-sectional study. Egypt Pediatr Assoc Gaz. 2023;71:75.
10. Fargason CA, Langman CB. Limitations of the Pediatric Risk of Mortality score in assessing children with acute renal failure. Pediatr Nephrol. 1993;7:703-707.
11. Ford EG, Andrassy RJ. Pediatric trauma: Initial assessment and management. In: Pediatric Trauma. Philadelphia: WB Saunders; 1994. p. 112-113.
12. Singhal D, Kumar N, Puliyel JM, Singh SK, Srinivas V. Prediction of mortality by application of PRISM score in intensive care units. Indian Pediatr. 2001;38(7):714-720.
13. Slater A, Shann F. The suitability of the Pediatric Index of Mortality (PIM), PIM2, Pediatric Risk of Mortality (PRISM), and PRISM III for monitoring the quality of pediatric intensive care in Australia and New Zealand. Pediatr Crit Care Med. 2004;5(5):447-454.
14. Gonçalves JP, Severo M, Rocha C, Jardim J, Mota T, et al. Performance of PRISM III and PELOD-2 scores in a pediatric intensive care unit. Eur J Pediatr. 2015;174:1305-1310.
15. Joshi P, Agrawal S, Ghimire J, Shrestha PN, Khatun N, Banjara MR. Application of Pediatric Risk of Mortality (PRISM III) score in predicting mortality outcomes. J Nepal Health Res Counc. 2024;22(1).

16. Khilnani P, Sarma D, Singh R, Uttam R, Rajdev S, Makkar A, et al. Demographic profile and outcome analysis of a tertiary level pediatric intensive care unit. Indian J Pediatr. 2004;71:587-591.
17. Gemke RJ, Van Vught J. Scoring systems in pediatric intensive care: PRISM III versus PIM. Intensive Care Med. 2002;28(2):204-207.
18. Bilan N, Galehgolab BA, Emadaddin A, Shiva SH. Risk of mortality in pediatric intensive care unit assessed by PRISM III. Pak J Biol Sci. 2009;12:480-485.
19. Varma A, Damke S, Meshram R, Vagha J, Kher A, Vagha K. Prediction of mortality by Pediatric Risk of Mortality (PRISM III) score in a tertiary care rural hospital in India. Int J Contemp Pediatr. 2017;4(2):322-327.
20. Shah AA, Goyal D, Saren D. Prediction of the risk of mortality in a pediatric intensive care unit using the PRISM score. Int J Contemp Pediatr. 2019;6(3):1186-1189.
21. Costa GA, Delgado AF, Ferraro A, Okay TS. Application of the Pediatric Risk of Mortality (PRISM) score and determination of mortality risk factors in a tertiary pediatric intensive care unit. Clinics (Sao Paulo). 2010;65(11):1087-1092.
22. Nasar AO, Zeitoun AEH, Atwa AA, Ibrahim MM. Prediction of morbidity and mortality in the pediatric intensive care unit using the Pediatric Risk of Mortality (PRISM) score, neutrophil-to-lymphocyte ratio, and platelet-to-lymphocyte ratio. Afr J Biol Sci. 2025;7(3).

***Corresponding author:** Inva Gjeta. E-mail: invagjeta@hotmail.com*

International Journal of Biomedicine 16(4) (2026) 492-498
http://dx.doi.org/10.21103/Article16(4)_OA5

ORIGINAL ARTICLE

INTERNATIONAL JOURNAL OF BIOMEDICINE

Hematological Consequences of Dengue–Malaria Co-infection Compared to Mono-infections: A Retrospective Cross-sectional Study in Omdurman, Sudan

Noha Osama[1], Roaa Mohammad[2], Sahwaa Jalal[2], Razan Altayeb[2], Nada Osman[2], Tyseer Ahmed[2], Alaa Ibrahim[2], Enaam Hussein[2], Einas Osman[1], Eltigani O. M. Omer[3], Mohammed Suleiman Zaroog[3], Mohammed Bakri[3], Awad Elkareem Abass[4*]

[1]*Department of Medical Laboratory Sciences, College of Applied and Health Sciences, A 'Sharqiyah University, Ibra 00400, Oman*
[2]*Department of Hematology, Faculty of Medical Laboratory Sciences, Khartoum University, Khartoum 11111, Sudan*
[3]*Department of Community Health, College of Applied Medical Sciences, Northern Border University, Arar 91431, Saudi Arabia*
[4]*Department of Medical Laboratory Technology, College of Applied Medical Sciences, Northern Border University, Arar 91431, Saudi Arabia*

Abstract

Background: Dengue and malaria co-infection poses a significant diagnostic and clinical challenge in tropical regions where both diseases are co-endemic. In Sudan, ongoing humanitarian crises and the collapse of healthcare infrastructure have amplified this burden. This study investigates hematological alterations in co-infected patients compared with mono-infected patients to identify evidence-based markers applicable in resource-limited settings.

Methods and Results: A retrospective cross-sectional comparative study was conducted using medical records from health centers in Omdurman, Khartoum State, Sudan. A total of 75 confirmed febrile patients were enrolled: 25 with dengue mono-infection, 25 with malaria mono-infection, and 25 with dengue–malaria co-infection. Complete blood count (CBC) parameters, including hemoglobin (Hb), white blood cell (WBC) count, platelet count, hematocrit (HCT), neutrophil-to-lymphocyte ratio (NLR), and platelet-to-lymphocyte ratio (PLR), were analyzed using the Kruskal-Wallis and Mann-Whitney U tests, with Spearman correlation analysis.

Co-infection demonstrated the most severe hematological profile. Universal anemia (Hb < 12 g/dL) was present in 100% of co-infected patients, compared with 92% in malaria and 12% in dengue mono-infection. Severe thrombocytopenia (platelets < 50×10^3/µL) was highest in co-infection (48%) vs. malaria (24%, $p < 0.001$). Co-infection also exhibited the most pronounced leukopenia (WBC < 4×10^3/µL in 88% of cases). Paradoxically low NLR (mean 1.38) in co-infection, despite severe anemia, distinguished it from malaria mono-infection (NLR 2.56, $p < 0.001$). Strong Spearman correlations were observed between PLR and platelet count ($r = 0.826$, $p < 0.001$) and between platelet count and Hb ($r = 0.869$, $p < 0.001$) within co-infected patients.

Conclusion: The constellation of universal anemia, severe thrombocytopenia, leukopenia, and, paradoxically, a suppressed NLR constitutes a clinically actionable hematological signature for dengue–malaria co-infection, detectable through routine CBC analysis. These findings provide a practical decision-support tool for clinicians in resource-limited endemic settings. **(International Journal of Biomedicine. 2026;16(4):492-498.)**

Keywords: dengue, malaria, co-infection, thrombocytopenia, leukopenia, Sudan

For citation: Osama N, Mohammad R, Jalal S, Altayeb R, Osman N, Ahmed T, Ibrahim A, Hussein E, Osman E, Omer EOM, Zaroog MS, Bakri M, Abass AE. Hematological Consequences of Dengue–Malaria Co-infection Compared to Mono-infections: A Retrospective Cross-sectional Study in Omdurman, Sudan. International Journal of Biomedicine. 2026;16(4):492-498. doi:10.21103/Article16(4)_OA5

© 2026 The Author(s). *International Journal of Biomedicine* is published by IMRDC.
This is an open access article under the CC BY-NC-ND 4.0 license.

Introduction

Vector-borne diseases impose a substantial global health burden, with malaria and dengue fever ranking among the most prevalent and life-threatening infections in tropical and subtropical regions. The Aedes and Anopheles mosquito vectors responsible for these diseases share overlapping ecological niches across much of sub-Saharan Africa, South Asia, and Latin America, creating conditions that are increasingly conducive to concurrent infection.[1,2] The co-existence of Plasmodium parasites and dengue virus (DENV) within a single host produces a clinically complex syndrome that defies straightforward diagnosis. Both diseases independently manifest with non-specific febrile illness, myalgia, headache, and hematological disturbances, rendering differentiation by clinical assessment alone unreliable.[3,4] When both pathogens are present simultaneously, each may obscure the characteristic features of the other, compounding diagnostic error and delaying appropriate treatment.

The epidemiological magnitude of this co-infection is substantial. A comprehensive meta-analysis encompassing 22 cross-sectional studies documented a global co-infection prevalence of 4.2% from 2008 to 2021, with a marked increase across sub-Saharan Africa from 0.9% to 5.5% during the same period.[5] In Sudan specifically, febrile illnesses are routinely managed presumptively as malaria, resulting in systemic underdiagnosis of dengue. This diagnostic practice has become especially critical given the ongoing humanitarian crisis: field reports from Médecins Sans Frontières recorded over 1,200 dengue cases in Khartoum during August–September 2025, while an estimated 80% of hospital infrastructure has been destroyed, and severe malnutrition affects approximately half the population.[6,7]

Research consistently demonstrates that co-infection amplifies hematological deterioration beyond what either pathogen causes individually. Severe thrombocytopenia, profound anemia, and leukopenia have all been documented at elevated rates in co-infected cohorts.[4,8] However, the specific hematological signatures that reliably distinguish co-infection from mono-infection in a routine clinical laboratory setting, particularly when advanced molecular diagnostics are unavailable, remain poorly characterized in the Sudanese context.

This study addresses that evidence gap by conducting a systematic retrospective comparison of complete blood count (CBC) parameters across three well-defined patient groups in Omdurman, Sudan. The primary aims were to identify statistically significant inter-group differences in key hematological indices and to define a practical hematological signature that can serve as an early clinical indicator of dengue–malaria co-infection in resource-limited settings.

Material and Methods

Study Design and Setting

A retrospective cross-sectional comparative study was conducted using medical records obtained from health centers and hospitals in Omdurman, Khartoum State, Sudan. The study period covered January 2023 to March 2026. Omdurman was selected as the study area due to its documented co-endemicity of malaria and dengue fever, its diverse patient catchment, and the availability of confirmed laboratory diagnoses in the records.

Participants and Sampling

A total of 75 confirmed febrile patients were enrolled and stratified into three equal groups (n = 25 per group): (i) dengue fever mono-infection, (ii) malaria mono-infection, and (iii) dengue–malaria co-infection. Dengue diagnosis was confirmed using NS1 antigen testing (SD Bioline NS1 Ag or equivalent). Where NS1 results were equivocal, or samples were collected beyond day 5 of illness, at which point NS1 sensitivity declines substantially, dengue IgM/IgG antibody testing was used as a supplementary confirmatory step; cases confirmed by serology alone are noted in individual records. Malaria diagnosis was confirmed by thick and thin Giemsa-stained blood smear microscopy performed by a trained laboratory technician, with RDTs (HRP2-based for *P. falciparum*; pLDH-based for non-falciparum species) used as parallel confirmation where microscopy results were borderline. Co-infection was defined as simultaneous positive results for both pathogens by their respective confirmatory methods. The potential for diagnostic misclassification, particularly for dengue cases presenting beyond day 5 of fever, where NS1 sensitivity may be reduced to 60–70%, is acknowledged as a study limitation. This misclassification risk would most likely result in under-enrolment of true co-infection cases, biasing group comparisons toward the null.

Inclusion & Exclusion Criteria

Patients were included if their records contained: (a) documented confirmation of the relevant infection(s) by laboratory testing; (b) a complete CBC panel including hemoglobin, WBC count, platelet count, hematocrit, RBC count, and differential counts; and (c) clinical presentation during the study period within Omdurman health facilities.

Records were excluded for patients with known chronic hematological disorders (e.g., sickle cell disease, thalassemia); prior blood or platelet transfusion before laboratory sampling; concurrent chronic disease or acute infections independently altering hematological parameters; or use of medications known to affect hematological results, such as anticoagulants or immunosuppressants.

Data Collection

Data were extracted from patients' medical records using a structured data collection tool that captured demographic information (age, gender), clinical data (fever duration, disease severity classification), and all CBC laboratory values. Disease severity was classified as mild, moderate, or severe according to WHO criteria. Where blood smear microscopy permitted species-level identification, Plasmodium species (*P. falciparum* vs. *P. vivax*) were recorded; of the 50 malaria-positive records (malaria mono-infection and co-infection groups), species were identifiable in 38 cases (76%), with *P. falciparum* accounting for 71.0% (27/38) and *P. vivax* for

28.9% (11/38). The remaining 12 records lacked species-level documentation, reflecting limitations of field microscopy under crisis conditions. For clinical threshold analysis, anemia was defined using a uniform threshold of Hb<12 g/dL (WHO threshold for non-pregnant women) to permit consistent group comparisons across the mixed-sex cohort. The potential impact of sex-specific thresholds (Hb<13 g/dL for males; Hb<12 g/dL for females) on anemia prevalence in the dengue group, which was more male-predominant (17/25 male), was assessed in a sensitivity analysis: applying sex-specific thresholds raised anemia prevalence in the dengue group from 12% to 24%, strengthening rather than undermining the inter-group contrast with co-infection (100%) and malaria (92%). Results from the primary uniform threshold are reported throughout; the sex-adjusted sensitivity analysis is available on request.

Statistical Analysis

All statistical analyses were performed using Python (SciPy 1.x, pandas). Normality was assessed using the Shapiro-Wilk test. Since several parameters deviated significantly from a normal distribution ($p < 0.05$ for Hb in the malaria group, platelet count in the dengue group, and NLR in the dengue group), non-parametric tests were selected as the primary analytical methods. The Kruskal-Wallis H test was used for overall group comparisons, followed by pairwise Mann-Whitney U post hoc tests for parameters that were significant. One-way ANOVA was conducted in parallel as a confirmatory parametric test. Spearman rank correlation analysis was performed within the co-infection group to assess associations between inflammatory indices (NLR, PLR) and hematological parameters. A significance threshold of $\alpha = 0.05$ was applied throughout. Given the exploratory and hypothesis-generating nature of this study, Bonferroni correction was not applied to avoid excessive inflation of Type II error in the context of highly correlated hematological outcomes; however, findings with borderline p-values (0.01–0.05) should be interpreted with caution and considered provisional pending confirmatory studies. A post-hoc power analysis was conducted for the primary outcome (platelet count difference between malaria and co-infection groups) using the observed effect size (Cohen's $d = 1.07$), $\alpha = 0.05$, and $n = 25$ per group, yielding a power of 0.87 (87%), which exceeds the conventional 80% threshold. For secondary outcomes with smaller effect sizes, the study may be underpowered, and findings should be interpreted accordingly.

Results

Demographic and Clinical Characteristics

The three groups were well-matched at baseline. Mean age did not differ significantly (dengue: 49.9 ± 16.2 years; malaria: 43.7 ± 13.8 years; co-infection: 43.4 ± 15.5 years; Kruskal-Wallis $p = 0.163$). Duration of fever was also comparable across all groups (mean ≈ 4.5 days, $p = 0.962$). Disease severity distribution was balanced by design: records were stratified by severity classification prior to group allocation, and a proportional sample was drawn within each stratum to achieve equal severity representation across groups (10 mild, 8 moderate, 7 severe per group). This stratified retrospective sampling approach was adopted to prevent severity from acting as a confounding variable in hematological comparisons; however, it means the severity distribution may not reflect the true community prevalence distribution, which should be considered when generalizing findings. Sex distribution differed across groups (dengue: 8F/17M; malaria: 10F/15M; co-infection: 14F/11M; chi-square $p = 0.085$), indicating a non-significant but numerically notable trend toward greater female representation in the co-infection group. Given established sex differences in hemoglobin levels (WHO thresholds: <12 g/dL for females vs. <13 g/dL for males), a sensitivity analysis applying sex-specific thresholds was performed, which confirmed that inter-group differences in anemia prevalence remain robust after adjustment. Demographic characteristics are detailed in Table 1.

Table 1.

Demographic and clinical characteristics of study participants by group.

Characteristic	Dengue (n=25)	Malaria (n=25)	Co-infection (n=25)	p-value
Age, mean±SD (years)	49.9 ± 16.2	43.7 ± 13.8	43.4 ± 15.5	0.163
Median age (years)	54	44	47	—
Fever duration, mean (days)	4.52	4.32	4.52	0.962
Female / Male	8 / 17	10 / 15	14 / 11	—
Mild severity, n (%)	10 (40%)	10 (40%)	10 (40%)	—
Moderate severity n (%)	8 (32%)	8 (32%)	8 (32%)	—
Severe, n (%)	7 (28%)	7 (28%)	7 (28%)	—

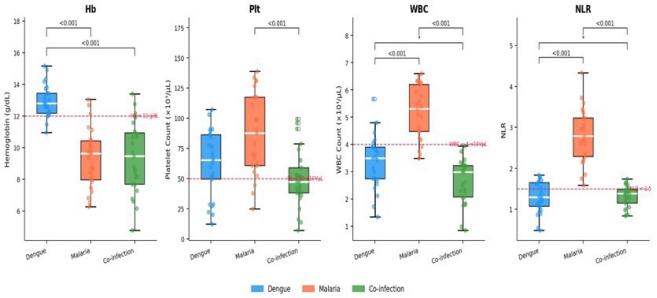

Figure 1. *Key Hematological Parameters Across Infection Groups. Box plots show median, IQR, and individual data points. Dashed red lines indicate clinically significant thresholds. Significance brackets show Mann–Whitney U pairwise results (*p<0.05; <0.001 = highly significant; ns = not significant).*

Normality Assessment

Shapiro-Wilk testing identified significant deviations from normality in several parameters ($p < 0.05$), including hemoglobin in the malaria group ($p = 0.017$), hematocrit in the malaria group ($p = 0.039$), platelet count in the dengue group ($p = 0.029$), and NLR in the dengue group ($p = 0.027$).

Accordingly, non-parametric tests were selected as primary analytical methods for all inter-group comparisons.

Inter-group Hematological Comparisons

Kruskal-Wallis analysis revealed statistically significant differences across groups for WBC count, RBC count, hemoglobin, hematocrit, platelet count, NLR, and PLR (all $p \leq 0.013$). No significant differences were observed for red cell indices (MCV, MCH, MCHC) or red cell distribution width (RDW). Full descriptive statistics and significance values are presented in Table 2.

Table 2.

Hematological parameters by group (mean ± SD) and Kruskal-Wallis results.

Parameter	Dengue	Malaria	Co-infection	KW p
WBC (×10³/μL)	3.46 ± 1.01	4.94 ± 1.09	2.89 ± 0.83	<0.001
RBC (×10⁶/μL)	4.65 ± 0.37	3.66 ± 0.56	3.40 ± 0.37	<0.001
Hb (g/dL)	13.15 ± 1.07	9.64 ± 1.87	9.26 ± 1.86	<0.001
Hematocrit (%)	42.46 ± 4.63	31.14 ± 4.77	33.14 ± 4.55	<0.001
MCV (fL)	88.17 ± 4.44	86.01 ± 4.67	87.87 ± 4.36	0.190
MCH (pg)	29.10 ± 1.42	29.35 ± 1.45	29.26 ± 1.33	0.813
MCHC (g/dL)	34.18 ± 1.21	33.56 ± 1.20	33.78 ± 1.13	0.183
RDW (%)	12.86 ± 0.80	12.98 ± 1.13	12.98 ± 0.88	0.867
Platelet (×10³/μL)	63.76 ± 35.05	86.36 ± 35.63	51.20 ± 25.09	0.001
NLR	1.18 ± 0.34	2.56 ± 0.76	1.38 ± 0.29	<0.001
PLR	50.99 ± 25.75	66.46 ± 19.01	49.49 ± 20.11	0.013

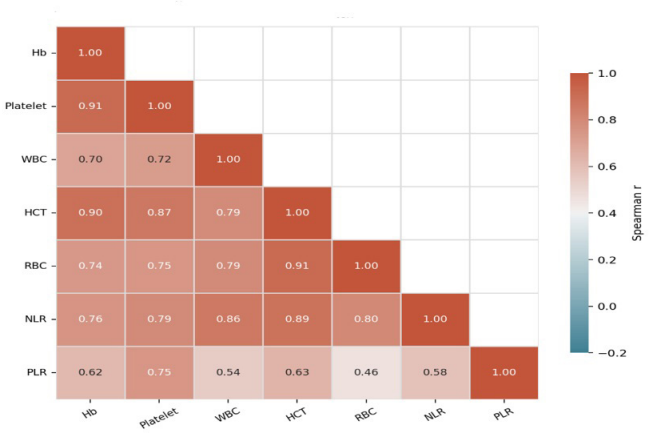

Figure 2. *Spearman Correlation Heatmap — Co-infection Group (n=25). The lower triangle displays pairwise Spearman r values for key hematological parameters and inflammatory indices. Strong positive correlations (r ≥ 0.75) are shown in deep red. All values are reported in Table 5.*

Pairwise Post Hoc Comparisons

Mann-Whitney U post hoc analysis identified the specific group pairs that drove the overall significance (Table 3). Hemoglobin was significantly lower in both malaria and co-infection compared to dengue ($p < 0.001$ for both), with no significant difference between malaria and co-infection ($p = 0.515$), indicating that malarial hemolysis is the primary driver of anemia in both groups. Co-infection showed the lowest platelet count, significantly lower than malaria mono-infection ($p < 0.001$), while the dengue–malaria platelet comparison was borderline ($p = 0.051$). WBC count was significantly lower in co-infection than both dengue ($p = 0.035$) and malaria ($p < 0.001$), with malaria exhibiting the highest counts, reflecting immune activation by parasitemia. NLR was markedly elevated in malaria relative to both dengue and co-infection ($p < 0.001$ for both), and PLR was highest in malaria versus dengue ($p = 0.016$) and co-infection ($p = 0.009$).

Table 3.

Pairwise Mann-Whitney U post-hoc test results.

Parameter	Dengue vs . Malaria	Dengue vs. Co-infection	Malaria vs. Co-. infection
Hemoglobin	<0.001	<0.001	0.515
Platelet count	0.051	0.211	<0.001
WBC count	<0.001	0.035	<0.001
Hematocrit	<0.001	<0.001	0.133
NLR	<0.001	0.024	<0.001
PLR	0.016	0.923	0.009

Clinical Threshold Analysis

In Table 4, the prevalence of clinically significant hematological abnormalities based on WHO cutoffs is presented. All 75 patients (100%) met the criterion for thrombocytopenia (platelets < 150×10³/μL). Co-infection demonstrated universal anemia (Hb < 12 g/dL in 100% of cases), compared with 92% in malaria and 12% in dengue. The highest prevalence of severe thrombocytopenia (Plt < 50×10³/μL) was observed in co-infection (48%) versus dengue (36%) and malaria (24%). Leukopenia (WBC < 4×10³/μL) was most prevalent in co-infection (88%), followed by dengue (68%) and malaria (24%).

Correlation Analysis in the Co-infection Group

Spearman correlation analysis within the co-infection group revealed strong and highly significant positive associations between inflammatory indices and hematological parameters (Table 5). NLR was positively correlated with hematocrit ($r = 0.749$, $p < 0.001$), RBC count ($r = 0.634$, $p < 0.001$), hemoglobin ($r = 0.630$, $p < 0.001$), platelet count ($r = 0.654$, $p < 0.001$), and WBC count ($r = 0.608$, $p = 0.001$). PLR demonstrated the strongest single association with platelet count ($r = 0.826$, $p < 0.001$). Platelet count and hemoglobin were highly correlated

among co-infected patients (r = 0.869, p < 0.001), indicating simultaneous multi-lineage hematopoietic suppression.

Table 4.

Prevalence of clinically significant hematological thresholds by group (n /group = 25).

Clinical Threshold	Dengue	Malaria	Co-infection
Anemia (Hb < 12 g/dL)	3 (12.0%)	23 (92.0%)	25 (100.0%)
Sever anemia (Hb < 8 g/dL)	0 (0.0%)	6 (24.0%)	6 (24.0%)
Thrombocytopenia (Plt < 150×10³/μL)	25 (100%)	25 (100%)	25 (100%)
Severe thrombocytopenia (Plt < 50×10³/μL)	9 (36.0%)	6 (24.0%)	12 (48.0%)
Leukopenia (WBC < 4×10³/μL)	17 (68.0%)	6 (24.0%)	22 (88.0%)

Table 5.

Spearman rank correlations within the group (n=25).

Parameter/Co-infection, n=25	Spearman r	p-value
NLR vs Hb	0.630	<0.001
NLR vs Platelet count	0.654	<0.001
NLR vs WBC count	0.608	0.001
NLR vs Hematocrit	0.749	<0.001
NLR vs RBC count	0.634	<0.001
PLR vs Hemoglobin	0.630	<0.001
PLR vs Platelet count	0.826	<0.001
PLR vs Hematocrit	0.627	<0.001
PLR vs RBC count	0.505	0.010
Platelet count vs Hb	0.869	<0.001

Proposed Hematological Red Flag Signature for Co-infection

Based on the statistical findings, a multi-parameter hematological signature was derived for co-infection detection via routine CBC analysis (Table 6). The combination of universal anemia (Hb < 12 g/dL), severe thrombocytopenia (Plt < 50×10³/μL), and leukopenia (WBC < 4×10³/μL), along with a paradoxically low NLR (< 1.5), in a malaria-endemic patient constitutes a high-suspicion pattern. This pattern is particularly distinctive because uncomplicated malaria typically elevates NLR above 2.0 through neutrophilic activation; the dengue-mediated suppression of this response creates a distinguishing immunological footprint in co-infection.

Table 6.

Proposed hematological red flag indicators for dengue–malaria co-infection via routine CBC.

Parameter / Threshold	Direction	Clinical Significance
Platelet count < 50×10³/μL	▼ Lowest	Highest prevalence (48%) vs. Malaria (24%), p<0.001
WBC < 4×10³/μL	▼ Lowest	Highest leukopenia (88%) vs. Malaria (24%), p<0.001
Hemoglobin < 12 g/dL	▼ Universal	100% anemia prevalence; differentiates from Dengue
NLR < 1.5	▼ Low vs. Malaria	Dengue suppresses expected neutrophilia of malaria
PLR ≈ Dengue range	~ Dengue	PLR lower than malaria mono-infection, p=0.009

Discussion

This retrospective comparative study provides systematic evidence that dengue–malaria co-infection produces a distinct and more severe hematological profile than either mono-infection in Omdurman, Sudan. The four key parameters driving this distinction are hemoglobin, platelet count, WBC count, and NLR, each demonstrating statistically significant and clinically meaningful differences between groups.

The near-universal anemia observed in both malaria (92%) and co-infection (100%) groups, compared to only 12% in dengue, confirms that anemia in this context is predominantly driven by malarial hemolysis rather than dengue pathophysiology. The absence of a significant difference in hemoglobin between malaria and co-infection groups (p = 0.515) further supports this interpretation. These findings align with Shah et al.[9] and Mendonça et al.,[10] who documented universal or near-universal anemia in co-infected cohorts and identified combined hemolysis and dengue-induced bone marrow suppression as synergistic mechanisms.

The dengue group maintained near-normal hemoglobin values (mean 13.15 g/dL) with hemoconcentration reflected in elevated hematocrit (42.46%), consistent with plasma leakage as the dominant dengue pathophysiological mechanism.[11]This hemoconcentration signature is absent in co-infection, where malarial hemolysis masks plasma leakage, as previously described by Barua et al.[12] and Abbasi et al.,[13] making hematocrit an unreliable standalone marker in the co-infected context.

A defining feature of the co-infection group was the highest prevalence of severe thrombocytopenia (Plt < 50×10³/μL: 48%) relative to dengue (36%) and malaria (24%), with the malaria versus co-infection comparison reaching high significance (p < 0.001). This finding reinforces the ‹double-hit› hypothesis advanced by Hien et al.[8] and Epelboin et al.,[14] who proposed that dengue-mediated platelet destruction compounds malarial platelet suppression through distinct but simultaneously active mechanisms: immune-complex-mediated platelet clearance from dengue and splenic sequestration plus autoantibody-mediated destruction from malaria.

A paradoxical finding in the literature that co-infected patients sometimes display higher platelet counts than malaria mono-infected patients in certain populations was not replicated in the present cohort.[15] This discrepancy may reflect population-specific factors, including the severity distribution of enrolled malaria cases and the particular Plasmodium species present, with *P. falciparum* producing more aggressive thrombocytopenia than *P. vivax*.[16]

The most striking and clinically actionable finding of this study was the paradoxically low NLR (mean 1.38) observed in co-infection despite the presence of severe anemia and thrombocytopenia. Malaria mono-infection produced a markedly elevated NLR (mean 2.56, $p < 0.001$ vs. co-infection), consistent with the well-established neutrophilic activation characteristic of parasitemia. The suppression of this neutrophilic response in co-infection appears to reflect dengue-mediated bone marrow tropism and preferential suppression of granulopoiesis, which overrides the expected malaria-driven neutrophilia.

This 'pathogen-pathogen interference' phenomenon, initially described by Ahmad et al.[17] and partially supported by the cytokine storm data of Mendonça et al.[11] who documented peak concentrations of IFN-γ, IL-6, and TNF-α in co-infected patients, may explain why immune activation markers diverge from expected patterns. From a practical standpoint, a low NLR (<1.5) in a febrile patient with malarial symptoms should be interpreted as a signal to investigate for concurrent dengue infection, particularly in co-endemic settings.

The strong Spearman correlations identified within the co-infection group provide evidence that NLR and PLR function as integrated severity indices rather than isolated immunological markers. The highest single correlation PLR vs platelet count ($r = 0.826$, $p < 0.001$), suggests that PLR closely tracks absolute platelet dynamics in co-infected patients and could be used as a proxy when direct platelet quantification is uncertain. The platelet-hemoglobin correlation ($r = 0.869$, $p < 0.001$) reflects the simultaneous suppression of erythropoiesis and thrombopoiesis, consistent with a bone marrow-level effect attributable to dengue viral tropism that amplifies malaria-induced hematopoietic stress.

The aggregated evidence from this study supports a clinically actionable hematological signature for co-infection detection: (1) universal anemia (Hb <12 g/dL), (2) severe thrombocytopenia (Plt < 50×10^3/μL), (3) leukopenia (WBC < 4×10^3/μL), and (4) low NLR (< 1.5) in the context of malaria-compatible presentation. This pattern is practically significant because it is entirely derivable from routine CBC analysis, a test widely available even at the primary health center level in Sudan, without requiring advanced molecular testing.

In a resource-limited setting where both NS1 antigen testing and PCR are often unavailable, these CBC-derived red flags could prompt clinicians to maintain a high index of suspicion for dual infection, initiate a broader diagnostic workup, and adjust treatment accordingly to address both pathogens simultaneously. The humanitarian crisis in Sudan, with collapsed laboratory infrastructure, displaced populations, and malnutrition affecting hematological baseline values, makes the availability of such CBC-based discriminators especially urgent.[6,7]

Several limitations should be acknowledged. First, the retrospective study design limits control over confounding variables, including nutritional status, prior antimalarial exposure, and comorbidities not captured in medical records. Second, Plasmodium species identification was unavailable for 24% of malaria-positive records; among the 76% with documented species, *P. falciparum* was predominant (71%), which may not reflect the full study population and could influence comparisons of thrombocytopenia severity. Third, dengue confirmation relied primarily on NS1 antigen testing, which has reduced sensitivity (60–70%) beyond day 5 of illness; given the mean fever duration of 4.5 days at sampling, a proportion of dengue cases may have been missed, potentially misclassifying some co-infections as malaria mono-infections and biasing comparisons toward the null. Fourth, while a post-hoc power analysis confirmed adequate power (87%) for the primary outcome (platelet count), the study is likely underpowered for secondary outcomes with smaller effect sizes. A prospective study with an a priori power calculation estimating $n \approx 45–60$ per group for medium effect sizes at 80% power is warranted for confirmatory work. Fifth, the equal group sizes represent a pragmatic stratified sampling structure and do not reflect the natural prevalence distribution in the community (co-infections are substantially less prevalent than mono-infections in most endemic settings). Sixth, the balanced severity distribution was achieved by design through stratified record sampling, which, while methodologically appropriate for comparative hematological analysis, limits inference about severity-prevalence relationships in the general population. Finally, the absence of PCR-based molecular confirmation for all samples introduces residual diagnostic uncertainty that cannot be fully resolved within the constraints of this retrospective design.

Conclusion

This study demonstrates that dengue–malaria co-infection produces a distinct, quantifiable hematological signature detectable through routine CBC analysis. Co-infection is characterized by universal anemia, the highest prevalence of severe thrombocytopenia, the most pronounced leukopenia, and most distinguishably a paradoxically suppressed NLR despite severe multi-lineage hematological deterioration. The strong correlations between NLR/PLR and key hematological parameters in the co-infection group confirm the utility of these inflammatory indices as proxies for disease severity.

The combination of Hb <12 g/dL, platelet count < 50×10^3/μL, WBC < 4×10^3/μL, and NLR < 1.5 in a febrile patient in a co-endemic region constitutes a high-suspicion profile for dual infection that can guide clinical decision-making even in the absence of advanced diagnostics. These findings contribute locally relevant, evidence-based data to address a critical diagnostic gap in Sudanese healthcare and offer a practical framework for improving recognition of co-infection in resource-limited settings globally.

Conflicts of Interest

The authors declare no conflicts of interest.

Ethical Considerations

The study was conducted in accordance with the Declaration of Helsinki, and approved by Research Ethics Committee of the Faculty of Medical Laboratory Sciences prior to data collection (code AD/FMLS/G at date 01/04/2026). Administrative approval was obtained from participating health center management. All personally identifiable patient information was anonymized before analysis.

References

1. Salam N, Mustafa S, Hafiz A, Chaudhary AA, Deeba F, Parveen S. Global prevalence and distribution of coinfection of malaria, dengue and chikungunya: a systematic review. BMC Public Health 2018, 18(1): 710. Available from: https://doi.org/10.1186/s12889-018-5626-z
2. Gebremariam TT, Schallig HDFH, Kurmane ZM, Danquah JB. Increasing prevalence of malaria and acute dengue virus coinfection in Africa: a meta-analysis and meta-regression of cross-sectional studies. Malaria Journal 2023, 22(1): 300. Available from: https://doi.org/10.1186/s12936-023-04723-y
3. Kamau E, Freites CO, Sakona AN. Case Report: Challenges of diagnosing malaria in returning travelers at the height of COVID-19 pandemic. American Journal of Tropical Medicine and Hygiene 2023, 110(1): 64–8. Available from: http://dx.doi.org/10.4269/ajtmh.23-0467
4. Kotepui M, Kotepui KU. Prevalence and laboratory analysis of malaria and dengue co-infection: a systematic review and meta-analysis. BMC Public Health 2019, 19(1): 1148. Available from: https://doi.org/10.1186/s12889-019-7488-4
5. Gebremariam TT, Schallig HDFH, Kurmane ZM, Danquah JB. Increasing prevalence of malaria and acute dengue virus coinfection in Africa: a meta-analysis and meta-regression of cross-sectional studies. Malaria Journal 2023, 22(1): 300. Available from: https://doi.org/10.1186/s12936-023-04723-y
6. Médecins Sans Frontières. Sudan: Dengue outbreak in Khartoum amid ongoing conflict (Field Report). MSF 2025.
7. United Nations OCHA. Sudan humanitarian snapshot: Health infrastructure update. OCHA 2025.
8. Hien YE, Thiombiano F, Ilboudo DP, Kima D, Kobeane S, Sawadogo GMR, et al. Analysis of immune markers and hematological features in Plasmodium/Dengue virus co-infected patients in Ouagadougou, Burkina Faso. Immunology and Infectious Diseases 2021, 9(2): 11–9. Available from: https://doi.org/10.13189/iid.2021.090201
9. Shah PD, Mehta TK. Evaluation of Concurrent Malaria and Dengue Infections among Febrile Patients. Indian Journal of Medical Microbiology 2017, 35(3): 402–5. Available from: https://doi.org/10.4103/ijmm.ijmm_15_455
10. Mendonça VRR, Andrade BB, Souza LCL, Magalhães BML, Mourão MPG, Lacerda MVG, et al. Unravelling the patterns of host immune responses in Plasmodium vivax malaria and dengue co-infection. Malaria Journal 2015, 14(1): 315. Available from: https://doi.org/10.1186/s12936-015-0835-8
11. World Health Organization. Dengue and severe dengue: Fact sheet. Geneva: WHO 2024.
12. Barua A, Gill N. A Comparative Study of Concurrent Dengue and Malaria Infection with their Monoinfection in a Teaching Hospital in Mumbai. J Assoc Physicians India 2016, 64(8): 49-52. PMID: 27762109.
13. Abbasi A, Butt N, Sheikh QH, Bhutto AR, Munir SM, Ahmed SM. Clinical features, diagnostic techniques and management of dual dengue and malaria infection. J Coll Physicians Surg Pak 2009,19(1): 25-9. PMID: 19149976.
14. Epelboin L, Hanf M, Dussart P, Ouar-Epelboin S, Djossou F, Nacher M, et al. Is dengue and malaria co-infection more severe than single infections? A retrospective matched-pair study in French Guiana. Malaria Journal 2012, 11(1): 142. Available from: https://doi.org/10.1186/1475-2875-11-142
15. Bhakhri BK, Singh DK, Singh N, Rai R. Does Malaria Co-Infection Alter the Clinical Course in Children Infected with Dengue? Analysis from 623 Indian Children Admitted with Dengue Infection. Journal of Tropical Pediatrics 2021, 67(2). Available from: https://doi.org/10.1093/tropej/fmab006
16. Ahmad S, Dhar M, Mittal G, Bhat NK, Shirazi N, Kalra V, et al. A comparative hospital-based observational study of mono- and co-infections of malaria, dengue virus and scrub typhus causing acute undifferentiated fever. European Journal of Clinical Microbiology & Infectious Diseases 2016, 35(4): 705–11. Available from: https://doi.org/10.1007/s10096-016-2590-3
17. Alsedig K, Eldigail MH, Elduma AH, Elaagip A, Altahir O, Siam HA, et al. Prevalence of malaria and dengue co-infections among febrile patients during dengue transmission season in Kassala, eastern Sudan. PLoS Neglected Tropical Diseases 2023, 17(10): e0011660. Available from: https://doi.org/10.1371/journal.pntd.0011660
18. Alsedig K, Eldigail MH, Elduma AH, Elaagip A, Altahir O, Siam HA, et al. Prevalence of malaria and dengue co-infections among febrile patients during dengue transmission season in Kassala, eastern Sudan. PLoS Neglected Tropical Diseases 2023, 17(10): e0011660. Available from: https://doi.org/10.1371/journal.pntd.0011660

***Corresponding author*: *Awad-Elkareem Abass. E-mail: awadko@hotmail.com*

International Journal of Biomedicine 16(4) (2026) 499-504
http://dx.doi.org/10.21103/Article16(4)_OA6

ORIGINAL ARTICLE

INTERNATIONAL JOURNAL OF BIOMEDICINE

Proinflammatory Mediators in Normal Weight Hypertensive Women of Reproductive Age

Zahir Hussain[1*]

[1]*Department of Physiology, Faculty of Medicine, Umm Al-Qura University, Makkah 21955, Saudi Arabia*

Abstract

Background: Based on age- and gender-specific studies, it has been revealed that hypertension (HTN) is an independent risk factor in the development and progression of cardiovascular diseases (CVDs). Therefore, the present study was designed to investigate the distinct impact of proinflammatory mediators -interleukin (IL-6), leptin (Lep), tumor necrosis factor-alpha (TNF-α), and homocysteine (Hcy) in normal weight (NW) normotensive (NTN) and HTN women of reproductive age with grade-1 HTN.
Methods and Results: The participants in the present study were NW women with NTN (n=200, age: 20-29 years) and HTN (n=198, age: 20-29 years) of reproductive age. The enzyme-linked immunosorbent assay (ELISA) kits were used to determine serum levels of pro-inflammatory mediators. Highly significant increases in serum levels ($p<0.001$) and significant positive linear correlations ($p<0.001$) for Lep, IL-6, and TNF-α in HTN compared to NTN women were investigated.
Conclusion: Results obtained in the present study in patients with HTN, independent of the influence of BW, indicate the pathophysiological significance of the interactive role of the inflammatory mediators (Lep, IL-6, and TNF-α) that would hopefully help further understanding of the mechanism of the development and progression of HTN and therapeutic implications for HTN. **(International Journal of Biomedicine. 2026;16(4):499-504.)**

Keywords: leptin, Interleukin-6, tumor necrosis factor-alpha, normal weight, hypertension, reproductive-age women

For citation: Hussain Z. Proinflammatory Mediators in Normal Weight Hypertensive Women of Reproductive Age. International Journal of Biomedicine. 2026;16(4):499-504. doi:10.21103/Article16(4)_OA6

Abbreviations

BMI, body mass index; **BP,** blood pressure; **BW,** body weight; **CVDs,** cardiovascular diseases; **DBP,** diastolic blood pressure; **DM,** diabetes mellitus; **ELISA,** enzyme linked immunosorbent assay; **Hb,** hemoglobin; **Hcy,** homocysteine; **HTN,** hypertension; **IL-6,** interleukin-6; **Lep,** leptin; **MCL,** menstrual cycle length; **MPD,** menstrual phase duration; **NTN,** normotension; **NW,** normal weight; **OW,** overweight; **PVAT,** perivascular adipose tissue; **R2,** coefficient of determination; **ROS,** radical oxygen species; **SBP,** systolic blood pressure; **SPSS,** Statistical Package for Social Sciences; **TNF-α,** tumor necrosis factor-alpha; **UQU,** Umm Al-Qura University.

Introduction

Based on age- and gender-specific studies, hypertension (HTN) is prevalent worldwide and is one of the major health problems requiring immediate attention.[1] It has been revealed that high blood pressure (BP) or HTN is an independent risk factor in the development and progression of cardiovascular diseases (CVDs).[2] Therefore, it is essential to study HTN thoroughly, considering various perspectives and screening, prevention, and therapeutic procedures.[1]

Considering systolic blood pressure (SBP) and diastolic blood pressure (DBP) levels irrespective of lifestyle and therapeutic criteria, HTN has been classified into three grades: grade 1 (SBP: 140-159 mmHg, DBP: 90-99 mmHg), grade 2 (SBP: 160-179 mmHg, DBP: 100-109 mmHg), and grade 3 (SBP: ≥180, DBP: ≥110).[3] Effective treatment of HTN and various other CVDs in women requires a better understanding of the sex-related differences that lead to a higher prevalence in women than men in view of more frequent female-related interactions,[4] e.g., heightened vasodilation in microvasculature and aortic stiffness due to small-sized coronary arteries in women.

The HTN-based information provides strong evidence of BP's influence on the development/progression of HTN.[5] Despite that, further clarification is required in view of controversial results due to different approaches/criteria employed for studying HTN patients.[5-7]

There are a variety of factors, including pro-inflammatory mediators-interleukin-6 (IL-6), leptin (Lep), tumor necrosis factor-alpha (TNF-α), and homocysteine (Hcy) that may

© 2026 The Author(s). *International Journal of Biomedicine* is published by IMRDC.
This is an open access article under the CC BY-NC-ND 4.0 license.

affect HTN and other vascular disorders.[8-16] However, no clear consensus exists on the interactive impact of various factors in understanding the mechanism of HTN, despite exploring the involvement of these factors,[17] though they have been studied in other CVDs, stroke, diabetes, and other disorders.[18-21] Therefore, the present study was designed to investigate the distinct impact of proinflammatory mediators in NW women of reproductive age with grade 1 HTN.

Materials and Methods

The present case-control study (HTN compared to NTN women) was carried out from January 2024 to January 2026 at the hospitals in Makkah (Saudi Arabia) collaborating with Umm Al-Qura University (UQU). Ethical approval for the current study (Approval No. HAPO-02-K-012-2022-01-1069) was obtained from the Faculty of Medicine, UQU. The methods, procedures, and techniques were employed in accordance with the instructions of the committee for institutional ethics on human experimentation and the Declaration of Helsinki (revised in 2013).

The sample size for the present work was calculated by: n=z2 *p* (1-p)/e2 (z, e and p respectively are: confidence level, margin of error/ confidence interval and proportion (p=0.5). The number of samples obtained using the formula was 385, and we planned to collect 420 samples for the present study. However, required patient/subject history and/or blood samples could not be properly managed for 22 participants (10 NTN and 12 HTN). Therefore, the sample size in the present study is 398 participants (200 NTN (Group 1) and 198 HTN (Group 2) with an age range of 20-29 years in both groups.

The subjects collected for both groups were well matched by age (20-29 years), sex (female subjects), and BW and, hence, body mass index (BMI) (≥18.5 and ≤24.9 kg/m²). Furthermore, all subjects in Group 2 (HTN) had grade-1 HTN (data for grade-2 and grade-3 HTN patients were not included). The participants in Group 1 (NTN) were healthy women without HTN, other cardiovascular disorders, or other disorders. The SBP and DBP were ≤120 and ≤80 mmHg, respectively, in NTN participants, and 140–159 and 90–99 mmHg, respectively, in HTN patients (grade 1). The BP measurements were taken by a manual mercury sphygmomanometer (MS-S1500-Mercury-Sphygmomanometer, Medical Sources Company Limited, Nanjing, Jiangsu, China).

Data from both groups were collected during the ovulatory cycle with the participants' permission/consent. The female individuals in both groups were of childbearing age (reproductive age) and free of anemia. Furthermore, they were not taking vitamin B, folic acid, or other supplements. They were all non-smokers, non-obese, non-pregnant, and non-diabetic. Those who were breastfeeding were not included in the present study.

The general features and patient/subject history were recorded and entered into a special questionnaire. The screening of the required participants was based on sex, age range, BW, and BP. The records of their menstrual cycle length (MCL in days) and 7 menstrual phase duration (MPD in days) were recorded. Their hemoglobin (Hb) levels were determined using a hematology analyzer, Sysmex XN 100i (Sysmex Europe SE, Norderstedt, Germany). The concentration of serum IL-6 was determined using a human interleukin-6 (IL-6) enzyme-linked immunosorbent assay (ELISA) kit. Serum homocysteine (Hcy) was measured using the Human-Hcy ELISA Kit. Serum Lep estimation was carried out using Lep human ELISA kit (ab100581)-Abcam's leptin human ELISA (Cambridge, UK), whereas serum TNF-α was measured by ELISA assay (catalog. STA00C, Quantikine ELISA, R&D Systems Inc., Minneapolis, MN, USA).

General biostatistical tests for the analysis of variation were performed using mean ± Standard Deviation (SD), and an unpaired t-test with two-tailed p-values was used to compare the HTN and NTN groups.[22] Whereas, to analyze and obtain the correlation between each pair of variables in both groups, the significance (p-value) was determined using the Statistical Package for the Social Sciences (SPSS), version 24.0 for Windows, and the coefficient of determination (R^2) was obtained. A p-value < 0.05 indicated significant variation or correlation between the two parameters.

Results

The present report in NW reproductive age women investigates the impact of serum proinflammatory mediators, IL-6, TNF-α, Hcy and Lep in NTN group (n=200, age: 25.05±2.95 years, MPD: 5.34±1.23 days, MCL: 28.37±1.39 days) and HTN group 8 (n=198, age: 25.00±2.96 years, MPD: 5.24±1.27 days, MCL: 28.45±1.40 days). Some of the general characteristics and variables studied in the current study are presented in Table 1.

Table 1.

General characteristics and variables of normal weight normotensive and hypertensive women of reproductive age.

Variables	Characteristics and variables in normal-weight normotensive and hypertensive women of reproductive age			
	NTN (n=200)	HTN (n=198)	Significance level	
			t-value	p-value
Number of subjects (n)	200	198	-	-
Age (years)	25.05±2.95	25.00±2.96	0.15	0.88
MPD (days)	5.34±1.23	5.24±1.27	0.80	0.42
MCL (days)	28.37±1.39	28.45±1.40	0.64	0.52
Hb (g/dL)	13.64±1.08	13.53±1.02	1.04	0.30
IL-6 (pg/mL)	3.83±1.82	6.39±2.72	11.03	<0.001
TNF-α (pg/ml)	4.20±2.28	6.35±2.69	8.63	<0.001
Hcy (µmol/L)	4.60±1.01	4.61±1.00	0.11	0.91
Lep (ng/mL)	4.65±1.86	9.16±3.24	17.04	<0.001

NTN: normotensive, HTN: hypertensive, MPD: menstrual phase duration, MCL: menstrual cycle length, Hb: hemoglobin, IL-6: interleukin-6, TNF- α: tumor necrosis factor alpha, Hcy: homocysteine, Lep: leptin.

Highly significant increases in serum levels of Lep, IL-6, and TNF-α were observed in HTN women compared

with NTN women (p<0.001; Table 1). The characteristics and variables in HTN women that did not show significant differences compared with NTN women were age, MPD, MCL, Hb, and Hcy (p>0.05; Table 1).

Serum Lep levels were plotted against other variables in both NTN and HTN groups of women. Significant positive linear correlations of serum Lep with IL-6 and TNF-α were observed in HTN women (p<0.001; Table 2). Serum Lep levels did not show a significant correlation with the remaining parameters (age, Hb, and Hcy) in HTN women (p>0.05, Table 2). All variables in the NTN group of women showed no significant correlation with serum Lep (p>0.05, Table 2).

Table 2.

Correlation of serum leptin levels with other variables in normal-weight hypertensive women of reproductive age.

Variables	R^2 and p-value for serum leptin against other variables in normal-weight normotensive and hypertensive women of reproductive age			
	NTN		HTN	
	R^2	p	R^2	p
Age	0.002	0.509	0.006	0.266
Hb	0.002	0.509	0.003	0.434
IL-6	0.001	0.590	0.560	<0.001
Hcy	0.001	0.590	0.000	0.895
TNF-α	0.003	0.475	0.290	<0.001

NTN: normotensive, HTN: hypertensive, Hb: hemoglobin, IL-6: interleukin-6, Hcy: homocysteine, TNF- α: tumor necrosis factor alpha.

A plot of serum IL-6 against Lep and TNF-α in HTN women showed a significant positive linear correlation (p<0.001; Table 3). Whereas age, Hb and serum Hcy showed non-significant correlation with serum levels of IL-6 (p>0.05, Table 3). Serum IL-6 did not show significant correlation with any of the parameters in NTN women (p>0.05, Table 3).

Table 3.

Correlation of serum IL-6 levels with other variables in normal-weight hypertensive women of reproductive age.

Variables	R^2 and p-value for serum IL-6 against other variables in normal-weight normotensive and hypertensive women of reproductive age			
	NTN		HTN	
	R^2	p	R^2	p
Age	0.006	0.286	0.001	0.733
Hb	0.012	0.110	0.006	0.281
Lep	0.001	0.590	0.560	<0.001
Hcy	0.001	0.590	0.001	0.590
TNF-α	0.001	0.594	0.190	<0.001

IL-6: interleukin-6, NTN: normotensive, HTN: hypertensive, Hb: hemoglobin, Lep: leptin, Hcy: homocysteine, TNF- α: tumor necrosis factor alpha.

Table 4 presents the results of the correlation between serum TNF-α levels and other variables in NW reproductive-age women with HTN. A significant positive linear correlation between TNF-α levels and each of Lep and IL-6 levels was found in the HTN group of women (p<0.001, Table 4). The other parameters, age, Hb, and serum Hcy, did not show a significant correlation with serum TNF-α levels (p>0.05, Table 4). Serum TNF-α levels showed no significant correlation with any parameter in NTN women (p>0.05, Table 4).

Table 4.

Correlation of serum TNF-α levels with other variables in normal-weight hypertensive women of reproductive age.

Variables	R^2 and p-value for serum TNF-α against other variables in normal-weight normotensive and hypertensive women of reproductive age			
	NTN		HTN	
	R^2	p	R^2	p
Age	0.000	0.976	0.009	0.178
Hb	0.001	0.706	0.002	0.559
Lep	0.003	0.475	0.290	<0.001
Hcy	0.001	0.649	0.001	0.665
IL-6	0.003	0.475	0.290	<0.001

TNF- α: tumor necrosis factor alpha, NTN: normotensive, HTN: hypertensive, Hb: hemoglobin, Lep: leptin, Hcy: homocysteine, IL-6: interleukin-6.

Discussion

Important findings in the present report are the highly significant increases in serum levels and significant positive linear correlations for Lep, IL-6, and TNF-α in HTN women of reproductive age with NW compared to NTN women of reproductive age with NW. The present work, comprising HTN grade-1 participants compared with NTN participants, is a well-controlled study considering sex, age, and BP status. Therefore, it is valuable to compare with already published reports and to interpret the results in light of the existing literature to understand the pathophysiological mechanisms and management of HTN.

Serum Lep-related studies provide evidence for our present findings on the impact of Lep in the progressive development of HTN[23,24] via endothelial dysfunction[25] and inflammation-related aortic stiffening, particularly in women, leading to ventricular stiffness.[26]

Other Lep-related mechanisms justifying the leading role of Lep in HTN in our present study are: enhanced sympathetic activity increasing BP and causing HTN,[24,27,28] Lep receptors in various blood vessels and atherosclerotic plaques causing arterial stiffness and HTN,[29] Lep-related increased immune activation, angiogenesis, increased platelet aggregation/production of radical oxygen species (ROS),[30] induction of endothelial related oxidative stress and the ROS,[31] and PVAT (perivascular adipose tissue)-derived contractile activity of Lep leading to decrease in vascular relaxation and development of HTN.[32]

Significantly increased levels of the most notorious pro-inflammatory cytokine, TNF-α, in women with HTN compared to women with NTN in the current study can be explained by previously published reports describing a vicious cycle[33] that links adiposity, inflammation, the immune system, and BP,

leading to HTN.[34] TNF-α causes low-grade inflammation and induces HTN, atherosclerosis, and other CVD dysfunctions.[35] IL-6 is another important risk factor in the present investigation that increases with increasing BP and, along with other important pro-inflammatory markers, is associated with immune system activation leading to HTN and other CVDs.[35-38] Serum Hcy and Hb in the current report did not show a significant difference between HTN and NTN subjects, consistent with earlier reports for HTN vs. NTN subjects.[39]

A study previously conducted in the Saudi Arabian population provides general information relevant to the present work.[40] However, our currently collected data did not correspond to the wide range of body weight/BMI investigated in that study.

The current investigation has merits as well as demerits/limitations. Since the participants in both groups (HTN and NTN) were non-obese, non-smoking, non-diabetic, non-pregnant, and non-anemic, and had similar ages and normal body weight within the reproductive age range, the present study is well-controlled and well-matched. Furthermore, women in the HTN group had grade 1 HTN.

The limitations or demerits in the present study are a narrow range of age, BW, and hence BMI, and BP, and the exclusion of male participants and overweight (OW), obese, anemic, and smoking female subjects, as well as women with HTN of grade 2 and grade 3. Furthermore, other pro-inflammatory and anti-inflammatory markers, along with other variables, need to be assessed in both groups to gain a clear idea of the role of inflammation in patients with HTN. Another limitation is that HTN women patients having comorbidities, including mainly other CHDs, diabetes mellitus, kidney diseases, stroke, and renal ischemia/failure, could not be consulted. However, these and other disorders are prevalent in HTN patients. It would be interesting and valuable to study HTN patients with various other medical comorbidities. Despite that, the present investigation provides a platform to carry out further studies to explore the pathophysiological mechanisms underlying the development of HTN in reproductive-age women and to provide insightful information for the management of patients with HTN.

Conclusion

The present study provides evidence of significant variation and correlation in Lep, TNF-α, and IL-6 among NW women with HTN compared to NTN women participants within the same age range, BW, and reproductive age status. The increased serum levels of Lep, TNF-α, and IL-6 in NW women with HTN compared to NW women with NTN indicate the pathophysiological significance of the interactive role of these inflammatory mediators independent of the influence of BW, which would hopefully help further understanding of the mechanism of the development and progression of HTN and therapeutic implications for HTN.

Ethical Considerations

The present study was approved by the Ethics Committee of the Faculty of Medicine, Umm Al-Qura University (UQU) (Approval Number: HAPO-02-K-012-2022-01-1069). All methods, procedures, and techniques used were in accordance with the Declaration of Helsinki of 1964, as revised in 2013. Written informed consent was obtained from all subjects who participated in the current study.

Author Contributions

Zahir Hussain contributed to supervision, conceptualization, investigation, data curation, formal analysis, writing the original draft, review and editing, and final approval of the article.

Sources of Funding

This research received no external funding.

Conflicts of Interest

The author declares that there are no competing interests/conflicts of interest.

Acknowledgments

The author thanks the medical and laboratory experts/personnel for their invaluable support.

References

1. Kearney PM, Whelton M, Reynolds K, Muntner P, Whelton PK, He J. Global burden of hypertension: analysis of worldwide data. Lancet. 2005;365(9455):217-23. doi: 10.1016/S0140-6736(05)17741-1.
2. Zhu L, Fang Z, Jin Y, Chang W, Huang M, Chen Y, et al. Circulating ERBB3 levels are inversely associated with the risk of overweight-related hypertension: a cross-sectional study. BMC Endocr Disord. 2021;21(1):130. doi: 10.1186/s12902-021-00793-8.
3. Williams B, Mancia G, Spiering W, Agabiti Rosei E, Azizi M, Burnier M, et al. ESC/ESH Guidelines for the management of arterial hypertension. Eur Heart J. 2018;39(33):3021-3104. doi: 10.1093/eurheartj/ehy339. Erratum in: Eur Heart J. 2019;40(5):475. doi: 10.1093/eurheartj/ehy686.
4. Pepine CJ, Kerensky RA, Lambert CR, Smith KM, von Mering GO, Sopko G, et al. Some thoughts on the vasculopathy of women with ischemic heart disease. J Am Coll Cardiol. 2006;47(3 Suppl):S30-5. doi: 10.1016/j.jacc.2005.09.023.
5. Linhart C, Tukana I, Lin S, Taylor R, Morrell S, Vatucawaqa P, et al., Continued increases in hypertension over three decades in Fiji, and the influence of obesity. J Hypertens. 2016;34(3):402-9. doi: 10.1097/HJH.0000000000000807.
6. Higashino R, Miyaki A, Kumagai H, Choi Y, Akazawa N, Ra SG, et al. Effects of lifestyle modification on central blood pressure in overweight and obese men. Blood Press Monit. 2013;18(6):311-5. doi: 10.1097/MBP.0000000000000006.
7. Malki MS, Babateen O, Hussain Z, Tawakul A, Subahi A, Obaid AA, et al. Low-Frequency Episodic Migraine with Aura and Associated Hypertension in Overweight Postmenopausal

Women: Interplay of Serum Interleukin-6 and Vitamin D. Medicina-Lithuania. Preprints 2026, 2026011619. doi:10.20944/preprints202601.1619.v1
8. Daiber A, Steven S, Weber A, Shuvaev VV, Muzykantov VR, Laher I, et al. Targeting vascular (endothelial) dysfunction. Br J Pharmacol. 2017;174(12):1591-1619. doi: 10.1111/bph.13517.
9. Pouvreau C, Dayre A, Butkowski EG, de Jong B, Jelinek HF. Inflammation and oxidative stress markers in diabetes and hypertension. J Inflamm Res. 2018;11:61-68. doi: 10.2147/JIR.S148911.
10. Aminuddin A, Salamt N, Ahmad Fuad AF, Chin KY, Ugusman A, Soelaiman IN, et al. Vascular Dysfunction among Malaysian Men with Increased BMI: An Indication of Synergistic Effect of Free Testosterone and Inflammation. Medicina (Kaunas). 2019;55(9):575. doi: 10.3390/medicina55090575.
11. Sohail S, Javaid A, Khan TA, Zahir H, Hussain Z. Diabetes mellitus, obesity and adipocytokines: Pathophysiological perspectives. Int J Biol Biotech. 2019;16 (2): 325-39.
12. Wu Y, Xu D, Shen HB, Qian SB, Qi J, Sheng XJ. The association between body mass index and testosterone deficiency in aging Chinese men with benign prostatic hyperplasia: results from a cross-sectional study. Aging Male. 2020;23(5):841-46. doi: 10.1080/13685538.2019.1604652.
13. Gonçalves CV, Ribeiro IS, Galantini MPL, Muniz IPR, Lima PHB, Santos GS, et al. Inflammaging and body composition: New insights in diabetic and hypertensive elderly men. Exp Gerontol. 2022;170:112005. doi: 10.1016/j.exger.2022.112005.
14. Hussain Z. Investigating the role of serum hepcidin and interleukin-6 in non-anemic women with acute ischemic stroke. International Journal of Biomedicine. 2024;14(2):260-64. doi:10.21103/Article14(2)_OA3
15. Hussain Z. Correlation of Serum Homocysteine, Interleukin-6 and Cholesterol in Overweight Women of Reproductive Age Group with Type 2 Diabetes Mellitus: A Case-control Study. Journal of Clinical and Diagnostic Research. 2025;19 (4):CC06-CC12. doi: 10.7860/JCDR/2025/77558.20844
16. Hussain Z. Comparative analysis of IL-6, hepcidin, homocysteine and cholesterol in normal-weight and overweight diabetic and non-diabetic adult men. Rawal Medical Journal. 2026; 51 (2):374-78. doi: 10.5455/rmj.20251014041148.
17. Phillips CL, Yee BJ, Trenell MI, Magnussen JS, Wang D, Banerjee D, et al. Changes in regional adiposity and cardio-metabolic function following a weight loss program with sibutramine in obese men with obstructive sleep apnea. J Clin Sleep Med. 2009;5(5):416-21.
18. Sohail S, Hussain Z. Pathophysiology of ischemic disorders- Ischemia, adipocytokines and diabetes mellitus. Int J Biol Biotech. 2013; 10 (2): 155-66.
19. Javaid A, Sohail S, Khan TA, Zahir H, Hussain Z. (2019). Ischemic disease and obesity: Plasma Lipids, Homocysteine and Hematological studies. Intern J Biol Biotech. 2019;16 (1): 49-58.
20. Hussain Z, Babateen O. Serum Vitamin D and Proinflammatory Markers Correlate Inversely in Overweight Postmenopausal Women with Type-2 Diabetes Mellitus. Pathophysiology. 2025; 32 (2). doi: 10.20944/preprints202503.1059.v1
21. Noorwali AA, Hussain Z. Interplay of serum IL-6 and vitamin D in overweight non-anemic reproductive age women with systemic lupus erythematosus. International Journal of Biomedicine. 2026; 16(1): 26-32. doi:10.21103/Article16(1)_OA2
22. Zahir H, Javaid A, Rehman R, Hussain Z. Statistical concepts in biology and health sciences. J Ayub Med Coll Abbottabad. 2014;26(1):95-7.
23. Seven E. Overweight, hypertension and cardiovascular disease: focus on adipocytokines, insulin, weight changes and natriuretic peptides. Dan Med J. 2015; 62(11):B5163.
24. Grassi G, Pisano A, Bolignano D, Seravalle G, D'Arrigo G, Quarti-Trevano F, et al. Sympathetic Nerve Traffic Activation in Essential Hypertension and Its Correlates: Systematic Reviews and Meta-Analyses. Hypertension. 2018;72(2):483-491. doi: 10.1161/HYPERTENSIONAHA.118.11038.
25. Zachariah JP, Hwang S, Hamburg NM, Benjamin EJ, Larson MG, Levy D, et al. Circulating Adipokines and Vascular Function: Cross-Sectional Associations in a Community-Based Cohort. Hypertension. 2016; 67(2):294-300. doi: 10.1161/HYPERTENSIONAHA.115.05949.
26. Zanoli L, Di Pino A, Terranova V, Di Marca S, Pisano M, Di Quattro R, et al. Inflammation and ventricular-vascular coupling in hypertensive patients with metabolic syndrome. Nutr Metab Cardiovasc Dis. 2018;28(12):1222-1229. doi: 10.1016/j.numecd.2018.08.003.
27. Grassi G, Seravalle G, Brambilla G, Buzzi S, Volpe M, Cesana F, et al. Regional differences in sympathetic activation in lean and obese normotensive individuals with obstructive sleep apnoea. J Hypertens. 2014;32(2):383-8. doi: 10.1097/HJH.0000000000000034.
28. Grassi G, Mark A, Esler M. The sympathetic nervous system alterations in human hypertension. Circ Res. 2015;116(6):976-90. doi: 10.1161/CIRCRESAHA.116.303604.
29. Purdham DM, Zou MX, Rajapurohitam V, Karmazyn M. Rat heart is a site of leptin production and action. Am J Physiol Heart Circ Physiol. 2004;287(6):H2877-84. doi: 10.1152/ajpheart.00499.2004.
30. Werner N, Nickenig G. From fat fighter to risk factor: the zigzag trek of leptin. Arterioscler Thromb Vasc Biol. 2004;24(1):7-9. doi: 10.1161/01.ATV.0000110908.43721.ad.
31. Yamagishi SI, Edelstein D, Du XL, Kaneda Y, Guzmán M, Brownlee M. Leptin induces mitochondrial superoxide production and monocyte chemoattractant protein-1 expression in aortic endothelial cells by increasing fatty acid oxidation via protein kinase A. J Biol Chem. 2001;276(27):25096-100. doi: 10.1074/jbc.M007383200.
32. Szasz T, Bomfim GF, Webb RC. The influence of perivascular adipose tissue on vascular homeostasis. Vasc Health Risk Manag. 2013;9:105-16. doi: 10.2147/VHRM.S33760.
33. Kaur J, Mukheja S, Varma S, Kalra HS, Khosa BS, Vohra K. Serum progranulin/tumor necrosis factor-α ratio as independent predictor of systolic blood pressure in overweight hypertensive patients: a cross-sectional study. Egypt Heart J. 2020;72(1):25. doi: 10.1186/s43044-020-00063-3.
34. Virdis A, Dell'Agnello U, Taddei S. Impact of inflammation on vascular disease in hypertension. Maturitas.

2014;78(3):179-83. doi: 10.1016/j.maturitas.2014.04.012.
35. Perticone M, Zito R, Miceli S, Pinto A, Suraci E, Greco M, et al. Immunity, Inflammation and Heart Failure: Their Role on Cardiac Function and Iron Status. Front Immunol. 2019;10:2315. doi: 10.3389/fimmu.2019.02315.
36. Raggi P, Genest J, Giles JT, Rayner KJ, Dwivedi G, Beanlands RS, et al. Role of inflammation in the pathogenesis of atherosclerosis and therapeutic interventions. Atherosclerosis. 2018;276:98-108. doi: 10.1016/j.atherosclerosis.2018.07.014.
37. Wolf D, Ley K. Immunity and Inflammation in Atherosclerosis. Circ Res. 2019;124(2):315-27. doi: 10.1161/CIRCRESAHA.118.313591.
38. Ruparelia N, Choudhury R. Inflammation and atherosclerosis: what is on the horizon? Heart. 2020;106(1):80-85. doi: 10.1136/heartjnl-2018-314230.
39. Naz L, Hussain Z, Husain T. (2009). Risk factors and biochemical variations in patients with ischemic stroke. Int J Biol Biotech. 2009;6 (1-2):83-87.
40. Harakeh S, Kalamegam G, Pushparaj PN, Al-Hejin A, Alfadul SM, Al Amri T, et al. Chemokines and their association with body mass index among healthy Saudis. Saudi J Biol Sci. 2020;27(1):6-11. doi: 10.1016/j.sjbs.2019.03.006.

***Corresponding author:** *Prof. Dr. Zahir Hussain, PhD. Department of Physiology, Faculty of Medicine, Umm Al-Qura University, Makkah 21955, Saudi Arabia. E-mail: zahirhussa@gmail.com*

International Journal of Biomedicine 16(4) (2026) 505-512
http://dx.doi.org/10.21103/Article16(4)_OA7

ORIGINAL ARTICLE

INTERNATIONAL JOURNAL OF BIOMEDICINE

Clinical Evaluation of a Novel Nanostructural Calcium Silicate–Hydroxyapatite Cement for Pulp Capping

Marija Lalović[1], Slavoljub Živković[2], Marijana Popović Bajić[2], Vukoman Jokanović[3], Vladimir Biočanin[4*]

[1]*Department of Endodontics and Dental Pathology, Faculty of Stomatology in Pančevo, University of Business Academy in Novi Sad, Serbia*
[2]*Department of Endodontics, School of Dental Medicine, University of Belgrade, Serbia*
[3]*ALBOS d.o.o., Belgrade, Serbia*
[4]*Department of Oral Surgery, Faculty of Stomatology in Pančevo, University of Business Academy in Novi Sad, Serbia*

Abstract

Background: Vital pulp therapy (VPT) is a conservative approach aimed at preserving pulp vitality in compromised teeth, contributing to long-term tooth survival. This study evaluated the clinical and radiographic outcomes of a novel hydroxyapatite-calcium silicate material (ALBO-MPCA) compared with commercially available mineral trioxide aggregate (MTA) in pulp-capping procedures, focusing on tertiary dentin formation.
Methods and Results: Twenty permanent teeth were treated with ALBO-MPCA (n = 15) or MTA (n = 5), and evaluated clinically and radiographically at baseline and after 6 months using cone-beam computed tomography (CBCT). The primary outcome was the thickness of tertiary dentin (μm), while secondary outcomes included pulp vitality, postoperative pain, and adverse events. Tertiary dentin formation was observed in all treated teeth in both groups. The mean thickness of newly formed tertiary dentin was higher in the MTA group compared to the ALBO-MPCA group (220 μm and 196 μm, respectively), with no statistically significant difference between the groups (p = 0.519). Pulp vitality was preserved in all cases. No adverse or serious adverse events were recorded, and only one patient in the MTA group reported mild postoperative pain.
Conclusion: ALBO-MPCA demonstrated clinical and radiographic performance comparable to MTA in vital pulp therapy. (**International Journal of Biomedicine. 2026;16(4):505-512.**)

Keywords: tertiary dentin • vital pulp therapy • mineral trioxide aggregate • cone-beam computed tomography

For citation: Lalović M, Živković S, Bajić MP, Jokanović V, Biočanin V. Clinical Evaluation of a Novel Nanostructural Calcium Silicate–Hydroxyapatite Cement for Pulp Capping. International Journal of Biomedicine. 2026;16(4):505-512. doi:10.21103/Article16(4)_OA7

Introduction

Vital pulp treatment (VPT) procedures are biologic and conservative treatment modalities, including direct or indirect pulp capping, aimed at maintaining the vitality of the dental pulp in teeth compromised by deep carious lesions, tooth wear, or trauma, thereby extending tooth longevity. Preservation of pulp vitality through minimally invasive approaches remains a key determinant of long-term tooth survival in contemporary restorative dentistry.

Traditionally, calcium hydroxide (CH) pulp-capping agents have been considered the gold standard of care for these procedures [1,2] because of their antibacterial properties and ability to promote healing and repair; however, their poor sealing ability and the formation of less homogeneous tertiary dentin compared with primary dentin represent notable limitations.[3] As a result, new generations of materials for VPT, namely calcium silicate cements, were subsequently introduced.[4,5]

One of the most widely investigated calcium silicate-based materials is mineral trioxide aggregate (MTA) due to its biocompatibility, bioactivity, and hard-tissue-inductive properties,[6-8] as well as favorable physical characteristics.[9] Hence, the indications for the use of MTA have expanded considerably beyond its original application, and it has become a widely accepted alternative to CH in several clinical

© 2026 The Author(s). *International Journal of Biomedicine* is published by IMRDC.
This is an open access article under the CC BY-NC-ND 4.0 license.

procedures, including direct [1,4] and indirect[7] pulp capping, root and furcation perforation repair,[10] apexification,[11] etc. Despite the considerable clinical advantages and expanded indications, MTA cements show several drawbacks. The major limitations include a prolonged setting time,[12] difficult handling, discoloration of the remaining tooth structure,[13] and the presence of heavy metals (arsenic, lead, and chromium) in the powder.[14] Therefore, researchers in this field have focused on synthesizing new materials to overcome the limitations of MTA cements.

In this context, an experimental material based on hydroxyapatite and calcium silicates, named ALBO-MPCA, has recently been synthesized.[15] The ALBO-MPCA material combines the advantages of hydroxyapatite, demonstrating excellent biocompatibility and bioactivity, along with similarity to the inorganic phases of biomineralized tissues. It also has the advantages of calcium silicates, whose progressive hydration enables the continuous transition of a hydrating cement paste from a fluid to a rigid material.[16] Several studies have evaluated the biocompatibility of the tested cement under both *in vitro* and *in vivo* conditions and compared it with MTA;[16-22] nevertheless, further clinical studies are required to assess its biocompatibility, effectiveness in tertiary dentin formation, and overall treatment outcomes.

Thus, the purpose of this *in vivo* study was to assess the clinical performance of the tested ALBO-MPCA cement for direct and indirect pulp capping and to compare it with MTA, focusing on clinical outcomes, including the occurrence of adverse events and the thickness of tertiary dentin.

Methods

Preparation of the Test Material

The experimental material (ALBO-MPCA) consists of 40% hydroxyapatite, 20% calcium silicates, 20% gypsum, and 20% barium sulfate ($BaSO_4$) as a radiopaque agent. Synthesis methods of hydroxyapatite and calcium silicates have been described in previous investigations.[16-22] Gypsum dihydrate and $BaSO_4$ were purchased from Whip Mix Corporation (USA) and Merck (Germany), respectively. Detailed physicochemical characterization of the material has also been reported in previous references.[16-22]

Study Design and Participants

This prospective clinical study was approved by the Ethics Committee of the Health Centre Foča, Bosnia and Herzegovina (Approval No. 01-78/2023). All participants provided written informed consent prior to inclusion, and the study was conducted in accordance with the Declaration of Helsinki.

The sample consisted of six females and fourteen males (n = 20), aged between 19 and 41 years. Eligible participants were adults (≥18 years) who provided written informed consent and presented with previously untreated Class II or Class IV carious lesions in permanent teeth. The distribution of participants by gender and age, treatment type, treated teeth, and pulp-capping material (ALBO-MPCA or MTA) is presented in Table 1.

Table 1.

Distribution of participants according to gender, age, type of treatment, treated teeth, and pulp-capping material used (ALBO-MPCA or MTA).

Patient No.	Gender	Age	Pulp capping	Tooth FDI notation	Smoker (Yes/No)	Pulp-capping material
P1	M	25	Direct	46	No	ALBO-MPCA
P2	M	19	Direct	37	No	ALBO-MPCA
P3	M	20	Direct	48	No	ALBO-MPCA
P4	M	22	Direct	25	No	ALBO-MPCA
P5	M	20	Indirect	16	No	ALBO-MPCA
P6	F	23	Indirect	17	No	ALBO-MPCA
P7	F	20	Indirect	27	No	ALBO-MPCA
P8	M	20	Indirect	24	No	ALBO-MPCA
P9	F	24	Direct	25	Yes	ALBO-MPCA
P10	M	29	Indirect	25	No	ALBO-MPCA
P11	M	20	Direct	14	No	ALBO-MPCA
P12	M	23	Direct	12	No	MTA
P13	M	22	Direct	24	No	ALBO-MPCA
P14	M	22	Indirect	15	No	ALBO-MPCA
P15	M	23	Indirect	25	Yes	ALBO-MPCA
P16	F	19	Direct	36	No	MTA
P17	M	19	Direct	25	No	MTA
P18	M	25	Direct	46	No	ALBO-MPCA
P19	F	41	Direct	44	Yes	MTA
P20	F	23	Direct	15	No	MTA

Abbreviations: *FDI, Fédération Dentaire Internationale; MTA, mineral trioxide aggregate; ALBO-MPCA, Calcium Silicate–Hydroxyapatite Cement for Pulp Capping*

Inclusion and Exclusion Criteria

Included participants were adults aged 18 years or older who provided written informed consent. Only carious teeth without prior restorative treatment were included. Eligible teeth presented with a pulpal diagnosis compatible with normal, healthy pulp and were asymptomatic, with accidental vital pulp exposure where present. Only symptomless vital teeth without clinical signs of pulp degeneration, such as spontaneous pain, tenderness to percussion, swelling, sinus tract formation, pathological mobility, or excessive pulpal bleeding, were included. All selected teeth were considered restorable. Radiographic inclusion criteria required the absence of internal or external resorption, interradicular and/or periapical bone destruction, and pulp stones.

Exclusion criteria comprised pregnancy or lactation within 6 months before or during the study period, a history of irreversible pulpal pain, immature teeth, non-restorable teeth, and teeth with active periodontal disease. Patients with systemic diseases, significant renal or hepatic impairment, or a life expectancy of less than 6 months were excluded. Subjects receiving concurrent systemic therapy with steroids, antibiotics, analgesics, immunomodulatory drugs, or cytostatics were not eligible for participation. Additionally, non-compliant patients, individuals with inadequate oral hygiene or unacceptable occlusal interferences, and participants enrolled in another clinical trial involving an investigational product within the previous 12 weeks were excluded. Any other condition that, in the opinion of the investigators, could compromise patient safety, influence study outcomes, or affect participation also constituted an exclusion criterion.

Clinical screening included thermal pulp testing using a cotton pellet sprayed with Endo-Frost cold spray (-50°C) (Coltene/Whaledent®, Altstatten, Switzerland), as well as percussion and palpation tests, and a standardized radiographic examination performed using the parallel cone technique with a Rinn holder (Dentsply Rinn®, Elgin, IL, USA) to exclude teeth with periradicular pathology.

Baseline Assessment

Before dental pulp capping, a baseline assessment was performed and included a detailed medical history, explanation and signing of the informed consent form, and a comprehensive oral clinical examination. Baseline pain assessment was conducted using a visual analogue scale (VAS). Pulp vitality was evaluated using thermal testing, and periapical status was assessed radiographically using standardized intraoral periapical radiographs obtained with the paralleling technique.

Clinical Procedure

All clinical procedures were performed under local anesthesia (4% articaine with adrenaline 1:100.000, Septanest®, Septodont, Saint-Maur-des-Fossés, France) and rubber dam isolation. The clinical crown was disinfected with 0.12% chlorhexidine (Hibideks®, Galenika, Belgrade, Serbia) before caries removal. Enamel was removed using round diamond burs in a high-speed handpiece with copious water spray, while carious dentin was removed using carbide burs in a low-speed handpiece under air-water spray. Complete caries excavation was performed from the peripheral to the central area using slow-speed round burs and hand instruments, with magnification (dental loupe).

In cases where caries removal resulted in a thin layer of remaining dentin without pulp exposure, indirect pulp capping was performed. When accidental pulp exposure occurred during caries excavation, the cavity was irrigated with sterile saline, and hemostasis was achieved using cotton pellets moistened with sodium hypochlorite or saline.

Following caries removal and, when present, pulp exposure management, a calcium silicate-based cement (ALBO-MPCA or MTA) was applied over the exposed pulp tissue or over the remaining dentin. The experimental material ALBO-MPCA was mixed with distilled water at a powder-to-liquid ratio of 2:1.[18] The control material MTA (MTA+®, Cerkamed, Poland) was prepared according to the manufacturer's instructions. To prevent displacement of the pulp-capping material during cavity sealing, a hard-setting protective glass-ionomer layer (GC Fuji IX GP®, GC Corporation, Tokyo, Japan) was applied. Subsequently, the cavity was gently rinsed with water to minimize potential adverse effects of disinfecting solutions on adhesive bonding (G-BOND®, GC Corporation, Tokyo, Japan), and the tooth was permanently restored using a resin composite restoration (Gradia Direct®, GC Corporation, Tokyo, Japan) during the same visit.

Clinical and Radiographic Evaluation

Clinical and radiographic evaluation was performed to assess the efficacy and clinical outcomes of the pulp-capping materials. The primary outcome measure was the formation and depth of tertiary dentin following direct or indirect pulp capping. Secondary outcome measures included changes in pulpal volume, presence of pulpal calcifications, postoperative pain, swelling or flare-up, analgesic consumption, sinus tract or fistula formation, and the occurrence of any adverse events.

Clinical follow-up examinations were conducted at 7 days, 3 months, and 6 months after treatment. Postoperative pain was assessed using a visual analogue scale (VAS). Pulp vitality was evaluated using thermal and electric sensitivity tests (Analytical Technologies®, Redmond, WA). Clinical assessment also included evaluation of tenderness to percussion and palpation, swelling, sinus tract formation, and pathological mobility.

Radiographic evaluation was performed using cone-beam computed tomography (CBCT) scans obtained at the 6-month follow-up. All CBCT scans were performed using a Romexis® 3D X-ray unit (Planmeca®, Helsinki, Finland) with standardized exposure parameters (90 kVp, 14 mA, voxel size 0.1 mm^3) to ensure consistency and comparability of radiographic measurements. A small field of view (5 × 5 cm) was used, and image reconstruction was performed with a matrix size of 1024 × 1024 pixels. CBCT data were analyzed using axial and coronal sections to identify tertiary dentin formation. The thickness of the newly formed tertiary dentin was measured in micrometers (μm) using a digital linear measurement tool at the narrowest point of the hard tissue formation. Coronal slices were used for occlusal locations, while axial slices were used for mesial and distal locations.

Radiographic analysis also included assessment of changes in pulpal chamber volume, presence of pulpal calcifications, and evaluation of periapical status and pathological root resorption. All measurements were independently performed by three examiners, and the mean value was used for statistical analysis to minimize potential measurement bias.

Adverse events were recorded during the follow-up period and included postoperative pain, analgesic use, swelling, flare-up, sinus tract formation, and any other procedure-related complications.

Statistical Analysis

Statistical analysis was performed to evaluate the primary outcome measure, defined as the thickness of tertiary dentin formed after pulp capping, and to compare the performance of the two pulp-capping materials (ALBO MPCA and MTA). Data distribution was assessed using the Shapiro-Wilk test.

For normally distributed data, comparisons between groups were performed using the independent *t*-test. For non-normally distributed data, the Mann-Whitney *U* test was applied. Effect size was calculated using Cohen's *d*. Categorical variables were analyzed using Cochran's test, where appropriate.

Statistical analyses were performed using standard statistical software, and the level of statistical significance was set at $p < 0.05$.

Results

During the study period, adverse events or serious adverse events were not recorded in either the ALBO-MPCA or MTA group. Clinical follow-up revealed no signs of postoperative infection, swelling, flare-up, sinus tract formation, pathological mobility, or tenderness to percussion or palpation.

Pulp vitality was preserved in all treated teeth in both groups throughout the follow-up period. Thermal and electric pulp tests showed normal responses in all treated teeth with ALBO-MPCA and MTA at all evaluation time points, while in the MTA group (patient No. 17), one tooth showed mild thermal sensitivity at the 3-month follow-up, which resolved by the 6-month examination.

No additional complications or adverse events related to direct or indirect pulp-capping procedures were observed, and VAS scores indicated the absence of postoperative pain (score 0) in all patients, except for a single case in the MTA group (patient No. 17), who reported mild pain.

Radiographic analysis performed using CBCT demonstrated tertiary dentin formation in all treated teeth in both groups. The mean tertiary dentin thickness was 196 ± 72 µm in the ALBO-MPCA group and 220 ± 57 µm in the MTA group. An independent *t*-test showed no significant difference in tertiary dentin thickness (µm) between the two materials ($p > 0.05$) (Table 2).

Representative original CBCT images demonstrating reparative dentin formation after direct pulp capping with ALBO-MPCA are shown in Figure 1.

Table 2.

Comparison of tertiary dentin thickness between ALBO-MPCA and MTA.

Group	n	Mean ± SD (µm)	*p*-value
ALBO-MPCA	14	196 ± 72	0.519
MTA	5	220 ± 57	

Independent t-test; $p > 0.05$.

***Abbreviations**: SD, standard deviation; MTA, mineral trioxide aggregate; n, number of samples.*

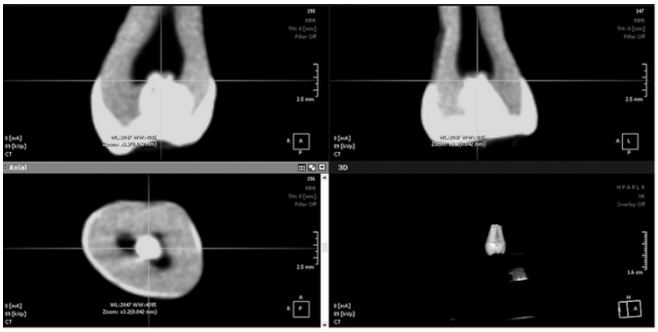

***Figure 1.** Original and multiplanar reconstructed CBCT images demonstrating tertiary dentin formation after pulp capping with ALBO-MPCA*

Discussion

Preservation of dental pulp vitality is essential for maintaining tooth health and long-term functionality. The present clinical study evaluated the performance of the experimental ALBO-MPCA cement compared with MTA in direct and indirect pulp capping procedures.

The clinical performance of the novel ALBO-MPCA material represented the primary endpoint and was assessed through systematic monitoring of adverse events and serious adverse events throughout the entire follow-up period. Special attention was given to potential complications, including postoperative infection, persistent pulp sensitivity, swelling, and sinus tract formation. No adverse or serious adverse events were recorded during the 6-month follow-up in either group. Pulp vitality was preserved in all treated teeth. VAS scores indicated absence of postoperative pain (score 0) in all cases, but only one tooth in the MTA group (patient No. 17) showed mild thermal sensitivity at the 3-month follow-up, which resolved by the 6-month examination. Although this isolated finding does not appear to be clinically significant, the overall results indicate favorable short-term clinical outcomes for both materials. These findings are in accordance with previous studies describing the high biocompatibility and favorable clinical performance of calcium silicate-based materials, particularly MTA, in vital pulp therapy procedures.[23-25] Furthermore, earlier *in vitro* and *in vivo* investigations of ALBO-MPCA have demonstrated promising biocompatibility and favorable biological properties,[16-22] which supports the clinical findings of the present study.

The present study is the first clinical study to assess tertiary dentin formation after the application of ALBO-MPCA pulp-capping materials using CBCT imaging. CBCT imaging

enables three-dimensional visualization and qualitative assessment of dentin structures.[26,27]

The CBCT results showed that the control material resulted in a higher tertiary dentin thickness than ALBO-MPCA (220 μm and 196 μm, respectively); however, this difference was not statistically significant. The thickness of tertiary dentin following pulp capping with MTA in the present study is comparable to the values reported by Agrawal et al.[28] and Mohanty et al.,[29] who reported mean thicknesses of 193 μm and 229.81 μm, respectively. These results suggest that the clinical performance of ALBO-MPCA is comparable to MTA and may be explained by the presence of calcium silicate phases in both materials. The reparative and reactive responses of VPT involve molecular activation of odontoblasts and, when necessary, the differentiation of undifferentiated stem cells within the dental pulp into odontoblast-like cells. Calcium silicate cements can stimulate cellular activity and promote the formation of tertiary dentin,[23] which is in accordance with the findings of the present study. This effect is attributed to their ability to release calcium ions during hydration, thereby promoting mineralization and stimulating tertiary dentin formation.[30] In addition, the hydroxyapatite component of ALBO-MPCA may further contribute to its bioactivity. Hydroxyapatite is one of the most commonly used calcium phosphate materials in medicine and dentistry, and its biocompatibility is closely related to its chemical composition, which is similar to that of dental and bone tissues.[31] Likewise, the lower cytotoxicity of the investigated material compared to MTA may be associated with a lower pH and the presence of hydroxyapatite, while the addition of calcium silicate improves mechanical properties.[32] Therefore, the ability of bioactive calcium silicate-based materials to stimulate tertiary dentin formation is considered a key factor in maintaining pulp vitality and promoting long-term tooth preservation.[33]

According to the results of the present *in vivo* study, ALBO-MPCA may represent a promising alternative to MTA for VPT procedures. However, the results should be considered within the limitations of the present study.

First, tertiary dentin formation was evaluated using CBCT imaging. Numerous studies have assessed tertiary dentin formation following indirect and direct pulp capping with different materials using the CBCT technique.[34-36] Nevertheless, for a more precise evaluation of tertiary dentin formation, methods that allow tissue assessment at the cellular level are required.[34] Although radiographic techniques such as CBCT and micro-CT provide valuable three-dimensional information, their resolution may be insufficient for detailed analysis of newly formed dentin. Therefore, histological and molecular techniques, including histologic analysis, immunohistochemical staining, in situ hybridization, and histomorphometric analysis, are considered more accurate for evaluating the structure and quality of tertiary dentin.[33] In the present clinical study, the application of these techniques was not feasible, as such analyses would require extraction of the treated teeth, which would be ethically unacceptable in cases where tooth preservation was the primary treatment goal. Another limitation of the present study is the heterogeneous sample, which included teeth from different tooth groups and both direct and indirect pulp capping procedures. However, this study aimed to evaluate the ability of the novel ALBO-MPCA material to stimulate tertiary dentin formation in comparison with MTA, which is widely accepted as a reference material in VPT procedures.[37-39]

Despite these limitations, the present *in vivo* study provides valuable clinical insight into the efficacy and clinical performance of the novel ALBO-MPCA material in VPT procedures. Both ALBO-MPCA and MTA induced tertiary dentin formation six months after pulp capping, with no significant difference in tertiary dentin thickness between the two materials. These findings suggest that ALBO-MPCA may represent a promising alternative to MTA. However, further clinical studies are needed to confirm the present findings, while long-term evaluation following potential commercialization will provide valuable information regarding the clinical performance and long-term success of ALBO-MPCA in routine clinical practice.

Author Contributions

Marija Lalović: Conceptualization, Data curation, Writing-original draft
Slavoljub Zivković: Investigation, Data curation and interpretation, Formal analysis
Marijana Popović Bajić: Investigation, Data curation, Formal analysis
Vukoman Jokanović: Conceptualization, Data interpretation, Writing-review and editing, Supervision
Vladimir Biočanin: Data curation and interpretation, Investigation, Conceptualization, Writing-review and editing, Supervision.

Funding

This research received no external funding

Disclosure and Conflicts of Interest

Author Vukoman Jokanovic was employed by the company ALBOS d.o.o., Belgrade, Serbia. He participated in resources, project administration, and funding acquisition in the study. The company's role was to synthesize the experimental mixture (ALBO-MPCA). Vukoman Jokanovic is among the masterminds behind the idea of composition and synthesis of experimental dental materials. The remaining authors declare that the research was conducted without any commercial or financial relationships that could be construed as a potential conflict of interest.

References

1. Tuna D, Olmez A. Clinical long-term evaluation of MTA as a direct pulp capping material in primary teeth. Int Endod J. 2008;41(4):273-278. doi:10.1111/j.1365-2591.2007.01339.x
2. Qudeimat MA, Barrieshi-Nusair KM, Owais AI. Calcium hydroxide vs mineral trioxide aggregates for partial pulpotomy of permanent molars with deep caries. Eur Arch Paediatr Dent.

2007;8(2):99-104. doi:10.1007/BF03262577
3. Didilescu AC, Cristache CM, Andrei M, Voicu G, Perlea P. The effect of dental pulp-capping materials on hard-tissue barrier formation: A systematic review and meta-analysis. J Am Dent Assoc. 2018;149(10):903-917.e4. doi:10.1016/j.adaj.2018.06.003
4. Nie E, Yu J, Jiang R, Liu X, Li X, Islam R, et al. Effectiveness of Direct Pulp Capping Bioactive Materials in Dentin Regeneration: A Systematic Review. Materials (Basel). 2021;14(22):6811. doi: 10.3390/ma14226811
5. Brizuela C, Ormeño A, Cabrera C, Cabezas R, Silva CI, Ramírez V, et al. Direct pulp capping with calcium hydroxide, mineral trioxide aggregate, and Biodentine in permanent young teeth with caries: A randomized clinical trial. J Endod. 2017;43(11):1776-1780. doi: 10.1016/j.joen.2017.06.031.
6. Benetti F, Gomes-Filho JE, de Araújo Lopes JM, Barbosa JG, Jacinto RC, Cintra LTA. In vivo biocompatibility and biomineralization of calcium silicate cements. Eur J Oral Sci. 2018;126(4):326-333. doi: 10.1111/eos.12539.
7. Covaci AM, Andrei M, Dinca I, Ciocan LT, Matei MN, Didilescu AC. Tertiary dentin barrier formation: A comparison between the effects of two calcium silicate-based materials. Curr Health Sci J. 2025;51(1):96-104. doi: 10.12865/CHSJ.51.01.10.
8. Davaie S, Hooshmand T, Ansarifard S. Different types of bioceramics as dental pulp capping materials: A systematic review. Ceram Int. 2021;47:20781-20792. doi: 10.1016/j.ceramint.2021.04.193.
9. Torabinejad M, Hong CU, McDonald F, Pitt Ford TR. Physical and chemical properties of a new root-end filling material. J Endod. 1995;21(7):349-53. doi: 10.1016/S0099-2399(06)80967-2.
10. Baroudi K, Samir S. Sealing ability of MTA used in perforation repair of permanent teeth: Literature review. Open Dent J. 2016;10:278-86. doi: 10.2174/1874210601610010278.
11. Muhamad A, Azzaldeen A, Hanali A. Mineral trioxide aggregate (MTA) in apexification. Endodontology. 2013;25(2):97-101. doi: 10.4103/0970-7212.352338.
12. Islam I, Chng HK, Yap AU. Comparison of the physical and mechanical properties of MTA and portland cement. J Endod. 2006;32(3):193-7. doi: 10.1016/j.joen.2005.10.043.
13. Kang SH, Shin YS, Lee HS, Kim SO, Shin Y, Jung IY, et al. Color changes of teeth after treatment with various mineral trioxide aggregate-based materials: An ex vivo study. J Endod. 2015;41(5):737-41. doi: 10.1016/j.joen.2015.01.019.
14. Schembri M, Peplow G, Camilleri J. Analyses of heavy metals in mineral trioxide aggregate and Portland cement. J Endod. 2010;36(7):1210-5. doi: 10.1016/j.joen.2010.02.011.
15. Jokanović V, Čolović B, Jokanović B, Živković S. Superplastic, Quick-Bonding Endodontic Mixtures and Their Hydration. Int J Appl Ceram Technol. 2015;12(6):E83-E91. doi: 10.1111/ijac.12234.
16. Paraš S, Trišić D, Mitrović Ajtić O, Antonijević Đ, Čolović B, Drobne D, et al. Biocompatibility Study of a New Dental Cement Based on Hydroxyapatite and Calcium Silicates: Focus on Liver, Kidney, and Spleen Tissue Effects. Int J Mol Sci. 2021;22(11):5468. doi: 10.3390/ijms22115468.
17. Petrović V, Opačić Galić V, Jokanović V, Jovanović M, Basta Jovanović G, Živković S. Biocompatibility of a new nanomaterial based on calcium silicate implanted in subcutaneous connective tissue of rats. Acta Vet Beogr. 2012;62(5-6):697-708. doi: 10.2298/AVB1206697P.
18. Opačić-Galić V, Petrović V, Zivković S, Jokanović V, Nikolić B, Knežević-Vukčević J, et al. New nanostructural biomaterials based on active silicate systems and hydroxyapatite: characterization and genotoxicity in human peripheral blood lymphocytes. Int Endod J. 2013;46(6):506-16. doi: 10.1111/iej.12017.
19. Petrović V, Opačić-Galić V, Živković S, Nikolić B, Danilović V, Miletić V, et al. Biocompatibility of new nanostructural materials based on active silicate systems and hydroxyapatite: in vitro and in vivo study. Int Endod J. 2015;48(10):966-75. doi: 10.1111/iej.12391.
20. Popović BM, Prokić B, Prokić BB, Jokanović V, Danilović V, Živković S. Histological evaluation of direct pulp capping with novel nanostructural materials based on active silicate cements and Biodentine® on pulp tissue. Acta Vet Beogr. 2013;63(2-3):347-360. doi: 10.2298/AVB1303347P.
21. Jokanović V, Čolović B, Prokić BB, Tomanović N, Popović Bajić M, Živković S. Subchronic Systemic Toxicity of New Endodontic Material Based on Calcium Hydroxyapatite and Calcium Silicates. Adv Mater Sci Eng. 2018;2018:1-6. doi: 10.1155/2018/8493439.
22. Cetenovic B, Prokic B, Vasilijic S, Dojcinovic B, Magic M, Jokanovic V, et al. Biocompatibility Investigation of New Endodontic Materials Based on Nanosynthesized Calcium Silicates Combined with Different Radiopacifiers. J Endod. 2017;43(3):425-432. doi: 10.1016/j.joen.2016.10.041.
23. Andrei M, Vacaru RP, Coricovac A, Ilinca R, Didilescu AC, Demetrescu I. The Effect of Calcium-Silicate Cements on Reparative Dentinogenesis Following Direct Pulp Capping on Animal Models. Molecules. 2021;26(9):2725. doi: 10.3390/molecules26092725.
24. Aeinehchi M, Eslami B, Ghanbariha M, Saffar AS. Mineral trioxide aggregate (MTA) and calcium hydroxide as pulp-capping agents in human teeth: a preliminary report. Int Endod J. 2003;36(3):225-31. doi: 10.1046/j.1365-2591.2003.00652.x.
25. Paranjpe A, Smoot T, Zhang H, Johnson JD. Direct contact with mineral trioxide aggregate activates and differentiates human dental pulp cells. J Endod. 2011;37(12):1691-5. doi: 10.1016/j.joen.2011.09.012.
26. Maret D, Molinier F, Braga J, Peters OA, Telmon N, Treil J, et al. Accuracy of 3D reconstructions based on cone beam computed tomography. J Dent Res. 2010;89(12):1465-9. doi: 10.1177/0022034510378011.
27. Scarfe WC, Farman AG, Sukovic P. Clinical applications of cone-beam computed tomography in dental practice. J Can Dent Assoc. 2006 Feb;72(1):75-80. PMID: 16480609.
28. Agrawal N, Singh V, Shrestha A, Jaisani M, Maharjan IK, Jain N. Evaluation of Mineral Trioxide Aggregate and Biodentine as Direct Pulp-capping Agents in Human Teeth: An Ex-Vivo Study. J Nepal Assoc Pediatr Dent.
29. Mohanty S, Ramesh S. Comparing Quality and Quantity of Dentin Bridge Formed Using Mineral Trioxide Aggregate, Biodentine, and Propolis: A Double-blinded Randomized Controlled Clinical Trial. World J Dent. 2020;11(5):373-379. doi: 10.5005/jp-journals-10015-1758.
30. Sarkar NK, Caicedo R, Ritwik P, Moiseyeva R, Kawashima I. Physicochemical basis of the biologic properties of mineral trioxide aggregate. J Endod. 2005;31(2):97-100. doi: 10.1097/01.don.0000133155.04468.41.

31. Suwanprateeb J, Thammarakcharoen F, Wasoontararat K, Chokevivat W, Phanphiriya P. Preparation and characterization of nanosized silver phosphate loaded hydroxyapatite by single step co-conversion process. Mater Sci Eng C Mater Biol Appl. 2012;32(7):2122-2128. doi: 10.1016/j.msec.2012.05.051.
32. Huan Z, Chang J. Calcium-phosphate-silicate composite bone cement: self-setting properties and in vitro bioactivity. J Mater Sci Mater Med. 2009;20(4):833-41. doi: 10.1007/s10856-008-3641-9.
33. Palczewska-Komsa MP, Gapiński B, Nowicka A. The Influence of New Bioactive Materials on Pulp-Dentin Complex Regeneration in the Assessment of Cone Beam Computed Tomography (CBCT) and Computed Micro-Tomography (Micro-CT) from a Present and Future Perspective: A Systematic Review. J Clin Med. 2022;11(11):3091. doi: 10.3390/jcm11113091.
34. Holiel AA, Mahmoud EM, Abdel-Fattah WM. Tomographic evaluation of direct pulp capping using a novel injectable treated dentin matrix hydrogel: a 2-year randomized controlled clinical trial. Clin Oral Investig. 2021;25(7):4621-4634. doi: 10.1007/s00784-021-03775-1.
35. Nowicka A, Wilk G, Lipski M, Kołecki J, Buczkowska-Radlińska J. Tomographic Evaluation of Reparative Dentin Formation after Direct Pulp Capping with Ca(OH)2, MTA, Biodentine, and Dentin Bonding System in Human Teeth. J Endod. 2015;41(8):1234-40. doi: 10.1016/j.joen.2015.03.017.
36. Oenning AC, Jacobs R, Pauwels R, Stratis A, Hedesiu M, Salmon B; DIMITRA Research Group. Cone-beam CT in paediatric dentistry: DIMITRA project position statement. Pediatr Radiol. 2018;48(3):308-316. doi: 10.1007/s00247-017-4012-9.
37. Kundzina R, Stangvaltaite L, Eriksen HM, Kerosuo E. Capping carious exposures in adults: a randomized controlled trial investigating mineral trioxide aggregate versus calcium hydroxide. Int Endod J. 2017;50(10):924-932.
38. Mente J, Hufnagel S, Leo M, Michel A, Gehrig H, Panagidis D, et al. Treatment outcome of mineral trioxide aggregate or calcium hydroxide direct pulp capping: long-term results. J Endod. 2014;40(11):1746-51. doi: 10.1016/j.joen.2014.07.019.
39. Matsuura T, Kawata-Matsuura VK, Yamada S. Long-term clinical and radiographic evaluation of the effectiveness of direct pulp-capping materials. J Oral Sci. 2019;61(1):1-12. doi: 10.2334/josnusd.18-0125.

***Corresponding author:** *Vladimir Bioč anin, Full Professor, University of Business Academy in Novi Sad, Faculty of Stomatology in Pančevo, Serbia, Žarka Zrenjanina 179, 26000 Pančevo, Serbia. E-mail: vladimirbiocanin@gmail.com*

Supplementary Material

Table S1.

Clinical follow-up parameters after VPT procedures.

Patient	Thermal sensitivity			Electric sensitivity			Tooth mobility		
	Baseline	3 months	6 months	Baseline	3 months	6 months	Baseline	3 months	6 months
P1	+	-	-	+ (2)	+ (3)	+ (3)	-	-	-
P2	+	-	-	+ (4)	+ (4)	+ (4)	-	-	-
P3	+	-	-	+ (2)	+ (3)	+ (3)	-	-	-
P4	+	-	-	+ (2)	+ (1)	+ (1)	-	-	-
P5	+	-	-	+ (3)	+ (2)	+ (2)	-	-	-
P6	-	-	-	+ (4)	+ (4)	+ (4)	-	-	-
P7	+	-	-	+ (3)	+ (4)	+ (4)	-	-	-
P8	+	-	-	+ (1)	+ (1)	+ (1)	-	-	-
P9	+	-	-	+ (1)	+ (1)	+ (1)	-	-	-
P10	-	-	-	+ (1)	+ (1)	+ (1)	-	-	-
P11	-	-	-	+ (1)	+ (1)	+ (1)	-	-	-
P12	-	-	-	+ (1)	+ (1)	+ (1)	-	-	-
P13	+	-	-	+ (2)	+ (2)	+ (2)	-	-	-
P14	+	-	-	+ (1)	+ (1)	+ (1)	-	-	-
P15	-	-	-	+ (1)	+ (1)	+ (1)	-	-	-
P16	+	-	-	+ (2)	+ (2)	+ (2)	-	-	-
P17	+	-	-	+ (2)	+ (2)	+ (2)	-	-	-
P18	+	-	-	+ (3)	+ (2)	+ (2)	-	-	-
P19	+	-	-	+ (2)	+ (2)	+ (2)	-	-	-
P20	+	-	-	+ (1)	+ (1)	0	-	-	-

Note: *In the "Electric sensitivity" column, the numerical values recorded in parentheses represent the response obtained during electric sensitivity testing, corresponding to the intensity of the tested current on a scale from 0 to 9. +, positive response; –, negative response.*

Table S2.

Types of carious lesions and treated teeth included in the study.

Patient	Type of caries		FDI Tooth notation
	Pit and fissure caries	Smooth-surface caries, class 2 and 4	
P1		+ 2	46
P2	+		37
P3	+		48
P4		+ 2	25
P5	+	+ 2	16
P6		+ 2	17
P7		+ 2	27
P8		+ 2	24
P9		+ 2	25
P10		+ 2	25
P11		+ 2	14
P12		+ 4	12
P13		+ 2	24
P14		+ 2	15
P15		+ 2	25
P16	+		36
P17		+ 2	25
P18	+	+ 2	46
P19		+ 2	44
P20		+ 2	15

Note: *"+" indicates the presence of the lesion. Numbers indicate the Black classification (Class II or Class IV). FDI, Fédération Dentaire Internationale.*

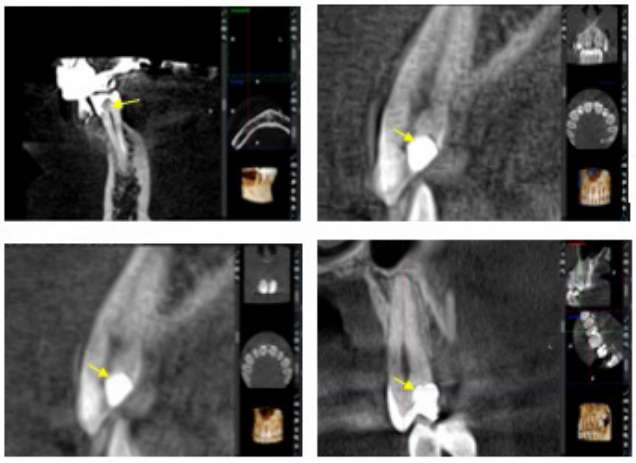

Figure S1.

Representative cone-beam computed tomography (CBCT) images showing a thin, continuous layer of tertiary dentin completely covering the pulp exposure site (yellow arrows). In all cases examined, the newly formed dentin exhibited radiopacity comparable to that of the surrounding dentin, indicating satisfactory mineralization.

International Journal of Biomedicine 16(4) (2026) 513-516
http://dx.doi.org/10.21103/Article16(4)_CR1

CASE REPORT

INTERNATIONAL JOURNAL OF BIOMEDICINE

Diagnosis of ANCA-Negative Eosinophilic Granulomatosis with Polyangiitis with Cardiac Involvement and Progressive Neuropathy via Cardiac Magnetic Resonance Imaging and Bone Marrow Biopsy

Musab A. bin Shuayl[1*]

[1]*Department of internal Medicine, College of Medicine, Prince Sattam Bin Abdulaziz University, Al-Kharj, Saudi Arabia*

Abstract

Eosinophilic granulomatosis with polyangiitis (EGPA) is a rare disorder that may present with cardiac involvement. EGPA diagnosis is a challenge. Our patient is a 57-year-old male with a history of adult-onset asthma who presented with hypoxemic respiratory failure and volume overload. Echocardiography displayed a reduced left ventricular ejection fraction (LVEF) of 42%. The patient didn't improve despite therapy for heart failure. The tests revealed eosinophilia and elevated serum IgE, but ANCA was negative. CMR and bone marrow biopsy findings confirmed secondary/reactive eosinophilia consistent with EGPA. The patient received induction, immunosuppressive, and maintenance therapies, and he improved. Therefore, the rapid and correct diagnosis of EGPA with cardiac involvement helps the patient improve and avoid poor prognosis and severe consequences. **(International Journal of Biomedicine. 2026;16(4):513-516.)**

Keywords: eosinophilic granulomatosis • polyangiitis • cardiac involvement • bone marrow biopsy

For citation: Shuayl MA. Diagnosis of ANCA-Negative Eosinophilic Granulomatosis with Polyangiitis with Cardiac Involvement and Progressive Neuropathy via Cardiac Magnetic Resonance Imaging and Bone Marrow Biopsy. International Journal of Biomedicine. 2026;16(4):513-516. doi:10.21103/ Article16(4)_CR1

Introduction

Eosinophilic granulomatosis with polyangiitis (EGPA) is a rare disorder characterized by late-onset asthma, blood and tissue eosinophilia, and small- to medium-vessel vasculitis,[1] with an annual incidence of 1-3 per 1000000 individuals.[2] EGPA has been described as progressing through three phases: the prodromal, the eosinophilic, and the vasculitic.[3] EGPA is one of the systemic vasculitides that affect the heart; the rate of cardiac involvement ranges from 1% to 29%.[3] Cardiac involvement causes mortality in almost 50%, and it is a poor prognostic factor.[4] However, diagnosing cardiac involvement in EGPA is challenging.[5] Here, we present a 57-year-old patient with ANCA-EGPA diagnosed by cardiac magnetic resonance (CMR) imaging and bone marrow biopsy (BMP).

Case Presentation

History and physical examination

A 57-year-old male was admitted to the emergency department with acute-onset hypoxemic respiratory failure and clinical signs of severe volume overload. His medical history revealed type 2 diabetes mellitus, systemic hypertension, dyslipidemia, and developed adult-onset asthma at 41 years of age, which has been relatively well-controlled with inhaled therapies, but he didn't experience asthmatic manifestations during childhood, and he had no known history of pre-existing ischemic or non-ischemic cardiomyopathy. He had respiratory distress with bilateral pulmonary rales, peripheral pitting edema, and elevated jugular venous pressure.

Laboratory tests and imaging

The tests revealed a markedly elevated B-type natriuretic peptide (BNP) level of 617 pg/mL. Electrocardiogram (ECG) showed normal sinus rhythm with no acute ischemic changes or conduction delays. Transthoracic echocardiography (TTE) showed a normal-sized left ventricle with mildly decreased systolic function (LVEF 42%) and global hypokinesia, and a mildly dilated right atrium. High-flow oxygen therapy and aggressive intravenous loop diuresis were used to stabilize the patient. A diagnostic coronary angiography was performed to rule out macrovascular coronary artery disease, which demonstrated non-significant atheromatous plaques in the mid-left anterior descending (LAD) and right coronary arteries (RCA). Based on optimized Guideline-Directed Medical Therapy (GDMT), our patient was diagnosed with

© 2026 The Author(s). *International Journal of Biomedicine* is published by IMRDC.
This is an open access article under the CC BY-NC-ND 4.0 license.

heart failure and reduced ejection fraction (HFrEF) and was prescribed sacubitril/valsartan 24/26 mg orally twice daily, empagliflozin 10 mg, and bisoprolol 2.5 mg orally once daily.

Outpatient assessment

Our patient was referred to the specialized Heart Failure Clinic (HFC); there was no active chest pain, orthopnea, paroxysmal nocturnal dyspnea (PND), or ankle swelling. There was no nausea, vomiting, gastroesophageal reflux disease (GERD), oral ulcers, bowel habit changes, generalized weakness, arthralgias, or inflammatory eye pain. However, he was still highly restricted from a functional standpoint with severe persistent dyspnea in agreement with New York Heart Association (NYHA) Functional Class III. He was complaining of a progressive, debilitating numbness in both hands and feet, which compromised his fine motor skills and balance. Laboratory tests, including CBC, kidney function, total serum IgE, and inflammatory markers, were performed. The tests were normal except for eosinophils (%), absolute eosinophil count, and total serum IgE, which were elevated at 14%, 1.4×10^9/L, and 563 IU/mL, respectively. Hepatitis B and C and HIV were negative, with an entirely negative autoimmune serology panel including anti-neutrophil cytoplasmic antibodies (ANCA) and anti-nuclear antibodies (ANA). During subsequent follow-up visits, spironolactone 12.5 mg daily was added to achieve full GDMT. The dyspnea and peripheral neuropathy failed to improve.

Further imaging and biopsy

The patient underwent CMR imaging to investigate the cause of non-ischemic cardiomyopathy and evaluate for suspected myocardial eosinophilic infiltration. The CMR displayed a moderately dilated left ventricle with a calculated LVEF of 46%. There was no evidence of acute myocardial edema. Late gadolinium enhancement (LGE) imaging showed non-ischemic mid-myocardial enhancement involving the basal septum, with a small, localized subendocardial region of enhancement in the mid-to-apical inferior portions. The patient underwent BMP, which displayed isolated eosinophilic hyperplasia with normal maturation and no excess of blasts, confirming secondary/reactive eosinophilia consistent with EGPA.

Management

Aggressive induction therapy was initiated in line with current international guidelines for severe EGPA. The treatment included systemic glucocorticoids, specifically prednisone, initiated at a high dose of 50 mg orally daily to achieve immediate suppression of eosinophilic activation and vascular inflammation, then gradually tapered over several months from the initial induction dose to a minimal chronic maintenance dose of 5 mg daily. He received intravenous cyclophosphamide pulse therapy for a total of three doses and azathioprine at a maintenance dose of 150 mg orally daily. Standard HFrEF therapy was continued, including immunosuppression, to support reverse ventricular remodeling.

Outcomes and follow-up

The response to targeted immunosuppression was quick and favorable. The numbness was resolved totally, with restoration of manual dexterity and balance. The dyspnea improved significantly to NYHA Class I. Follow-up echocardiography and clinical parameters revealed stable cardiac metrics (LVEF at 46%) without recurrence of systemic volume overload or asthmatic exacerbations. The patient remains adherent to azathioprine and a low-dose prednisone regimen under close multidisciplinary surveillance by cardiology and rheumatology.

Discussion

In EGPA with an asthma history, eosinophilia, and both eosinophilic and vasculitic organ damage, the suspicion of EGPA is straightforward. However, some cases lack evidence of vasculitis or ANCA, and there is debate over whether such patients can be recognized as having EGPA.[6] Our patient had asthma, but he displayed negative serology for ANCA, which made EGPA diagnosis hard. The patient was diagnosed as HFrEF based on GDMT; however, the treatment wasn't effective.

Laboratory investigations revealed elevated eosinophils (%), absolute eosinophil count, and total serum IgE. Active EGPA is characterized by eosinophilia > 10%, which correlates with disease activity.[7,8] Additionally, a non-specific rise in IgE levels was discovered in 75% of patients.[9] Therefore, our patient was suspected to have EGPA. However, the cardiac manifestations couldn't be explained as he lacked a history of cardiovascular problems.

ANCA is positive in 30-40% of patients with EGPA. ANCA-negative type is associated with organ damage related to Eosinophilic inflammation[1] and is more prone to develop cardiac involvement.[4] The rate of cardiac involvement in EGPA ranges from 16% to 29%.[3] Clinically evident cardiac manifestations are uncommon despite the wide range of cardiac manifestations, including cardiomyopathy, heart failure, and myocarditis.[10] The patient was not suspected of having EGPA with cardiac involvement, as the signs of cardiac involvement include chest pain, palpitations, arrhythmia, hypotension, and cardiogenic shock.[5] However, the patient didn't experience any of the previous signs.

Cardiac involvement is associated with a poor prognosis; therefore, all patients should undergo basic cardiological examinations, including ECG, troponin, BNP, and echocardiography.[1] Our patient's BNP was significantly elevated, and the initial ECG showed normal sinus rhythm with no acute ischemic changes or conduction delays. Therefore, a more advanced imaging modality was needed to identify the cause of non-ischemic cardiomyopathy in our patient.

Recently, CMR imaging has been considered the gold standard for cardiomyopathy; it is a safe, non-invasive tool for assessing cardiac involvement in ANCA-associated vasculitis.[11] LGE by CMR is characterized by high specificity and sensitivity in detecting fibrosis and cardiac inflammation.[12] The signs of cardiac involvement in EGPA based on CMR

include subendocardial LGE, myocardial edema, and left ventricular dysfunction.[1] Cardiac involvement in EGPA can affect the coronary arteries, endocardium, myocardium, pericardium, and valvular structures.[5]

In our patient, the CMR revealed a moderately dilated left ventricle with an LVEF of 46%, and LGE showed non-ischemic mid-myocardial enhancement involving the basal septum, with a small, localized region of subendocardial enhancement.

Additionally, our patient underwent BMP, as EGPA shares features of vasculitis and hypereosinophilic syndrome (HES),[13] which causes heterogeneity in clinical symptoms, making diagnosis a challenging process.[1] The similarities in clinical presentations made the exclusion of HES and, in some cases, the identification of overlapping HES possible only with BMP or trepanobiopsy and genetic testing.[14] The BMP of our patient revealed marked, isolated eosinophilic hyperplasia with normal maturation and no excess of blasts, confirming secondary/reactive eosinophilia consistent with EGPA. Cardiac involvement in EGPA is strongly linked with eosinophilia.[5]

Therefore, our patient was diagnosed with EGPA based on CMR and BMP. Our patient was diagnosed as an EGPA case with cardiac involvement represented as heart failure with left ventricular dysfunction (46%). A previous meta-analysis revealed that the most common echocardiographic finding was systolic left ventricular dysfunction (83.9%), whereas clinical heart failure was the most common clinical presentation (51.6%).[3]

In the vasculitic phase, manifestations including those related to the nervous system can be observed, and it is often preceded by general manifestations such as muscle pain, fever, and weakness.[1] Additionally, our patient experienced numbness in the hands and feet, which wasn't improved after the initial therapy. However, the patient didn't experience fever, weakness, or muscle pain.

The management of EGPA depends on disease severity and consists of induction and maintenance phases; the former aims to achieve disease remission, whereas the latter aims to prevent relapse.[3] The cornerstone therapy in EGPA is systemic corticosteroids with a recommended initial dose of 1mg/kg/day of prednisolone followed by gradual reduction to the minimal effective dose.[15] Cyclophosphamide is recommended as an immunosuppressant for those who don't respond well to corticosteroids or have poor prognostic factors as defined by the five-factor score, which predicts disease severity and prognosis.[4] Maintenance therapy is preferably azathioprine at a dose of 2-3mg/kg/day.[15] Our patient received induction, immunosuppression, and maintenance therapies, and he improved; these improvements included reduced dyspnea and stable cardiac metrics, with no recurrence of systemic volume overload or asthma exacerbation.

Conclusion

The diagnosis of EGPA with cardiac involvement and neuropathy is challenging, especially with the absence of ANAC. CMR and BMP served as effective non-invasive diagnostic tools that helped correctly diagnose the patient; consequently, he was prescribed appropriate treatment, improved, and a poor prognosis associated with EGPA cardiac involvement was avoided. Therefore, ANCA-negative asthma patients with eosinophilia and cardiac manifestations should undergo CMR and BMP to rapidly confirm the diagnosis of EGPA with cardiac involvement to establish early treatment and avoid poor prognosis and severe consequences.

References

1. Fijolek J, Radzikowska E. Eosinophilic granulomatosis with polyangiitis - Advances in pathogenesis, diagnosis, and treatment. Front Med (Lausanne). 2023 May 3;10:1145257. doi: 10.3389/fmed.2023.1145257. PMID: 37215720; PMCID: PMC10193253.
2. Springer JM, Kalot MA, Husainat NM, Byram KW, Dua AB, James KE, Chang Lin Y, Turgunbaev M, Villa-Forte A, Abril A, Langford CA, Maz M, Chung SA, Mustafa RA. Eosinophilic Granulomatosis with Polyangiitis: A Systematic Review and Meta-Analysis of Test Accuracy and Benefits and Harms of Common Treatments. ACR Open Rheumatol. 2021 Feb;3(2):101-110. doi: 10.1002/acr2.11194. Epub 2021 Jan 29. PMID: 33512787; PMCID: PMC7882521.
3. Pakbaz M, Pakbaz M. Cardiac Involvement in Eosinophilic Granulomatosis with Polyangiitis: A Meta-Analysis of 62 Case Reports. J Tehran Heart Cent. 2020 Jan;15(1):18-26. PMID: 32742288; PMCID: PMC7360870.
4. Watanabe R, Hashimoto M. Eosinophilic Granulomatosis with Polyangiitis: Latest Findings and Updated Treatment Recommendations. J Clin Med. 2023 Sep 15;12(18):5996. doi: 10.3390/jcm12185996. PMID: 37762936; PMCID: PMC10532073.
5. Srikantharajah M, Gopalan D, Wilson-Morkeh H, Siddiqui S, McAdoo SP, Youngstein T. Cardiac Involvement in Eosinophilic Granulomatosis with Polyangiitis. Curr Cardiol Rep. 2025 Jul 9;27(1):109. doi: 10.1007/s11886-025-02258-z. PMID: 40632386; PMCID: PMC12241301.
6. Churg A. Recent advances in the diagnosis of Churg-Strauss syndrome. Mod Pathol. 2001 Dec;14(12):1284-93. doi: 10.1038/modpathol.3880475. PMID: 11743052.
7. White J, Dubey S. Eosinophilic granulomatosis with polyangiitis: A review. Autoimmun Rev. 2023 Jan;22(1):103219. doi: 10.1016/j.autrev.2022.103219. Epub 2022 Oct 22. PMID: 36283646.
8. Nguyen Y, Guillevin L. Eosinophilic Granulomatosis with Polyangiitis (Churg-Strauss). Semin Respir Crit Care Med. 2018 Aug;39(4):471-481. doi: 10.1055/s-0038-1669454. Epub 2018 Nov 7. PMID: 30404114.
9. Khoury P, Grayson PC, Klion AD. Eosinophils in vasculitis: characteristics and roles in pathogenesis. Nat Rev Rheumatol. 2014 Aug;10(8):474-83. doi: 10.1038/nrrheum.2014.98. Epub 2014 Jul 8. PMID: 25003763; PMCID: PMC4849122.
10. Lagan J, Naish JH, Fortune C, Bradley J, Clark D, Niven R, Chaudhuri N, Schelbert EB, Schmitt M, Miller CA. Myocardial involvement in eosinophilic granulomatosis with polyangiitis evaluated with cardiopulmonary magnetic resonance. Int J Cardiovasc Imaging. 2021 Apr;37(4):1371-1381. doi: 10.1007/s10554-020-02091-1. Epub 2020 Nov 19. PMID: 33211241; PMCID: PMC8026437.
11. Garcia-Vives E, Rodriguez-Palomares JF, Harty L, Solans-Laque R, Jayne D. Heart disease in eosinophilic

granulomatosis with polyangiitis (EGPA) patients: a screening approach proposal. Rheumatology (Oxford). 2021 Oct 2;60(10):4538-4547. doi: 10.1093/rheumatology/keab027. PMID: 33493294.
12. Fijolek J, Wiatr E, Gawryluk D, Nowicka U, Martusewicz-Boros MM, Kober J, Piotrowska-Kownacka D, Roszkowski-Sliz K. "The significance of cardiac magnetic resonance imaging in detection and monitoring of the treatment efficacy of heart involvement in eosinophilic granulomatosis with polyangiitis patients". Sarcoidosis Vasc Diffuse Lung Dis. 2016 Mar 29;33(1):51-8. PMID: 27055836.
13. Valent P, Klion AD, Horny HP, Roufosse F, Gotlib J, Weller PF, Hellmann A, Metzgeroth G, Leiferman KM, Arock M, Butterfield JH, Sperr WR, Sotlar K, Vandenberghe P, Haferlach T, Simon HU, Reiter A, Gleich GJ. Contemporary consensus proposal on criteria and classification of eosinophilic disorders and related syndromes. J Allergy Clin Immunol. 2012 Sep;130(3):607-612.e9. doi: 10.1016/j.jaci.2012.02.019. Epub 2012 Mar 28. PMID: 22460074; PMCID: PMC4091810.
14. Sebastian A, Kosałka-Węgiel J. A variety of clinical presentations of eosinophilic granulomatosis with polyangiitis: a comprehensive review. Reumatologia. 2024;62(6):456-465. doi: 10.5114/reum/196141. Epub 2024 Dec 24. PMID: 39866310; PMCID: PMC11758110.
15. Groh M, Pagnoux C, Baldini C, Bel E, Bottero P, Cottin V, Dalhoff K, Dunogué B, Gross W, Holle J, Humbert M, Jayne D, Jennette JC, Lazor R, Mahr A, Merkel PA, Mouthon L, Sinico RA, Specks U, Vaglio A, Wechsler ME, Cordier JF, Guillevin L. Eosinophilic granulomatosis with polyangiitis (Churg-Strauss) (EGPA) Consensus Task Force recommendations for evaluation and management. Eur J Intern Med. 2015 Sep;26(7):545-53. doi: 10.1016/j.ejim.2015.04.022. Epub 2015 May 9. PMID: 25971154.

***Corresponding author:** *Musab A. bin Shuayl. E-mail: m.binshuayl@psau.edu.sa*

International Journal of Biomedicine 16(4) (2026) 517-517
http://dx.doi.org/10.21103/Article16(4)_CRR

CORRIGENDUM

INTERNATIONAL JOURNAL OF BIOMEDICINE

[Corrigendum] Deep Learning-Based Convolutional Neural Networks for Brain Tumor Detection on CT Scans: A Systematic Review

Sara Ali[1], Meaad Elbashir[1], Noor Hamzi [1], Imad Akour[1], Anwar Sheikhain[1], Raed Al-Shahri[1], Turkey Refaee[1], Ali Abdelrazig[1], Awatif M. Omer[2]

[1]Diagnostic Radiography Technology Department, Faculty of Nursing and Health Sciences, Jazan University, Jazan, Saudi Arabia
[2]Diagnostic Radiography Technology Department, College of Applied Medical Sciences, Taibah University, Madinah, Saudi Arabia

Abstract

Corrigendum for ' Deep Learning-Based Convolutional Neural Networks for Brain Tumor Detection on CT Scans: A Systematic Review' by Ali S, Elbashir M, Hamzi A, Akour I, Sheikhain A, Al-Shahri R, Refaee T, Abdelrazig A, Omer AM. Deep Learning–Based Convolutional Neural Networks for Brain Tumor Detection on CT scans: A Systematic Review. 2026;16(3):306-313. doi:10.21103/Article16(3)_RA2.

Following the publication of this article, A.Hamzi has realized that his name has legally changed to 'Noor Hamzi' with documentation of the name change and the government ID. Therefore, the author's name in this paper should have appeared as Noor Hamzi.

For citation: Ali A, Elbashir M, Hamzi N, Akour I, Sheikhain A, Al-Shahri R, Refaee T, Abdelrazig A, Omer AM. [Corrigendum] Deep Learning-Based Convolutional Neural Networks for Brain Tumor Detection on CT Scans: A Systematic Review. International Journal of Biomedicine. 2026;16(4):517-517. doi:10.21103/Article16(4)_CRR.

© 2026 The Author(s). *International Journal of Biomedicine* is published by IMRDC.
This is an open access article under the CC BY-NC-ND 4.0 license.

IJBM

INTERNATIONAL JOURNAL OF BIOMEDICINE

Instructions for Authors

International Journal of Biomedicine (IJBM) publishes peer-reviewed articles on the topics of basic, applied, and translational research on biology and medicine. International Journal of Biomedicine welcomes submissions of the following types of paper: Original Articles, Reviews, Viewpoints, Case Reports, and Brief Communications.

All research studies involving animals must have been conducted following animal welfare guidelines such as *the National Institutes of Health (NIH) Guide for the Care and Use of Laboratory Animals*, or equivalent documents. Studies involving human subjects or tissues must adhere to the *Declaration of Helsinki and Title 45, US Code of Federal Regulations, Part 46, Protection of Human Subjects*, and must have received approval of the appropriate institutional committee charged with oversight of human studies. Informed consent must be obtained.

Pre-submissions

Authors are welcome to send an abstract or draft manuscript to obtain a view from the Editor about the suitability of their paper. Our Editors will do a quick review of your paper and advise if they believe it is appropriate for submission to our journal. It will not be a full review of your manuscript.

Manuscript Submission

Manuscript submissions should conform to the guidelines set forth in the Recommendations for the Conduct, Reporting, Editing and Publication of Scholarly Work in Medical Journals (ICMJE Recommendations), available from www.ICMJE.org.

Original works will be accepted with the understanding that they are contributed solely to the Journal, are not under review by another publication, and have not previously been published except in abstract form.

All manuscripts must be submitted through the International Journal of Biomedicine`s online submission system (www.ijbm.org/submission.php). Manuscripts must be typed, double-spaced using a 14-point font, including references, figure legends, and tables. Leave 1-inch margins on all sides. Assemble the manuscript in this order: Title Page, Abstract, Keywords, Text (Introduction, Methods, Results, and Discussion), Acknowledgments, Sources of Funding, Disclosures, References, Tables, Figures, and Figure Legends. References, Figures, and Tables should be cited in numerical order according to first mention in the text.

The preferred order for uploading files is as follows: Cover letter, Full Manuscript PDF (PDF containing all parts of the manuscript including references, legends, figures and tables), Manuscript Text File (MS Word), Figures (each figure and its corresponding legend should be presented together), and Tables. Files should be labeled with appropriate and descriptive file names (e.g., SmithText.doc, Fig1.eps, Table3.doc). Text, Tables, and Figures should be uploaded as separate files. (Multiple figure files can be compressed into a Zip file and uploaded in one step; the system will then unpack the files and prompt the naming of each figure. See www.WinZip.com for a free trial.)

Authors who are unable to provide an electronic version or have other circumstances that prevent online submission must contact the Editorial Office prior to submission to discuss alternate options (editor@ijbm.org).

Cover Letter

The cover letter should be saved as a separate file for upload. In it, the authors should (1) state that the manuscript, or parts of it, have not been and will not be submitted elsewhere for publication; (2) state that all authors have read and approved the manuscript; and (3) disclose any financial or other relations that could lead to a conflict of interest. If a potential conflict exists, its nature should be stated for each author. When there is a stated potential conflict of interest a footnote will be added indicating the author's equity interest in or other affiliation with the identified commercial firms.

The corresponding author should be specified in the cover letter. All editorial communications will be sent to this author. A short paragraph telling the editors why the authors think their paper merits publication priority may be included in the cover letter.

Types of articles

Original articles

Original articles present the results of original research. These manuscripts should present well-rounded studies reporting innovative advances that further knowledge about a topic of importance to the fields of biology or medicine. These can be submitted as either a full-length article (no more than 6,000 words, 4 figures, 4 tables) or a Short Communication (no more than 2,500 words, 2 figures, 2 tables). An original

article may be Randomized Control Trial, Controlled Clinical Trial, Experiment, Survey, and Case-control or Cohort study.

Case Reports

Case reports describe an unusual disease presentation, a new treatment, a new diagnostic method, or a difficult diagnosis. The authors must make it clear what the case adds to the field of medicine and include an up-to-date review of all prior cases. These articles should be no more than 5,000 words with no more than 6 figures and 3 tables. Case Reports should consist of the following headings: Abstract (no more than 100 words), Introduction, Case Presentation, Discussion, and Conclusions. The number of authors for a clinical case description must not exceed seven. Those who contributed to the patient's care but did not contribute directly to the intellectual work of the manuscript should be listed in the acknowledgments section.

Reviews

Reviews analyze the current state of understanding on a particular subject of research in biology or medicine, the limitations of current knowledge, future directions to be pursued in research, and the overall importance of the topic. Reviews could be non-systematic (narrative) or systematic. Reviews can be submitted as a Mini-Review (no more than 2,500 words, 3 figures, and 1 table) or a long review (no more than 6,000 words, 6 figures, and 3 tables). Reviews should contain four sections: Abstract, Introduction, Topics (with headings and subheadings, and Conclusions and Outlook.

Viewpoints

Viewpoint articles include academic papers, which address any important topic in biomedicine from a personal perspective than standard academic writing. Maximum length is 1,200 words, ≤70 references, and 1 small table or figure.

Short Communications

Short communications are concise scientific papers (typically 1,500–2,500 words) that present novel, preliminary, or urgent findings without the length or depth of a full research article. Main body of text, excluding tables (<2), figures (<2), and references (<15), not to exceed 1,000 words. Short Communications should contain Abstract, Introduction, Materials and Methods, Results, and Conclusion.

Research Reporting Guidelines

Authors are encouraged to adhere to recognized research reporting guidelines for study types:

• Randomized trials: CONSORT (https://www.equator-network.org/reporting-guidelines/consort/)

• Observational studies: STROBE (https://www.equator-network.org/reporting-guidelines/strobe/)

• Systematic reviews: PRISMA (https://www.equator-network.org/reporting-guidelines/prisma/)

• Case reports: CARE (https://www.equator-network.org/reporting-guidelines/care/)

• Qualitative research: SRQR (https://www.equator-network.org/reporting-guidelines/srqr/)

• Diagnostic / prognostic studies: STARD (https://www.equator-network.org/reporting-guidelines/stard/)

• Animal pre-clinical studies: ARRIVE (https://www.equator-network.org/reporting-guidelines/improving-bioscience-research-reporting-the-arrive-guidelines-for-reporting-animal-research/)

• Study protocols: SPIRIT (https://www.equator-network.org/reporting-guidelines/spirit-2013-statement-defining-standard-protocol-items-for-clinical-trials/)

Genetic Nomenclature and Sequence Data

DNA sequence variants should be described in the text and tables according to HGVS (Human Genome Variation Society) nomenclature (varnomen.hgvs.org). DNA-level changes must be specified relative to a specific reference sequence, such as NCBI RefSeq or a Locus Reference Genomic (LRG) record. Tabular listings of the described sequence variants must include columns for DNA, RNA, and protein, and clearly indicate whether the changes were determined experimentally or predicted exclusively theoretically.

Nucleotide sequence data can be submitted to any of the three major collaborative databases:

• DNA Data Bank of Japan (DDBJ): http://www.ddbj.nig.ac.jp

• European Nucleotide Archive (ENA): ebi.ac.uk/ena

• GenBank: https://www.ncbi.nlm.nih.gov/genbank/

Manuscript Preparation

Title Page

The first page of the manuscript (title page) should include (1) a full title of the article, (2) a short title of less than 60 characters with spaces, (3) the authors' names, academic degrees, and affiliations, (4) the total word count of the manuscript (including Abstract, Text, References, Tables, Figure Legends), (5) the number of figures and tables, and (6) the name, email address, and complete address of corresponding author.

Disclaimers. An example of a disclaimer is an author's statement that the views expressed in the submitted article are his or her own and not an official position of the institution or funder.

Abstract

The article should include a brief abstract of no more than 200 words. Limit use of acronyms and abbreviations. Define at first use with acronym or abbreviation in parentheses. The abstract should be structured with the following headings: Background, Methods and Results, and Conclusions. The Background section should describe the rationale for the study. Methods and Results should briefly describe the methods and present the significant results. Conclusions should succinctly state the interpretation of the data. Authors should supply a list of up to four key words not appearing in the title, which will be used for indexing. The key words should be listed immediately after the Abstract. Use terms from the Medical Subject Headings (MeSH) list of Index Medicus when possible.

Main text in the IMRaD format

Introduction should describe the purpose of the study and its relation to previous work in the field; it should not include an extensive literature review.

Methods should be concise but sufficiently detailed to permit repetition by other investigators. Previously published methods and modifications should be cited by reference. A subsection on statistics should be included in the Methods section.

Results should present positive and relevant negative findings of the study, supported when necessary by reference to Tables and Figures.

Discussion should interpret the results of the study, with emphasis on their relation to the original hypotheses and to previous studies. The importance of the study and its limitations should also be discussed.

The IMRaD format does not include a separate Conclusion section. The conclusion is built into the Discussion. More information on the structure and content of these sections can be found in the Recommendations for the Conduct, Reporting, Editing and Publication of Scholarly Work in Medical Journals (ICMJE Recommendations), available from www.ICMJE.org.

Author Contributions, Acknowledgments, Sources of Funding, and Disclosures

CRediT (Contributor Roles Taxonomy) author statement should be provided during the submission process**.**

Acknowledgments : All contributors who do not meet the criteria for authorship should be listed in an acknowledgments section. Examples of those who might be acknowledged include a person who provided purely technical help, writing assistance, or a department chairperson who provided only general support. Authors should declare whether they had assistance with study design, data collection, data analysis, or manuscript preparation. If such assistance was available, the authors should disclose the identity of the individuals who provided this assistance and the entity that supported it in the published article.

Sources of Funding: All sources of financial support for the study should be cited on the title page, including federal or state agencies, nonprofit organizations, and pharmaceutical or other commercial sources.

Disclosure and conflicts of interest: All authors must disclose any financial or other relations that could lead to a conflict of interest. If a potential conflict exists, its nature should be stated for each author. All sources of financial support for the study should be cited, including federal or state agencies, nonprofit organizations, and pharmaceutical or other commercial sources. Please use ICMJE Form for Disclosure of Potential Conflicts of Interest (http://www.icmje.org/conflicts-of-interest/).

References

References should follow the standards summarized in the NLM's International Committee of Medical Journal Editors (ICMJE) Recommendations for the Conduct, Reporting, Editing and Publication of Scholarly Work in Medical Journals: Sample References webpage (www.nlm.nih.gov/bsd/uniform_requirements.html) and detailed in the NLM's Citing Medicine, available from www.ncbi.nlm.nih.gov/books/NBK7256/. MEDLINE abbreviations for journal titles (www.ncbi.nlm.nih.gov/nlmcatalog/journals) should be used.

References should be presented in the Vancouver style. The first six authors should be listed in each reference citation (if there are more than six authors, "et al" should be used following the sixth). Periods are not used in authors' initials or journal abbreviations. Examples of journal reference style:

Journal Article: Serruys PW, Ormiston J, van Geuns RJ, de Bruyne B, Dudek D, Christiansen E, et al. A Polylactide Bioresorbable Scaffold Eluting Everolimus for Treatment of Coronary Stenosis: 5-Year Follow-Up. J Am Coll Cardiol. 2016;67(7):766-76. doi: 10.1016/j.jacc.2015.11.060.

Book: Murray PR, Rosenthal KS, Kobayashi GS, Pfaller MA. *Medical Microbiology*. 4th ed. St. Louis: Mosby; 2002.

Chapter in Edited Book: Meltzer PS, Kallioniemi A, Trent JM. Chromosome alterations in human solid tumors. In: Vogelstein B, Kinzler KW, editors. *The Genetic Basis of Human Cancer*. New York: McGraw-Hill; 2002:93–113.

References should be numbered consecutively in the order in which they are first mentioned in the text. Identify references in text, tables, and legends by Arabic numerals in parentheses and listed at the end of the article in citation order.

Tables

Tables should be comprehensible without reference to the text and should not be repetitive of descriptions in the text. Every table should consist of two or more columns; tables with only one column will be treated as lists and incorporated into the text. All tables must be cited in the text and numbered in order of appearance. Tables should include a short title. Place explanatory matter in footnotes, not in the heading. Explain all nonstandard abbreviations in footnotes, and use symbols to explain information if needed. Each table submitted should be double-spaced, each on its own page. Each table should be saved as its own file as a Word Document. Explanatory matter and source notations for borrowed tables should be placed in the table footnote.

Figures and Legends

All illustrations (line drawings and photographs) are classified as figures. All figures should be cited in the text and numbered in order of appearance. Figures should be provided in .tiff, .jpeg or .eps formats. Color images must be at least 300 dpi. Gray scale images should be at least 300 dpi. Line art (black and white or color) and combinations of gray scale images and line art should be at least 1,000 dpi. The optimal size of lettering is 12 points. Symbols should be of a similar size. Figures should be sized to fit within the column (86 mm) or the full text width (180 mm). Line figures must be sharp, black and white graphs or diagrams, drawn professionally or with a computer graphics package. Legends should be supplied for each figure and should be brief and not repetitive of the text. Any source notation for borrowed figures should appear at the end of the legend. Figures should be uploaded as individual files.

Units of Measurement

Measurements of length, height, weight, and volume should be reported in metric units (meter, kilogram, or liter) or their decimal multiples. Temperatures should be in degrees Celsius. Blood pressures should be in millimeters of mercury. All measurements must be given in SI or SI-derived units. Drug concentrations may be reported in either SI or mass units, but the alternative should be provided in parentheses where appropriate

Style and Language

The journal accepts manuscripts written in English. Spelling should be US English only. The language of the manuscript must meet the requirements of academic

publishing. Reviewers may advise rejection of a manuscript compromised by grammatical errors. Non-native speakers of English may choose to use a copyediting service.

Abbreviations and Symbols

Use only standard abbreviations; use of nonstandard abbreviations can be confusing to readers. Avoid abbreviations in the title of the manuscript. The spelled-out abbreviation followed by the abbreviation in parenthesis should be used on first mention unless the abbreviation is a standard unit of measurement.

Drugs should be referred to by their generic names. If proprietary drugs have been used in the study, refer to these by their generic name, mentioning the proprietary name, and the name and location of the manufacturer, in parentheses.

Permissions

To use tables or figures borrowed from another source, permission must be obtained from the copyright holder, usually the publisher. Authors are responsible for applying for permission for both print and electronic rights for all borrowed materials and are responsible for paying any fees related to the applications of these permissions. This is necessary even if you are an author of the borrowed material. It is essential to begin the process of obtaining permission early, as a delay may require removing the copyrighted material from the article. The source of a borrowed table should be noted in a footnote and of a borrowed figure in the legend. It is essential to use the exact wording required by the copyright holder. A copy of the letter granting permission, identified by table or figure number, should be sent along with the manuscript. A permission request form is provided for the authors use in requesting permission from copyright holders.

Journal Policy on Affiliation with Sanctioned Institutions

At IJBM, we uphold the highest standards of academic integrity and compliance with international laws and regulations. To ensure the ethical and legal standing of all submitted research papers, authors are required to adhere to the following policy regarding affiliation with sanctioned institutions:

1. Declaration of Non-Affiliation: Authors must provide a clear and unambiguous statement confirming their non-affiliation with any institution, organization, or individual subject to sanctions imposed by international sanctions, laws, or regulations. This declaration should be included in the cover letter accompanying their manuscript submission.

2. Sanctioned Entities: Sanctioned entities include those listed on sanctions lists maintained by international authorities, such as the United Nations, the United States Department of the Treasury's Office of Foreign Assets Control (OFAC), the European Union, or any other relevant governing body.

3. Independence and Ethical Research: Authors should affirm that their research is conducted independently and ethically, without receiving any funding, resources, or support from sanctioned sources in connection with the submitted research.

4. Disclosure of Conflicts of Interest: Authors must disclose any potential conflicts of interest that may compromise the ethical and legal standing of their submission. This includes any financial interests or affiliations that could be perceived as influencing the research.

5. Consequences of Non-Compliance: Failure to adhere to this policy, misrepresentation of affiliations, or non-disclosure of conflicts of interest may result in the rejection of the submitted manuscript or further investigation into the matter.

Authors submitting their research papers to IJBM are responsible for ensuring their compliance with this policy. We reserve the right to verify the accuracy of the provided information and take appropriate action in cases of non-compliance.

Page Proofs

Page proofs are sent from the Publisher electronically and must be returned within 72 hours to avoid delay of publication. Generally, peer review is completed within 11-12 weeks, and the editor’s decision is made within 7-14 days of this. A timeline from submission to publication is an average of 14 weeks.

It is important to note that when citing an article from IJBM, the correct citation format is **International Journal of Biomedicine.**